

Evaluation of the Impact of Spectral Power Distribution on Driver Performance

PUBLICATION NO. FHWA-HRT-15-047

AUGUST 2015



U.S. Department of Transportation
Federal Highway Administration

Research, Development, and Technology
Turner-Fairbank Highway Research Center
6300 Georgetown Pike
McLean, VA 22101-2296

FOREWORD

The Federal Highway Administration's Office of Safety Research and Development focuses on conducting research that promotes a safe driving environment while offering practical considerations to address the needs of practitioners. Roadway lighting offers significant safety benefits but also represents a substantial share of the operating budgets of agencies tasked with maintaining the lighting infrastructure. Therefore, there is a need to optimize the safety implications and budgetary considerations.

This report provides the details and results of a comprehensive investigation of the impact of light-source spectrum on driver visual performance. In a series of human factors experiments, the effect of overhead lighting and headlamp spectral power distribution was evaluated with respect to driver detection and recognition of large and small objects. The report also discusses the spectral interaction of headlamp and roadway lighting on the detection of pedestrians, including an evaluation of enhanced pedestrian detection through a momentary peripheral illumination mechanism of the vehicle headlamps.

Monique R. Evans
Director, Office of Safety Research and
Development

Notice

This document is disseminated under the sponsorship of the U.S. Department of Transportation in the interest of information exchange. The U.S. Government assumes no liability for the use of the information contained in this document. This report does not constitute a standard, specification, or regulation.

The U.S. Government does not endorse products or manufacturers. Trademarks or manufacturers' names appear in this report only because they are considered essential to the objective of the document.

Quality Assurance Statement

The Federal Highway Administration (FHWA) provides high-quality information to serve Government, industry, and the public in a manner that promotes public understanding. Standards and policies are used to ensure and maximize the quality, objectivity, utility, and integrity of its information. FHWA periodically reviews quality issues and adjusts its programs and processes to ensure continuous quality improvement.

TECHNICAL REPORT DOCUMENTATION PAGE

1. Report No. FHWA-HRT-15-047	2. Government Accession No.	3. Recipient's Catalog No.		
4. Title and Subtitle Evaluation of the Impact of Spectral Power Distribution on Driver Performance		5. Report Date August 2015		
		6. Performing Organization Code:		
7. Author(s) Ronald B. Gibbons, Jason Meyer, Travis Terry, Rajaram Bhagavathula, Alan Lewis, Michael Flanagan, Caroline Connell		8. Performing Organization Report No.		
9. Performing Organization Name and Address Virginia Tech Transportation Institute 3500 Transportation Research Plaza (0536) Blacksburg, VA 24061		10. Work Unit No.		
		11. Contract or Grant No. DTFH61-10-C-00032		
12. Sponsoring Agency Name and Address Office of Safety Research and Development Federal Highway Administration 6300 Georgetown Pike McLean, VA 22101-2296		13. Type of Report and Period Covered 09/24/2010–01/31/2015		
		14. Sponsoring Agency Code		
15. Supplementary Notes The Contracting Officer's Representatives were Clayton Chen and Abdul Zineddin, Office of Safety Research and Development.				
16. Abstract This project is a complete investigation of the impact of light-source spectrum on driver visual performance. In a series of human factors experiments, the effect of overhead lighting and headlamp spectral power distribution was evaluated with respect to driver detection and recognition of large and small objects and pedestrians. The potential for applying mesopic multiplying factors to roadway lighting was also evaluated, as was a momentary peripheral illuminator system's effects on driver visual performance and eye-glance behavior. The results indicate that, although the momentary peripheral illuminator improved one measure of pedestrian detection, it was also a distraction to drivers. The results also indicate that at higher speeds, neither light-source spectrum nor mesopic multiplying factors apply, but mesopic multiplying factors are applicable to lighting design for lower-speed roadways and other nondriving environments.				
17. Key Words Light sources, Spectral effects roadway lighting, Roadway safety, Lighting levels, Lighting and safety		18. Distribution Statement No restrictions. This document is available through the National Technical Information Service; Springfield, VA 22161. http://www.ntis.gov/about/contact.aspx		
19. Security Classif. (of this report) Unclassified	20. Security Classif. (of this page) Unclassified	21. No. of Pages 236	22. Price	

SI* (MODERN METRIC) CONVERSION FACTORS				
APPROXIMATE CONVERSIONS TO SI UNITS				
Symbol	When You Know	Multiply By	To Find	Symbol
LENGTH				
in	inches	25.4	millimeters	mm
ft	feet	0.305	meters	m
yd	yards	0.914	meters	m
mi	miles	1.61	kilometers	km
AREA				
in ²	square inches	645.2	square millimeters	mm ²
ft ²	square feet	0.093	square meters	m ²
yd ²	square yard	0.836	square meters	m ²
ac	acres	0.405	hectares	ha
mi ²	square miles	2.59	square kilometers	km ²
VOLUME				
fl oz	fluid ounces	29.57	milliliters	mL
gal	gallons	3.785	liters	L
ft ³	cubic feet	0.028	cubic meters	m ³
yd ³	cubic yards	0.765	cubic meters	m ³
NOTE: volumes greater than 1000 L shall be shown in m ³				
MASS				
oz	ounces	28.35	grams	g
lb	pounds	0.454	kilograms	kg
T	short tons (2000 lb)	0.907	megagrams (or "metric ton")	Mg (or "t")
TEMPERATURE (exact degrees)				
°F	Fahrenheit	5 (F-32)/9 or (F-32)/1.8	Celsius	°C
ILLUMINATION				
fc	foot-candles	10.76	lux	lx
fl	foot-Lamberts	3.426	candela/m ²	cd/m ²
FORCE and PRESSURE or STRESS				
lbf	poundforce	4.45	newtons	N
lbf/in ²	poundforce per square inch	6.89	kilopascals	kPa
APPROXIMATE CONVERSIONS FROM SI UNITS				
Symbol	When You Know	Multiply By	To Find	Symbol
LENGTH				
mm	millimeters	0.039	inches	in
m	meters	3.28	feet	ft
m	meters	1.09	yards	yd
km	kilometers	0.621	miles	mi
AREA				
mm ²	square millimeters	0.0016	square inches	in ²
m ²	square meters	10.764	square feet	ft ²
m ²	square meters	1.195	square yards	yd ²
ha	hectares	2.47	acres	ac
km ²	square kilometers	0.386	square miles	mi ²
VOLUME				
mL	milliliters	0.034	fluid ounces	fl oz
L	liters	0.264	gallons	gal
m ³	cubic meters	35.314	cubic feet	ft ³
m ³	cubic meters	1.307	cubic yards	yd ³
MASS				
g	grams	0.035	ounces	oz
kg	kilograms	2.202	pounds	lb
Mg (or "t")	megagrams (or "metric ton")	1.103	short tons (2000 lb)	T
TEMPERATURE (exact degrees)				
°C	Celsius	1.8C+32	Fahrenheit	°F
ILLUMINATION				
lx	lux	0.0929	foot-candles	fc
cd/m ²	candela/m ²	0.2919	foot-Lamberts	fl
FORCE and PRESSURE or STRESS				
N	newtons	0.225	poundforce	lbf
kPa	kilopascals	0.145	poundforce per square inch	lbf/in ²

*SI is the symbol for the International System of Units. Appropriate rounding should be made to comply with Section 4 of ASTM E380.
(Revised March 2003)

TABLE OF CONTENTS

EXECUTIVE SUMMARY	1
CHAPTER 1. INTRODUCTION.....	5
PROJECT OBJECTIVES	5
CHAPTER 2. BACKGROUND.....	7
IMPACT OF ROADWAY LIGHTING	7
Color	10
MESOPIC EFFECTS AT NIGHT FOR DRIVERS	11
Models of Mesopic Vision.....	13
LIGHTING AND THE DRIVING ENVIRONMENT	17
Visual Acuity	17
Age Effects on Vision and Driving.....	18
Visibility and Contrast	18
Size (Visual Angle).....	20
Contrast Polarity Factor	21
Exposure Time	21
Age Factor.....	21
Transient Adaptation.....	22
Eccentricity	22
MOMENTARY PERIPHERAL ILLUMINATORS.....	22
Problems Detecting Pedestrians at Night.....	23
Headlamp Technologies.....	24
SPECIFICATION DEVELOPMENT FOR AN MPI SYSTEM.....	27
Conceptual Design of an MPI System	27
Pedestrian-Detection Systems.....	28
CHAPTER 3. EXPERIMENTAL APPROACH.....	31
MATERIALS AND FACILITIES	32
Virginia Smart Road	32
Overhead-Lighting Systems.....	33
Vehicles and Headlamp Systems	35
Visual Objects	37
DEPENDENT VARIABLES	40
Detection Distance	40
Color-Recognition Distance.....	41
Orientation-Recognition Distance	42
PROCEDURES.....	42
Participant Selection	42
Participant Screening	43
Experimental Runs.....	44
PHOTOMETRIC SYSTEMS.....	44
Luminance-Based Systems	44
Illuminance-Based Systems	45

DATA REDUCTION PROCEDURES	46
Detection/Recognition Distances	46
Luminance Data	46
CHAPTER 4. SCOPING EXPERIMENT	47
INTRODUCTION	47
Research Objectives	47
EXPERIMENTAL DESIGN	47
Independent Variables	48
Dependent Variables	51
METHODS	51
Facilities and Equipment	51
Participants	51
Procedure	52
Data Analysis	52
RESULTS	53
Overhead-Lighting Type and Level	53
No Overhead Lighting	65
Luminance Analysis	69
DISCUSSION	73
CONCLUSIONS	74
Design of Further Experiments	76
LIMITATIONS	76
CHAPTER 5. MPI SYSTEM PERFORMANCE EXPERIMENT	77
INTRODUCTION	77
Research Objectives	77
EXPERIMENTAL DESIGN	78
Independent Variables	78
Dependent Variables	81
Facilities and Equipment	83
Participants	83
Procedure	84
Data Analysis	84
RESULTS	85
Detection and Color-Recognition Distances	85
Detection Rate by Pedestrian Illuminated by MPI System	96
Mean Fixation Duration by MPI System Configuration	97
DISCUSSION	98
CONCLUSIONS	99
FUTURE RESEARCH	99
CHAPTER 6. OVERHEAD-LIGHTING LEVEL EXPERIMENT	101
INTRODUCTION	101
Research Objectives	101
EXPERIMENTAL DESIGN	102
Independent Variables	102
Dependent Variables	106

METHODS	107
Participants	107
Procedure	107
Data Analysis	108
RESULTS	108
Lighting Characteristics	108
Detection Distance Versus Lighting Conditions	109
Orientation-Recognition Distance	120
Luminance	123
DISCUSSION	128
Zones of Visibility	128
Stopping Sight Distance	129
Weber Contrast and Detection Distance	131
Visibility Level	139
CONCLUSIONS	142
CHAPTER 7. MESOPIC MODELING EXPERIMENT	145
INTRODUCTION	145
Research Objectives	145
EXPERIMENTAL DESIGN	146
Independent Variables	146
Dependent Variables	148
METHODS	149
Facilities and Equipment	149
Participants	150
Procedure	151
Data Analysis	151
RESULTS	152
Static	152
Dynamic	158
DISCUSSION	163
Static Experiment	164
Dynamic Experiment	168
CONCLUSIONS	173
CHAPTER 8. FINAL PERFORMANCE EXPERIMENT	175
INTRODUCTION	175
Research Objectives	176
EXPERIMENTAL DESIGN	176
Independent Variables	177
Covariate	179
Dependent Variables	179
Facilities and Equipment	180
Participants	180
Procedure	180
Data Analysis	180

RESULTS	181
Main Effects	181
Two-Way Interactions.....	188
Contrast and Detection Distance.....	195
DISCUSSION	199
MPI.....	199
Age.....	200
Color	201
Adaptation Luminance.....	201
Offset.....	202
Speed.....	202
CHAPTER 9. SUMMARY.....	205
CHAPTER 10. CONCLUSIONS AND FUTURE CONSIDERATIONS	207
CONCLUSIONS	207
Effect of Overhead-Lighting SPD on Driver Visual Performance	207
Combined Effect of Overhead Lighting and Headlamps on Driver Visual Performance	207
Applicability of Mesopic Models to the Driving Environment	208
Impact of MPI System on Driver Visual Performance	208
Additional Findings	208
CONSIDERATIONS.....	209
FUTURE RESEARCH.....	209
CHAPTER 11. APPLICATION TO PRACTICE	211
REFERENCES.....	213

LIST OF FIGURES

Figure 1. Graph. Spectral power distribution of HPS light sources.....	8
Figure 2. Graph. Spectrum power distribution of three LED light sources.....	9
Figure 3. Diagram. Change in light source appearance with CCT	10
Figure 4. Diagram. Ranges of visual sensitivity	12
Figure 5. Equation. CIE formula for calculating mesopic spectral sensitivity	16
Figure 6. Equation. Luminance difference threshold.....	19
Figure 7. Equation. VL formula.....	19
Figure 8. Equation. Formula for calculating Weber contrast.....	20
Figure 9. Diagram. Variables for calculating visual angle	20
Figure 10. Equation. Formula for visual angle in degrees	20
Figure 11. Equation. Calculation for negative contrast threshold	21
Figure 12. Equation. Calculation of the contrast polarity factor.....	21
Figure 13. Equation. Age factor calculation for younger age group (23 to 64 years)	22
Figure 14. Equation. Age factor calculation for older age group (64 to 75 years)	22
Figure 15. Graph. Headlamp beam pattern	24
Figure 16. Chart. Comparison between halogen and HID headlamps.....	25
Figure 17. Graph. Comparison of reaction times between halogen and HID headlamps.....	25
Figure 18. Graph. Reaction times with different HID headlamp types	26
Figure 19. Diagram. MPI headlamp illuminating pedestrian by flashing on and swiveling	27
Figure 20. Diagram. Conceptual design of an MPI system	28
Figure 21. Diagram. General structure of a pedestrian-detection system.....	29
Figure 22. Flowchart. Relationship among experiments performed.....	31
Figure 23. Diagram. Smart Road test track.....	33
Figure 24. Graph. Mesopic modeling experiment—SPDs of overhead-lighting types used in the study.....	34
Figure 25. Photo. Test vehicle with headlamps and interchangeable gels.....	35
Figure 26. Graph. SPD of low-power, color-filtered headlamps.....	36
Figure 27. Graph. SPD of high-power, color-filtered headlamps.....	36
Figure 28. Graph. SPD of low-power, neutral-density-filtered headlamps	37
Figure 29. Photo. Clothing colors on confederate pedestrian	38
Figure 30. Graph. Pedestrian clothing reflectance.....	38
Figure 31. Photo. Targets.....	39
Figure 32. Graph. Target reflectance relative to diffuse white	40
Figure 33. Diagram. Measuring detection and color-recognition distances	41
Figure 34. Screenshot. Luminance analysis software	45
Figure 35. Photo. Pedestrian on roadway	50
Figure 36. Photo. Target on roadway.....	51
Figure 37. Chart. Scoping experiment—mean pedestrian-detection distance by overhead- lighting type and level, with SNK results	54
Figure 38. Chart. Scoping experiment—mean pedestrian color-recognition distance by overhead-lighting type and level, with SNK results	55
Figure 39. Chart. Scoping experiment—mean pedestrian-detection distance by clothing color	56

Figure 40. Chart. Scoping experiment—mean pedestrian clothing color-recognition distance by clothing color	57
Figure 41. Chart. Scoping experiment—mean off-axis pedestrian-detection distance by overhead-lighting type and level.....	58
Figure 42. Chart. Scoping experiment—mean off-axis pedestrian color-recognition distance by overhead-lighting type and pedestrian position	59
Figure 43. Chart. Scoping experiment—pedestrian-detection distance by position and clothing color	60
Figure 44. Chart. Scoping experiment—pedestrian color-recognition distance by position and clothing color	60
Figure 45. Chart. Scoping experiment—mean pedestrian-detection distance by pedestrian position, speed, and overhead-lighting type	61
Figure 46. Chart. Scoping experiment—detection distances by overhead-lighting type and level for constant-contrast pedestrians.....	62
Figure 47. Chart. Scoping experiment—mean target-detection distance by target color	64
Figure 48. Chart. Scoping experiment—mean target color-recognition distance by target color	64
Figure 49. Chart. Scoping experiment—target color-recognition distance by target color and overhead-lighting type	65
Figure 50. Chart. Scoping experiment—mean pedestrian-detection distance by clothing color for no overhead lighting.....	66
Figure 51. Chart. Scoping experiment—mean pedestrian color-recognition distance by clothing color for no overhead lighting	67
Figure 52. Chart. Scoping experiment—mean target-detection distance by target color for no overhead lighting	68
Figure 53. Chart. Scoping experiment—mean target color-recognition distance by target color for no overhead lighting.....	69
Figure 54. Scatter Plot. Scoping experiment—pedestrian-detection distance, luminance, and clothing color	70
Figure 55. Chart. Scoping experiment—pedestrian mean Weber contrast at time of detection by overhead-lighting color and clothing color	71
Figure 56. Photo. Uniformity of HPS and LED lighting	72
Figure 57. Scatter Plot. Scoping experiment—target-detection distance and luminance.....	73
Figure 58. Photo. MPI system with straight (left) and swiveling (right) headlamp	79
Figure 59. Diagram. MPI system performance experiment—MPI system configurations	80
Figure 60. Diagram. MPI system performance experiment—pedestrian opposite from area illuminated by MPI system	81
Figure 61. Photo. MPI system performance experiment—eye-tracker goggles	82
Figure 62. Screenshot. MPI system performance experiment—pupil location (left) and dot representing gaze direction overlaid on scene (right)	83
Figure 63. Chart. MPI system performance experiment—pedestrian-detection and color-recognition distances versus headlamp color.....	87
Figure 64. Chart. MPI system performance experiment—pedestrian-detection and color-recognition distances versus headlamp color and overhead lighting.....	87
Figure 65. Chart. MPI system performance experiment—pedestrian-detection and color-recognition distance versus MPI system configuration	88

Figure 66. Chart. MPI system performance experiment—pedestrian-detection and color-recognition distances versus MPI system configuration and overhead lighting.....	89
Figure 67. Chart. MPI system performance experiment—pedestrian-detection and color-recognition distances versus MPI system configuration and headlamp color	90
Figure 68. Chart. MPI system performance experiment—pedestrian-detection and color-recognition distances versus MPI system configuration and pedestrian on left or right	91
Figure 69. Chart. MPI system performance experiment—pedestrian-detection and color-recognition distances versus pedestrian clothing color.....	92
Figure 70. Chart. MPI system performance experiment—pedestrian-detection and color-recognition distances versus pedestrian clothing color and overhead lighting.....	93
Figure 71. Chart. MPI system performance experiment—pedestrian-detection and color-recognition distances versus pedestrian on left or right.....	94
Figure 72. Chart. MPI system performance experiment—pedestrian-detection and color-recognition distances versus pedestrian in overhead lighting.....	95
Figure 73. Photo. MPI system performance experiment—visual clutter on the Smart Road.....	96
Figure 74. Chart. MPI system performance experiment—percentage of detections of pedestrian versus MPI system configuration and whether the pedestrian was illuminated by the MPI system	97
Figure 75. Chart. MPI system performance experiment—mean fixation duration versus MPI system configuration.....	98
Figure 76. Diagram. Overhead-lighting level experiment—target I (low VI) placement	104
Figure 77. Diagram. Overhead-lighting level experiment—target II (high VI) placement.....	105
Figure 78. Graph. Overhead-lighting level experiment—VI on objects by overhead-lighting level	106
Figure 79. Graph. Overhead-lighting level experiment—VI at target, vehicle with headlamps on at between 91 and 8 m (300 and 25 ft) from target, luminaires from 0 to 100 percent.....	109
Figure 80. Chart. Overhead-lighting level experiment—SNK groupings for pedestrian-detection distance with headlamps off by overhead-lighting level.....	111
Figure 81. Chart. Overhead-lighting level experiment—SNK groupings for pedestrian-detection distance with headlamps on by overhead-lighting level	112
Figure 82. Chart. Overhead-lighting level experiment—SNK groupings for target I detection distance with headlamps off by overhead-lighting level.....	113
Figure 83. Chart. Overhead-lighting level experiment—SNK groupings for target I detection distance with headlamps on by overhead-lighting level	114
Figure 84. Chart. Overhead-lighting level experiment—SNK groupings for target II detection distance with headlamps off by overhead-lighting level.....	115
Figure 85. Chart. Overhead-lighting level experiment—SNK groupings for target II detection distance with headlamps on by overhead-lighting level	116
Figure 86. Chart. Overhead-lighting level experiment—mean detection distance for all objects by headlamp on/off.....	117
Figure 87. Chart. Overhead-lighting level experiment—mean detection distance for all objects by participant age and lighting conditions combined	118
Figure 88. Chart. Overhead-lighting level experiment—mean detection distances for pedestrians by overhead-lighting level	119

Figure 89. Chart. Overhead-lighting level experiment—mean detection distances for targets by overhead-lighting level.....	120
Figure 90. Chart. Overhead-lighting level experiment—mean recognition distance of pedestrian by headlamps on and off and overhead-lighting level.....	121
Figure 91. Chart. Overhead-lighting level experiment—mean recognition distance of target I by headlamps on and off and overhead-lighting level.....	122
Figure 92. Chart. Overhead-lighting level experiment—mean recognition distance of target II by headlamps on and off and overhead-lighting level	123
Figure 93. Graph. Overhead-lighting level experiment—pedestrian log luminance by overhead-lighting level, headlamp condition, and distance.....	124
Figure 94. Graph. Overhead-lighting level experiment—target I luminance by overhead-lighting level, headlamp condition, and distance.....	126
Figure 95. Graph. Overhead-lighting level experiment—target II luminance by overhead-lighting level, headlamp condition, and distance.....	127
Figure 96. Graph. Overhead-lighting level experiment—pedestrian contrast and detection distance at 100-percent overhead lighting	131
Figure 97. Graph. Overhead-lighting level experiment—pedestrian contrast and detection distances at 50-percent overhead lighting.....	133
Figure 98. Graph. Overhead-lighting level experiment—pedestrian contrast and detection distances at 10-percent overhead lighting.....	133
Figure 99. Image Table. Overhead-lighting level experiment—images of target I at 100-percent overhead lighting for from 15.2 to 123 m (50 to 400 ft) to the target	134
Figure 100. Graph. Overhead-lighting level experiment—target I contrast and detection distance at 100-percent overhead lighting	135
Figure 101. Image Table. Overhead-lighting level experiment—images of target I at 40-percent overhead lighting for from 15.2 to 123 m (50 to 400 ft) to the target	136
Figure 102. Graph. Overhead-lighting level experiment—target I contrast and detection distances versus distance from target at 40-percent overhead lighting.....	137
Figure 103. Graph. Overhead-lighting level experiment—target II contrast and detection distances versus distance from target at 100-percent overhead lighting.....	138
Figure 104. Graph. Overhead-lighting level experiment—target II contrast and detection distances versus distance from target at 40-percent overhead lighting.....	139
Figure 105. Graph. Overhead-lighting level experiment—pedestrian VL with headlamps on and with and without overhead lighting.....	140
Figure 106. Graph. Overhead-lighting level experiment—target I VL with headlamps on and with and without overhead lighting.....	141
Figure 107. Graph. Overhead-lighting level experiment—target II VL with headlamps on and with and without overhead lighting.....	142
Figure 108. Diagram. Arrangement of target lights for static experiments on the Smart Road	148
Figure 109. Photo. Mesopic modeling experiment—target, target light, and background.....	150
Figure 110. Graph. Mesopic modeling experiment (static portion)—threshold contrast by overhead-lighting type	153
Figure 111. Graph. Mesopic modeling experiment (static portion)—threshold contrast by adaptation luminance	154

Figure 112. Graph. Mesopic modeling experiment (static portion)—threshold contrast by eccentricity	155
Figure 113. Equation. Formula for calculating mesopic output	155
Figure 114. Equation. Formula for calculating mesopic threshold contrast	156
Figure 115. Graph. Mesopic modeling experiment (static portion)—threshold contrasts calculated with photopic and mesopic luminances for the three lighting types and three eccentricities	157
Figure 116. Graph. Mesopic modeling experiment (dynamic portion)—detection distance by adaptation luminance	160
Figure 117. Graph. Mesopic modeling experiment (dynamic portion)—effect of overhead-lighting type and adaptation luminance on detection distance	161
Figure 118. Chart. Mesopic modeling experiment (dynamic portion)—effect of eccentricity and speed on detection distance	161
Figure 119. Graph. Mesopic modeling experiment (dynamic portion)—effect of adaptation luminance and eccentricity on detection distance	162
Figure 120. Graph. Mesopic modeling experiment (dynamic portion)—effect of overhead-lighting type, adaptation luminance, and eccentricity on detection distance	163
Figure 121. Graph. Mesopic modeling experiment (static portion)—threshold contrasts of targets under different overhead-lighting sources at different adaptation luminances	164
Figure 122. Graph. Mesopic modeling experiment (static portion)—mesopic contrast thresholds as predicted by the CIE Mesopic Spectral Sensitivity Model	166
Figure 123. Equation. Formula for calculating the mesopic luminance difference between 2,100-K HPS and 6,000-K LED lighting	167
Figure 124. Graph. Mesopic modeling experiment (static portion)—calculated versus predicted deltas (difference in mesopic luminance expressed as a percentage) between HPS lighting and each of the LED lighting types	168
Figure 125. Graph. Mesopic modeling experiment (dynamic portion)—effect of eccentricity and speed on detection distance	170
Figure 126. Graph. Mesopic modeling experiment—peripheral visual performance in both static and dynamic experiments at different adaptation luminances	171
Figure 127. Graph. Mesopic modeling experiment—peripheral visual performance of overhead lighting types at different adaptation luminances	172
Figure 128. Diagram. Final performance experiment—pedestrian positions and offsets from the roadway	178
Figure 129. Graph. Final performance experiment—detection distance and color-recognition distance by adaptation luminance	185
Figure 130. Chart. Final performance experiment—detection and color-recognition distances by pedestrian clothing color	187
Figure 131. Chart. Final performance experiment—detection distance and color-recognition distance versus offset for all pedestrian clothing colors	188
Figure 132. Chart. Final performance experiment—detection distance by adaptation luminance and offset for all clothing colors	189
Figure 133. Chart. Final performance experiment—detection distance by adaptation luminance and offset for gray-clothed pedestrians only	189
Figure 134. Chart. Final performance experiment—missed detections by age and offset	190

Figure 135. Chart. Final performance experiment—detection distance by offset and overhead-lighting type for gray-clothed pedestrians	191
Figure 136. Chart. Final performance experiment—missed detections by MPI system configuration and offset	192
Figure 137. Graph. Final performance experiment—detection distance by speed and offset for all clothing colors	193
Figure 138. Graph. Final performance experiment—detection distance by speed and offset for gray only	194
Figure 139. Chart. Final performance experiment—detection distance by adaptation luminance and overhead-lighting type with the MPI system off	195
Figure 140. Graph. Final performance experiment—detection distance and Weber contrast by adaptation luminance	197
Figure 141. Graph. Detection distance and Weber contrast by adaptation luminance for MPI system on and off	198
Figure 142. Graph. Final performance experiment—detection distance and Weber contrast by offset	199
Figure 143. Graph. Final performance experiment—VL and Weber contrast by adaptation luminance	201

LIST OF TABLES

Table 1. Light type, color, and problems (from Shaflik, 1997)	11
Table 2. Overhead-lighting system characteristics	34
Table 3. Characteristics of headlamp filters	36
Table 4. Integral of pedestrian clothing reflectance.....	39
Table 5. Integral of target reflectance	40
Table 6. Scoping experiment independent variables and values	48
Table 7. Scoping experiment dependent variables and measurement method	48
Table 8. Scoping experiment participant characteristics	52
Table 9. Scoping experiment on-axis pedestrian significant results summary for runs in overhead-lighting type and level.....	53
Table 10. Scoping experiment constant-contrast pedestrian results summary	61
Table 11. Scoping experiment target results summary for overhead lighting	63
Table 12. Scoping experiment pedestrian results summary for no overhead lighting.....	66
Table 13. Scoping experiment target results summary for no overhead lighting	67
Table 14. Scoping experiment best and worst colors for target and pedestrian detection and color recognition, with and without overhead lighting	75
Table 15. MPI system performance experiment independent variables and values	78
Table 16. MPI system performance experiment dependent variables and measurement method.....	78
Table 17. MPI system performance experiment participant characteristics	84
Table 18. MPI system performance experiment detection distance results per independent variable.....	85
Table 19. MPI system performance experiment color-recognition distance results per independent variable	86
Table 20. Overhead-lighting level experiment independent variables	102
Table 21. Overhead-lighting level experiment dependent variables	102
Table 22. Overhead-lighting level experiment—VI of targets and pedestrian with luminaires and no headlamps.....	106
Table 23. Overhead-lighting level experiment participant characteristics	107
Table 24. Overhead-lighting level experiment—significant effects on detection distance of targets and pedestrian	110
Table 25. Overhead-lighting level experiment—zones of visibility for pedestrian and targets	129
Table 26. Overhead-lighting level experiment—object stopping sight distance and corresponding speed.....	130
Table 27. Mesopic modeling experiment—-independent variables and values.....	146
Table 28. Mesopic modeling experiment—covariate and value/measurement method	146
Table 29. Mesopic modeling experiment—dependent variables and measurement method.....	146
Table 30. Mesopic modeling experiment—adaptation luminance by overhead-lighting level and pavement type.....	147
Table 31. Mesopic modeling experiment participant characteristics.....	151
Table 32. Mesopic modeling experiment (static portion)—independent variables and their effect on threshold contrast.....	152

Table 33. Mesopic modeling experiment (dynamic portion)—independent variables and their effect on threshold contrast.....	159
Table 34. Final experiment—independent variables and values	176
Table 35. Final experiment—covariate and measurement method	176
Table 36. Final experiment—dependent variables and measurement method	176
Table 37. Final performance experiment—adaptation luminance per overhead lighting level and pavement type.....	177
Table 38. Final performance experiment—VI for all pedestrian positions, overhead lighting levels, and visual angles	179
Table 39. Final performance experiment participant characteristics	180
Table 40. Final performance experiment results.....	181
Table 41. Final performance experiment significant main effects, gray only	184
Table 42. Final performance experiment results for Weber contrast and detection distance for gray pedestrians only.....	196

ACRONYMS AND ABBREVIATIONS

ANCOVA	Analysis of Covariance
ANOVA	Analysis of Variance
BAT	Brightness Acuity Tester
BSM	Binocular Simultaneity Method
CCT	Correlated Color Temperature
CIE	Commission Internationale d'Eclairage
GPS	Global Positioning System
HID	High-Intensity Discharge
HPS	High-Pressure Sodium
HSD	Honest Significant Difference
IES	Illuminating Engineering Society
K	Kelvin
LED	Light-Emitting Diode
MH	Metal Halide
MOA	Minutes of Arc
MOVE	Mesopic Optimization of Visual Efficiency
MPI	Momentary Peripheral Illumination
OD	Optical Density
RLMMS	Roadway Lighting Mobile Measurement System
S/P	Scotopic Output/Photopic Output
SAE	Society for Automotive Engineering
SNK	Student-Newman-Keuls
SPD	Spectral Power Distribution
TOF	Time of Flight
UFOV	Useful Field of View
VI	Vertical Illuminance
VL	Visibility Level
VTI	Virginia Tech Transportation Institute

EXECUTIVE SUMMARY

Traditional roadway lighting uses high-pressure sodium (HPS) light sources, which provide high photometric efficacy. HPS light itself, however, is amber and does not render object color correctly. With the advent of light-emitting diode technology in roadway lighting, a new aspect of the light source is now being considered—its spectral power distribution (SPD). Broad-spectrum sources, with significant spectral output across the entire visible spectrum, potentially provide additional benefits to the driver; these light sources can provide better color information and can activate all of the photoreceptors in the eye more efficiently. This project investigates these effects and considers the potential benefits of a broad-spectrum light source.

This project is a comprehensive review of the applicability of mesopic factors to roadway-lighting applications particularly for higher speed roadways. These factors are based on the transition in the human eye from cone sensitivity to rod sensitivity and represent the potential benefit of broad-spectrum sources over traditional sources. While the model to determine the impact of mesopic adaptation to visual performance is well established and verified, both in the laboratory and in some very carefully prescribed experiments, the real-world applicability of the model has remained in question. Determining the impact of mesopic lighting on high-speed roadways is the focus of this effort.

In addition, a momentary peripheral illumination (MPI) system for highlighting pedestrians was developed and tested. The MPI system's effect on visibility may have also been affected by the overhead lighting source's SPD and level because pedestrians on the roadside might be detected in the periphery of the visual field, where mesopic effects occur.

This project was developed as a stepwise approach to the problems noted above. The first two steps were to develop a scoping experiment that defined the nature of the effect of the SPD of overhead lighting on visibility and to provide guidance for development of the subsequent experiments. The primary outcomes from this scoping experiment were that both the type and level of overhead lighting significantly affected the detection and recognition of objects on the roadway. This was also evident for objects that were off of the roadway. One of the primary determinants for detection was the color of the pedestrian clothing and the targets in the roadway, thus indicating that color contrast is a significant component of object detection. The results also indicated that roadway lighting uniformity has an important role in object detection. The final aspect was that of headlamp color and intensity. In scenarios when overhead lighting was used, headlamp configuration did not affect visibility.

These results drove the direction of the next two experiments. The first was an investigation of conditions when headlamps have an impact on object detection and when they do not. The second was the investigation of the applicability of the mesopic model to roadway lighting.

In addition to spectral experiments that were performed, an investigation of the applicability of an MPI system was conducted to determine whether a system could be developed to leverage the spectral aspects of the visual response. Although the scoping experiment showed a minimal spectral effect of headlamp color on detection distance, two headlamp colors were used to further explore this relationship of headlamp color and the MPI. A mock-up MPI system was created with servo-activated headlamps that either tracked the pedestrians as the vehicle approached or

highlighted them for a short time during which the vehicle approached. The results of this experiment were that the MPI system resulted in both shorter detection distances and an increase in detection rate. Headlamp color did not seem to have a significant impact on detection. When the MPI system highlighted an area across from a pedestrian, participants' detection rates and distances for that pedestrian were lower. This highlights the importance of careful design of a full-featured MPI system; participants' behavior indicated that they expected it to work properly, so it must not produce false positives, which could distract drivers from actual roadside hazards.

The next experiment was an investigation of the interaction of vehicle headlamps and overhead lighting on roadway-object detection. Small targets and a pedestrian were located in specific positions along the roadway that created high- and low-visibility conditions. The overhead lighting was then dimmed, and headlamps were turned off and on while participant drivers tried to detect the objects. Results indicated that the impact of the headlamps varied by object size. For most lighting levels, the overhead lighting was the dominant force driving object detection, but that was not the case when the overhead lighting was at the lowest levels. Headlamps were the driving factor for orientation-recognition distances—recognition of the direction the object was facing. The applicability of these results is critical for roadway lighting design. Headlamps dominate object recognition and also drive adaptation luminance. Therefore, the effect of the SPD of the roadway lighting may be overridden by the headlamps' effect on adaptation level and the contribution of headlamp illumination to object luminance.

The other experiment resulting from the scoping experiment considered the mesopic model. Here both static and dynamic target-detection experiments allowed the research team to evaluate the mesopic model in the field. The static portion of the experiment was performed by determining the threshold contrast for small targets, and the dynamic portion examined target detection from a moving vehicle. The results indicate that overhead-lighting level significantly affected object detection; higher adaptation levels resulted in a lower threshold contrast. The results also showed that in the dynamic experiment, higher speeds typically resulted in longer detection distances. In terms of the mesopic model, for white overhead-lighting sources, the experimental results corresponded well to the model; however, for HPS sources, they did not. One of the important aspects of the project was the consideration of the off axis or object eccentric to the line of sight. An issue with the mesopic model could be that it does not include a term for eccentricity that accounts for different retinal sensitivities at different angles. The main conclusion was that, although the mesopic model predicted some of the results at lower lighting levels, it also had limitations.

The final experiment performed did not attempt to limit driver eye glances or fix eccentricities at detection. This experiment included an MPI system, overhead lighting, two speeds, and pedestrian detection in the periphery of the visual field. The results indicate that, for pedestrians close to the roadway, there was no impact of overhead lighting's spectral distribution on detection distance. For those pedestrians, adaptation luminance was the most influential factor affecting visibility. For pedestrians farther from the roadway, spectral effects were more significant, but those results might not be applicable to roadway lighting design because objects that far away would have to be moving fairly quickly and on a collision path with the vehicle to become a hazard. The MPI performance results were similar to those of the initial MPI experiment. The MPI reduced detection distances and increased detection rates for objects in the periphery of the visual field.

The results of this experiment show that in a natural driving environment at the speeds tested, there is limited applicability of the mesopic model to lighting design. It is likely that drivers scan the roadway and detect objects in the fovea, where mesopic effects are not seen. Headlamps might also cause a higher adaptation luminance than predicted from the road luminance, further limiting the applicability of the mesopic model to lighting design for nighttime driving.

In general, the conclusions from the project are that the spectral component of the light source affects driver visual performance but only in certain conditions. The adaptation luminance of the driver is by far the dominant component of driver visual performance. The speed of the vehicle also affects the driver visual performance. In general, for high-speed roadways, it is recommended that spectral effects not be included in the design of the lighting systems. For lower speed roadways where the lighting system is predominantly for pedestrians, it is believed that spectral effects may still apply.

CHAPTER 1. INTRODUCTION

Traditional roadway lighting uses high-pressure sodium (HPS) light sources, which provide high photometric efficacy. HPS light itself, however, is amber and does not render object color correctly. With the advent of light-emitting diode (LED) technology in roadway lighting, a new aspect of the light source is now being considered by roadway lighting designers and road agencies: its spectral power distribution (SPD). Broad-spectrum sources, with significant spectral output across the entire visible spectrum, potentially provide additional benefits to the driver because these light sources can provide better color information and can activate the photoreceptors in the eye more efficiently. These benefits from broad-spectrum sources may include the ability to reduce lighting levels without sacrificing visibility, improved visual performance (speed and accuracy of performing a visual task), better object color recognition, and increased visual comfort. A model has been developed that may predict these benefits, but it has not been verified in the field.⁽¹⁾ This project investigates these effects and considers the potential benefits of a broad-spectrum light source.

In addition to investigating the application of broad-spectrum sources to overhead lighting, this project highlights a significant issue in the design and analysis of the roadway visual environment. Lighting for motorists is typically provided by two different sources: headlamps and, if warranted and installed, a fixed overhead-lighting system. These two systems are typically independent. The design of a vehicle headlamp is specified by Society for Automotive Engineering (SAE) *J1383-2010: Performance Requirements for Motor Vehicle Headlamps* and *Federal Motor Vehicle Safety Standard 108*.^(3,4) Requirements for overhead lighting are documented in the American National Standards Institute–Illuminating Engineering Society of North America RP-8 publication, with more practical specifications in the *American Association of State Highway and Transportation Officials Roadway Lighting Design Guide*.^(5,6) Another interesting issue is that jurisdiction governing these two light sources is bifurcated: the National Highway Traffic Safety Administration regulates vehicle-based systems, while State and local agencies are responsible for roadway lighting infrastructure. Because these two systems are both designed and managed separately, their interaction is rarely considered in evaluating the visible road environment. Therefore, in addition examining the spectral effects of overhead lighting, the integration of vehicle headlamps and overhead lighting and the subsequent effect on visibility was also considered in this project.

The final aspect of the project was to take advantage of the potential spectral effectiveness of broad-spectrum lighting systems and of video detection and instrumentation systems to develop an integrated approach to highlight pedestrians on the side of the roadway. Because many of the spectral differences in the eye occur in the periphery of the visual field, a broad-spectrum peripheral detection system could potentially benefit visibility to the sides of the road. A momentary peripheral illumination (MPI) system was developed and tested for this project to determine whether this adaptive lighting system benefited drivers by increasing their detecting pedestrians and animals on and along the side of the roadway. The impacts of the MPI system on driver behavior were also investigated.

PROJECT OBJECTIVES

The objectives of this project were to evaluate the following:

- Impact of the spectra of overhead-lighting systems on driver visual performance for higher speed roadways.
- Interaction of vehicle headlamps and overhead lighting in terms of object visibility.
- Applicability of mesopic models and scaling factors in a roadway lighting design.
- Impact of a peripheral illumination system on driver visual performance.

The approach for this project was multiphased. The first phase of the project involved a scoping experiment to identify the critical aspects of spectral interactions. The second phase evaluated the overall performance of the MPI system. Based on these two experiments, the subsequent phase of the project included a study of headlamp and overhead lighting interaction, and a study of the models of spectral impact of light sources. Last, an indepth study evaluated all of these factors in a single experiment.

CHAPTER 2. BACKGROUND

This literature review considers all aspects of the project that were investigated. The first aspect is roadway lighting and the overall impact of spectrum on human vision. The second component covers the mechanisms for describing visual performance and calculating the impact of lighting conditions on the detection of objects in the roadway. The third component considers mesopic models. Finally, the fourth component describes the MPI system.

IMPACT OF ROADWAY LIGHTING

Although 25-percent less travel occurs at night compared with daytime, more than 50 percent of all fatal crashes occur at night. The fatality rate (number of fatalities per 100 million vehicle-mi traveled) for drivers is three times higher at night compared with daylight conditions.⁽⁷⁻⁹⁾

Roadway lighting has long been used as a crash countermeasure, and the link between crash safety and lighting level has been established through several investigations. (See references 10–15). In the most recent study, Gibbons et al. show that there is a significant link between lighting level and crash safety based on roadway type.^(16,17) These investigations consider roadway lighting design criteria such as luminance (how much light is reflected from the roadway toward the eye of the observer) and uniformity (how evenly the light is distributed on the roadway), but none of these investigations have used the color of the light source as a design criterion.

The color of the lighting for the roadway light source has recently become a more critical issue in roadway lighting design, but as yet, it is not accounted for in lighting design criteria.⁽⁵⁾ The human eye responds to electromagnetic waves in the range of about 360 to 800 nm. This is known as the visible light spectrum. The light emitted from a light source on a wavelength-by-wavelength basis is called spectral power distribution (SPD). The SPD is a result of the physics of how the light is produced (i.e., arc tube, emission, phosphor transition, LED, etc.) and can be broadband, with emissions across all of the visible light spectrum, or narrowband, with emissions in only a small portion of the spectrum. As an example, the SPD of an HPS lamp and three types of LED sources are shown in figure 1 and figure 2. Here the HPS lamp would be classified as narrowband because it does not have significant output below 500 nm (blue), whereas the LED sources would be considered broad spectrum because they have output across the entire spectrum. The other curves in the figure, $V(\lambda)$ and $V'(\lambda)$, represent human visual response at high (daytime) illuminance levels and low (nighttime) illuminance levels, respectively.

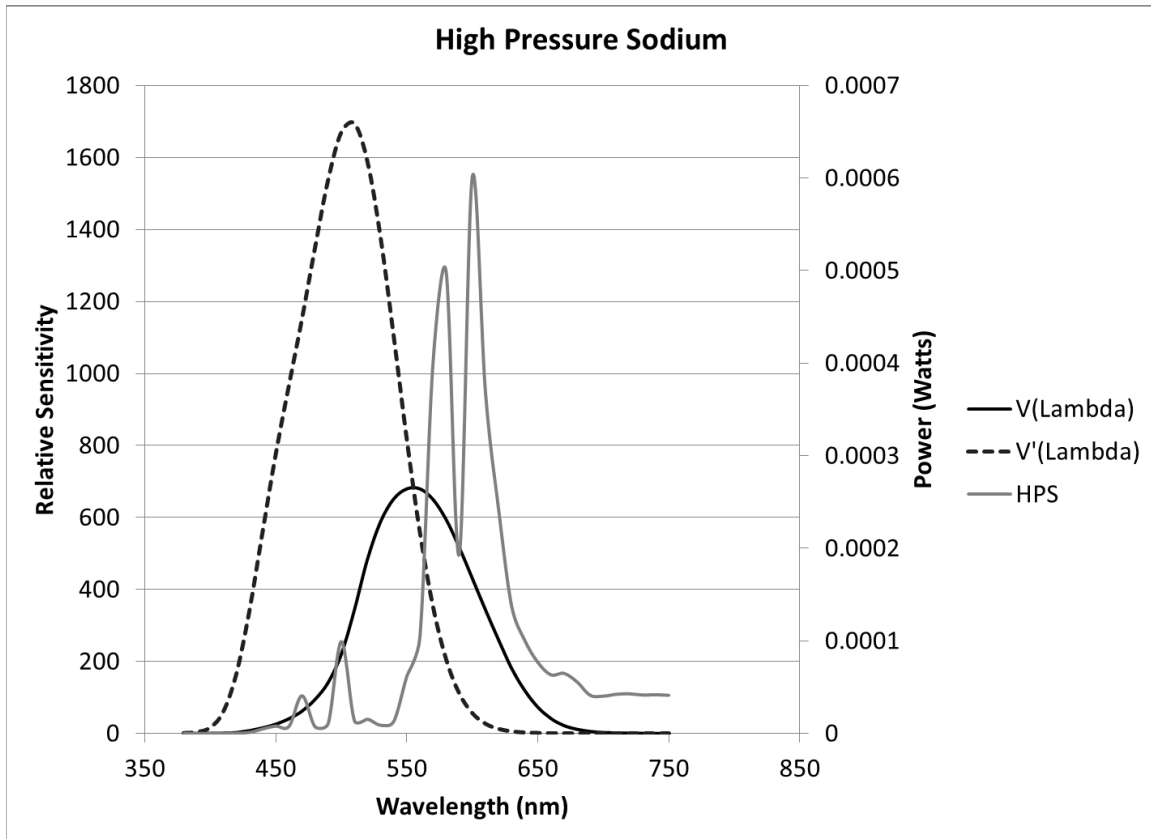


Figure 1. Graph. Spectral power distribution of HPS light sources.⁽¹⁸⁾

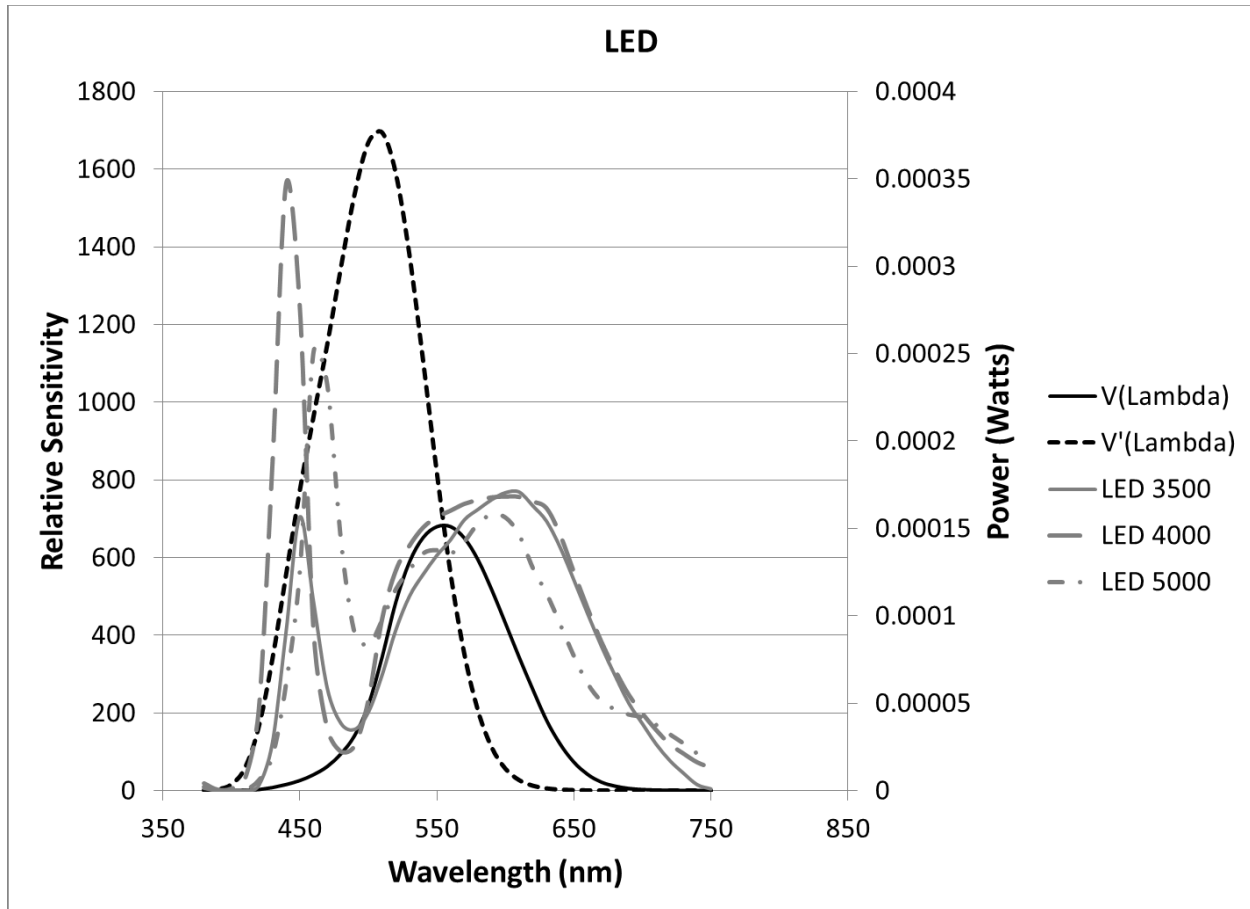


Figure 2. Graph. Spectrum power distribution of three LED light sources.⁽¹⁸⁾

Light sources have a color component typically measured in correlated color temperature (CCT) measured in Kelvin (K). The CCT is a measure of how the appearance of a light source relates to the temperature of a black body radiator. As the radiator is heated, it typically changes from appearing as yellow toward blue as the temperature rises. This color shift is shown in figure 3. Typically, light sources that are 3,000 K and higher are categorized as white sources because their output is broad spectrum, and they do not have gaps in their color output.

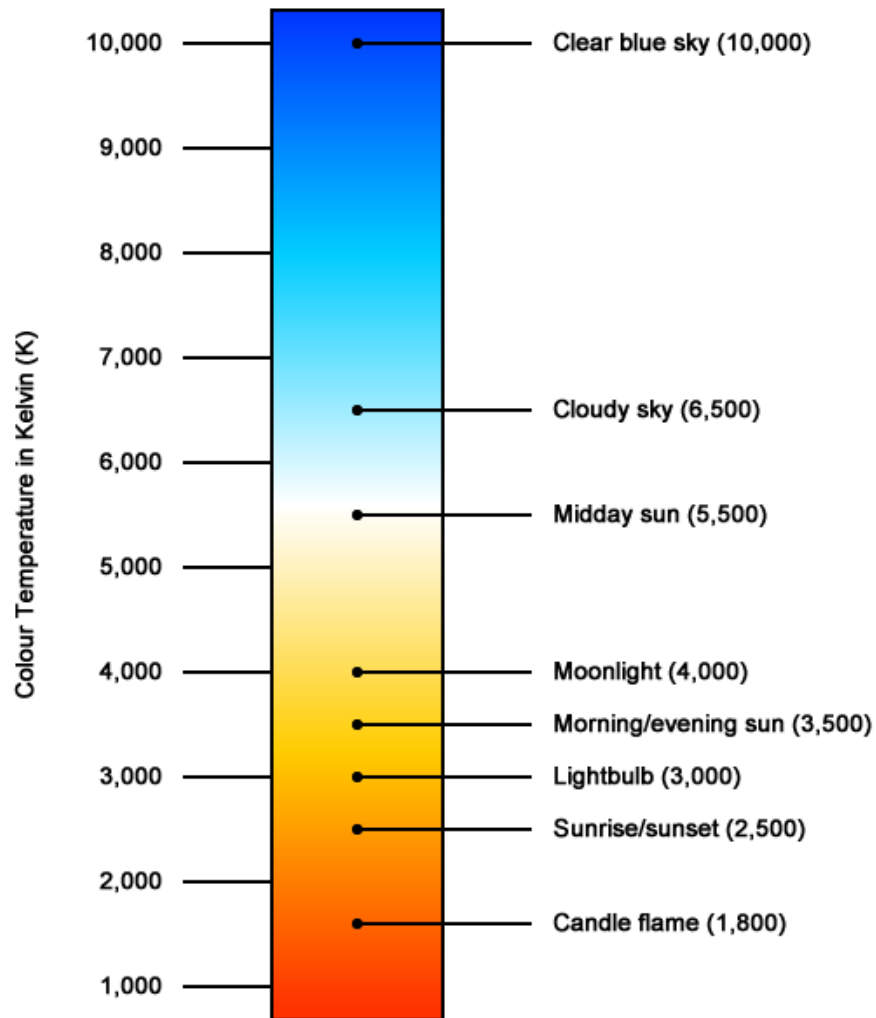


Figure 3. Diagram. Change in light source appearance with CCT.⁽¹⁸⁾

Recent research has shown a benefit of broad-spectrum light in the detection of objects along the side of a roadway when compared with traditional narrow-spectrum light sources. (See references 19–23.) The potential of this benefit is that a lower light level provides the same visual performance under broad spectrum sources as a higher light level under a narrowband source. This benefit may be a result of the responsiveness of the human eye to lower levels of light (mesopic vision issues), or it may be a result of color information provided by the light source in the visual application. The potential for having similar visual performance with reduced lighting levels translates directly to reduced energy costs while maintaining driver safety. The magnitude of this benefit in an actual driving environment, as well as its relationship to the spectral character of the light source, is unknown.

Color

Shaflik detailed differing light types, their colors, and the issues with these light types.⁽²⁴⁾ Table 1 is derived from this information. Shaflik notes that blue and white light sources are more preferred by the general public, but town planners and astronomers resist them because of light

trespass and light pollution issues. From Shaflik's review, most blue and white light sources tend to be more energy-inefficient than HPS light sources, which lack color-rendering capabilities and are less preferred by motorists. It should be noted that Shaflik's review was in 1997, before the advent of high-power LED sources, and he does not consider them in his review.

Table 1. Light type, color, and problems (from Shaflik, 1997).⁽²⁴⁾

Light Type	Color	Problem
Mercury vapor	Blue-white	Energy inefficient
Metal halide	White	Lower efficiency, upward sky glow
High-pressure sodium	Amber-pink	Poor color rendition
Low pressure sodium	Amber-orange	Very poor color rendition

Terry and Gibbons compared two LED luminaires of 3,500- and 6,000-K correlated color temperature to a 4,200-K fluorescent luminaire for the detection and color recognition of small targets and pedestrians.⁽²⁵⁾ Pedestrians were clad in two different colors, and the small targets were painted four different colors. Their results were mixed. The 3,500- and 6,000-K sources were nearly equal in terms of target color recognition distance; however, the 6,000-K luminaires outperformed the 3,500-K luminaires in pedestrian clothing color recognition distance by nearly 30 percent. The 4,200-K fluorescent light outperformed both LEDs for small target color recognition, but for pedestrian clothing color recognition, the 4,200-K fluorescent light was found to be equal to the 3,500-K LED. When considering both detection distance and color recognition distance, the authors suggested that the 6,000-K LED might be the superior light type for rendering color. The differences in color recognition between small targets and pedestrians were likely a result of the chosen colors for each: pedestrians wore black or denim scrubs, while targets were red, blue, gray, or green.

MESOPIC EFFECTS AT NIGHT FOR DRIVERS

The nature of the lighting conditions for a nighttime driver can define how the spectral output from a light source affects the driver's vision. Eye performance changes based on the ambient light level surrounding the driver. This process is typically called dark adaptation and represents both changes in overall sensitivity as well as the spectral response of the eye. The dark adaptation process represents the transition between the two types of photoreceptors in the retina: the rod and cone systems.

At high light levels, where visual field luminances are in excess of approximately 3.4 cd/m^2 (.99 fL) (about early twilight level) conditions are considered to be photopic, and human eye response follows a curve known as $V(\lambda)$. When the light level is very low (well below moonlight levels, less than 0.001 cd/m^2 (0.0003 fL)), the conditions are described as scotopic. Conditions between these two levels are referred to as mesopic, which is typically where roadway lighting levels fall. In the mesopic range, both rods and cones are active, and visual sensitivity is a combination of the two sensitivity functions. $1 \text{ cd/m}^2 = 0.3 \text{ fL}$

Figure 4 illustrates these ranges.⁽²⁶⁾ This figure also illustrates typical recommended street and roadway lighting levels, in terms of averages and minima, for Illuminating Engineering Society of North America and Commission Internationale d'Eclairage (CIE) practice.^(1,26) Lighting levels

for security are generally in the same range or lower and are usually specified in terms of illuminance.

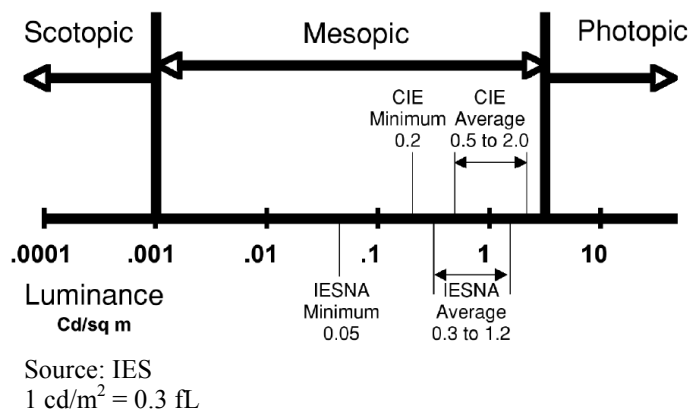


Figure 4. Diagram. Ranges of visual sensitivity.⁽¹⁸⁾

The spectral response of the eye is also a result of the cone/rod transition. The spectral response of the cone system, active at high lighting levels, corresponds to the photopic $V(\lambda)$ sensitivity curve, which peaks at 555 nm. The spectral response of the rod system, active at low lighting levels, corresponds to the scotopic $V'(\lambda)$ sensitivity curve, which peaks at 507 nm. Thus, at the transition between photopic and scotopic lighting levels during dark adaptation, the eye's maximum sensitivity changes from green in photopic conditions to blue-green in scotopic conditions. This effect—the well-known Purkinje shift, where the eye's sensitivity shifts from longer to shorter wavelengths—has been known for more than a century.

One of the difficulties with this spectral change is that it unevenly affects the retina. It is based on the relative densities of the rods and cones and receptor areas across the retina. In the retinal periphery, the rod-dominated receptive fields outweigh the cone-dominated fields, which creates a stronger mesopic effect in that portion of the visual field. In the fovea centralis, the central portion of the retina that provides maximum visual resolution, and at adaptation levels sufficient to stimulate the small cone-dominated receptive fields, there is no rod contribution, which means there is no mesopic impact in this region. Therefore, because the mesopic effect varies across the retina, care must be taken in the design and application of an experiment to provide visual tasks that are both fovea based and periphery based.

One of the important aspects of this effect of dark adaptation is that the specifications for light outputs of light sources are determined using the photopic $V(\lambda)$ curve. This means that all luminaires are characterized photopically, but their implementation in the roadway environment is mesopic, where the photopic curve does not accurately indicate their visual effect. However, the extent of any deviations between the photopic and mesopic conditions depends on the actual luminance levels and viewing conditions in the roadway.

Models of Mesopic Vision

To evaluate lighting systems in the mesopic adaptation range, a model of the sensitivity of the eye during the change from photopic into mesopic lighting conditions was established.

The luminous efficiency function, $V(\lambda)$, is based on data collected in 1922–23 and was adopted in 1924 by the CIE for a central visual angle of 2 degrees.⁽²⁷⁾ It is the basis of most lighting measurements, as well as for manufacturer descriptions of a light source's output. Other luminous efficiency functions are $V_{10}(\lambda)$, the photopic luminous efficiency function for a visual angle of 10 degrees, and $V'(\lambda)$, the scotopic luminous efficiency function, derived from data acquired at a visual angle of approximately 10 degrees.⁽²⁷⁾ The ratio of the lamp's scotopic output to its photopic output (S/P) is calculated using $V(\lambda)$ and $V'(\lambda)$, and describes the SPD of a light source in mesopic conditions. The models suggest that the higher a lamp's S/P ratio, the better its light is for peripheral detection in the mesopic region.^(28,29)

For nighttime driving, in the mesopic vision region, $V(\lambda)$ remains fairly accurate for foveal detection but does not describe the eye's behavior for the kind of off-axis vision commonly used in driving. A number of models using various combinations of the photopic and scotopic luminous efficiency functions have been developed in an effort to better describe mesopic vision. The models discussed here fall into two broad groups, based on how the data to create them were collected: brightness-matching models and performance-based models.

Any mesopic model that is to be implemented as a model of photometry must meet two basic requirements. First, the model should obey Abney's Law of additivity, that the luminance of the light source is equal to the sum of its comprised wavelengths, which is a fundamental law of photometry. The second constraint is that the mesopic spectral sensitivity function should be the same as the photopic spectral sensitivity function, $V(\lambda)$, at the upper end of the mesopic region, and also should be the same as the scotopic spectral sensitivity function, $V'(\lambda)$, at the lower end of the mesopic region.

Brightness Matching

To develop a function for mesopic luminous efficiency, a number of researchers had participants view two adjacent semicircles of light and match them for brightness. The lower section was either white light or 570 nm, and the top section was light of varying wavelengths throughout the spectrum.^(30–32) Observers identified the point when the two semicircles appeared equally bright; researchers then measured their comparative radiances to develop the luminous efficiency function. The resulting functions describe the mesopic luminosity of a light source as a linear relationship between the log of the mesopic luminous efficiency function and the sum of the photopic and scotopic luminous efficiency functions, each weighted by a factor that describes where in the mesopic region the test occurred. (See references 30, 32, 33, and 34.) Additional brightness-matching functions include contributions of the different types of cones.⁽³⁵⁾

Brightness-matching functions accurately describe monochromatic light sources in the mesopic region. However, they are inaccurate when describing multichromatic sources such as roadway lighting. This is because humans perceive narrow-bandwidth saturated colors as brighter than other colors. Thus, two saturated colors together appear less bright than the sum of the

constituent colors' brightness, a phenomenon known as the Helmholtz-Kohlrausch effect.⁽³⁵⁾ Brightness matching is performed with narrow-bandwidth stimuli, so the resulting luminous efficiency function applies to those stimuli—but not multichromatic sources, which will appear dimmer than would be predicted by brightness-matching luminous efficiency functions.

The main problem with using brightness-matching models as a basis for photometry is that they tend to violate Abney's law of additivity. This is because they account for interactions between chromatic and achromatic channels of the visual system, which are nonlinear in nature, thereby resulting in nonadditive models.

Performance-Based Models

X-Model:

In an effort to correct for problems with brightness-matching functions and to collect data on visual perception in a context more similar to driving, the X-model was developed using data collected with the binocular simultaneity method (BSM). The researchers' goal was to create an easy-to-use model of mesopic vision, grounded in human vision, that does not suffer from additivity problems, using the familiar luminous efficiency functions $V(\lambda)$ and $V'(\lambda)$.⁽³⁶⁾

In the BSM, participants view two stimuli, one for each eye, against two backgrounds set to the same adaptation level. Superimposed on the backgrounds are a reference stimulus at 589 nm at a reference radiance level for one eye and a test stimulus of varying wavelengths and radiances for the other eye. The stimuli are arranged so that, when using binocular vision, they appear 12 degrees off-axis, one on top of the other. The experimenters flash the stimuli and adjust the radiance of the test stimulus until the participant sees the two stimuli appear at the same time. Using this method, the experimenters can measure the comparative radiances needed to detect the two stimuli simultaneously. From these results, luminous efficiency for the stimuli for a number of background adaptation levels can be measured.⁽²⁷⁾

The resulting mesopic luminous efficiency function requires an iterative process to calculate the mesopic luminous intensity of a source with respect to the $V_{10}(\lambda)$ and $V'(\lambda)$ functions and the adaptation level (X) in the mesopic range. Detection time does not suffer from the same bias toward saturated colors that brightness matching does; the function is additive and can describe multichromatic light sources.^(28,36) One major criticism of the X-model is that it was developed using data from a very limited number of participants.

Mesopic Optimization of Visual Efficiency (MOVE) Model:

Like the creators of the X-model, the researchers who developed the MOVE model wanted a practical model for mesopic vision designed with realistic nighttime driving in mind and based on the existing luminous efficiency functions. They defined a set of common experimental parameters and, as a consortium, conducted a large number of experiments based on contrast detection threshold, reaction time, and target recognition.^(35,37)

Like the X-model, the resulting luminous efficiency function uses $V'(\lambda)$ and x , a factor defining the adaption of the eye—the region in the mesopic range where luminous efficiency is calculated. Unlike the X-model, it uses $V(\lambda)$ and not $V_{10}(\lambda)$, because the researchers found that

differences between the two were small, and using the more-common $V(\lambda)$ was more practical.^(37,38) The MOVE model also incorporates the S/P ratio of the light sources, and the luminance and spectrum of the background.⁽³⁸⁾ The MOVE model accurately predicted luminous efficiency for both off-axis tasks and tasks with multichromatic light but did not accurately predict luminous efficiency for narrow-bandwidth targets or on-axis tasks with monochromatic light at 0.01 cd/m^2 (0.03 fL). These latter conditions are rarely encountered in nighttime driving.⁽³⁷⁾

Problems With Models of Mesopic Vision:

Lighting designers have criticized both the X-model and the MOVE model for incorrectly placing the transition point from mesopic to photopic ranges. For the X-model, the transition occurs at 0.6 cd/m^2 (0.18 fL); in the MOVE model, it falls at 10 cd/m^2 (2.9 fL). In practice, many lighting experts assume it falls somewhere in between.⁽³⁹⁾ Therefore, Viikari and Ekrias decided to test those models, alongside a modified version of the MOVE model with a transition at 5 cd/m^2 (1.5 fL), using data from three previous experiments.⁽³⁹⁾ They found the modified MOVE model was the most accurate in predicting the experimental results in 9 of 17 test cases. The original MOVE model was the most accurate in another seven cases, and the X-model was the most accurate in one case. The fact that no single model stood apart as predicting performance under all conditions indicates that more research is needed.

Another example of mixed results using different models of mesopic vision stemmed from research on lighting type and level and pedestrian visibility.⁽⁴⁰⁾ Results indicated HPS lighting outperformed metal halide (MH) lighting for a black-clad pedestrian but not for a blue-clad pedestrian. The pedestrians were likely detected foveally (where $V(\lambda)$ accurately predicts performance), so mesopic effects, including the benefit of broader-spectrum sources, would not be as obvious. Experiments testing off-axis detection are more likely to produce mesopic effects.

Raphael and Leibenfer used a projector-based simulator to project a roadway and targets at 2, 6, 10, and 14 degrees off-axis with a range of background luminances and target contrasts.⁽⁴¹⁾ They found that for targets near the fovea, $V(\lambda)$ more accurately predicted the threshold contrast than mesopic models (including the X-model and the MOVE model), but for the 10- and 14-degree targets, the mesopic models predicted the contrast threshold better than photopic luminance.

***CIE Recommended System for Mesopic Photometry Based on Visual Performance:*⁽¹⁾**

Because in some aspects both the X-model and the MOVE-model can be considered to represent two extreme ends of a single system, the *CIE Recommended System for Mesopic Photometry Based on Visual Performance* adopted an intermediate system that operates in a region between the X-model and the MOVE model.⁽¹⁾ The objective of the recommended system was not only to make it widely applicable but also to increase the weight given to achromatic tasks. Two intermediate models were considered, with upper and lower luminance limits of 3 cd/m^2 (0.88 fL) – 0.01 cd/m^2 (0.003 fL) and 5 cd/m^2 (1.5 fL) – 0.005 cd/m^2 (0.00015 fL), respectively. After extensive testing, CIE recommended the intermediate system with an upper luminance limit of 5 cd/m^2 (1.5 fL) and lower luminance limit of 0.005 cd/m^2 (0.00015 fL) as the recommended system for mesopic photometry. It takes the form shown in figure 5.

$$M(m)V_{mes}(\lambda) = mV(\lambda) + (1 - m)V(\lambda) \text{ for } 0 \leq m \leq 1$$

$$\text{and } L_{mes} = \frac{683}{V_{mes}(\lambda)} \int V_{mes}(\lambda) L_e(\lambda) d\lambda$$

Figure 5. Equation. CIE formula for calculating mesopic spectral sensitivity.

Where:

$M(x)$ = A normalizing function such that $V_{mes}(\lambda)$ attains a maximum value of 1.

$V_{mes}(\lambda_0)$ = Value of $V_{mes}(\lambda)$ at 555 nm.

L_{mes} = Mesopic luminance.

$L_e(\lambda)$ = Spectral radiance in $\text{W}\cdot\text{m}^{-2}\cdot\text{sr}^{-1}\cdot\text{nm}^{-1}$.

if $L_{mes} \geq 5.0 \text{ cd}\cdot\text{m}^{-2}$, then $m = 1$.

if $L_{mes} \leq 0.0005 \text{ cd}\cdot\text{m}^{-2}$, then $m = 0$.

if $0.005 \text{ cd}\cdot\text{m}^{-2} < L_{mes} < 5 \text{ cd}\cdot\text{m}^{-2}$ then $m = 0.3334 \cdot \log L_{mes} + 0.767$.

It should be noted that the recommended system does not correlate well with visual performance when recognition of color is important, when the target has a very narrow SPD, or when assessing brightness in the mesopic region.

Applying Models of Mesopic Vision to Roadway Lighting

Most nighttime driving occurs in the mesopic region, where the eye is more sensitive to blue light than photopic luminance, the standard for lighting design, would predict.^(28,38) Because they are more efficient, broad-spectrum sources can be dimmer—consuming less energy while providing the same safety benefit—so those results are promising for energy savings. However, models of mesopic vision incorporated into CIE *Recommended System for Mesopic Photometry Based on Visual Performance*, including the MOVE model, were produced using laboratory data and must be further validated in roadway conditions before they can be fully applied to roadway lighting design.⁽¹⁾ Furthermore, broader-spectrum sources might be more efficient because they provide color information, or because they are better suited to mesopic vision. Experiments investigating mesopic vision and roadway lighting are described here and are the foundation for the work performed in this project.

X-Model Testing:

As part of the team that created the X-model, Bullough and Rea described a number of studies examining roadway lighting.⁽²⁸⁾ A test-track study found that reaction times with MH lighting were shorter than those with HPS lighting for peripheral targets, that headlamps had no effect on target detection for targets 15 and 23 degrees off-axis, and that glare reduced reaction time.⁽⁴²⁾ Another study, using a roadway lighting simulation with MH lamps (S/P ratio = 1.63) and HPS lamps (S/P ratio = 0.64), found that for foveal-target detection, participants had similar reaction times with the two lighting types.⁽⁴³⁾ However, for off-axis detection, reaction times with HPS lighting were slower than those for MH lighting, especially at lower light levels. To obtain similar reaction times, the HPS lighting had to be about 10 times as bright as the MH lighting, a ratio far greater than the ratio of S/P ratios of the lighting types ($1.63:0.64 \approx 2.5:1$) would predict. Therefore, a comparison of the $V(\lambda)$ and $V'(\lambda)$ functions, on which S/P ratios are based,

does not describe visual performance for off-axis detection in the mesopic range.⁽⁴³⁾ Two simulator studies found that HPS lighting needed to be much brighter than MH lighting, and brighter than the ratio of S/P ratios would suggest, to get the same target-detection performance.^(44,45) Bullough and Rea concluded that, while photopic models accurately predict foveal detection and driving performance in the mesopic range for multiple lighting types, the S/P ratios underestimate MH performance for peripheral object detection—an important task in driving—and that the X-model is more accurate than using $V(\lambda)$ and $V'(\lambda)$ alone.⁽²⁸⁾ They recommended that roadway lighting should be designed with peripheral tasks in mind and to take a systems approach that accounts for headlamps, roadway lighting, and the cognitive demands of nighttime. Research into energy savings has acknowledged the importance of more accurate models of mesopic vision and recommends using MH lighting over HPS lighting based on the X-model and to use the newer models of mesopic visual performance.^(46,47)

MOVE Model Testing:

The MOVE model has also been applied to roadway lighting. Eloholma and Halonen measured the photopic luminance of HPS and MH lighting with identical wattages and took background luminance measurements for selected areas of the roadway.⁽³⁸⁾ They found that the photopic luminance of MH lighting was lower than its MOVE-calculated mesopic luminance and that the photopic luminance of HPS lighting was higher than its MOVE-calculated mesopic luminance. The result was similar to that of the X-model testing: MH lighting performed better than HPS lighting in the mesopic range—more so than predicted by their S/P ratios alone—and MH lighting is more efficient than HPS lighting in the mesopic range.⁽³⁸⁾ Other experiments showed that both MH and LED lighting enable better roadside object detection than more common narrow-spectrum sources, like HPS lighting. (See references 19, 20, 22, and 23.)

LIGHTING AND THE DRIVING ENVIRONMENT

As discussed previously, roadways are illuminated for nighttime driving with vehicle headlights and, on many roads, with overhead roadway lights. These different light sources have a combinative effect on roadway visibility. Several components affect this visibility in the roadway, as discussed in the following subsections.

Visual Acuity

Driving involves object detection, which in turn relies on detection of motion, luminance contrast, and color contrast. Some aspects of driving require higher acuity, such as reading signs or differentiating between similar objects. Object detection and categorization affects driver behavior; the difference between a tire tread and a pothole, or a pedestrian and a fixed structure, or a small animal and highway debris, are all significant in terms of driver reaction. Other aspects of driving, such as maintaining lane position, instead rely on peripheral vision and can be accomplished with lower acuity.

For nighttime driving, the lack of understanding of mesopic vision's effect on visual acuity makes it difficult to predict driver's visual behavior. Predicting this behavior at night is further complicated by changing lighting conditions as drivers pass under and away from roadway lighting fixtures and by glare from both luminaires and the headlamps of oncoming vehicles.

This study examines visual behavior on a road with overhead lighting while driving a vehicle with headlamps.

Age Effects on Vision and Driving

As drivers' eye age, changes occur in the optical density (OD) of the eye's crystalline lens. With age, the lens becomes more yellow, reducing older persons' ability to see color and color contrast.⁽⁴⁸⁾ Contrast contributes more to visibility than any other factor, so contrast sensitivity significantly affects hazard perception. That impact has been measured in driving studies; for example, in a study of older drivers, those with cataracts and poor contrast sensitivity had slower response times to traffic conflicts.⁽⁴⁹⁾ Another study measured the response time of younger and older drivers to roadside objects. Elderly participants were often surprised by the objects regardless of the lighting level, but younger participants identified the objects and avoided them.⁽⁵⁰⁾ The authors hypothesized that the age-related decrease in target detection was likely a result of diminished visual systems in older drivers, including diminished contrast sensitivity.

Aging affects older drivers' response times and ability to steer, which may also be related to visual behavior. In a study by Wood et al., older drivers detected and recognized only 59 percent of pedestrians, whereas younger drivers recognized 94 percent of pedestrians.⁽⁵¹⁾ Older drivers also recognized pedestrians much later than did younger drivers.⁽⁵¹⁾ Another study found that older drivers' steering accuracy in low-luminance settings was poorer than that of younger drivers.⁽⁵²⁾ However, Owens and Wood found that older drivers tended to drive more cautiously in low light than did younger drivers, showing they might be aware of, and compensating for, poorer vision.⁽⁵⁰⁾

Despite the possibility that older drivers compensate for poorer vision, older drivers (ages 55+) comprised 16 percent of nighttime crash fatalities and nearly 25 percent of all crash-related fatalities, day and night.⁽⁵³⁾ Understanding how aging affects visual behavior, especially in mesopic night driving conditions, could increase traffic safety and reduce fatalities like those above. This study adds to that understanding.

Visibility and Contrast

Roadway and roadway-lighting design address increasing the visibility of roads and roadway objects to drivers. Contrast is a key component of visibility because the amount of contrast an object has is often directly related to how well it can be seen. There are two different types of contrast: luminance contrast, the comparative brightness of objects irrespective of color; and color contrast, the comparative difference in color between objects of the same or different luminances.

Contrast is directly related to visibility in static environments: the higher an object's contrast, the more visible it is. However, because driving is dynamic—with overhead luminaires, moving headlamps, and potentially moving roadside objects—factors affecting visibility other than luminance contrast might come into play. Two of those factors, roadway and headlamp lighting, are investigated in this study and discussed in following sections.

When driving at night and using mesopic vision, a motorist's ability to discern color varies with the amount of light available. Because the effect of color-contrast measurements on overall

visibility changes with differing ambient lighting and vision conditions, most researchers measure luminance contrast, not color contrast, in night-driving studies.

Luminance Difference Thresholds

One of the key components of evaluating contrast is a model that quantifies the visibility of targets using the luminance difference threshold.⁽⁵⁴⁾ The calculation model uses variables that include target size, contrast, observer age, exposure time, eccentricity angle, adaptation, and distance to determine the visibility level (VL) of the target. A luminance difference (ΔL) is the difference between the luminance of a background and a target. A luminance difference threshold is the luminance difference at which the target is just perceived with a probability of 99.93 percent (ΔL_{th}), the formula for which is shown in Figure 6:

$$\Delta L = 2.6 \left(\frac{\phi^{\frac{1}{2}}}{\alpha} + L^{\frac{1}{2}} \right)^2 F_{CP} \frac{a(L_b, \alpha) + t}{t} AF$$

Figure 6. Equation. Luminance difference threshold.

Where:

ΔL = Threshold luminance difference.

L_b = Background luminance.

α is the target size in minutes of arc FCP is the Contrast Polarity Factor.

t = Observation time.

AF = Age factor.

ϕ and L are models of Ricco and Weber's Law.

VL is a term introduced by Blackwell to better describe the level luminance difference must reach for a target to be rendered conspicuous. The formula for calculating VL is given in figure 7^(54,55):

$$VL = \frac{\Delta L_{actual}}{\Delta L_{threshold}}$$

Figure 7. Equation. VL formula.

Where:

ΔL_{actual} = Luminance difference between the target and the background

$\Delta L_{Threshold}$ = Calculated luminance difference from the equation in figure 6.

Luminance contrast is the degree to which the luminance of a target distinguishes itself from the background luminance. The Weber contrast formula is commonly used because it accounts for contrast polarity. Positive contrast occurs when a light target is against a darker background; negative contrast occurs when a dark target is against a lighter background. Higher contrasts or high luminance differences do not always correlate with increased visibility. Therefore, by

incorporating the variables included in the VL calculation, visibility becomes possible to quantify. The Weber contrast formula (figure 8) requires target luminance (L_t) and background luminance (L_b):

$$\text{Weber Contrast} = \frac{L_t - L_b}{L_b}$$

Figure 8. Equation. Formula for calculating Weber contrast.

VL expresses how much a target's luminance exceeds the perception threshold and is a function of adaptation luminance. As cited by Adrian, VL values of 10 to 20 are considered to be safe traffic conditions.⁽⁵⁴⁾ The following sections describe the variables used for calculation in the VL model and how they are determined.

Size (Visual Angle)

The visibility calculation considers the size of the target in the viewer's visual field. A target can be as small as the wooden targets used in this project or as large as a pedestrian. Visual angle is used to describe object size because relative size in the visual field changes with distance from the object; the closer the object, the larger the visual angle.

The visual angle (α) can be calculated from the object's size, S , and its distance from the eye, D , from the viewer, as described in figure 9.

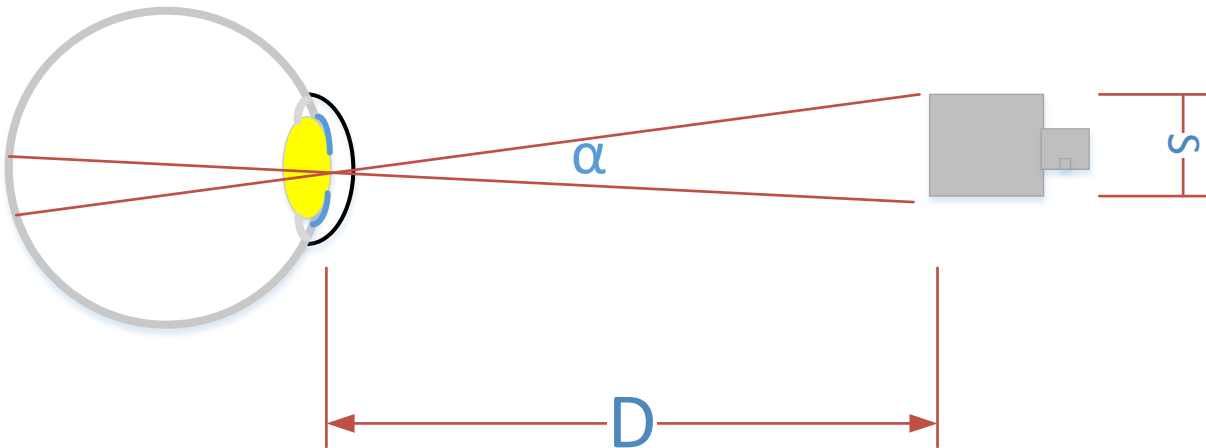


Figure 9. Diagram. Variables for calculating visual angle.

For small visual angles, such as the ones encountered when detecting the presence of small wooden targets on the roadside, the formula in figure 10 is used. To convert the visual angle from degrees to minutes of arc (MOA), α is multiplied by 60.

$$\alpha = \tan^{-1} \frac{S}{2D}$$

Figure 10. Equation. Formula for visual angle in degrees.

Contrast Polarity Factor

The contrast polarity factor (F_{CP}), is a phenomenon explained by Aulhorn in 1964 as cited by Adrian.⁽⁵⁴⁾ Two figures with equal minimum luminance differences but different polarities, positive or negative, are not perceived the same way. A dark target on a light background (negative contrast) is detected sooner and with more distinguishable detail than is a light target on a dark background (positive contrast) with the same absolute value of minimum luminance difference. The luminance difference threshold for a target in negative contrast, ΔL_{neg} , is calculated by multiplying the positive contrast, ΔL_{pos} , by the contrast polarity factor, F_{CP} , as described by the equation in figure 11.

$$\Delta L_{neg} = \Delta L_{pos} F_{CP}$$

Figure 11. Equation. Calculation for negative contrast threshold.

The magnitude of the difference between the minimum positive and negative contrasts, F_{CP} , required for object detection depends on the background and target size, as described by the equations in figure 12.

$$F_{CP}(\alpha, L_b) = 1 - \frac{m\alpha^{-\beta}}{2.4\Delta L_{pos} \text{ } t=2}$$

For $L_b \geq 0.1 \text{ cd/m}^2$:

$$m = 10^{-10 - (.0125 (\log L_b + 1)^2 + 0.0245)}$$

For all L_b :

$$\beta = 0.6L^{-0.1488}$$

Figure 12. Equation. Calculation of the contrast polarity factor.

Exposure Time

The model for visibility incorporates the increment of time that an observer views a target. For viewing times shorter than 0.2 s, a greater luminance difference threshold is needed for object detection. Typically a glance duration of 0.2 s is most commonly used for design criteria.⁽⁵⁴⁾

Age Factor

Age is a critical factor in the visual perception of objects, especially in low light settings such as nighttime driving. As discussed above, the crystalline lens of the eye begins to yellow with increased age, limiting the amount and color of light entering the eye.⁽⁵⁶⁻⁵⁸⁾ Adrian's model accounts for age with two different age-factor calculations for two age groups: one for ages 23 to 64 and another for ages 64 to 75. The small target visibility model uses the following equations for the age groups listed in figure 13 and figure 14.

$$AF = \frac{(Age + 19)^2}{2160} + 0.99$$

Figure 13. Equation. Age factor calculation for younger age group (23 to 64 years).

$$AF = \frac{(Age - 56.6)^2}{116.3} + 1.43$$

Figure 14. Equation. Age factor calculation for older age group (64 to 75 years).

Transient Adaptation

Transient adaptation occurs when the eyes are in the process of adapting and have not established a steady state of adaptation. This adaptation process has two speeds: a quick neural process related to the photoreceptors and a slower physical process occurring when the pupil expands and constricts to adjust to the amount of light in the environment. During nighttime driving, light-level changes occur when a vehicle passes under and then beyond overhead-lighting fixtures, when the road surface and its reflectivity change, and when oncoming vehicles with headlamps approach. Adaptation typically occurs very quickly; however, if drivers' eyes do not sufficiently adapt to the ambient lighting, their ability to detect contrast can be negatively affected.⁽⁵⁹⁾ Age can also negatively affect transient adaptation. The model for calculating VL with luminance threshold difference includes transient adaptation as an element of overall target visibility.

Eccentricity

Eccentricity is defined as the angle, measured in degrees, along the horizontal axis of the visual field. Studies have shown that contrast sensitivity depends on several factors, including target size, eccentricity of the target, and the background luminance of the visual field. Increases in eccentricity are associated with increase in contrast threshold for targets of same size and background luminance.⁽⁶⁰⁾

MOMENTARY PERIPHERAL ILLUMINATORS

In 2009, approximately 4,872 non-motor vehicle occupants (pedestrians, bicyclists, etc.) were fatally injured, and about 85 percent of those were pedestrians.⁽⁶¹⁾ About 56 percent of the crashes occurred in rural areas, and 83 percent occurred where the speed limit was greater than 72 km/h (45 mi/h). It is likely that the absence of crosswalks, sidewalks, or shoulders on rural high-speed roads contributed to those crash fatalities.⁽⁶¹⁾ In addition, approximately 51 percent of fatal pedestrian crashes occurred at dawn, dusk, or at night,⁽⁶¹⁾ when visibility is more of an issue; most pedestrian crashes occur because vehicle drivers fail to see the pedestrians. Therefore, technology that helps drivers to see pedestrians on dark rural roads could contribute significantly to pedestrian safety.

An MPI system incorporates vehicle-based sensors that detect pedestrians with servo-actuated headlamps that pivot to highlight them, thus directing a driver's attention to pedestrians. This section discusses a theoretical MPI system and its components, and proposes design criteria to ensure such a system is effective and successful.

Problems Detecting Pedestrians at Night

In the design of an MPI system, the following must be considered to establish the required specifications. Similarly, the experimental evaluation must account for these roadway visibility issues.

Peripheral Detection

When driving at night, drivers focus on the center of the roadway. However, pedestrians usually walk on the side of the road, where drivers must use peripheral vision to detect them. One of the limiting performance factors for the visibility of objects on the side of the road is that the human eye has low peripheral sensitivity and visual acuity; the eye's sensitivity decreases as the object is detected farther away from the fovea.⁽¹⁸⁾ Some research has found visual sensitivity plateaus between 8 and 30 degrees; other research in peripheral visibility found that target detection decreased with increasing angle, dropping off rapidly beyond 15 degrees. (See references 62–65.) In a road test, more than 80 percent of targets were not detected at a peripheral viewing angle of 17.5 degrees.⁽⁶⁶⁾ In all cases, peripheral object detection is poor, especially at greater angles. Motion of the object may help; however, most objects' movement in the visual field is much slower than the flow of objects due to the motion of the vehicle. In addition, during nighttime driving, peripheral vision is mesopic, where the eye's sensitivity to colors shifts toward blue as the environment's luminance decreases (see Impact of Roadway Lighting section above), making accurately modeling visual performance problematic (see Models of Mesopic Vision section).

Headlamps

Headlamps are designed to help drivers see down the road and to minimize glare to oncoming traffic. Illuminating the oncoming lane causes glare to oncoming traffic, so headlamps are aimed to illuminate the roadway ahead of the vehicle and the right-hand side of the roadway.⁽¹⁸⁾ Figure 15 shows a headlamp beam's center, marked by "X," and the beam pattern resulting from aiming the headlamp for the lower right-hand quadrant. Pedestrians usually appear in the lower left-hand and the upper right-hand quadrants, where the beam intensity tapers off.⁽¹⁸⁾ If a car is far enough away from a pedestrian, the driver might use foveal vision to detect them, but vehicle headlamps might not illuminate the roadway to that distance. Therefore, by the time the headlamps illuminate a pedestrian, he or she is likely on the periphery of the visual field, making him or her difficult to see, and the driver may be too close to avoid a collision. This problem is compounded by roadside objects adding visual clutter and/or occluding the view of pedestrians.

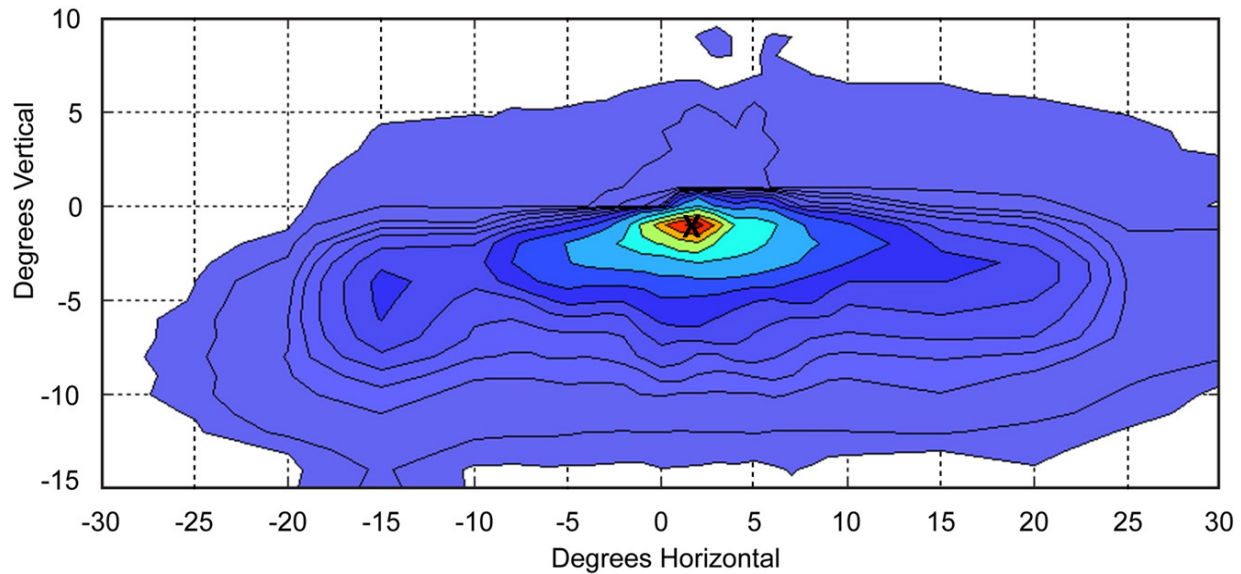


Figure 15. Graph. Headlamp beam pattern.⁽¹⁸⁾

One additional problem with headlamp design with respect to pedestrian detection is that drivers detect pedestrians using the contrast created when headlamps illuminate pedestrians against the background.⁽¹⁸⁾ However, by design, headlamps are aimed low, illuminating both the pedestrian's legs and the ground immediately surrounding them, thus decreasing contrast and hindering detection.⁽¹⁸⁾ Increasing headlamp power mitigates that problem but increases glare to oncoming vehicles.

Headlamp Technologies

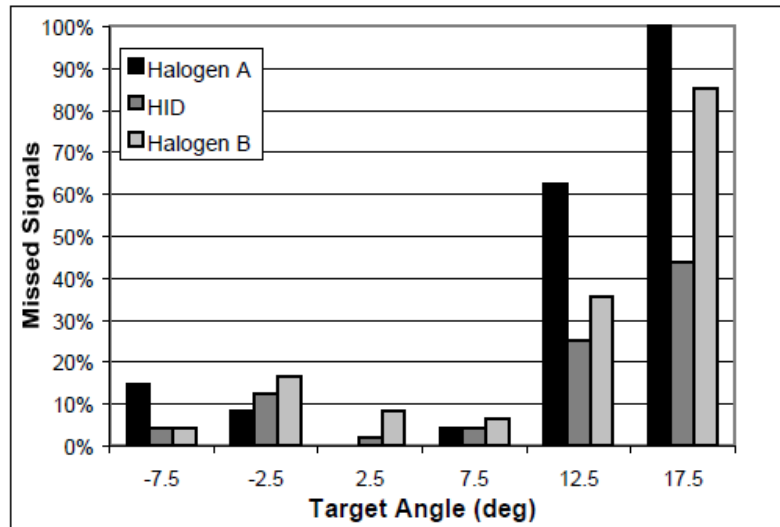
The headlamp system for the MPI system has two points of consideration: headlamp type and headlamp behavior.

Headlamp Type

During low lighting conditions, the headlamp should have an SPD efficient in the mesopic range and favor shorter wavelengths. High-intensity discharge (HID) lamps, tuned HID lamps, and LED lamps have all provided better off-axis visual performance than traditional headlamp types because of their SPDs. (See references 66 and 88–90.)

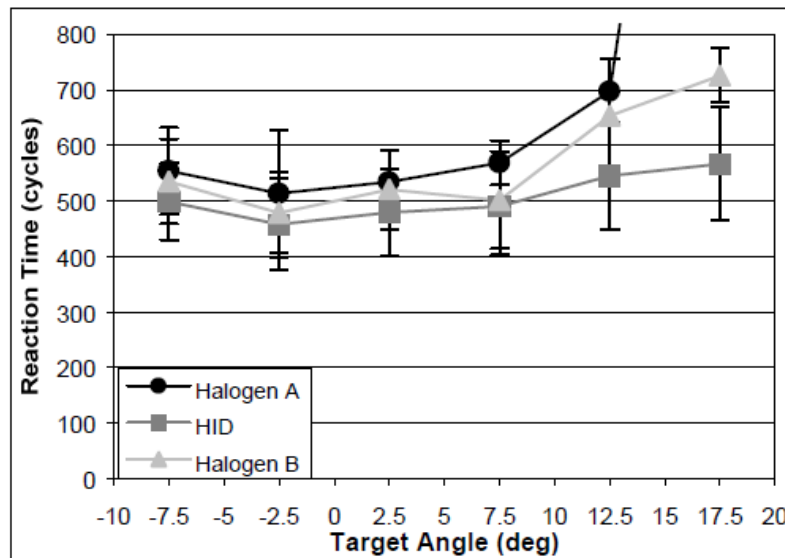
HID Headlamps:

HID headlamps have higher luminous efficacy, higher color temperature, and longer life compared with more traditional halogen headlamps. These lamps are more intense in the beam's periphery. When tested using off-axis targets, participants driving with HID headlamps have longer detection distances, fewer missed targets (figure 16), and shorter reaction times (figure 17) than participants driving with halogen headlamps.⁽⁶⁶⁾ HID headlamps enable better peripheral detection because of their higher color temperature, brighter area in front of the vehicle, and different light spectra. HID lamps have a wider spread of light than halogen lamps.



Reprinted with permission from SAE paper 2001-01-0298 Copyright ©2001 SAE International Further use and distribution is not permitted with permission from SAE.

Figure 16. Chart. Comparison between halogen and HID headlamps.⁽⁶⁶⁾



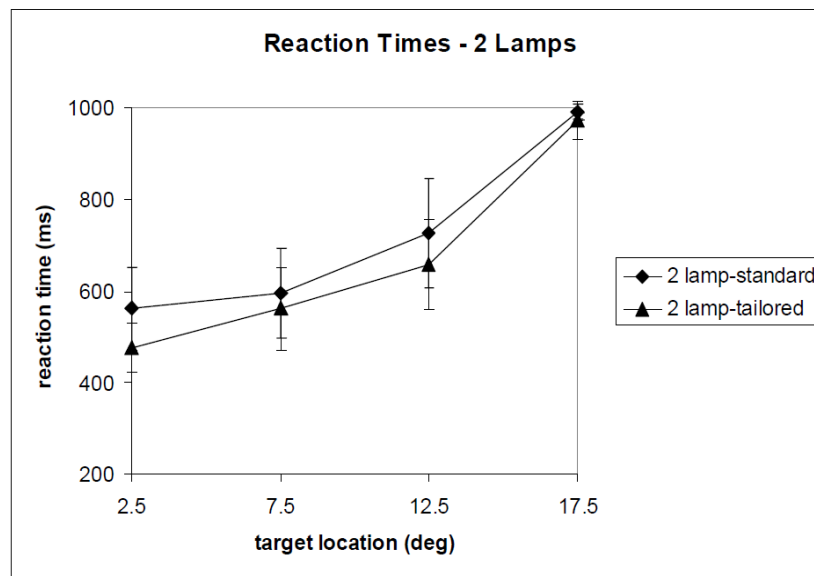
Reprinted with permission from SAE paper 2001-01-0298 Copyright ©2001 SAE International Further use and distribution is not permitted with permission from SAE.

Figure 17. Graph. Comparison of reaction times between halogen and HID headlamps.⁽⁶⁶⁾

Spectrally Tuned HID Headlamps:

Using special filters, HID headlamps can be tuned to emit a higher percentage of shorter wavelengths. Participants in a vehicle with tuned HID headlamps detected off-axis targets with shorter reaction times and fewer missed detections than those with regular HID headlamps.⁽⁸⁸⁾

(See figure 18.) A major limitation of the study was that the test vehicle was stationary; visual performance of drivers in moving vehicles with tuned HID headlamps should be further studied.



Source: Van Derlofske, J.F., Bullough, J.D., and Gribbin, C.

Figure 18. Graph. Reaction times with different HID headlamp types.⁽⁸⁸⁾

LED Headlamps:

The use of LEDs is rapidly increasing in automotive headlamps. They have a longer life cycle, lower power requirements, and different spectra than HID lamps. In 2008, the Audi® R8 was the first car to have full LED headlamps, incorporating 54 high-performance LEDs.⁽⁹¹⁾

Researchers at the Lighting Research Center in Troy, NY, investigated the spectral distributions of 17 white LEDs used in headlamps. The S/P ratios of three white LEDs were found to be similar to or greater than a tuned HID headlamp, indicating that LED headlamps should permit drivers to see off-axis targets as effectively as tuned HID headlamps.⁽⁶⁴⁾

Headlamp System Configuration

Typical headlamps are stationary and aimed down the road, where pedestrians are less likely to be detected. The headlamp portion of an MPI system would have two sets of headlamps, one stationary and the other directed by the MPI system controller to highlight pedestrians and roadway objects, increasing the probability of detection.

The MPI headlamps could be installed at a fixed angle with respect to the vehicle and flash momentarily as the car approaches a pedestrian. Alternately, the headlamps could be controlled by a servo and thus swivel and track the pedestrian as the vehicle moves down the road. These options are shown in figure 19. Both technologies require the MPI system to identify and track the pedestrian and then calculate the pedestrian's position with respect to the vehicle.

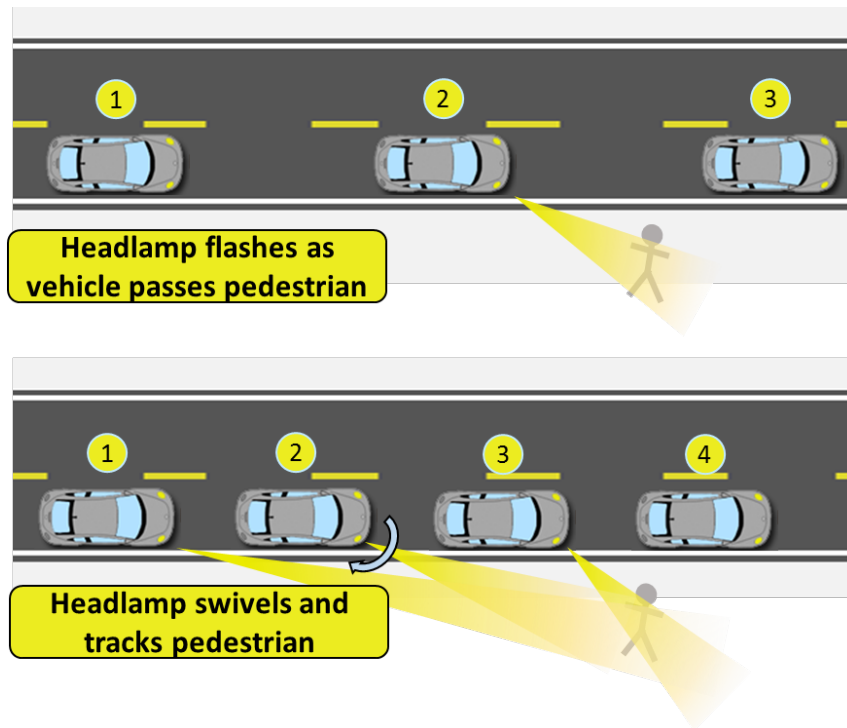


Figure 19. Diagram. MPI headlamp illuminating pedestrian by flashing on and swiveling.

Potential issues in tracking and illuminating pedestrians include deciding which type of headlamp to use, determining how long it is safe to illuminate a pedestrian and how to track and illuminate multiple pedestrians, and ensuring pedestrians are comfortable with the system. Research on MPI systems should determine which approach is best for pedestrian detection, pedestrian comfort, multiple-pedestrian tracking, and avoiding driver distraction.

SPECIFICATION DEVELOPMENT FOR AN MPI SYSTEM

As part of the development of the background for this project, the specifications of a functioning MPI system need to be developed.

Conceptual Design of an MPI System

An MPI system would overcome limitations in human vision and vehicle headlamp design by automatically detecting pedestrians and using side-aimed headlamps that illuminate the pedestrian in sufficient time for the driver to react. MPI headlamp light would be efficient in activating the eye's photoreceptors in the mesopic range and not produce glare for oncoming drivers.

Such a system requires two primary components: a detection system and a lighting system. A conceptual design for one version of an MPI system is shown in figure 20. That system uses vision-based detection that enters pedestrian locations into a control system, which activates swiveling headlamps. Those and other detection and lighting systems are discussed in this section.

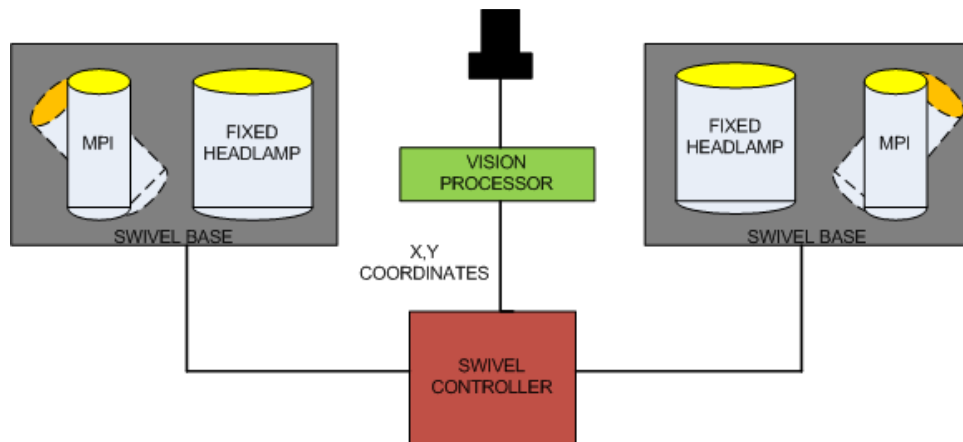


Figure 20. Diagram. Conceptual design of an MPI system.

Pedestrian-Detection Systems

An ideal pedestrian collision warning system would detect a pedestrian and the pedestrian's position in time for the headlamp control system and headlamps to illuminate them. The detection system would need to have a low false-positive rate because drivers would not continue to pay attention to a system with a high false-positive rate. Prior research in pedestrian detection points to three commonly used sensor types, described in this section: vision-based sensors, infrared sensors, and sensors based on time of flight (TOF), such as radar and laser scanners.^(67–69)

Vision-Based Sensors

Vision-based sensors detect high-resolution information from the environment, extract shapes from that information, and compare the shapes with a large sample of example images. If a shape matches an image of a pedestrian, a pedestrian is detected.

Extracting shapes from a complex visual environment can be accomplished in a variety of ways. Edge tracking and motion estimating, active frame subtraction, texture property analysis, are some possible approaches.^(70–72) Other promising approaches analyze image intensity and motion information, leg symmetry, motion analysis and parallax, or use stereo matching.^(73–75) Systems could also be trainable.^(72,76) There are a large number of approaches for vision-based systems, but all are limited by darkness, where objects and background have no luminance contrast, and are also negatively affected by glare.

Thermal Infrared Sensors

Thermal infrared sensors detect human body heat and are effective when vision-based systems are not—at night—when the environment is cooler than human skin. A number of researchers have used thermal infrared sensors to detect and track pedestrians. Systems can use a single camera or stereo cameras, and detect pedestrians using size and aspect ratio, profile and contrast, and pedestrian contour. (See references 77–81.) Other systems use head detection, comparative motion of the pedestrian and background and relative motion of the vehicle and pedestrian.^(78,82)

One system even detected pedestrians and warned drivers.⁽⁸²⁾ Although thermal infrared sensors work in the dark, they are less effective in poor and hot weather.

TOF Sensors

TOF systems include radar and laser systems. They scan the environment, collect reflected radiation, and estimate the relative velocity of nearby objects based on the differences in time it takes for reflected radiation to arrive back at the sensor. TOF systems can be used to select objects of interest in the environment for further vision processing, reducing the computational load on the vision portion of the system.⁽⁸³⁾ They could also process data from a TOF system and an infrared system in parallel.⁽⁸⁴⁾

Vision-based and infrared sensors provide high-resolution information about a captured scene. This high level of information comes at the expense of the amount of processing and computation. TOF sensors locate objects accurately, but their resolution is limited. Systems using both TOF and vision and/or infrared data would be effective in a variety of conditions but can be very expensive.

Pedestrian-Detection Algorithms

Vision-based, infrared-based, and TOF systems all require an algorithm to process the incoming data and determine whether a pedestrian is present. Despite the variation in detection technology, the detection algorithms are similar, with the basic algorithm structure shown in figure 21.⁽⁶⁷⁾

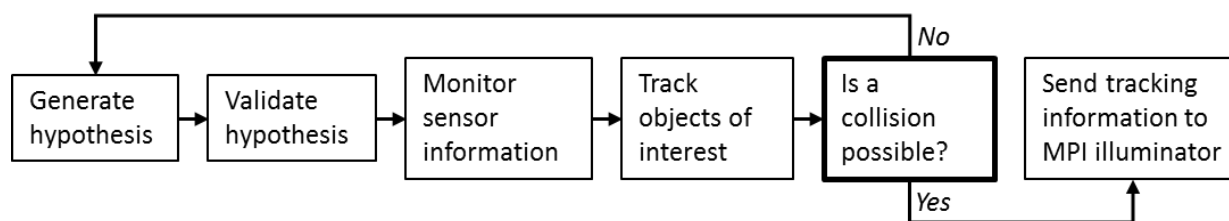


Figure 21. Diagram. General structure of a pedestrian-detection system.⁽⁶⁷⁾

This algorithm begins by hypothesizing that an object in the field of view is an object of interest and then validates whether or not the object in the field of view is actually an object of interest. The system then monitors the input from the sensors to further validate the hypothesis and tracks validated objects of interest. Using tracking information, the system calculates whether or not a collision is imminent. If a collision is imminent, the tracking information is forwarded to the MPI illuminator, which lights up the object of interest. If not, the system continues monitoring and tracking objects of interest.

Pedestrian-Detection System Development

DaimlerChrysler developed and tested the PROTECTOR system in traffic conditions.⁽⁸⁵⁾ The system detects pedestrians, estimates trajectories, assesses collision risk, and warns drivers. Although its performance was promising, PROTECTOR requires more research and development before it is implemented. Volvo also developed a pedestrian-detection system for the S60, using radar and a camera mounted on the front of the car to detect pedestrians and other

objects.⁽⁸⁶⁾ It can detect pedestrians 0.8 m (32 inches) and taller, and, if a collision is imminent, it will alert the driver and automatically brake. Mobileye® technology has been used by automakers such as BMW, Volvo, and General Motors, and Mobileye® has developed several technologies for detecting pedestrians.⁽⁸⁷⁾ Mobileye® systems use a monocular approach and advanced spatiotemporal classification techniques based on machine learning, where the system is trained with static and dynamic information. This Mobileye® system does not, however, function in the dark.

Pedestrian-Detection System Requirements

Based on previous work, the pedestrian-detection portion of an MPI system should do the following:

- Detect standing and moving pedestrians.
- Detect multiple pedestrians and their direction and speed of movement.
- Detect pedestrians of different sizes and orientations.
- Categorize and prioritize among pedestrians based on collision risk, if more than one pedestrian is present.
- Locate pedestrian positions on the side of the road and calculate the distance between the pedestrian and car.
- Detect pedestrians in the dark and in rain, fog, and snow.
- Have a light source spectrum that maximizes peripheral detection.
- Have minimal latency and issue timely alerts.

CHAPTER 3. EXPERIMENTAL APPROACH

Five experiments were undertaken as part of this project. The progression of the experiments is shown in figure 22. Later experiments were built from two basic efforts undertaken in the first two experiments, a scoping experiment and an MPI experiment. Those two experiments were designed to explore the range of the possible experiments' conditions and to develop the boundaries of the future efforts. The two subsequent experiments, the overhead-lighting level and mesopic modeling experiments, were performed to investigate other facets of spectral interactions. A final performance experiment investigated the results of the first four experiments in a full driving environment. Each of the experiments is summarized in the following paragraphs.

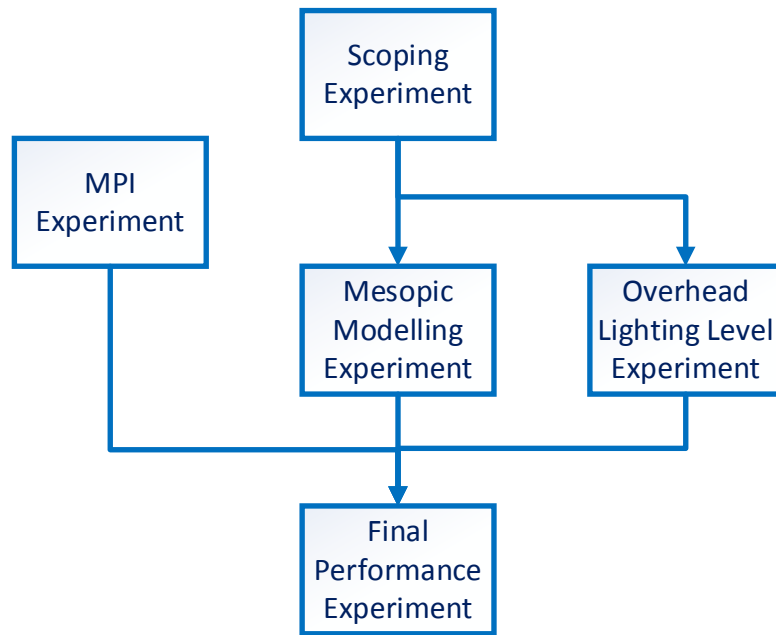


Figure 22. Flowchart. Relationship among experiments performed.

The scoping experiment compared the detection and recognition distances of pedestrians and small targets under two different overhead-lighting sources, two overhead-lighting levels, two headlamp colors, and two headlamp levels. The objects detected and recognized were four different colors and were located both along the roadway and in the periphery of the roadway. The purpose of this experiment was to provide an initial review of the interactions of light source spectrum and level and to identify the specific characteristics of the lighting conditions to be further investigated.

The MPI system performance experiment investigated the effect of using a momentary peripheral illuminator on object visibility. The goal of this experiment was to investigate whether the possible spectral improvement in the periphery could be enhanced by the light source type. The experiment considered the MPI system under two headlamp light source characteristics, two headlamp light levels, three different MPI behaviors, and two different ambient lighting conditions. The results of this experiment were used to identify the critical components of the

MPI system, the impact of the light source spectrum on the MPI performance and to identify variables to be carried forward to the final performance experiment.

The overhead-lighting level experiment was designed to investigate the interaction between overhead lighting and vehicle headlamps on visibility. The spectral effects of a light source depend on the adaptation level of the human eye, and headlamps may be the dominant aspect in a driver's field of view; thus, headlamps may be the main contributor to adaptation level. This experiment was designed to investigate this aspect of the lighted area by looking at the detection and recognition of both small objects and pedestrians in a carefully controlled manner by dimming the overhead-lighting system from 100 percent to off, in 10-percent increments.

The mesopic modeling experiment was designed to provide a real-world validation of the CIE Recommended Model for Mesopic Photometry.⁽¹⁾ Because most of the previous work performed for mesopic models was done in highly controlled environments, even for the experiment that included driving, external validation of the model was required.⁽⁴²⁾ The experiment implemented here used both a static and a dynamic approach to the detection of objects in the roadway. These results were then compared with the expected results of the mesopic models.

The final performance experiment combined all of the efforts of the previous experiments to perform an overall assessment of the spectral aspects of the overhead lighting. In all, three overhead-lighting systems, off-axis pedestrians, five different adaptation luminance levels, different vehicle speeds, and three pedestrian clothing colors were used to explore the spectral effects of the overhead-lighting system. This experiment was a true driving experiment, used to assess the overall applicability of spectral aspects of the light source in a realistic scenario.

There were common elements to each of the experiments undertaken as part of the project. In particular, each experiment was performed on the Virginia Smart Road (hereafter referred to as the Smart Road) using the same overhead-lighting systems and vehicle headlamp systems. Similar objects for detection were also used in all of the experiments. Common components and aspects of the experiments are described in this chapter. Experimental methods unique to each experiment are described in the chapters on those experiments.

MATERIALS AND FACILITIES

Virginia Smart Road

The research was conducted at the Virginia Tech Transportation Institute's (VTTI) Smart Road. The Smart Road is a 3.54-km (2.2-mi) restricted-access test track with guard rails, pavement markings, and a variety of overhead-lighting installations, as shown in figure 23. The Smart Road has two pavement surfaces—asphalt and concrete, and overhead-lighting levels can be adjusted to match luminance levels between lighting types, if required.

During the experiments, participant drivers completed a number of laps on the Smart Road, turning their vehicles around at the top turn, the bottom turn, or turn three, depending on which protocol they were following.

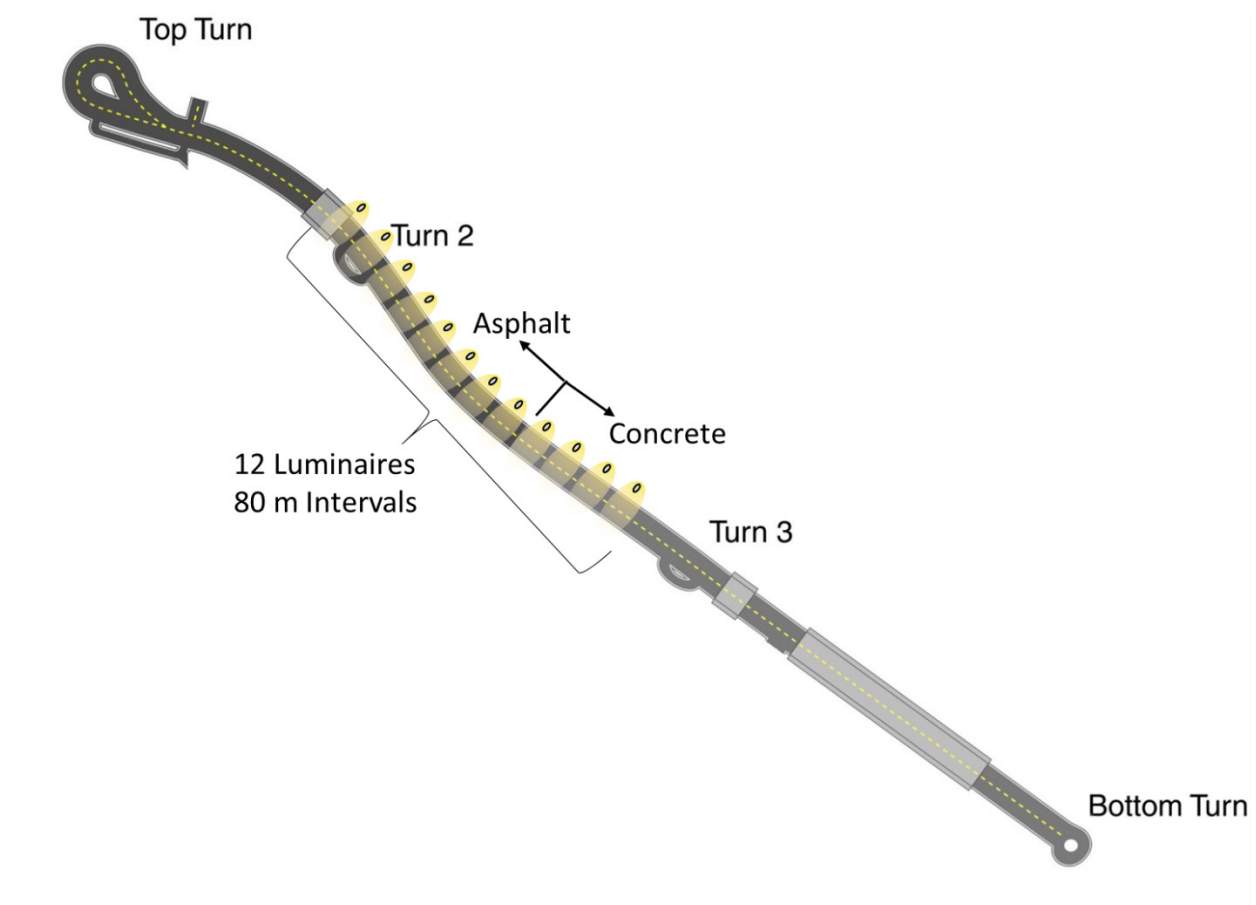


Figure 23. Diagram. Smart Road test track.

Overhead-Lighting Systems

For this project, three lighting systems installed on the Smart Road were used. One was a traditional HPS system, and two were solid-state LED systems. All luminaires were dimmable, mounted 15 m (49 ft) high, and spaced 80 m (262 ft) apart. The characteristics of the luminaires used for this project are listed in table 2, and their SPDs are shown in figure 24.

Table 2. Overhead-lighting system characteristics.

Lighting System	Wattage	Color Temperature (K)	Luminaire Type	Driver
2,100-K HPS	150 W	2,100	General Electric model M2AC-15S4-A1-GMC2-1253, Type II M	Greentek 0- to 10-V dimming
3,500-K LED	234 W	3,500	Cree® LEDway® BetaLED® model STRLWY, Type II M. 3500	Advance 0- to 10-V dimming
6,000-K LED	234 W	6,000	Cree® LEDway® BetaLED® model STR-LWY, Type II M. 6000	Advance 0- to 10-V dimming

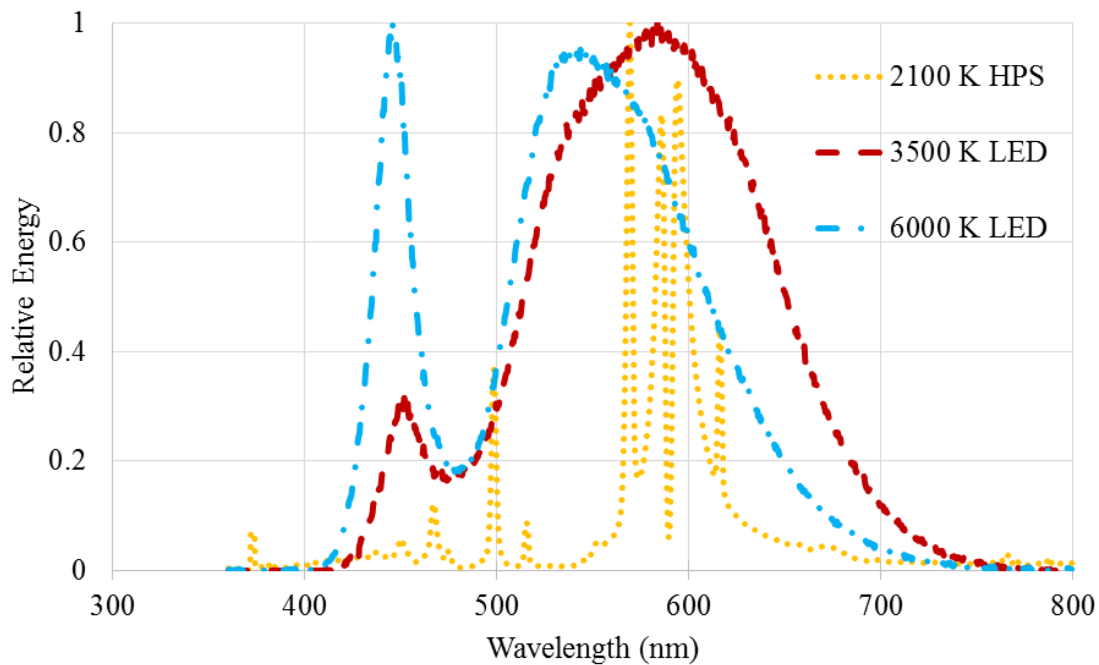


Figure 24. Graph. Mesopic modeling experiment—SPDs of overhead-lighting types used in the study.

Each of the lighting systems was equipped with a wireless control system to provide dimming and on/off control for the luminaires. The control system is a Synapse® Wireless, Inc., SNAP DIM-10 0- to 10-V system that provides simultaneous 255-step remote-dimming control for all 3 luminaire systems.

The overhead-lighting systems were calibrated using the VTTI-developed Roadway Lighting Mobile Measurement System (RLMMS).⁽²³⁾ This allowed each system to be dimmed accurately and allowed lighting level characteristics to be matched between lighting systems depending on the conditions required for the experiments.

Vehicles and Headlamp Systems

Two mid-sized sport-utility vehicles with the same body style and internal layout were used in the study. Both were instrumented with digital audio and video recorders, luminance cameras (described under Luminance-Based Systems in the Procedures section of this chapter), small monitors, and keyboards. The data collected included driving distance, vehicle speed, Global Positioning System (GPS) location, and the user-input button used to calculate detection and color recognition distances. During the experiments, the rear view and side mirrors were covered to prevent headlamp glare from the other test vehicle.

HID headlamps were installed on the test vehicles. The headlamps selected were Hella™ 90-mm Bi-Xenon projector lamps, rated at 35 W, that use an internal shutter to provide an SAE beam pattern with a sharp vertical cutoff. A single 1-F capacitor stabilized headlamp input voltage on each vehicle. Low beams only were used. Before each night of experiments, the headlamps were aligned according to manufacturer specifications using a Hopkins® Manufacturing Hoppy Vision 100 laser aiming system.

Gels were placed in front of the headlamps and were mounted so they could be easily changed, as shown in figure 25.

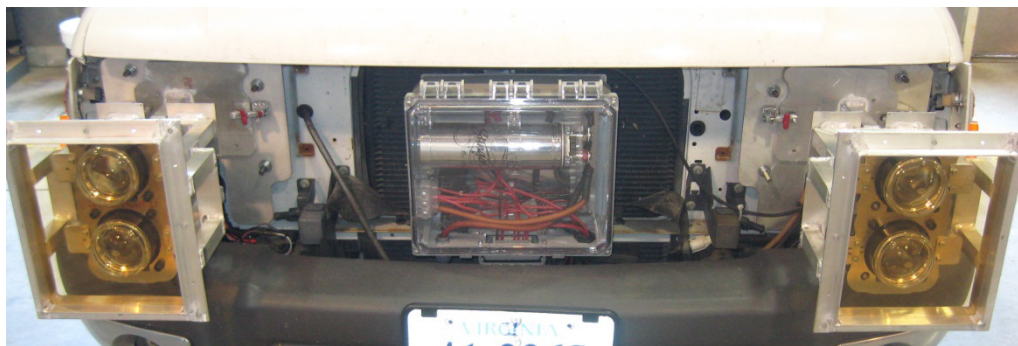


Figure 25. Photo. Test vehicle with headlamps and interchangeable gels.

Depending on the experiment, one of five sets of filters was used: white/yellow high intensity, white/yellow low intensity, white/blue high intensity, white/blue low intensity, and neutral density low intensity. Recommendations for the headlamp configurations were provided by the University of Michigan Transportation Research Institute. The headlamp and gel intensity and spectral characteristics are listed in table 3, and the SPDs of the headlamps using different filters are shown in figure 26 through figure 28. In the first two of these figures, it can be seen that the blue light is truncated by the yellow filter and vice versa.

Table 3. Characteristics of headlamp filters.

Headlamp Color	Intensity	Transmittance	Correlated Color Temperature (K)
White/yellow—high	High	0.49	2,926
White/yellow—low	Low	0.38	2,910
White/blue—high	High	0.44	5,357
White/blue—low	Low	0.31	5,120
Neutral density	Low	0.34	3,530

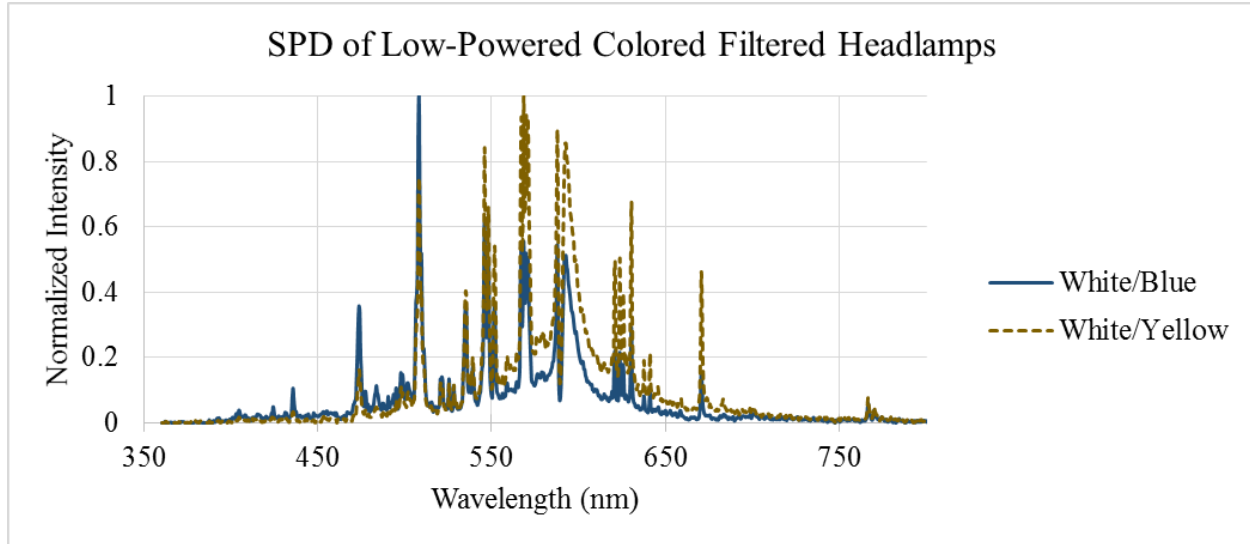


Figure 26. Graph. SPD of low-power, color-filtered headlamps.

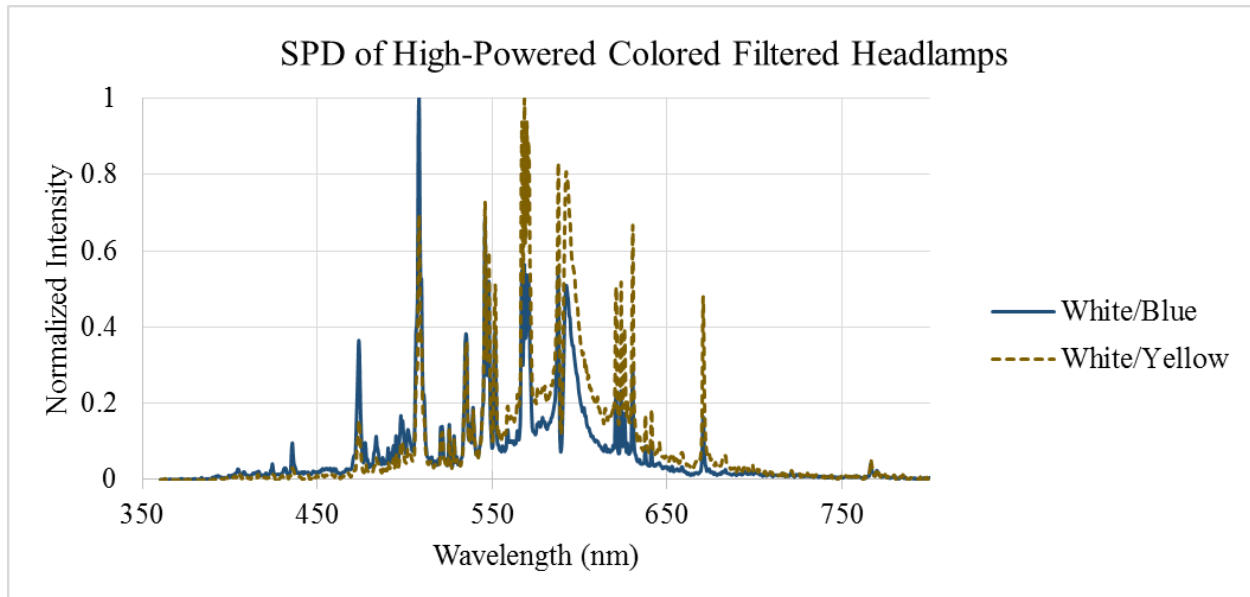


Figure 27. Graph. SPD of high-power, color-filtered headlamps.

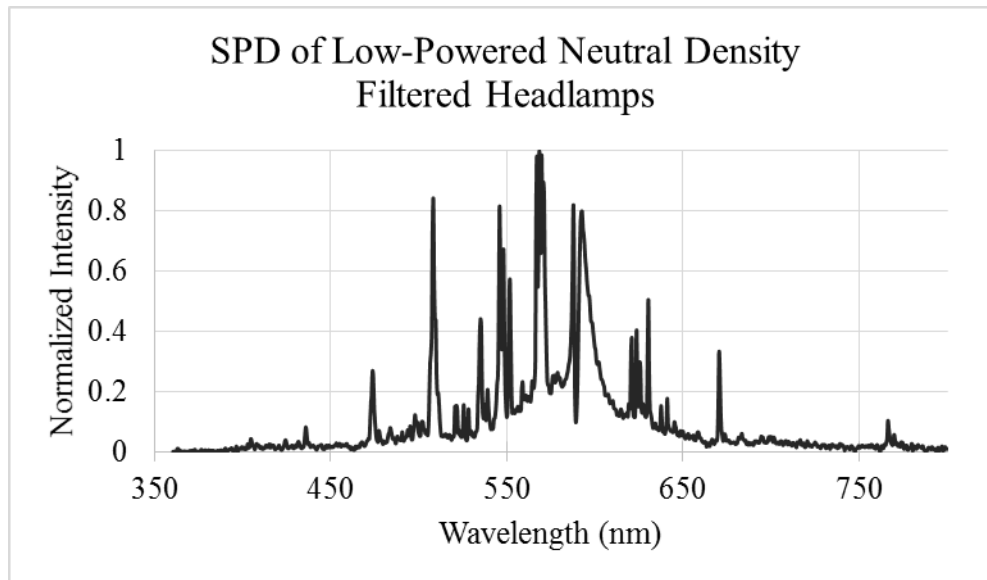


Figure 28. Graph. SPD of low-power, neutral-density-filtered headlamps.

Depending on the experiment, yellow filters were used to create an SPD similar to HPS roadway lighting, and blue filters were used to create an SPD similar to LED headlamps. When the 50-percent filters were used, the headlamps were about the same intensity as typical HID headlamps installed in vehicles. For the white/yellow headlamp configurations, the CCT was slightly different between the high and low settings, because the team used standard, off-the-shelf filters (gels) to reduce transmittance, and these off-the-shelf gels did not necessarily have precisely the same color properties. The same applied to the white/blue headlamp configurations.

Visual Objects

For each of the experiments, a visual object was used to measure visual performance. Dependent variables characterizing visual performance were detection distance, orientation-recognition distance, and color-recognition distance, depending on the experiment. The characteristics, type, size, and color of the visual objects were standardized. The objects were either pedestrians or small targets and are described in the following subsections.

Pedestrians

Confederates acted as pedestrians. Pedestrians wore four colors of scrubs, depending on the experiment—red, black, gray, or blue—as shown in figure 29. Pedestrians were not allowed to wear shoes with reflective materials or any other reflective clothing or accessories.



Figure 29. Photo. Clothing colors on confederate pedestrian.

Red was chosen to highlight the amber hue of the HPS overhead lighting and the yellow-filtered headlamps. Blue was chosen because LED luminaires have a blue component and because two headlamp configurations are white/blue. Gray was chosen as a more neutral color, and black was chosen to represent a worst-case, least-visible scenario for a pedestrian at night. The spectral reflectance of the four clothing colors, calculated as a percentage relative to a diffuse white reflector, is shown in figure 30. The integral of the reflectances for the four clothing colors, calculated between 360 and 800 nm using the trapezoid rule and weighted for the eye's spectral sensitivity, are listed in table 4. These integrals give a direct comparison of how visible these colors would be in ideal conditions in bright light (photopic) and very low light (scotopic).

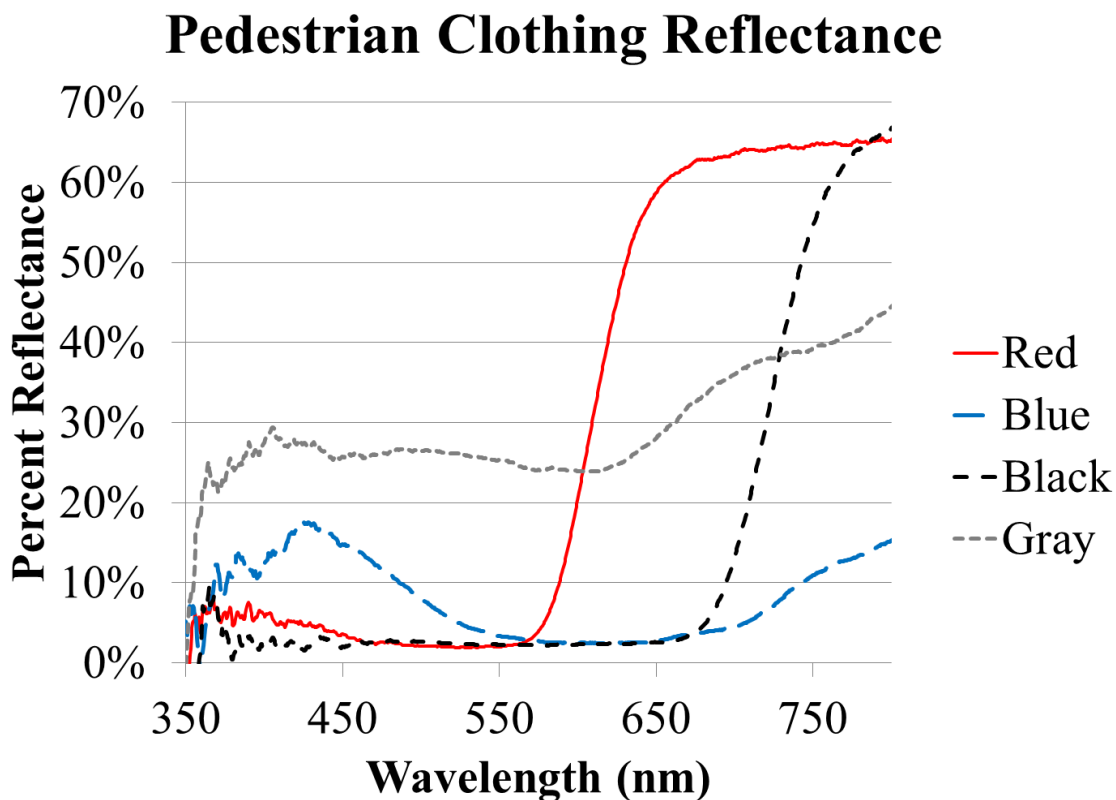


Figure 30. Graph. Pedestrian clothing reflectance.

Table 4. Integral of pedestrian clothing reflectance.

Clothing Color	Red	Blue	Black	Gray
Integral of reflectance (photopic)	11.0	4.3	2.5	26.9
Integral of reflectance (scotopic)	2.7	8.1	2.4	25.3

Targets

Participants also identified targets during the experiment. The targets represented roadway obstacles and were 18 by 18 cm (7 by 7 inches)—small and difficult to see but still potentially dangerous to drivers. The targets were two-dimensional to remove the effect that viewing angle has on a three-dimensional object. Their flat faces facilitated the team’s collection of accurate luminance and contrast data, and they were designed to break if a participant ran them over.

The targets were painted one of four colors: red, gray, blue, or green. The red, blue, and green were chosen because they are additive primaries; the red, blue, and gray were chosen for the same reasons that they were used on the pedestrians’ scrubs. Photos of the targets are shown in figure 31, and the spectral reflectance of the targets is shown in figure 32. The integral of the reflectances for the four target colors, calculated between 360 and 800 nm using the trapezoid rule and weighted for the eye’s spectral sensitivity, are listed in table 5.

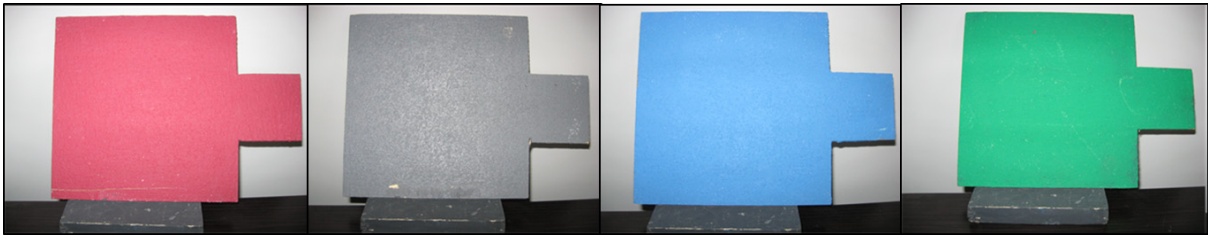


Figure 31. Photo. Targets.

Percent Target Reflectance Relative to Diffuse White

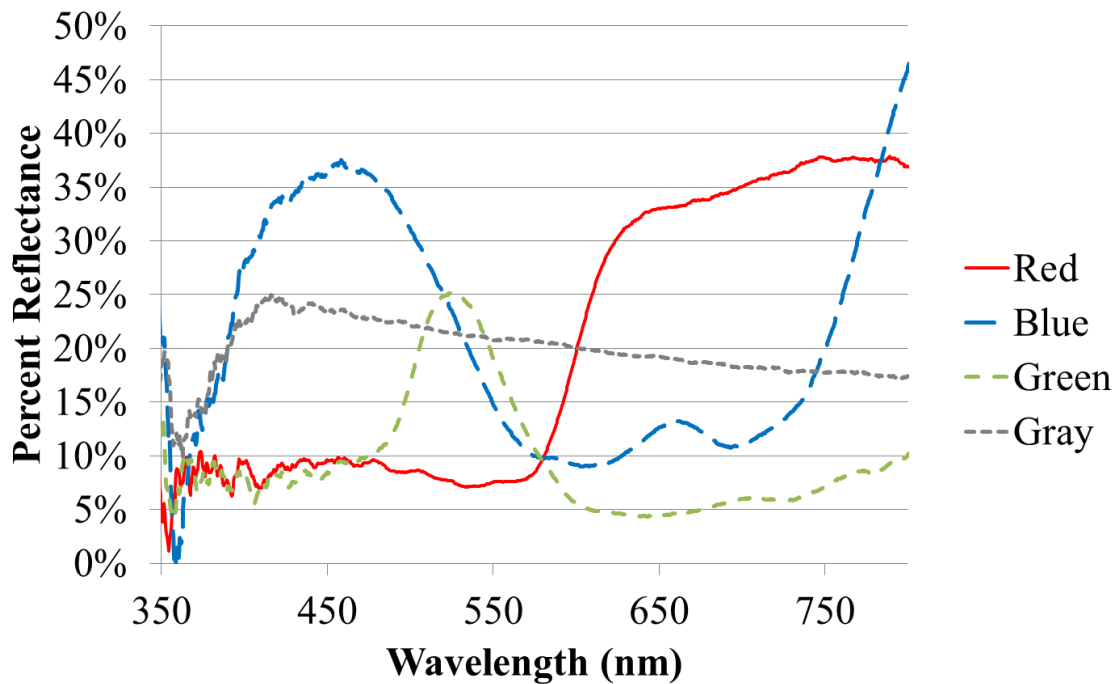


Figure 32. Graph. Target reflectance relative to diffuse white.

Table 5. Integral of target reflectance.

Target Color	Red	Blue	Green	Gray
Integral of reflectance (photopic)	13.0	17.3	15.4	22.3
Integral of reflectance (scotopic)	8.3	27.1	15.6	21.5

DEPENDENT VARIABLES

Three dependent variables measuring visibility were used in the experiments for this project: detection distance, color-recognition distance, and orientation-recognition distance. The variables used depended on the experimental goals and are described in the following subsections.

Detection Distance

The detection distance was the distance at which a participant was able to detect the presence of an on- or off-axis pedestrian or target. To measure detection distance, researchers instructed participants to say “person” or “target” when they first saw the pedestrian or target. At that moment, an in-vehicle experimenter pressed a button to flag the data. The in-vehicle experimenter also pressed a button to flag the data when the vehicle passed the pedestrian or target. If a participant failed to see an object, it was counted as a miss. Later analysis calculated the distance between these two points to determine the detection distance.

Color-Recognition Distance

The color-recognition distance was the distance at which a participant was able to accurately recognize the color of an on- or off-axis pedestrian or target. Participants were instructed to call out the color of an on- or off-axis pedestrian's clothing, or the color of the target, as soon as they saw it. The researcher in the vehicle then pressed a button to flag the data. The in-vehicle experimenter also pressed a button to flag the data when the vehicle passed the pedestrian or target, as stated above, so the distance between where the participant could identify the color and when the vehicle passed the pedestrian or target itself was calculated. That distance was the color-recognition distance. If participants recognized the wrong color, it was recorded as a miss. Figure 33 is a diagram of how detection and color-recognition distances were measured.

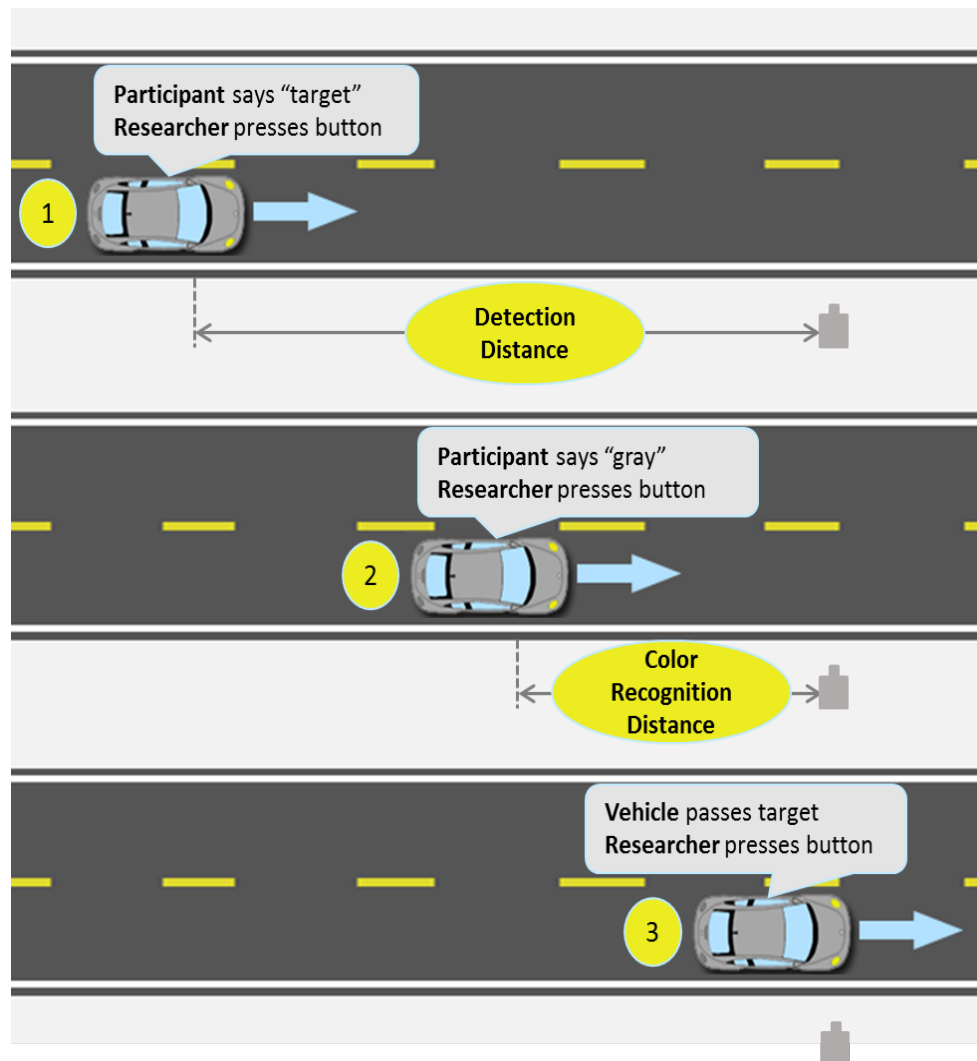


Figure 33. Diagram. Measuring detection and color-recognition distances.

Orientation-Recognition Distance

The orientation-recognition distance was the distance at which a participant was able to accurately recognize the direction a pedestrian was facing, or the direction the tab on the target was pointing. Participants were instructed to call out the direction as soon as they were able to discern it. The researcher in the vehicle used button presses to flag the data as was done for the other dependent variables, and the orientation-recognition distances were calculated. If a participant failed to recognize which way an object was facing, it was recorded as a miss.

PROCEDURES

Participant Selection

Participants were selected from the VTTI subject database based on their age and gender to form two gender-balanced groups, older and younger.

Screening criteria for participant selection included the following:

- Must hold a valid driver's license.
- Must not have more than two moving violations in the past 3 years.
- Must have normal (or corrected to normal) vision.
- Must be able to drive an automatic transmission vehicle without assistive devices.
- Must not have caused an injurious accident in the past 3 years.
- Females must not be pregnant.
- Must not have lingering effects of a heart condition, brain damage from stroke, tumor, head injury, recent concussion, or infection. Must not have had epileptic seizures within 12 months. Must not have current respiratory disorders, motion sickness, inner ear problems, dizziness, vertigo, balance problems, diabetes for which insulin is required, or chronic migraine or tension headaches.
- Must not currently be taking any substances that may interfere with driving ability, cause drowsiness, or impair motor abilities.
- Must be eligible for employment in the United States.
- Must drive at night at least two times per week.
- Must not have had eye surgery.

Participants were compensated \$30 for every hour they participated in the study, including time spent responding to questionnaires.

Participant Screening

Telephone Screening

After participants conforming to the age and gender requirements were identified, a research assistant called them to ask whether they were interested in participating in the study, to gain consent for a screening, and to perform the screening. Those eligible based on the telephone screening were scheduled to come to VTTI for the vision screening.

Vision Screening

When the participant arrived, a researcher obtained consent, had the participant fill out a W9 form and health questionnaire, and administered vision tests: useful field of view (UFOV), brightness acuity, visual acuity, color vision, and contrast sensitivity. Not all vision tests were administered for all experiments. Results for participant vision testing are listed in the chapters describing the individual experiments. The following describes elements of vision screening:

- **Health Questionnaire:** Participants filled out a health questionnaire with basic demographic information, questions regarding health concerns in the last 24 h, and questions regarding their comfort with driving at night. Those with serious health concerns or a fear of driving at night were excluded.
- **UFOV:** Participants used a computer program that tested their UFOV. Scores ranged from 0 to 5; those with a score of 3 and higher were excluded.
- **Photopic and Mesopic Visual Acuity:** Participants' binocular visual acuity was measured using a Snellen Early Treatment Diabetic Retinopathy Study acuity chart. Those with binocular vision worse than 20/40 were excluded. The test was performed in both photopic and mesopic lighting conditions.
- **Glare Visual Acuity:** Although glare was not a focus of this study, participants' sensitivity to glare was measured using a brightness acuity tester (BAT). The BAT is a handheld device with an adjustable light that directs glare toward one eye. While holding the BAT over one eye and with the other eye closed, participants read lines off of the Snellen eye chart, and their scores were recorded.
- **Color Vision:** Participant's color vision was tested using an Ishihara color vision exam. Those responding incorrectly on one or more items were considered colorblind and excluded.
- **Contrast Sensitivity:** Contrast plays a major role in differentiating between objects and their backgrounds. The contrast sensitivity test used an illuminator with a Snellen eye chart with 25-percent contrast. Participants' binocular and monocular performance were measured. There was no exclusion criterion for the contrast sensitivity evaluation.

Experimental Runs

Almost all of the experiments required participants drive on the Smart Road while detecting/recognizing objects.

In-Vehicle Experimenter Activities

After participants completed the consent and testing portion of the session, in-vehicle experimenters escorted the participants to the test vehicles, where the participants were familiarized with the vehicle controls. They then drove the vehicles to the Smart Road and drove a practice lap, followed by the number of experimental laps required by the experiment. Most experiments used two vehicles. During the experiment, the vehicles were driven through the test section of the road one at a time, pausing at one of the turnarounds while the other vehicle completed its lap, so that the two vehicles would not interfere with each other. Participants completing experimental laps would state whether they saw a target or pedestrian, what color they saw, and which way the object was facing, and the researcher recorded the detections/recognitions with button presses, as described in the section on dependent variables. The in-vehicle researcher ensured that the participant was driving safely and at the correct speed. For safety reasons, when using confederate pedestrians, after the participant saw the pedestrian, the researcher radioed the pedestrian and asked him or her to move away from the road.

On-Road Experimenter Activities

On-road experimenters acted as confederate pedestrians and positioned themselves and/or the targets alongside the road according to the protocol for that experiment and lap. They were asked to clear the road when instructed by the in-vehicle experimenter, or when a vehicle approached within about 24 m (80 ft). Experimenters also ensured the overhead lighting was set to the correct level and changed headlamp filters as required by the experiment and lap. The test vehicles would only pass through the test portion of the road once the on-road experimenters confirmed the apparatus was in place.

PHOTOMETRIC SYSTEMS

For each of the experiments, photometric analyses were performed to determine the lighting conditions and the visibility conditions during the experiment. Photometric systems were also used to monitor the lighting levels during the experiment and characterize the lighting system's performance. Four different photometric measurement systems were used during the experiments, two were luminance-based systems and two were illuminance-based systems, and all are described the following subsections.

Luminance-Based Systems

Both of the two luminance-based photometric systems were imaging systems providing the luminance distribution across a scene.

The first system was a Radiant Imaging® ProMetric® 1600 photometer, a stand-alone commercial test system providing a 1,024- by 1,024-pixel image of a scene. This system can be mounted in the vehicle and provides static luminance measurements from stationary vehicles.

The second system was a calibrated luminance camera recording luminance data regarding the road in front of the vehicle. The luminance cameras in the two vehicles were calibrated by comparing their video to known luminance values.⁽⁹²⁾ The luminance camera systems were mounted to the windshields, linked with the vehicle instrumentation system, and took dynamic data from moving vehicles. Every time the participant detected a target or pedestrian, luminance data were captured.

The reduction of the data from the two luminance-measurement system was performed in a similar manner. For data from the ProMetric® Radiant Imaging® camera, data were analyzed with ProMetric® software. For data taken with the luminance cameras, VTTI developed data-reduction software was used.⁽⁹³⁾ In both cases, the analysis software displayed the captured image, allowing the user to select an area of interest, and then calculated the luminance of that area of interest. Multiple areas of interest were selected to calculate luminance contrast. A screenshot of the VTTI program is shown in figure 34.

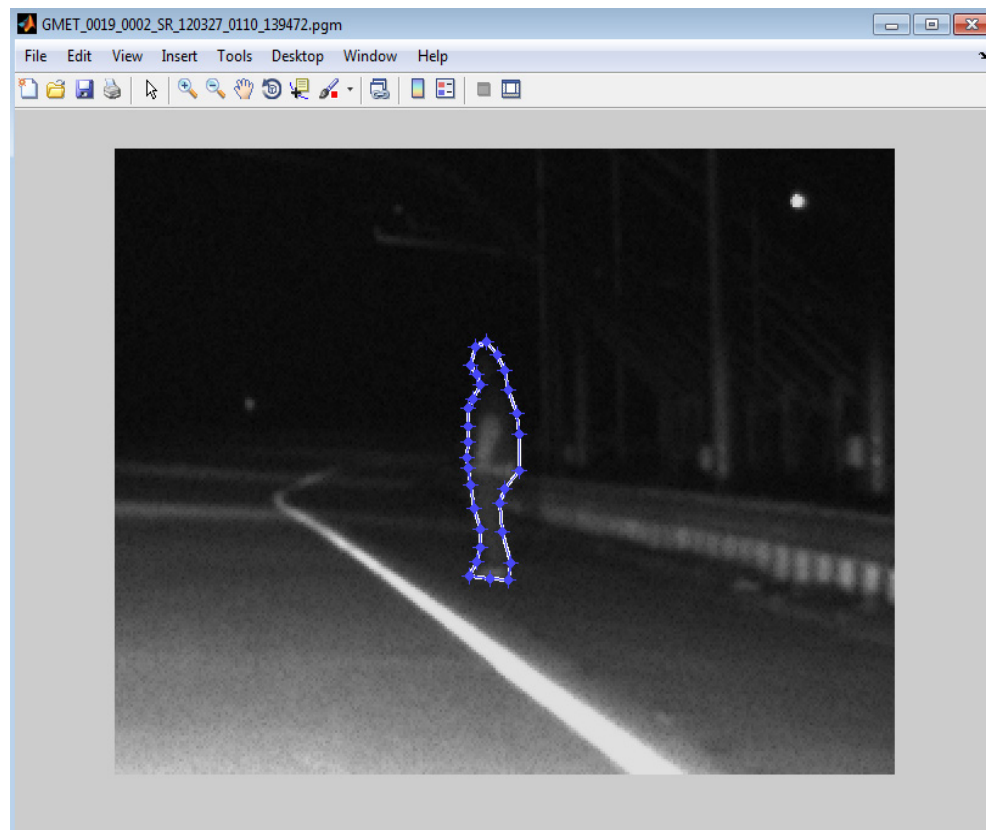


Figure 34. Screenshot. Luminance analysis software.

Illuminance-Based Systems

The two illuminance-based systems are a handheld Minolta® T10 system and the VTTI RLMMS system. The handheld meter was used to measure the vertical illuminance (VI) and to verify the lighting level on the road during the experiment. The RLMMS is a mobile-based measurement system that allowed for the illuminance characterization of the entire roadway and was used to calibrate the lighting system.

DATA REDUCTION PROCEDURES

Detection/Recognition Distances

The detection, color-recognition, and orientation-recognition distances for objects were the primary independent variables in almost all of the experiments. These distances were reduced from the data stream provided by the instrumentation system in the vehicle. Typically these distances were calculated based on the in-vehicle experimenter's button press at the moment of detection or color recognition and a button press at the moment the vehicle passed the visual object. The button presses are accurate to within 100 ms and logged to a data file. Using either technique, the moment of detection/recognition was identified in the data file containing the vehicle's GPS coordinates, accurate to within 5 cm (2 inches) and recorded using the vehicle data acquisition system. Detection/recognition distances were calculated from the GPS coordinates at the moment of detection and the moment the vehicle passed the object.

In the scoping and MPI system performance experiments, button presses were the main method for identifying the moment of detection/recognition. If an error occurred and the button presses were suspected to be inaccurate, video and audio data, continuously recorded in the vehicles, were used to determine the moment when a participant detected/recognized the object. Once the exact point of detection was recorded, the time stamp associated with the detection was matched to a GPS location recorded by the vehicle's radar unit. The distance from the point of detection to the target or pedestrian was calculated.

In the other three experiments, the overhead-lighting level, mesopic modeling, and the final performance experiments, all moments of detection/recognition were verified by examining video data, not by relying on button presses alone. Video verification is more precise because it removes any delay caused by an experimenter's reaction time. This method was used for these three experiments because the differences sought were small and accuracy was paramount.

Luminance Data

If the experiment used the luminance camera, the video from the moment when the participant detected or recognized the color of a pedestrian's clothing or a target was correlated with a screen capture from the luminance camera. Data reductionists then selected regions of interest in the image from which luminance and contrast values were calculated.

CHAPTER 4. SCOPING EXPERIMENT

INTRODUCTION

This experiment was the initial investigation of the spectral impact of overhead lighting and vehicle headlamps on driver visual performance. It was a scoping experiment that provided the framework for subsequent investigations.

Research Objectives

The purpose of the scoping experiment was to accomplish the following tasks:

- Evaluate the effect of the spectral distribution of overhead-lighting sources on driver ability to detect pedestrians and targets and recognize colors in the environment.
- Evaluate the effect of the spectral distribution of vehicle headlamp color on driver ability to detect pedestrians and targets and recognize colors in the environment.
- Evaluate the impact of the overhead-lighting color and headlamp color in mesopic conditions on driver ability to detect pedestrians and targets and recognize colors in the environment.
- Evaluate the impact of spectral distribution of overhead lighting and headlamp lighting on detection of pedestrians and targets located peripherally.
- Provide a framework upon which to design subsequent experiments.

EXPERIMENTAL DESIGN

A 2 by 4 by 2 by 2 by 4 mixed-factors experiment was designed to investigate the relationship of the spectral distribution and level of overhead lighting and headlamps on object detection and recognition on a roadway. A partial factorial design was used to ensure participants of both age groups were exposed to all combinations of vehicle speed, overhead lighting, and headlamp colors and intensities. Experimental variables are listed in table 6 and table 7.

Table 6. Scoping experiment independent variables and values.

Independent Variables	Levels
Age	Younger (25–35), Older (65+)
Overhead-Lighting Type and Level	2,100-K HPS High (5 lx (0.46 fc)), 2,100-K HPS Low (1.25 lx (0.12 fc)), 6,000-K LED High (5 lx (0.46 fc)), 6,000-K LED Low (1.25 lx (0.12 fc))
Headlamp Type	White/Blue White/Yellow
Headlamp Intensity	High (50-percent transmittance), Low (30-percent transmittance)
Pedestrian Clothing Color	Red, Black, Gray, Blue
Pedestrian Position	Constant VI (On axis), Constant contrast (On axis), Off axis
Target Color	Red, Gray, Blue, Green
Speed	89 km/h (55 mi/h), 56 km/h (35 mi/h)

lx = lux

fc = foot-candle

Table 7. Scoping experiment dependent variables and measurement method.

Dependent Variables	Measurement Method
On-Axis Pedestrian-Detection Distance	Participant first sees pedestrian
On-Axis Pedestrian Color-Recognition Distance	Participant first correctly identifies pedestrian clothing color
Off-Axis Pedestrian-Detection Distance	Participant first sees pedestrian
Off-Axis Pedestrian Color-Recognition Distance	Participant first correctly identifies pedestrian clothing color
Target Detection Distance	Participant first sees target
Target Color-Recognition Distance	Participant first correctly identifies target color

Independent Variables

Age

Age negatively affects visual perception.⁽⁴⁸⁾ There are two components to this visual reduction. The first is the yellowing of the lens as a person ages, which acts as a filter across the eye, and the second is intraocular scatter, in which light is significantly scattered as it passes through the ocular media thus reducing the contrast and the ability of the driver to detect objects. (See reference 49, 51, 57, and 94.) Burton, Owsley, and Sloane found that the reduction in retinal image quality is almost linear with the age of the observer.⁽⁹⁴⁾ However, it is noteworthy that driver performance may not follow the same trend as the reduction in the retinal image because older drivers have more experience driving in general and at night.

To examine the effects of age on visual performance, two age groups were investigated: younger drivers (25–35 years old) and older drivers (65 years old and older).

Overhead-Lighting Type and Level

For this experiment, the 2,100-K HPS and the 6,000-K LED overhead-lighting systems were used. Two lighting levels were used: 1.25 lx and 5 lx (0.12 and 0.46 fc).

Headlamp Configuration

Four headlamp configurations were used in this experiment: white/yellow low intensity, white/yellow high intensity, white/blue low intensity, and white/blue high intensity. These colors were chosen to match the color temperature of the HPS overhead lighting and LED vehicle headlamps, respectively. Details regarding the headlamps and filters are included in chapter 3, Experimental Approach.

Pedestrian Clothing Color

All four pedestrian clothing colors were used in this experiment.

Pedestrian Position

During the experiment, the confederate pedestrians stood in three sets of positions to satisfy three experimental needs.

The first set of positions was designed to isolate the effect of roadway lighting type and level. The VI falling on the pedestrians was controlled. The pedestrians were placed along the length of the Smart Road so that the roadway lighting types (HPS and LED) would project the same VI on the pedestrian across both lighting types and levels. Depending on the lighting type and level, each pedestrian would have to move to one of four possible locations along the road to achieve the same VI. In each location, the pedestrian was 0.6 m (2 ft) to the right of the right shoulder line, shown in figure 35. This was called the constant-VI position.

The second set of positions (the constant-contrast positions) was designed to keep the pedestrian's contrast with the background constant. For the constant-contrast position, the pedestrian stayed in the same place, 0.6 m (2 ft) from the right shoulder line, for both intensity levels of the same lighting type. This means that when the lighting system dimmed, the VI would change but the object contrast would not because the background would also be dimmed.



Figure 35. Photo. Pedestrian on roadway.

The last set of positions was designed to investigate off-axis visibility and to represent a possible collision hazard instead of an immediate collision hazard. This pedestrian was placed beyond the right guardrail, approximately 18 m (59 ft) off the roadway. That was called the off-axis position.

The design was balanced so that all clothing colors and pedestrian positions were viewed under all the overhead lighting and vehicle headlamp lighting combinations.

In the two positions close to the road, pedestrians stepped away from the road when the participant identified them or when participant vehicle reached a certain point.

Target Color and Position

All four colors of targets were used in this experiment. During the experiment, the targets were placed 0.6 m (2 ft) to the right of the shoulder with the flat face aimed toward the oncoming participant driver. The target positions controlled for VI, similar to the constant-VI position of the pedestrians. Figure 36 is a photo of the target in the roadway.



Figure 36. Photo. Target on roadway.

Speed

The experiment was performed at 89 and 56 km/h (55 and 35 mi/h).

Dependent Variables

Detection and color-recognition distances were measured in this experiment, as described in chapter 3. Orientation-recognition distance was not measured, and pedestrians and targets faced the same direction for all runs.

METHODS

Facilities and Equipment

The experiment was performed on the Smart Road using the equipment described in chapter 3, Experimental Approach.

Participants

The participants were recruited and screened, as described in chapter 3. Thirty-two participants completed the experiment and were balanced by both age and gender. Mean and standard deviation of participant age, visual acuity, mesopic visual acuity, low contrast visual acuity, and UFOV are listed in table 8.

Table 8. Scoping experiment participant characteristics.

Participant Characteristic	Older Drivers Mean	Older Drivers Standard Deviation	Young Drivers Mean	Younger Drivers Standard Deviation
Age	67.2	1.4	26.1	2.3
Visual Acuity	20/20.5	4.7	20/16.4	4.8
Mesopic Visual Acuity	20/35.5	13	20/24.3	6.6
Low Contrast Visual Acuity	20/28.6	7	20/21.3	6.4
UFOV	1.4	0.5	1.3	0.4

Procedure

Experimental Sessions

Those eligible for the experiment, based on the vision and health screening, were asked to come to two experimental sessions, with each session testing one overhead-lighting type and speed. Two participants completed the experiment during each session.

Data Collection

Once on the Smart Road, participants drove one practice lap followed by eight experimental laps. During the experiment, on-road experimenters altered the overhead-lighting conditions, headlamp filters, object types, colors, and positions according to the protocol. In-vehicle experimenters directed the participant to drive at the correct speed and recorded detection and color-recognition distances using button presses.

Data Analysis

After data reduction, dependent variables were analyzed with respect to the independent variables. If the participant failed to detect a pedestrian or target, it was counted as a miss. If the participant recognized the incorrect color, it was counted as a miss.

The detection and color-recognition distances for pedestrians and targets were compared across the experimental conditions using analysis of covariance (ANCOVA) in Statistical Analysis System® software. Individual and interaction effects were analyzed. Independent variables were compared within three groups: on-axis pedestrians, off-axis pedestrians, and targets. There were too few detections of off-axis pedestrians to draw meaningful conclusions; however, results are described here. Results for on- and off-axis pedestrians were also compared.

Student-Newman-Keuls (SNK) post hoc tests were performed for all significant effects to determine the contribution of the individual factors to the statistical significance. In all figures reporting SNK results, mean values sharing a letter label are not significantly different from each other.

RESULTS

Overhead-Lighting Type and Level

For runs in overhead lighting, independent variables were analyzed with respect to on- and off-axis pedestrian and target detection and color-recognition distances. Results for on- and off-axis pedestrians were also compared.

On-Axis Pedestrian

ANCOVA results are listed in table 9, with significant main effects described below the table.

Table 9. Scoping experiment on-axis pedestrian significant results summary for runs in overhead-lighting type and level.

Factor(s)	Detection Distance, <i>F</i>	Detection Distance, <i>p</i>	Color-Recognition Distance, <i>F</i>	Color-Recognition Distance, <i>p</i>
Age	7.78	0.0092 ^a	7.42	0.0108 ^a
Overhead-Lighting Type and Level	5.55	0.0023 ^a	1.62	0.1963
Clothing Color	4.27	0.0073 ^a	28.67	< 0.0001 ^a
Clothing Color by Overhead-Lighting Type and Level	2.1	0.0327 ^a	2.06	0.0379 ^a
Headlamp Color and Intensity	0.57	0.5674	1.22	0.3016
Age By Headlamp Color and Intensity	0.64	0.5329	0.68	0.5131
Age by Clothing Color	0.71	0.5494	2.02	0.1172
Headlamp Color and Intensity by Clothing Color	0.44	0.8513	1.62	0.1464
Age by Overhead-Lighting Type and Level	1.13	0.3461	1.13	0.3453
Headlamp Color and Intensity by Overhead-Lighting Type and Level	0.42	0.8648	0.83	0.5532

^aSignificant at $p < 0.05$.

Age:

Driver age significantly affected pedestrian-detection distance. Younger drivers detected pedestrians from significantly farther away (the mean $M = 118$ m (386 ft)) than older drivers ($M = 88.5$ m (290 ft), $p = 0.0092$). Age significantly affected color-recognition distance for pedestrian clothing. Younger participants recognized the clothing color from significantly farther away ($M = 69.3$ m (227 ft)) than older participants ($M = 49.1$ m (161 ft), $p = 0.0108$). Both effects were expected because previous research has shown these types of effects. These may be a result of intraocular scatter or the natural yellowing of the lens as a person ages.

Overhead Lighting:

Overhead-lighting type and level significantly affected detection distances and color-recognition distances. Higher lighting levels of both types corresponded to longer detection distances, as seen in figure 37, where bars sharing a letter are not significantly different from each other. What is important to note is the difference within overhead-lighting type. The difference in detection distances between the high and low levels for the 6,000-K LED luminaires was statistically significantly greater than the difference between the high and low levels for 2,100-K HPS ($p = 0.0023$) sources. This indicates an impact that can be attributed to the spectral distribution of the light source.

Overhead-lighting type and level affected pedestrian color-recognition distance similarly to how they affected pedestrian-detection distance—detection distances were significantly longer for higher level lighting. Again, the difference between the high and low levels was more pronounced for the LED lighting than for the HPS lighting, again showing an impact owing to the overhead lighting's spectral distribution. The color-recognition distance results are shown in figure 38, where bars sharing a letter are not significantly different from each other.

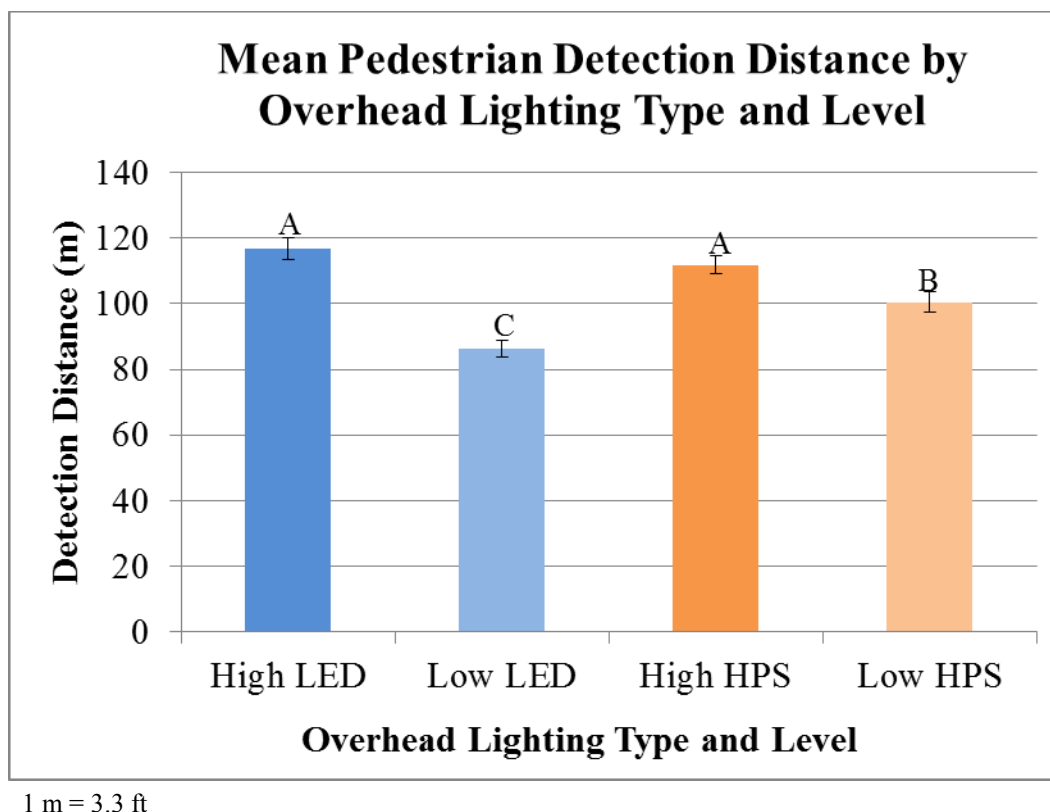
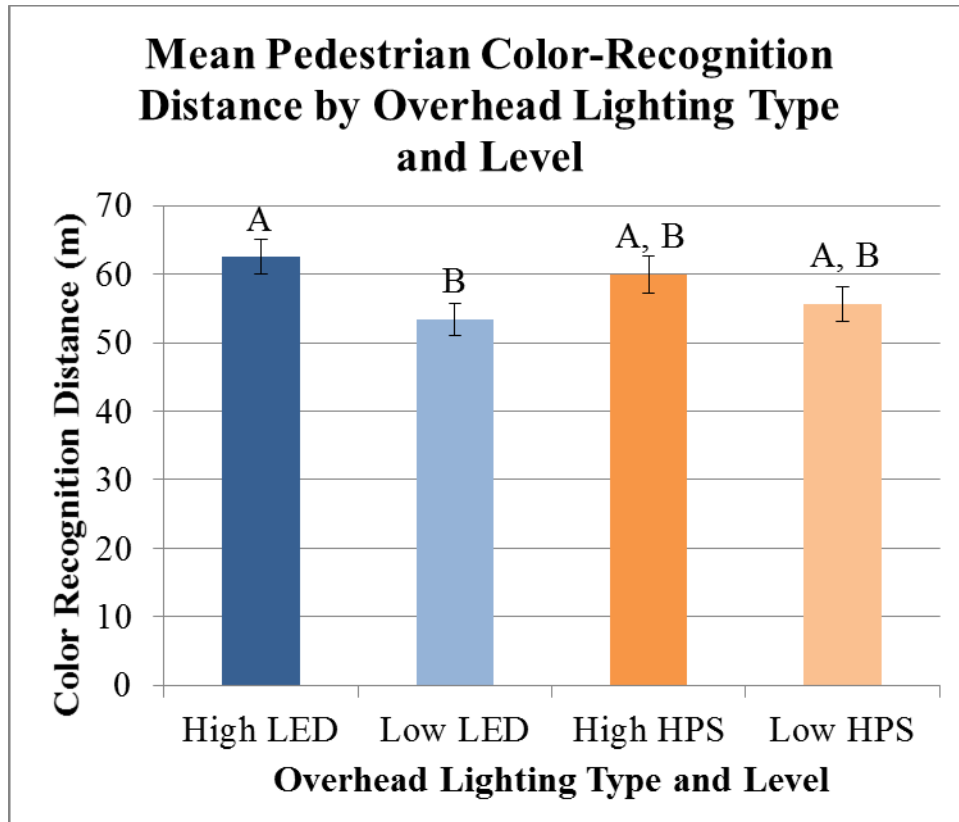


Figure 37. Chart. Scoping experiment—mean pedestrian-detection distance by overhead-lighting type and level, with SNK results.



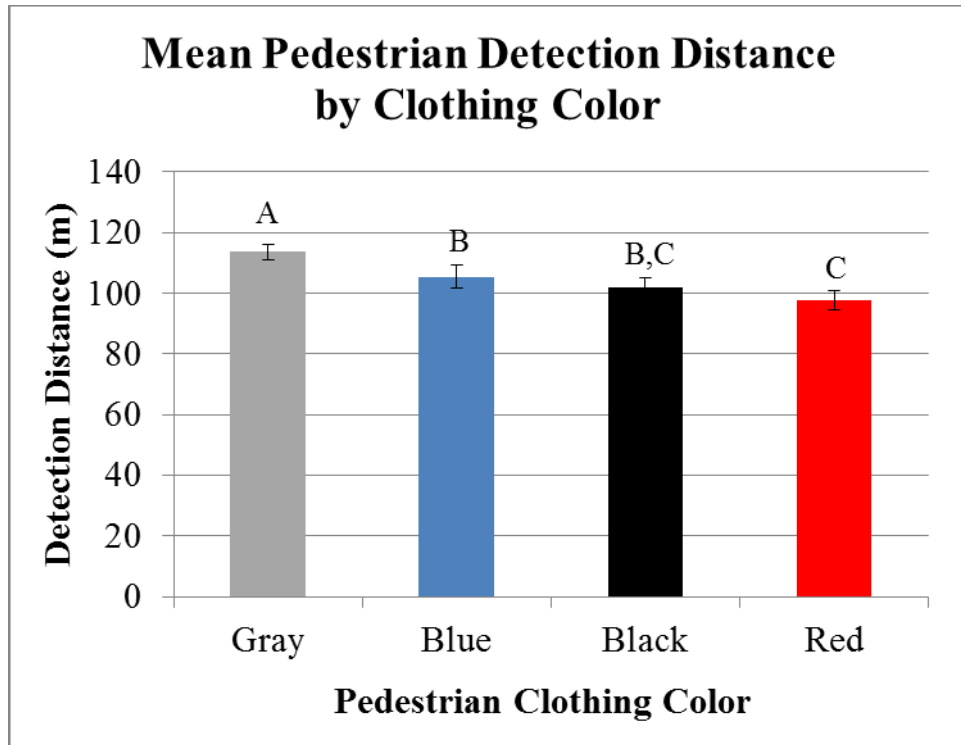
1 m = 3.3 ft

Figure 38. Chart. Scoping experiment—mean pedestrian color-recognition distance by overhead-lighting type and level, with SNK results.

Pedestrian Clothing Color:

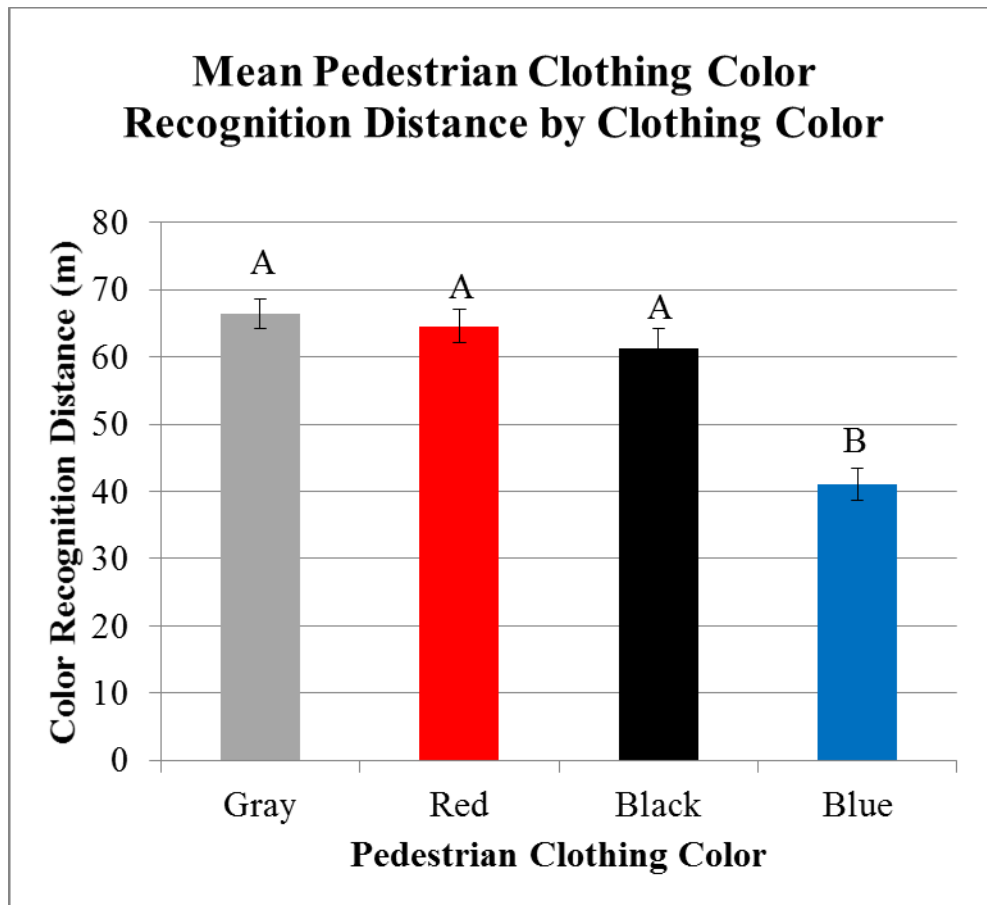
Pedestrian clothing color significantly affected detection distances. Figure 39 shows that when the four lighting conditions were compared, gray clothing was detected from significantly farther away than any other color, and red was detected from significantly closer than any other color. Bars sharing a letter are not statistically significantly different from each other.

Pedestrian clothing color also significantly affected color-recognition distance but in a different manner than detection distance. The pedestrian with blue clothing was detected, on average, at significantly shorter distances than the pedestrians wearing the other colors see (figure 40). Bars sharing a letter are not significantly different from each other.



1 m = 3.3 ft

Figure 39. Chart. Scoping experiment—mean pedestrian-detection distance by clothing color.



1 m = 3.3 ft

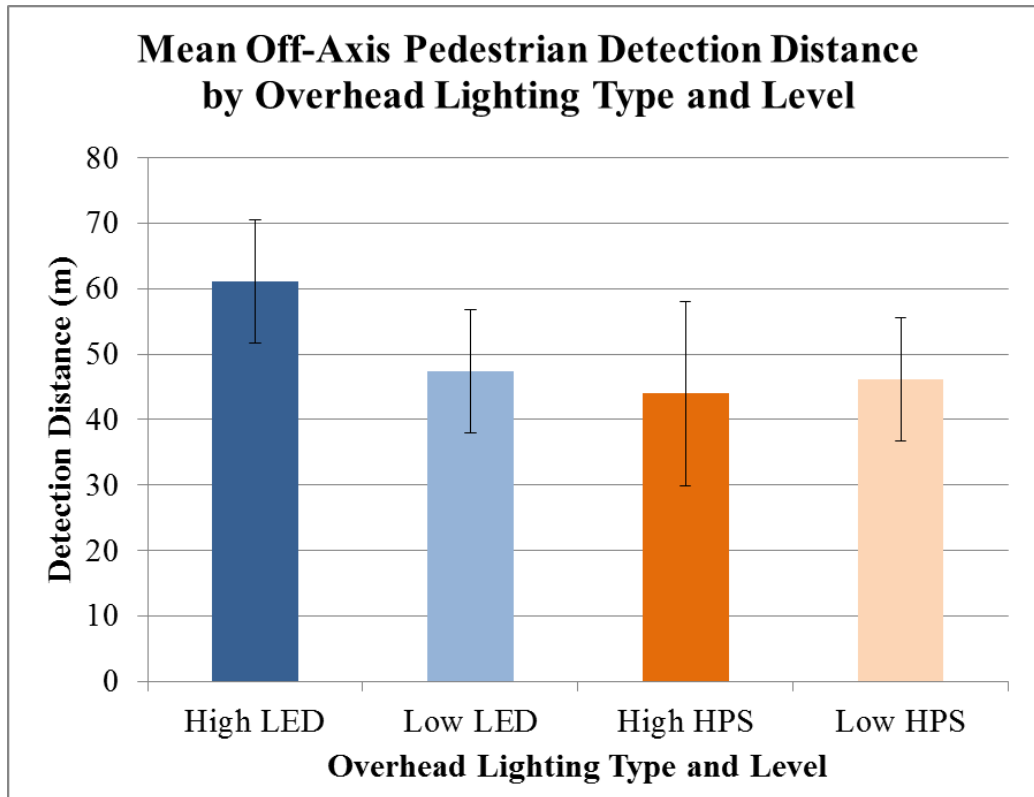
Figure 40. Chart. Scoping experiment—mean pedestrian clothing color-recognition distance by clothing color.

Off-Axis Pedestrian

Participants detected 23 percent of off-axis pedestrians. Participants had only five opportunities to detect off-axis pedestrians during the course of the experiment, too few to draw strong conclusions, and no effects were found to be significant. However, those results provided direction to the research team for future experiments and are discussed.

Overhead-Lighting Type and Level:

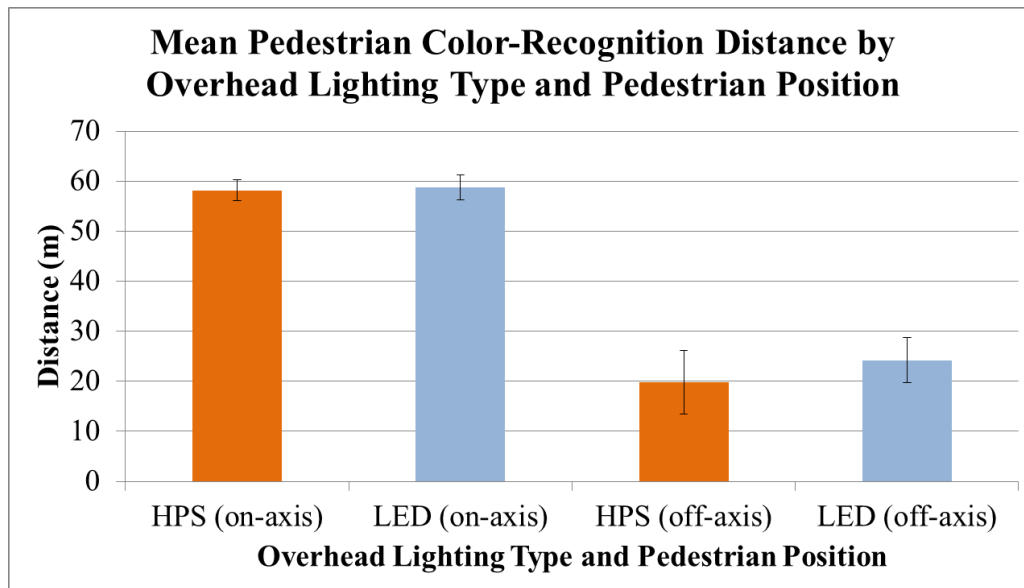
Off-axis pedestrians were detected from farther away, on average, in LED overhead lighting ($M = 55.7$ m (183 ft)) than in HPS overhead lighting ($M = 44.7$ m (147 ft)). The difference was not statistically significant, but it is in the expected direction, and overhead lighting is capable of off-axis illumination. In addition, when overhead lighting was broken down by color and level, off-axis pedestrians were detected from farthest away in high-level LED lighting, followed by low-level LED lighting. Those results show promise that LED lighting, efficient in the mesopic range, allowed objects on the road's periphery to be detected from farther away, more so than HPS lighting at higher levels. A comparison between on- and off-axis pedestrian-detection distances in the two lighting types is shown in figure 41.



1 m = 3.3 ft

Figure 41. Chart. Scoping experiment—mean off-axis pedestrian-detection distance by overhead-lighting type and level.

When overhead-lighting type and level were combined, they had a significant effect on off-axis pedestrian color-recognition distance. Participants recognized the color of off-axis pedestrian clothing color from farther away in LED lighting ($M = 24.2$ m (79.4 ft)), than in HPS lighting ($M = 19.8$ m (64.9 ft), $p > 0.05$). The results, shown in figure 42, were in the expected direction given off-axis spectral effects in the mesopic range but were not significant.



1 m = 3.3 ft

Figure 42. Chart. Scoping experiment—mean off-axis pedestrian color-recognition distance by overhead-lighting type and pedestrian position.

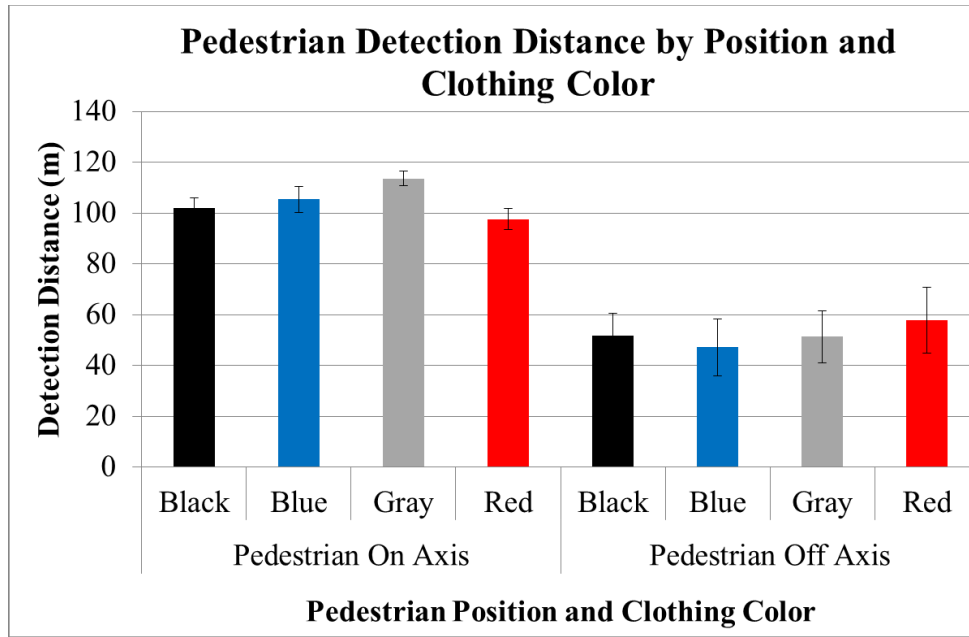
On- Versus Off-Axis Pedestrian

Overhead-Lighting Type:

Overhead-lighting type did not significantly affect color-recognition distance for either on- and off-axis pedestrians, but in both cases, the mean color-recognition distances for LED lighting were greater than for HPS. The effect was more so for the off-axis pedestrian, visible in figure 43. This could indicate a spectral effect in which bluer LED lighting, which is more efficient for off-axis mesopic vision than HPS lighting, led to better pedestrian detection. Subsequent experiments in this project examined off-axis object detection in detail.

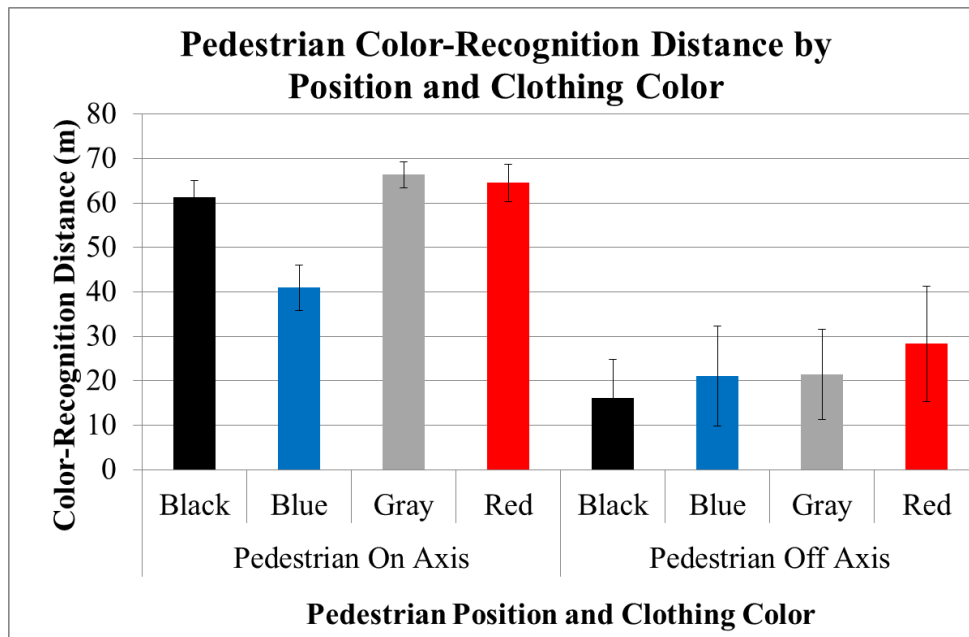
Clothing Color:

For on-axis pedestrians, blue clothing had a much shorter color-recognition distance than clothing of the other colors, but the same trend was not seen for off-axis pedestrians, nor for the detection distance of this blue-clothed pedestrian (figure 44). Theoretical explanations regarding human vision do not explain those findings. One environmental factor could be that the on-axis pedestrians were seen against the road, and the off-axis pedestrians were seen against the hills and brush on the roadside. It could be that the differently contrasting environments affected color recognition differently and unpredictably.



1 m = 3.3 ft

Figure 43. Chart. Scoping experiment—pedestrian-detection distance by position and clothing color.



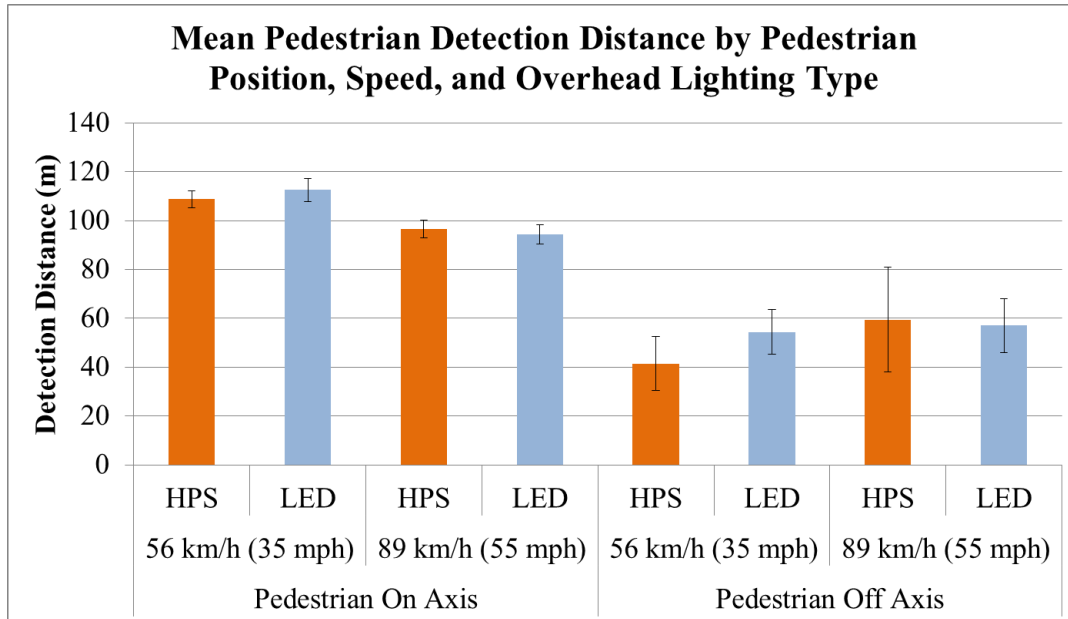
1 m = 3.3 ft

Figure 44. Chart. Scoping experiment—pedestrian color-recognition distance by position and clothing color.

Speed and Overhead-Lighting Type:

Overhead-lighting levels were pooled for this analysis. For on-axis pedestrians, mean detection distances at 89 km/h (55 mi/h) were shorter than at 56 km/h (35 mi/h), but the opposite trend,

visible in figure 45, was seen for off-axis pedestrians. The detection distance for 56 km/h (35 mi/h) was particularly short because detection distances for HPS were short. However, with so few detections of off-axis pedestrians, it is difficult to draw a firm conclusion that the shorter distance is due to the overhead-lighting type.



1 m = 3.3 ft

Figure 45. Chart. Scoping experiment—mean pedestrian-detection distance by pedestrian position, speed, and overhead-lighting type.

Constant Contrast Pedestrian

An analysis of the constant-contrast pedestrian found a significant effect of participant age on detection and color-recognition distances. Results for all factors are listed in table 10.

Table 10. Scoping experiment constant-contrast pedestrian results summary.

Factor(s)	Detection Distance <i>F</i>	Detection Distance <i>p</i>	Color-Recognition Distance <i>F</i>	Color-Recognition Distance <i>p</i>
Age	7.33	0.0113 ^a	1.43	0.2407
Headlamp Color	1.97	0.1712	0.24	0.6292
Age By Headlamp Color	2.82	0.1036	3.13	0.0874
Overhead-Lighting Type	3.66	0.1043	4.57	0.0763
Headlamp Color by Overhead-Lighting Type	7.46	0.0719	11.03	0.0800
Overhead-Lighting Level	0.84	0.3678	2.20	0.1489

^aSignificant at $p < 0.05$.

Overhead-lighting level and type did not significantly affect detection distance for the constant-contrast pedestrians. The constant-contrast pedestrian was in the same location for each

detection, with the same background, regardless of overhead-lighting level. Lower lighting levels had slightly longer detection distances for both overhead-lighting types, as shown in figure 46, but the effect was not statistically significant.

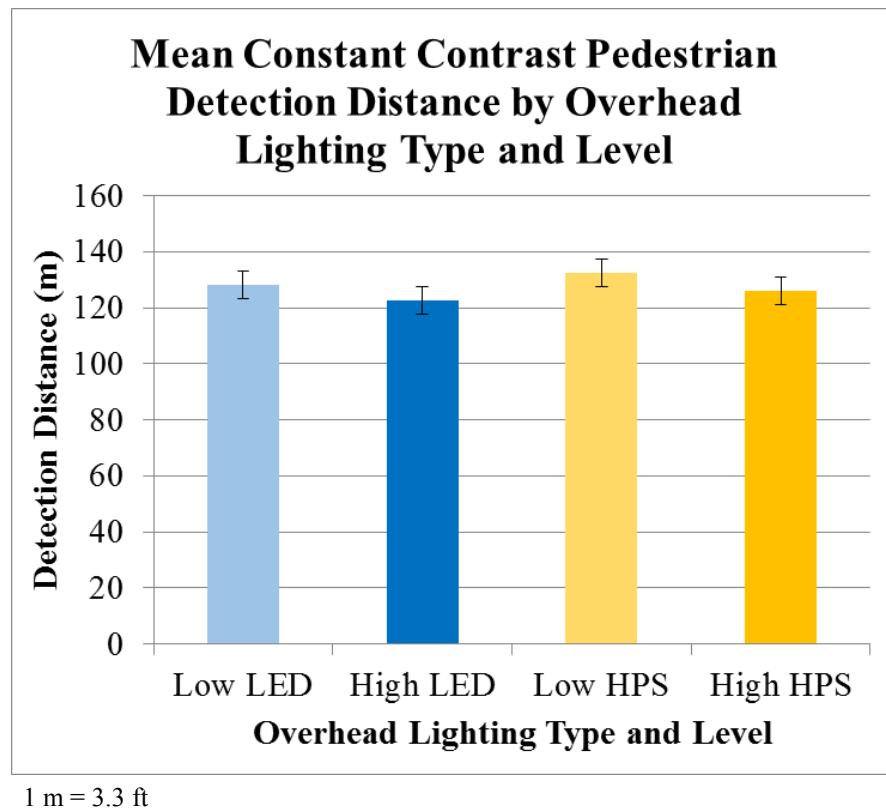


Figure 46. Chart. Scoping experiment—detection distances by overhead-lighting type and level for constant-contrast pedestrians.

Targets

The significant effects of the independent variables on detection and color-recognition distances of the targets for detections performed in overhead lighting are summarized in table 11.

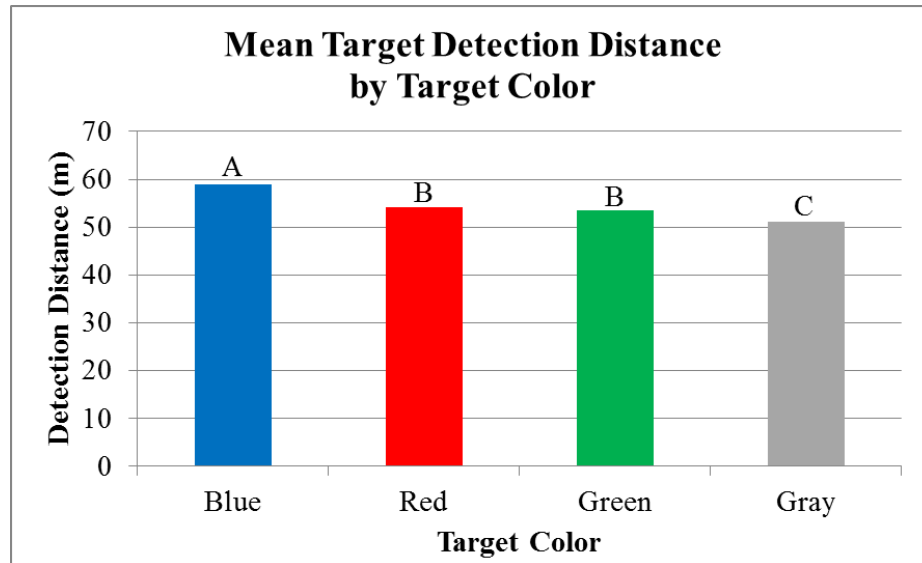
Table 11. Scoping experiment target results summary for overhead lighting.

Factor(s)	Detection Distance F	Detection Distance p	Color-Recognition Distance F	Color-Recognition Distance p
Target color	12.35	< 0.0001 ^a	3.6	0.0169 ^a
Target color by overhead-lighting type and level	1.32	0.2321	3.25	0.0018 ^a
Age	1.46	0.2372	0.39	0.5369
Headlamp color and intensity	1.51	0.2287	0.33	0.7186
Age by headlamp color and intensity	0.88	0.4196	0.59	0.5581
Age by target color	0.91	0.4406	0.45	0.7145
Headlamp color and intensity by target color	0.92	0.4833	0.83	0.5474
Overhead-lighting color and level	2.19	0.1013	0.67	0.5717
Age by overhead-lighting color and level	0.26	0.8525	0.07	0.9763
Headlamp color and intensity by overhead-lighting color and level	0.71	0.642	0.66	0.682

^aSignificant at $p < 0.05$.

Target Color:

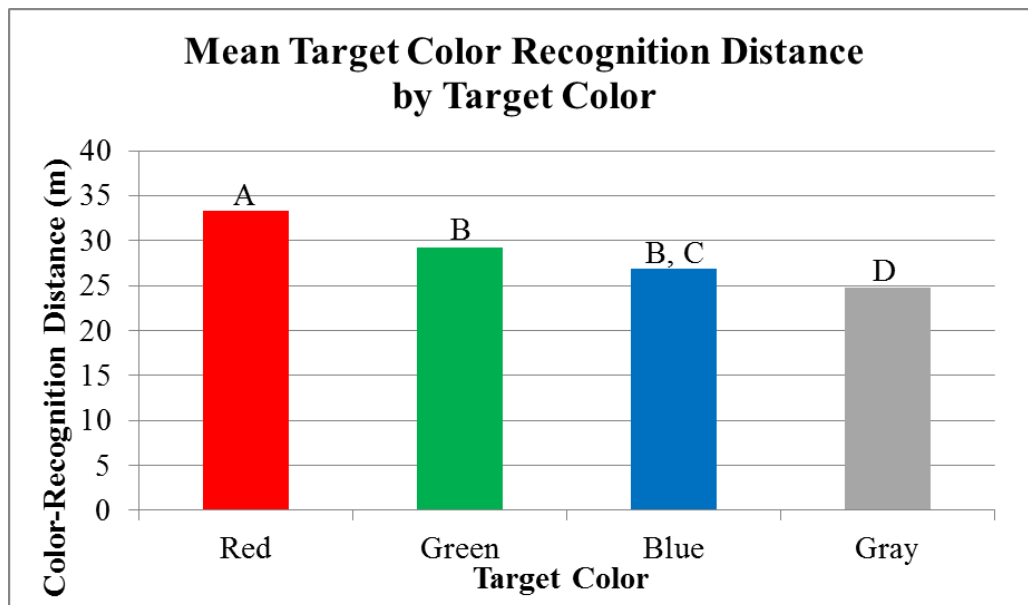
Only target color significantly affected target detection distances in all overhead-lighting conditions. When the four overhead-lighting conditions were combined, the blue target was detected from significantly farther away than the other targets, and the gray target was detected from significantly closer (figure 47), where bars sharing a letter do not statistically differ from each other. The road targets were detected on-axis, and color would not necessarily be prone to mesopic effects. More experiments were performed during this project to examine spectral effects in the mesopic range.



1 m = 3.3 ft

Figure 47. Chart. Scoping experiment—mean target-detection distance by target color.

Target color significantly affected target color-recognition distance. Red was detected from the farthest away, followed by green, blue, and gray (figure 48). All color-recognition distances differed significantly from each other. The color-recognition distances (red, green, blue, and gray) are in a different order than the detection distances (blue, red, green, and gray). That could be because of confusion between blue and green. Color contrast between the target and the background could have an effect, but the luminance camera did not take color-contrast data, so color contrast could not be analyzed.



1 m = 3.3 ft

Figure 48. Chart. Scoping experiment—mean target color-recognition distance by target color.

Target Color and Overhead-Lighting Type:

Target color and overhead-lighting type combined to affect target color-recognition distance. Overhead-lighting levels were pooled for this analysis. In LED lighting, the red and green targets were visible from a greater distance than in HPS lighting. That effect was not seen for the blue and gray targets, as shown in figure 49.

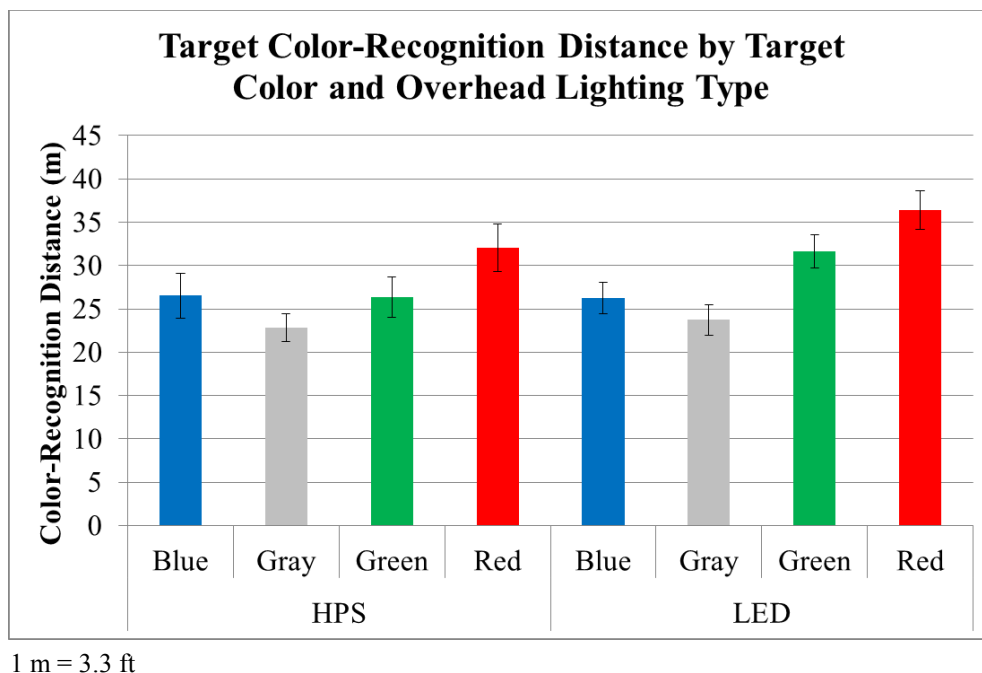


Figure 49. Chart. Scoping experiment—target color-recognition distance by target color and overhead-lighting type.

No Overhead Lighting

For experiments without overhead lighting, independent variables were analyzed with respect to pedestrian and target detection and color-recognition distances, and results are shown in table 12 for pedestrians and table 13 for targets. Results for off-axis pedestrians were not analyzed for runs without overhead lighting because there were too few detections for results to be meaningful.

Pedestrian

Table 12 summarizes scoping experiment results for pedestrians with no overhead lighting.

Table 12. Scoping experiment pedestrian results summary for no overhead lighting.

Factor(s)	Detection Distance F	Detection Distance p	Color-Recognition Distance F	Color-Recognition Distance p
Clothing Color	16.15	< 0.0001 ^a	21.04	< 0.0001 ^a
Age	1.25	0.2731	1.35	0.2539
Headlamp Intensity	0.77	0.3887	1.29	0.2659
Age by Headlamp Intensity	1.81	0.1895	4.3	0.077
Headlamp Color	0.04	0.8503	0.6	0.4446
Age by Headlamp Color	0.68	0.4151	0.06	0.8006
Headlamp Intensity by Headlamp Color	0.07	0.7876	0.02	0.9668
Age by Clothing Color	1.26	0.2943	1.75	0.163
Headlamp Intensity by Clothing Color	0.82	0.4886	0.16	0.9225
Headlamp Color by Clothing Color	0.46	0.7129	0.75	0.5266

^aSignificant at $p < 0.05$.

Pedestrian Clothing Color: Pedestrian clothing color significantly affected detection distance, with gray clothing being detected from significantly farther away than the other clothing colors ($p < 0.0001$) (figure 50). As shown in figure 50, the red and gray clothing colors had higher reflectances than the blue and black. When illuminated with vehicle headlamps alone, the higher-reflectance pedestrians were more positively contrasted and more visible.

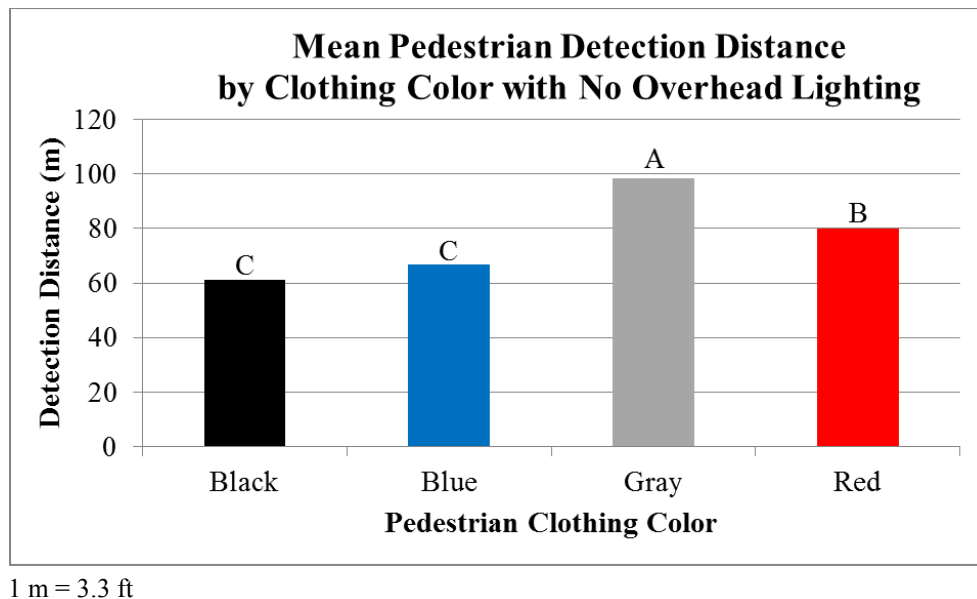


Figure 50. Chart. Scoping experiment—mean pedestrian-detection distance by clothing color for no overhead lighting.

Pedestrian clothing color significantly affected pedestrian clothing color-recognition distance ($p < 0.0001$) (figure 51). Pedestrians with red and gray clothing were recognized from farther away than with black and blue clothing. The similar and shorter color-recognition distances for black and blue might be because participants found it difficult to differentiate between the two dark colors. Target detection followed the same pattern.

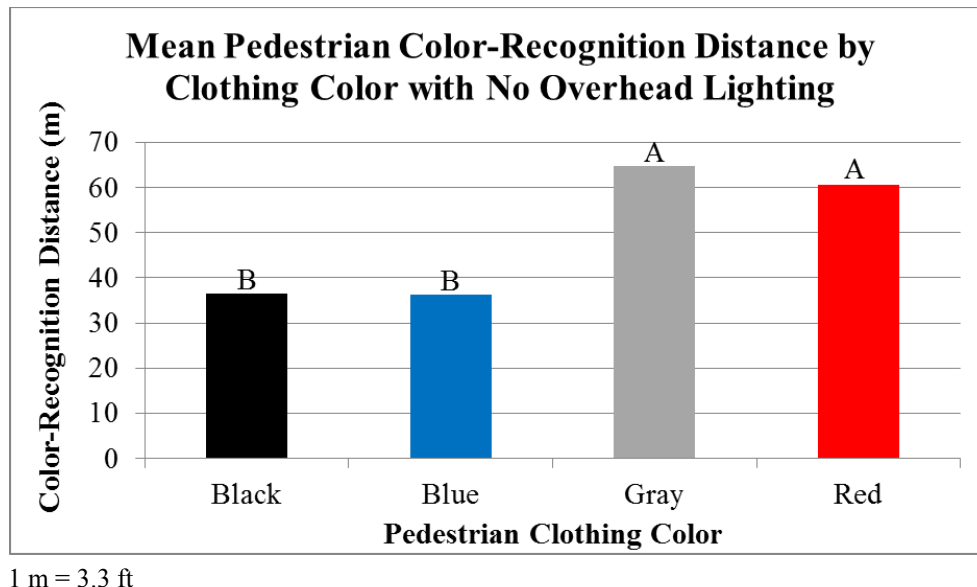


Figure 51. Chart. Scoping experiment—mean pedestrian color-recognition distance by clothing color for no overhead lighting.

Targets

Table 13 summarizes scoping experiment results for targets with no overhead lighting.

Table 13. Scoping experiment target results summary for no overhead lighting.

Factor(s)	Detection Distance F	Detection Distance p	Color-Recognition Distance F	Color-Recognition Distance p
Target Color	3.3	0.0242 ^a	3.1	0.0312 ^a
Age	0.71	0.4059	0.23	0.6335
Headlamp Intensity	4.29	0.0673	0.98	0.3303
Age by Headlamp Intensity	0.76	0.3919	0.04	0.8467
Headlamp Color	0.34	0.565	0.11	0.7469
Age by Headlamp Color	0.08	0.7856	0.37	0.5462
Headlamp Intensity by Headlamp Color	3.3	0.0801	1.75	0.1975
Age by Target Color	0.5	0.6818	0.3	0.827
Headlamp Intensity by Target Color	1.03	0.3854	0.87	0.4614
Headlamp Color by Target Color	1.11	0.3492	2.65	0.0572

^aSignificant at $p < 0.05$.

Target Color:

Target color significantly affected target detection distance ($p = 0.0242$), with gray targets detected from significantly farther away than green targets, but no other pairwise comparisons were significant (figure 52).

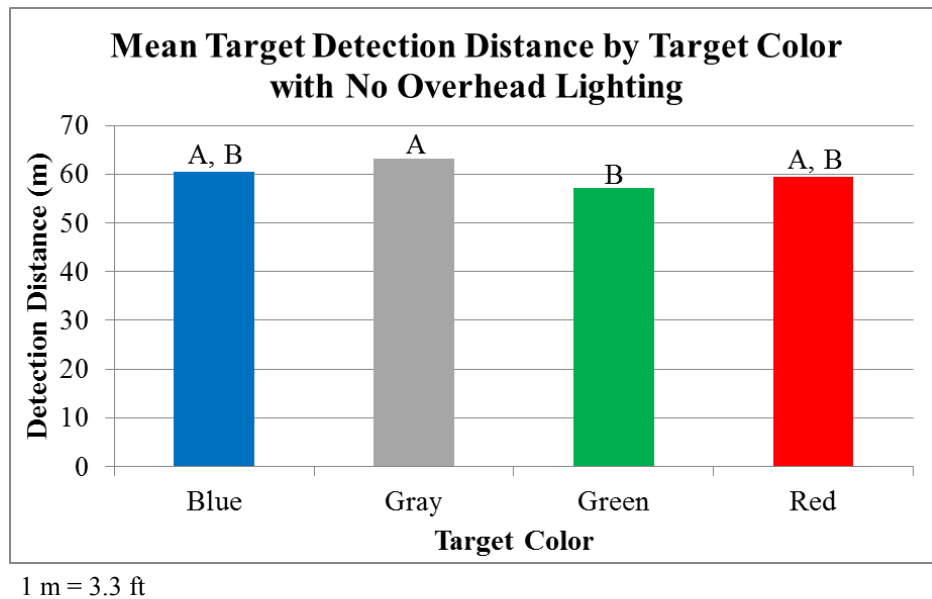
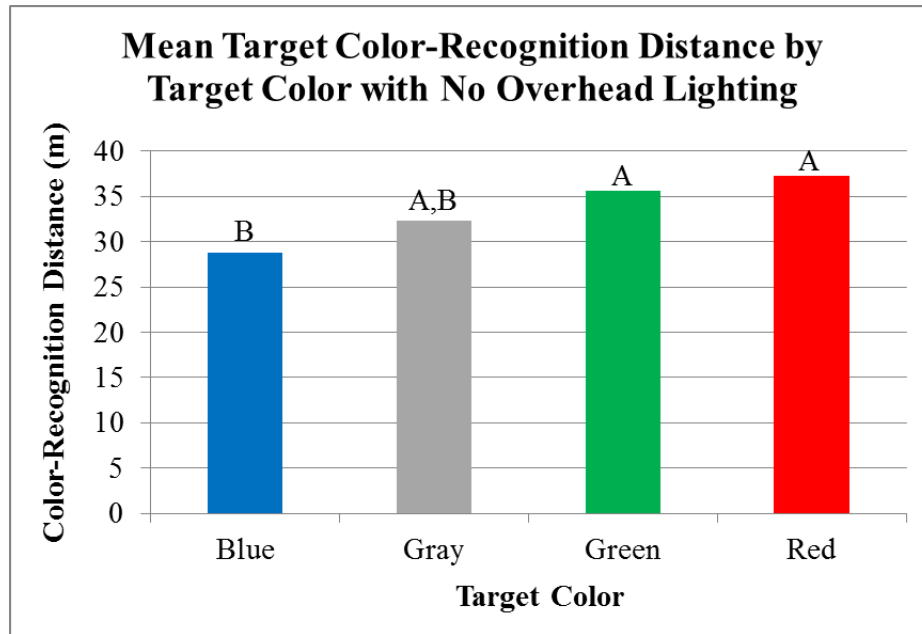


Figure 52. Chart. Scoping experiment—mean target-detection distance by target color for no overhead lighting.

Target color significantly affected color-recognition distance, with red and green target colors recognized from significantly farther away (red $M = 37.3$ m (122 ft); green $M = 35.6$ m (117 ft)) than blue targets ($M = 28.8$ m (94.4 ft), $p = 0.0312$) (figure 53).



1 m = 3.3 ft

Figure 53. Chart. Scoping experiment—mean target color-recognition distance by target color for no overhead lighting.

Luminance Analysis

Luminance camera images taken at the moment a participant detected a pedestrian or target were analyzed. They were also analyzed at color recognition, but those results largely mirrored the detection results and are not discussed. Luminance analyses were only performed for runs with overhead lighting.

Pedestrian-Detection Distance

Luminance:

At the moment participants detected pedestrians under HPS lighting, the average pedestrian luminance was 0.327 cd/m^2 (0.095 fL), less than that in LED lighting, 0.464 cd/m^2 (0.14 fL). Figure 54 shows a threshold at a luminance of approximately 0.2 cd/m^2 (0.06 fL) where on-axis pedestrians, regardless of clothing color, were able to be detected.

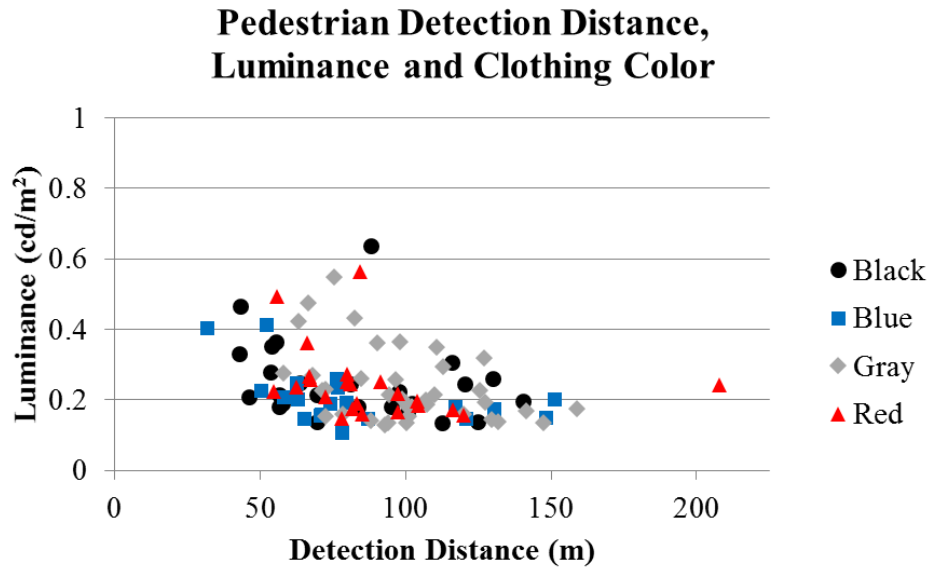


Figure 54. Scatter Plot. Scoping experiment—pedestrian-detection distance, luminance, and clothing color.

Contrast:

The average contrast when pedestrians were detected was also different between the lighting types, with the contrast in HPS lighting at -0.086 and LED lighting at -0.032. A lower negative contrast, as seen in HPS lighting, means a darker pedestrian with respect to the background was needed than in LED lighting.

When further broken down by clothing color, a combined effect of clothing color and lighting type on contrast at time of detection is seen in figure 55. For all clothing colors except red, pedestrians were more highly contrasted in LED lighting than in HPS lighting, as measured by detection distance. In HPS lighting, red clothing requires the lowest contrast for detection, meaning it is particularly visible in that lighting type. The opposite trend is seen in LED lighting, where red requires the greatest contrast for detection, meaning it is less visible in that lighting type. That is because the spectrum of HPS lighting is redder than that of LED lighting, making red clothing visible, while the opposite is true in LED lighting.

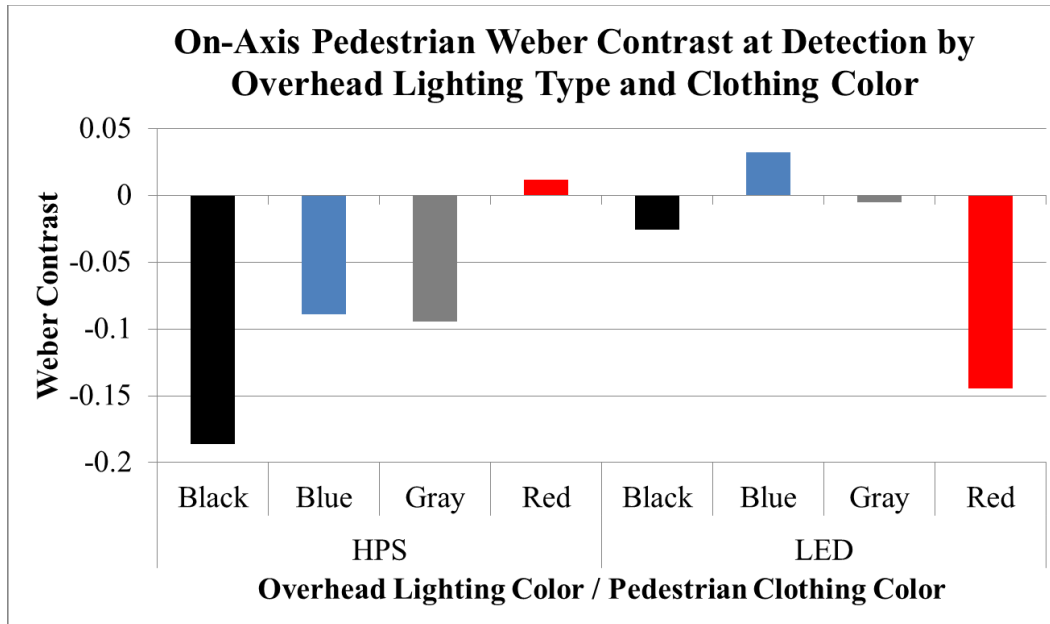


Figure 55. Chart. Scoping experiment—pedestrian mean Weber contrast at time of detection by overhead-lighting color and clothing color.

Uniformity:

LEDs have a more uniform horizontal light distribution than HPS sources, as shown in figure 56, where the photo of HPS lighting has bright streaks across the road, and the photo of LED lighting does not. Even though VI on the pedestrians was matched between HPS and LED lighting, less negative contrast was needed in LED lighting for pedestrian detection. That is because HPS lighting created bright lines across the roadway that increased background luminance values and therefore increasing the absolute contrast.

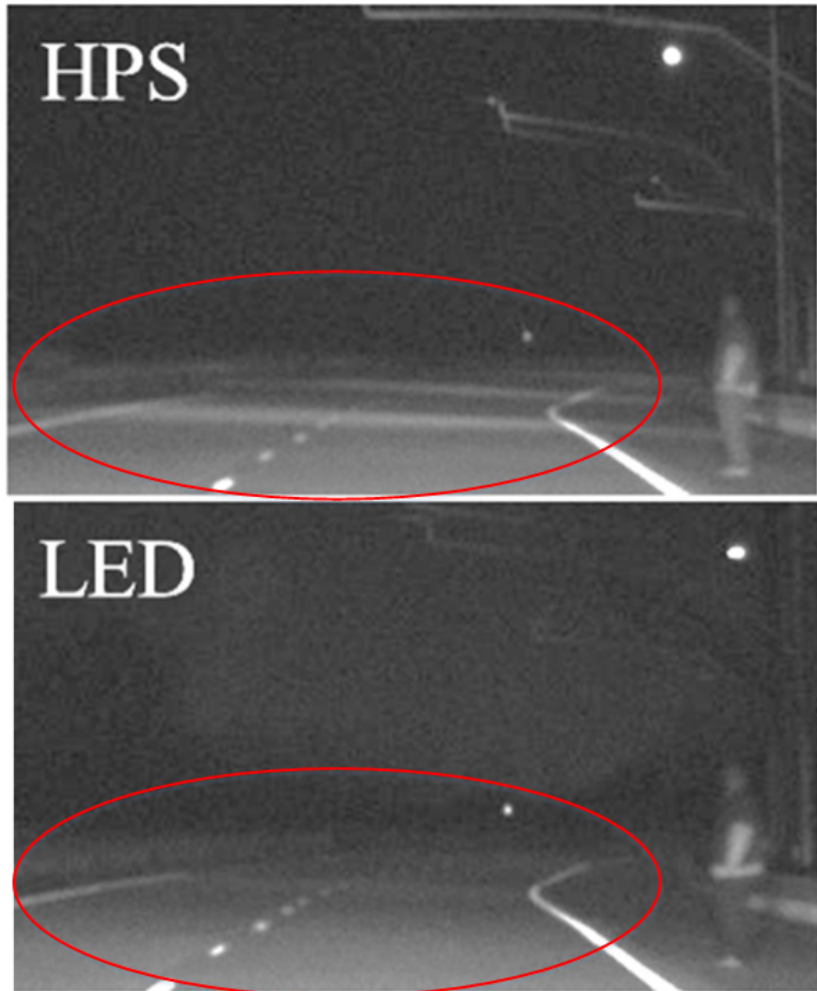


Figure 56. Photo. Uniformity of HPS and LED lighting.

Target Detection Distance

Luminance:

At the moment participants detected targets under HPS lighting, the average target luminance was 0.916 cd/m^2 (0.267 fL), greater than that in LED lighting, 0.683 cd/m^2 (0.199 fL). There appears to be a threshold at a luminance of approximately 0.2 cd/m^2 (0.06 fL) where targets were detected, shown in figure 57.

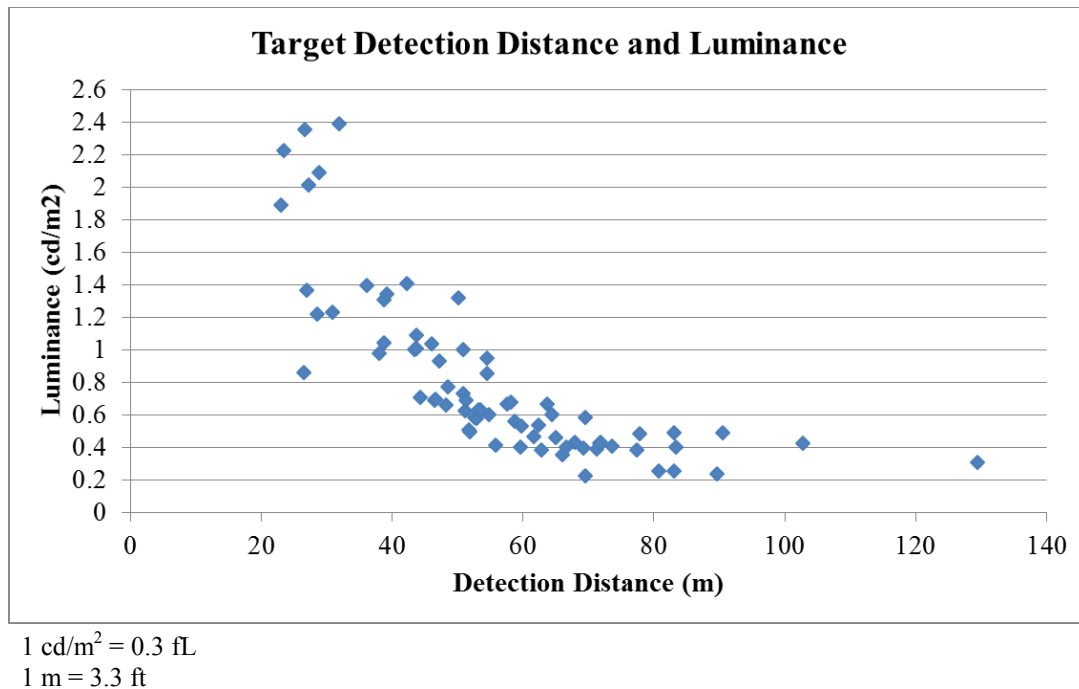


Figure 57. Scatter Plot. Scoping experiment—target-detection distance and luminance.

Contrast:

The average contrast when targets were detected was also different between the lighting types, with the contrast in HPS lighting at 0.788 and LED lighting at 0.734. Unlike the pedestrians, the targets were in positive contrast at detection. Similar to the pedestrians, a higher absolute contrast was needed in HPS than LED lighting to detect the targets.

DISCUSSION

The study considered many factors, including overhead-lighting type (2,100-K HPS and 6,000-K LED) and intensity, and headlamp color and intensity.

A project objective was to measure the combined effect of vehicle headlamps and overhead lighting on visibility. Results of this experiment indicated that headlamp color and intensity did not significantly affect detection and color-recognition distances. While that result may be expected in situations where the overhead lighting is the predominant lighting source, when there was no overhead lighting present and the driver relied solely on headlamp light, there was still no statistically significant difference in visibility between the white/blue or white/yellow headlamps or between high- and low-powered headlamps. That result held true for detection and color-recognition for both targets and pedestrians. Interestingly, results were closest to approaching significance for targets positioned low to the ground in the dark section of the road. A possible explanation for this could be that the beam pattern of the headlamps is critical for highlighting low targets on the roadway.

The project also aimed to measure the impact of spectra of overhead-lighting systems on visibility, another project objective. The results regarding the effect of overhead-lighting type,

(HPS with a correlated color temperature of 2,100 K and LED with a correlated color temperature of 6,000 K) and overhead-lighting intensity on pedestrian detection were mixed. For the constant-contrast pedestrian, there was no significant difference between the effects of overhead-lighting type and effects of level of the overhead lighting on detection distance. However, results combining all pedestrian locations indicated a very strong impact of overhead-lighting type and level on pedestrian-detection distance. This is an interesting result because it highlights the importance of contrast for detection. A few aspects of the experiment could have produced this result. First, constant-contrast pedestrians only wore gray clothing, so interactions between the spectral distribution of the overhead lighting and clothing color contrast would not be present. Second, this task was likely foveal, so mesopic effects would be minimal. The constant-contrast result shows that contrast is by far the more dominant impact on detection compared with other factors such as overhead-lighting SPD and intensity. It also demonstrates that the spectral effects are by far more evident in the periphery, as shown by the off-axis results and by the fact that changing the light source spectrum did not improve performance when all other factors were controlled.

Despite informing participants that pedestrians could be located both along the roadway and off to the side of the roadway, there were very few detections of off-axis pedestrians. The low detection rate for the off-axis pedestrians did not produce enough data to draw firm conclusions. However, for off-axis pedestrians, high-level LED overhead lighting resulted in a greater detection distances than high-level HPS overhead lighting; the same was not true for low-level lighting. The results were not statistically significant but are worth considering because they might indicate an effect of the overhead lighting's uniformity. One possible reason for the greater detection distances in high-level LED lighting could be the distribution of the light source and how it illuminates the environment outside the roadway. The off-axis pedestrians stood on a grassy and rocky area, much less uniform than a typical roadway surface. The LED overhead lighting was more uniformly distributed than the HPS lighting. Thus, the more-uniform LED overhead lighting combined with the less-uniform background for off-axis pedestrians could have allowed participants to detect those pedestrians from farther away.

CONCLUSIONS

A research objective of this experiment was to evaluate the effect of the spectral distribution of overhead-lighting sources on drivers' ability to detect pedestrians and targets and recognize colors in the environment. Results found that overhead-lighting type and level significantly affected detection and color-recognition distances for pedestrians, with brighter lighting corresponding to longer detection and color-recognition distances. The effect of a change in overhead-lighting level for a particular type of lighting was significant. For example, lighting level significantly affected detection and color-recognition distances for LED lighting. For HPS lighting, lower levels of lighting also resulted in shorter detection and color-recognition distances, but the effect was not significant. The different results for LED and HPS lighting indicate a spectral effect occurred with the LED lighting that did not occur with HPS lighting.

Another research objective for this experiment was to evaluate the impact of spectral distribution of overhead lighting and headlamp lighting on detection of pedestrians and targets located peripherally. Results indicate that, for off-axis pedestrians, LED overhead lighting had greater

(though not statistically significantly greater) color-recognition distances than HPS lighting, possibly indicating a spectral effect of overhead-lighting type.

Evaluating the effect of the spectral distribution of vehicle headlamp color on drivers' ability to detect pedestrians and targets and recognize colors in the environment was an additional research objective. Results found that headlamp color and intensity did not significantly affect detection and color-recognition distances when overhead lighting was used. Because overhead lighting had a greater effect on visibility than headlamps, overhead lighting was the focus of subsequent experiments.

Other noteworthy results include that age significantly affected detection distances when there was overhead lighting but not without overhead lighting. Age-related response times might have been a factor, but responses were not corrected for this factor. Also, age-related response times would not explain why age significantly affected detection distances in overhead lighting only. Age effects were not a main research objective, and these results were not further analyzed in this experiment.

Pedestrian clothing color and target color both significantly affected detection and color-recognition distances, whether or not overhead lighting was used. The best and worst colors for detection and color recognition varied between pedestrians and targets, and between whether or not there was overhead lighting, as listed in table 14. However, clothing and target color were not the focus of this project on light-source spectra.

Table 14. Scoping experiment best and worst colors for target and pedestrian detection and color recognition, with and without overhead lighting.

Condition	Dependent Variable	Color	On-Axis Pedestrian	Off-Axis Pedestrian	Target
Overhead lighting	Detection distance	Best	Gray	Red	Blue
Overhead lighting	Detection distance	Worst	Red	Black	Gray
Overhead lighting	Color-rec. distance	Best	Gray	Red	Red
Overhead lighting	Color-rec. distance	Worst	Blue	Black	Gray
No overhead lighting	Detection distance	Best	Gray	N/A	Gray
No overhead lighting	Detection distance	Worst	Black	N/A	Green
No overhead lighting	Color-rec. distance	Best	Gray	N/A	Red
No overhead lighting	Color-rec. distance	Worst	Blue	N/A	Blue

rec. = Recognition.

N/A = Not applicable.

The uniformity of the overhead lighting appeared to affect the results. At the time of detection, pedestrians contrasted more against the background under HPS lighting than under LED lighting, likely because HPS lighting was less uniform and created bright lines across the roadway. Future experiments included HPS and LED lighting to further investigate the effect of the overhead lighting's uniformity on object detection.

Design of Further Experiments

The results of the scoping experiment were used to inform the design of the subsequent phase of the project. This project's subsequent investigation of the spectral impact of the overhead-lighting sources included the following efforts:

- Evaluate the full range of the spectral impact of the light source on the visibility of both on-axis and off-axis targets because the scoping experiment showed that a wider range of off-axis detection objects was required to more fully describe the impact of overhead lighting's spectral effect.
- Test an MPI peripheral highlighting system's effectiveness in increasing off-axis pedestrian visibility, possibly increasing detection rates from the very low 23-percent rate found in the scoping experiment.
- Evaluate further the interaction of overhead lighting and headlamps on visibility because results from the scoping experiment regarding this interaction were not statistically significant.
- Evaluate the effectiveness of the CIE-developed mesopic model for describing nighttime driving visibility conducted both in a static and a dynamic environment because the scoping experiment was not specifically designed to address this project objective.

LIMITATIONS

Participant fatigue and learning effects might have affected the results. There were too few off-axis detections to draw strong conclusions regarding off-axis detection.

CHAPTER 5. MPI SYSTEM PERFORMANCE EXPERIMENT

INTRODUCTION

As discussed earlier, one promising technology for increasing pedestrian and object visibility on nighttime roadways is an MPI system that would detect and highlight crash hazards. With this technology, objects located in the areas of a driver's peripheral vision could be illuminated more effectively than with a traditional headlamp design. With illuminating objects in a driver's peripheral vision comes the consideration of how a driver's eyes process headlamp color. It is also worth exploring driver reactions to that technology. For example, it is unknown whether moving headlamps would distract drivers to the extent that visibility would be decreased instead of increased. Therefore, the goal of this experiment was to test the visual performance and extent of distraction of participant drivers using an MPI system to relate such a system to detection and recognition of color located in the periphery of driver's visual field.

Designing an actual MPI system was outside the scope of this project. However, a mockup MPI system that could not detect pedestrians but instead moved the headlamps to illuminate pedestrians at predetermined locations, was designed, built, and used. The MPI system behaved in two ways, either turning on the headlamp at a set distance and spot-lighting the pedestrian for a short period of time, or swiveling the headlamp to keep the pedestrian in its beam while the vehicle approached. Two headlamp colors were used—the white/yellow and white/blue used in the scoping experiment—but only the high-intensity filters were used. Because small target detection is difficult using machine vision software, MPI systems would likely be designed to illuminate only pedestrians. Thus, this experiment used pedestrians only to test visibility. Pedestrians were placed on both sides of the road and wore two clothing colors.

Detection distance, detection rate, and color-recognition distance quantified visual performance. A major concern with using MPI systems is the extent to which they would distract the driver. Detection distances cannot entirely capture driver distraction, so an eye tracker was used in this experiment to measure the driver's fixation duration.

Research Objectives

One of this project's objectives was to evaluate the impact of a peripheral illumination system on driver visual performance. To achieve that objective, the purpose of the MPI system performance experiment was to evaluate the following:

- How different highlighting behaviors of the MPI system affect driver visual performance.
- How the MPI system and overhead lighting interact to affect driver visual performance.
- How different headlamp colors on an MPI system affect driver visual performance.
- How an MPI system affects driver eye-glance behavior.

EXPERIMENTAL DESIGN

A mixed-factors experiment was conducted investigating the effects on participant detection distances and detection rates and on participant eye-glance behavior. Factors considered were participant age, headlamp color, overhead-lighting level, MPI system configuration, pedestrian position, pedestrian clothing color, and whether the pedestrian was illuminated. Variables are listed in table 15 and table 16.

Table 15. MPI system performance experiment independent variables and values.

Independent Variable	Levels
Age	Younger (25–35), Older (65+)
Headlamp Color	White/Yellow, White/Blue
Overhead Roadway Lighting Level	On, Off
MPI System Configuration	Highlighting, Tracking, Off
Pedestrian Position on Road	Left, Right
Pedestrian Clothing Color	Red, Blue
Pedestrian Illumination by MPI System	Yes, No

Table 16. MPI system performance experiment dependent variables and measurement method.

Dependent Variables	Measurement Method
Pedestrian-Detection Distance	Participant first sees pedestrian
Pedestrian Color-Recognition Distance	Participant first correctly identifies pedestrian clothing color
Fixation Duration	Measured with eye tracker

Independent Variables

Age

For the same reason as in the scoping experiment, this experiment included two age groups: younger (25–35) and older (65+).

Headlamp Color

Two headlamp configurations were used in this experiment: white/yellow high intensity and white/blue high intensity. The high-intensity filters were used because they more closely matched the intensity of headlamps on the market.

MPI System Configuration

The purpose of this experiment was to measure driver reactions to a system with moving headlamps that illuminate pedestrians, rather than to develop a full-featured working MPI system. Therefore, the team designed and built a mockup MPI system with headlamps swiveled and aimed according to a predetermined program, rather than by detecting the pedestrians in real time. The headlamps are shown in figure 58.

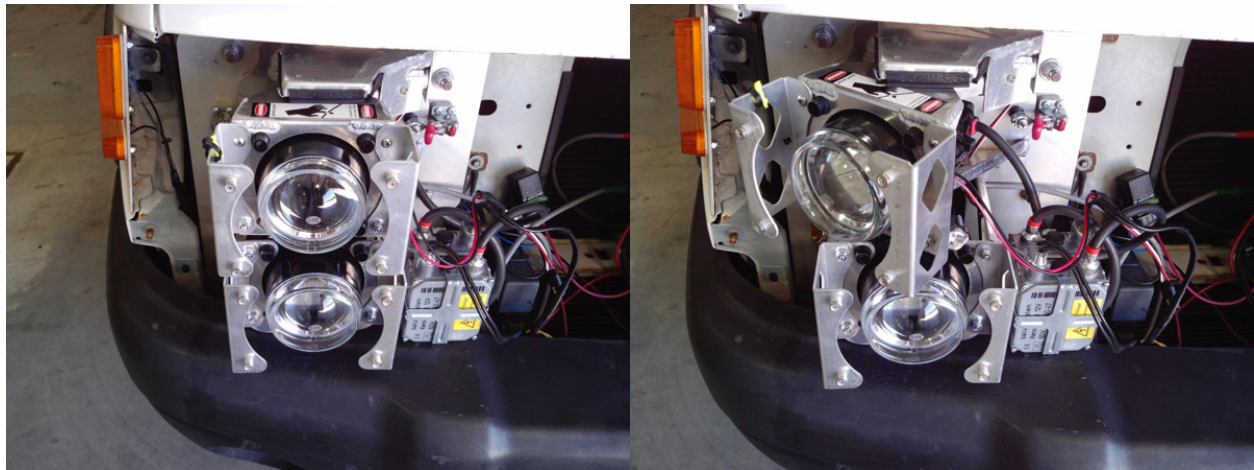


Figure 58. Photo. MPI system with straight (left) and swiveling (right) headlamp.

Confederate pedestrians stood on the roadway in the positions the headlamps were programmed to illuminate. The mockup MPI system had three configurations. The first was highlighting, in which the system would aim a headlamp at a pedestrian and turn it on momentarily, illuminating the pedestrian for a short period of time. Highlighting occurred when the vehicle was about 46.7 m (150 ft) from the pedestrian, and only the headlamp closest to the pedestrian would highlight him or her. The second MPI system configuration was tracking, in which the MPI system turned on the headlamp closest to the pedestrian when the vehicle was about 183 m (600 ft) from him or her and then swiveled the headlamp to keep the pedestrian in the beam as the vehicle approached. The last configuration was when the MPI system was off, with the headlamps aimed down the roadway as in a normal vehicle. The three MPI system configurations are illustrated in figure 59. The MPI system illuminated pedestrians on both sides of the road.

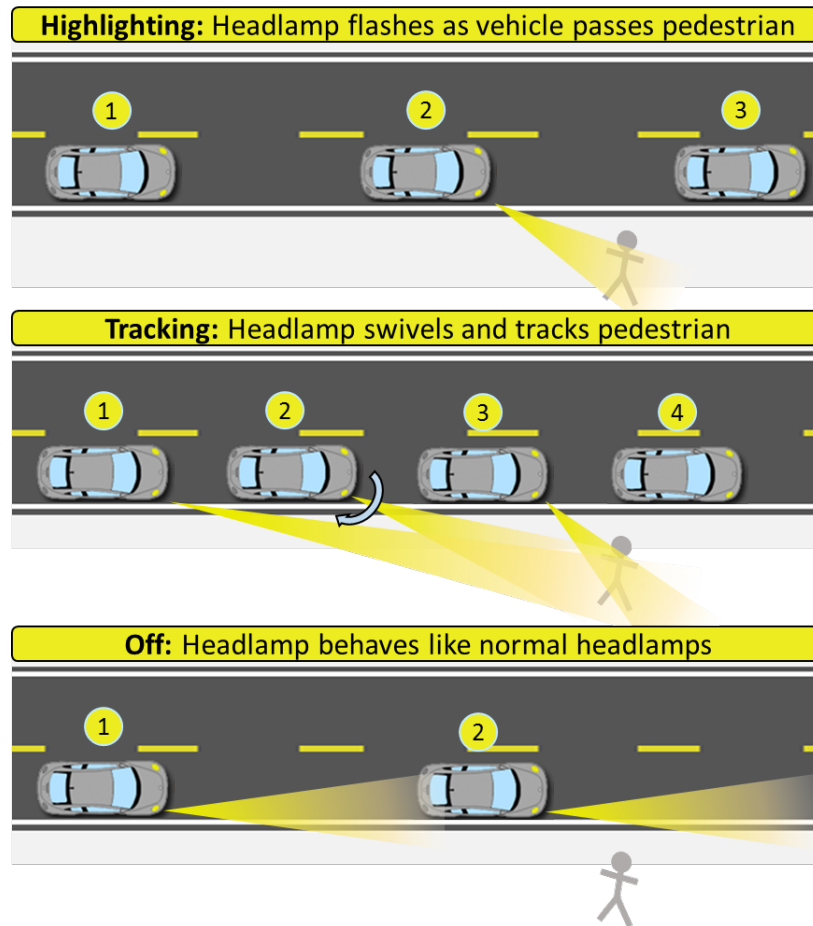


Figure 59. Diagram. MPI system performance experiment—MPI system configurations.

Pedestrian Clothing Color

Pedestrians wore blue or red scrubs. The blue color was chosen because both the 6,000-K LED overhead lighting and white/blue headlamps have strong blue components. The red was chosen because the white/yellow headlamps have a strong amber component. Both red and blue are common clothing colors.

Pedestrian Stations

Pedestrians were placed at various locations along the road to create the independent variables described in the following sections. All pedestrian stations were placed away from curves in the road, so line-of-sight would not be shorter than the detection distance. Stations were placed far enough apart so that participants would not detect two pedestrians at two different distances at the same time. VI on the pedestrians' faces was kept constant at 0.40 lx (.037 fc) for all pedestrian stations. Although the pedestrians' faces were illuminated at 0.40 lx (0.037 fc), the background behind the pedestrians was necessarily different, creating different contrasts.

Pedestrian on Left or Right

Pedestrians were placed on the left-hand or right-hand side of the roadway with respect to the oncoming vehicle, approximately 12 m (40 ft) away from the shoulder.

Pedestrian in Overhead Lighting

Pedestrians stood at five different stations. Two of those stations were illuminated by overhead lighting, and three were not. The areas with overhead lighting used 6,000-K LED luminaires dimmed to 20 percent. At that dim level, the horizontal illuminance was 1.97 lx (0.183 fc) when measured on the ground, halfway between two luminaires, on the shoulder of the road opposite the luminaires. That dim level also resulted in a VI of 0.40 lx (0.037 fc) on the pedestrian's face and enabled researchers to consistently illuminate the pedestrians in the sections of the road with overhead lighting.

Pedestrian Illuminated by MPI System

To test whether the MPI system would distract drivers from seeing pedestrians or objects outside of its beam path, some runs were performed with a pedestrian on the side of the road opposite from where the MPI system illuminated, illustrated in figure 60.

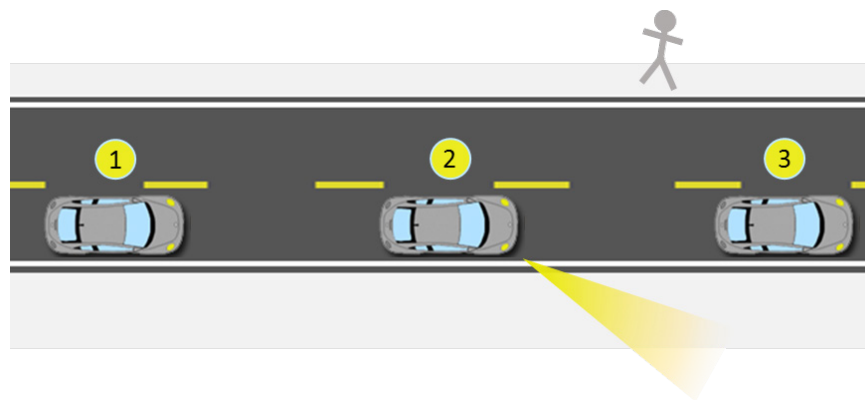


Figure 60. Diagram. MPI system performance experiment—pedestrian opposite from area illuminated by MPI system.

Dependent Variables

Detection and color-recognition distances were measured in this experiment, as described in chapter 3. Orientation-recognition distance was not measured, and pedestrians faced the same direction for all runs. Fixation duration was also measured and is described the following subsections.

Fixation Duration

Fixation duration was measured using an Arrington Research ViewPoint EyeTracker® and its accompanying software. The eye tracker was mounted on a pair of clear goggles with two cameras, one under each eye, to determine the direction the pupil was aimed. A third camera mounted on the bridge of the goggles was aimed forward to record the scene the user was seeing.

After calibration, the software overlays a dot corresponding to gaze direction onto the video from the forward-facing camera, and researchers then use the dot to determine where the participant was looking at any point in time. The eye-tracker goggles are shown in figure 61, and screenshots from the eye tracker software showing pupil identification and dot overlaid on a scene are shown in figure 62.



Figure 61. Photo. MPI system performance experiment—eye-tracker goggles.

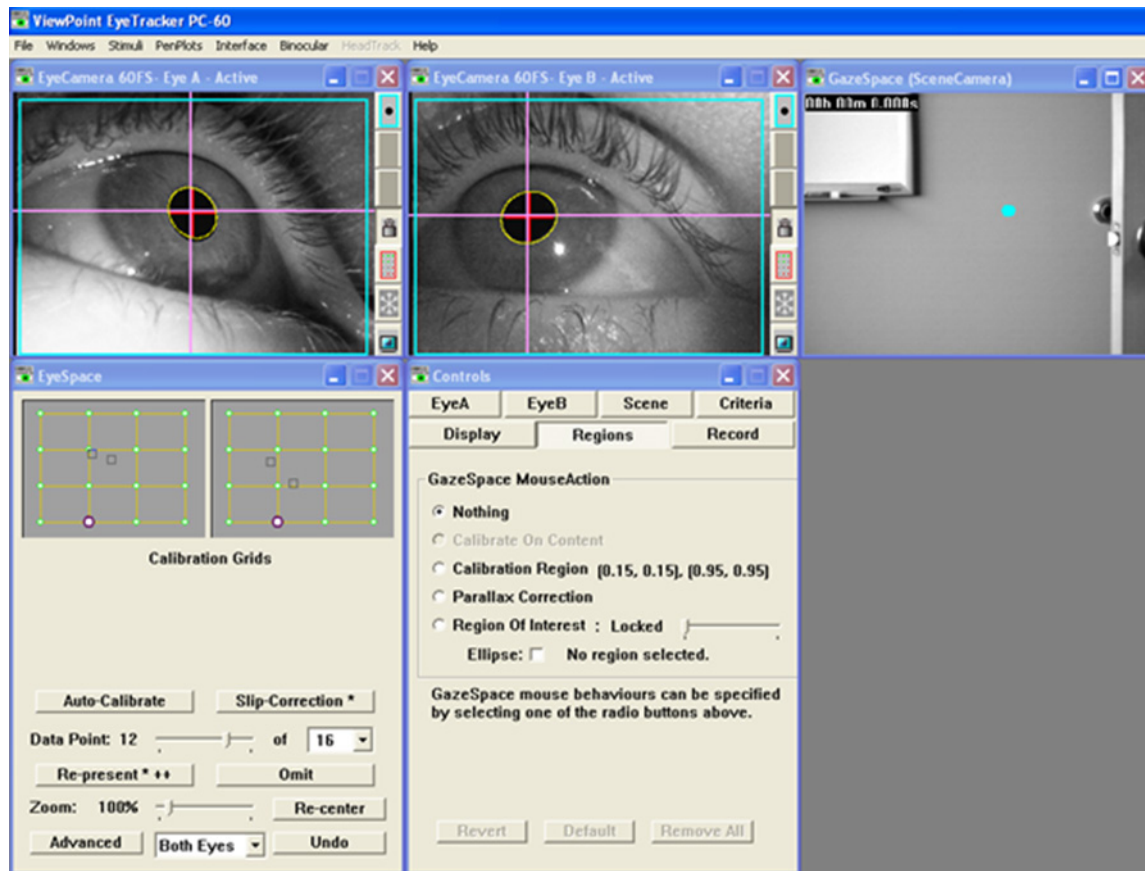


Figure 62. Screenshot. MPI system performance experiment—pupil location (left) and dot representing gaze direction overlaid on scene (right).

Facilities and Equipment

The experiment was performed on the Smart Road using one of the same test vehicles as in the scoping experiment. The vehicle headlamps were aligned each evening before experiments were conducted.

Participants

Participants were recruited and screened as described in chapter 3. A total of 13 participants performed the experiment. Seven were older, and six were younger. Seven were female, and six were male. Mean and standard deviation of participant age, visual acuity, mesopic visual acuity, low contrast visual acuity, and UFOV are listed in table 17.

Table 17. MPI system performance experiment participant characteristics.

Participant Characteristic	Older Drivers Mean	Older Drivers Standard Deviation	Young Drivers Mean	Younger Drivers Standard Deviation
Age	66.8	1.7	28.4	2.4
Visual Acuity	20/26.9	9.8	20/19.1	3.9
Mesopic Visual Acuity	20/39	15.7	20/28.1	5.8
Low Contrast Visual Acuity	20/30.8	17.5	20/20	5
UFOV	1.6	0.5	1	0

Procedure

One participant completed the testing protocol during each session. Upon arrival, participants followed the procedure outlined in chapter 3 but were also fitted for the eye tracker, which was then calibrated. They next proceeded to the Smart Road, where they drove one practice lap followed by eight experimental laps at a maximum speed of 56 km/h (35 mi/h). During the experiment, the confederate pedestrians positioned themselves at the stations and changed the headlamp filters according to the protocol. The in-vehicle researchers configured the MPI system according to protocol and recorded detection and color-recognition distances.

Data Analysis

After reduction, analysis of variance (ANOVA) tests were performed comparing detection and color-recognition distances across the independent variables. ANOVAs show whether the mean values of multiple variables differ significantly from each other. They do not report which means differ significantly from other means. Therefore, Tukey's honest significant difference (HSD) tests were also performed to determine which individual variables significantly differed from other individual variables. When Tukey HSD results are shown in charts, bars sharing a letter are not significantly different from each other.

Detection Rates

Detection rate is the percentage of instances a pedestrian, either on the same side of the road illuminated by the MPI system or opposite the side illuminated by the MPI system, was detected. Detection rates were only calculated with respect to the pedestrian-illuminated-by-MPI-system variable.

Mean Fixation Duration

Video clips of participants detecting pedestrians were isolated from the video files using button presses as flags. A custom MATLAB® program allowed data reductionists to calculate the fixation duration, i.e., the length of time the participant gazed at a pedestrian. Mean fixation durations were calculated for the three MPI configurations (off, tracking, and highlighting).

RESULTS

Detection and Color-Recognition Distances

For detection distance, three independent variables resulted in significantly different means: age, headlamp color, and pedestrian clothing color. There was also a significant effect of the interaction between MPI system performance and headlamp color. Detection-distance results are shown in table 18.

For color-recognition distance, two independent variables resulted in significantly different means: age and pedestrian clothing color. There was also a significant effect of the interaction between MPI system configuration and headlamp color. Color-recognition results are shown in table 19.

Table 18. MPI system performance experiment detection distance results per independent variable.

Independent Variable(s)	<i>F</i> -value	Pr > <i>F</i>
Age	57.51	< 0.0001 ^a
Headlamp Color	5.90	0.0355 ^a
Headlamp Color and Pedestrian in Overhead Lighting	0.09	0.7650
MPI System Configuration	2.50	0.1076
Pedestrian Clothing Color	17.49	0.0015 ^a
Pedestrian Clothing Color and Pedestrian in Overhead Lighting	1.28	0.2825
Pedestrian on Left or Right	3.81	0.0767
Pedestrian in Overhead Lighting	1.52	0.2430
MPI System Configuration by Pedestrian in Overhead Lighting	0.99	0.3917
MPI System Configuration by Headlamp Color	3.90	0.0405 ^a
MPI System Configuration by Pedestrian on Left or Right	1.79	0.1967

^aSignificant at $p < 0.05$.

Pr = Probability.

Table 19. MPI system performance experiment color-recognition distance results per independent variable.

Independent Variable(s)	<i>F</i>-value	Pr > <i>F</i>
Age	36.08	< 0.0001 ^a
Headlamp Color	3.02	0.1131
Headlamp Color and Pedestrian in Overhead Lighting	0.85	0.3792
MPI System Configuration	0.52	0.6037
Pedestrian Clothing Color	31.79	0.0002 ^a
Pedestrian Clothing Color and Pedestrian in Overhead Lighting	0.08	0.7811
Pedestrian on Left or Right	4.80	0.0562
Pedestrian in Overhead Lighting	0.67	0.4322
MPI System Configuration by Pedestrian in Overhead Lighting	0.93	0.4161
MPI System Configuration by Headlamp Color	6.56	0.0090 ^a
MPI System Configuration by Pedestrian on Left or Right	2.95	0.0832

^aSignificant at $p < 0.05$.

Pr = Probability.

Results are discussed in detail in following subsections.

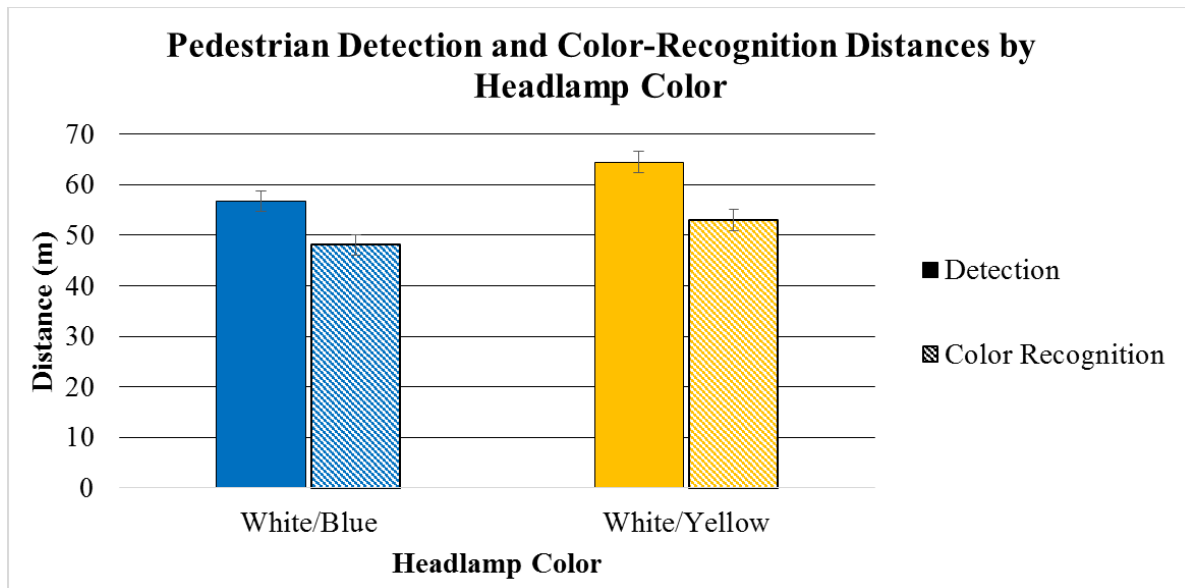
Age

Age significantly affected detection distance because younger participants ($M = 70.2$ m (230 ft)) detected pedestrians from significantly farther away than older participants ($M = 49.2$ m (161 ft)), $p < 0.0001$).

Age also significantly affected color-recognition distance because younger participants ($M = 57.2$ m (188 ft)) recognized clothing color from significantly farther away than older participants ($M = 42.1$ m (138 ft)), $p < 0.0001$).

Headlamp Color

Headlamp color significantly affected detection distances. When using white/yellow headlamps, participants detected pedestrians from significantly farther away ($M = 64.5$ m (212 ft)) than when using white/blue headlamps ($M = 56.7$ m (186 ft), $F=5.90$, $p<0.05$) (figure 63). Headlamp color did not significantly affect color-recognition distances. When using white/yellow headlamps, participants recognized the clothing color from a mean of 53.0 m (174 ft) away, and when using white/blue headlamps, participants recognized the clothing color from 48.2 m (158 ft) away. The results are shown in figure 63.

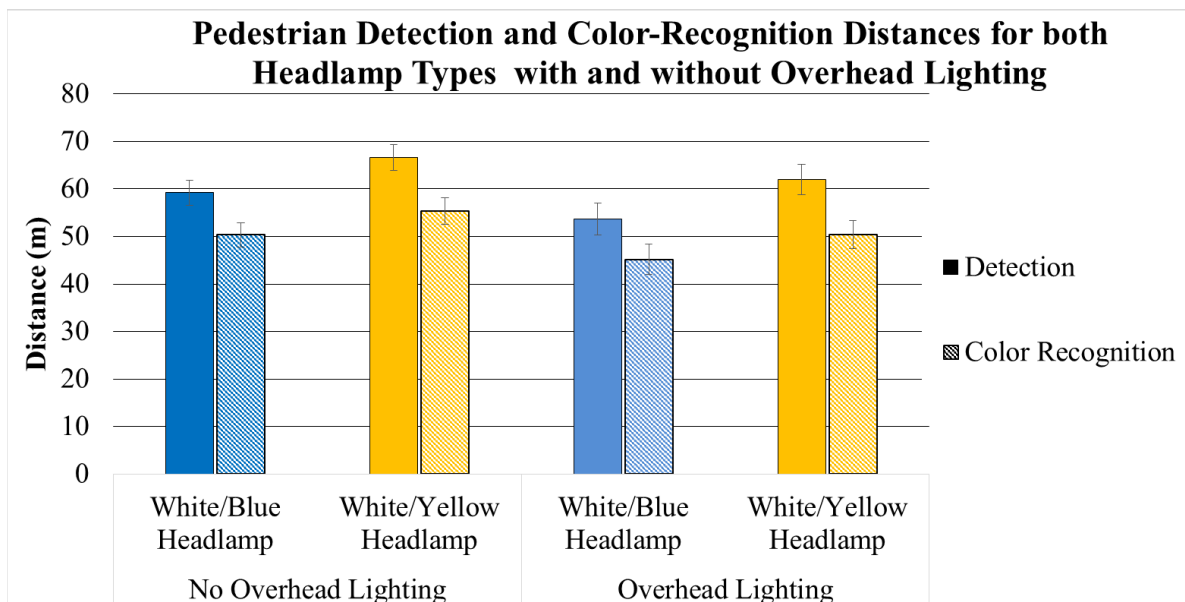


1 m = 3.3 ft

Figure 63. Chart. MPI system performance experiment—pedestrian-detection and color-recognition distances versus headlamp color.

Headlamp Color and Pedestrian in Overhead Lighting

Headlamp color significantly affected detection distances when the pedestrian was in sections of the road with and without overhead lighting. In both cases, detection distances were greater with the white/yellow headlamps than with white/blue headlamps, as illustrated in figure 64.



1 m = 3.3 ft

Figure 64. Chart. MPI system performance experiment—pedestrian-detection and color-recognition distances versus headlamp color and overhead lighting.

The effects of headlamp color on detection and color recognition were robust enough to be replicated in different ambient-light scenarios. One would expect white/blue to have greater detection and color-recognition distances than white/yellow, because mesopic vision is more sensitive to blue. However, pedestrian detection was performed with participants free to move their heads and eyes. Thus, detection probably occurred in the fovea, less sensitive to mesopic effects than peripheral vision. The transmittance of the white/yellow filters was 49 percent, and the white/blue filters was 44 percent, making the white/yellow headlamps slightly brighter, perhaps causing the greater detection distances.

MPI System Configuration

The MPI system was configured three ways: set to off, set to appear to track the pedestrian, or set to appear to highlight the pedestrian.

The ANOVA revealed that the MPI system configuration's effect on detection distance approached significance at the 0.10 level ($F = 2.5$, $p = 0.1076$). A Tukey HSD test found that pedestrians were detected from significantly farther away when the MPI system was off ($M = 67.4$ m (221 ft)) than when it highlighted ($M = 56.7$ m (186 ft)) or tracked pedestrians ($M = 61.1$ m (200 ft)), as shown in figure 65. That could be because the MPI system's actions distracted the participant, making it more difficult to detect pedestrians.

MPI system configuration did not approach significance with respect to color-recognition distance ($F = 0.52$, $p = 0.6037$).

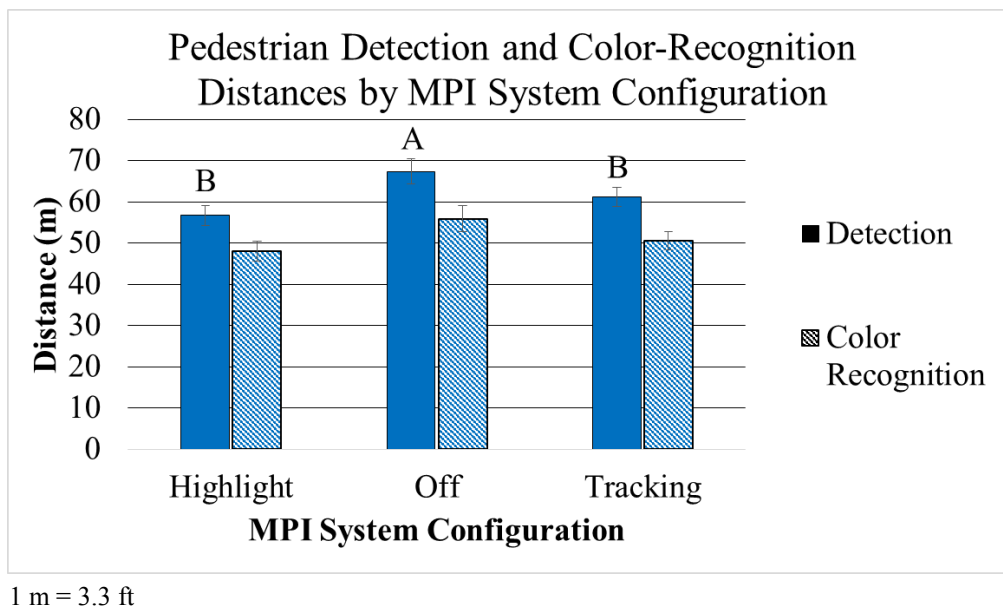


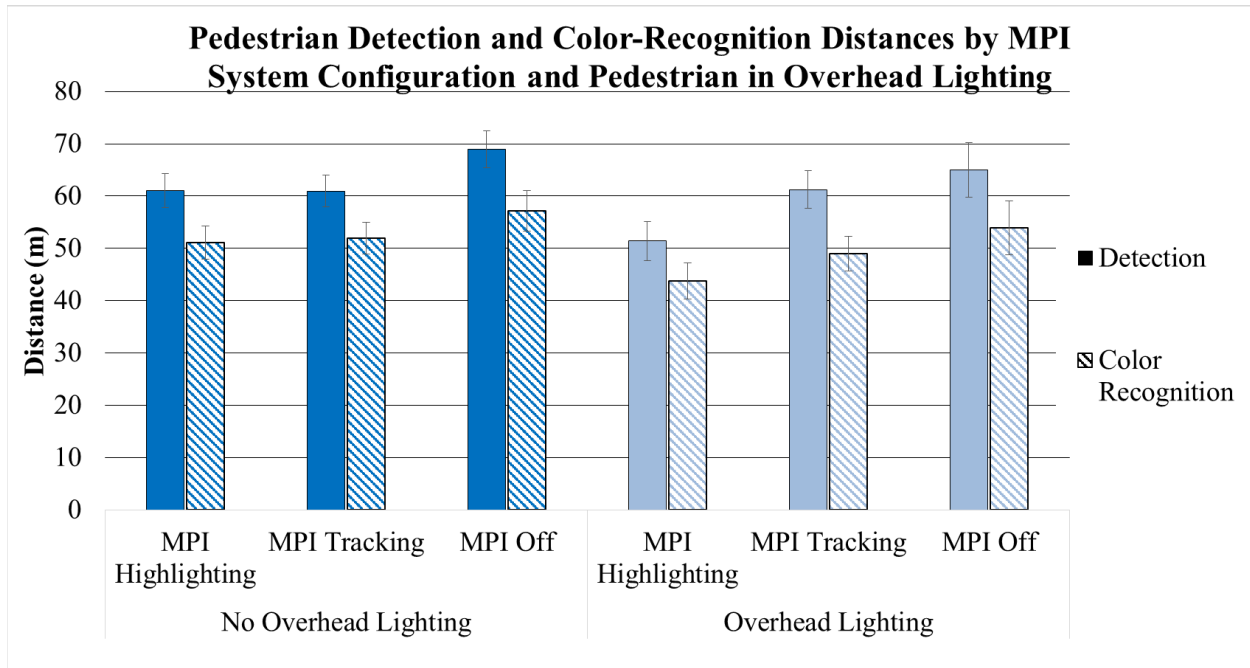
Figure 65. Chart. MPI system performance experiment—pedestrian-detection and color-recognition distance versus MPI system configuration.

MPI System Configuration and Pedestrian in Overhead Lighting

There was no significant effect on detection distance from the interaction between MPI system configuration and whether the pedestrian was in overhead lighting. In the area with no overhead

lighting, pedestrian-detection distances were similar to the overhead-lighting condition for the three MPI system configurations. In the area with overhead lighting, the pedestrian-detection distance for the highlighting MPI system configuration ($M = 51.4$ m (169 ft)) was shorter than for the other two configurations (tracking ($M = 61.2$ m (201 ft)) and MPI off ($M = 65.0$ m (213 ft))), visible in figure 66, but not to a statistically significant degree.

There was also no significant effect on color-recognition distance from the interaction between MPI system configuration and whether the pedestrian was in overhead lighting.

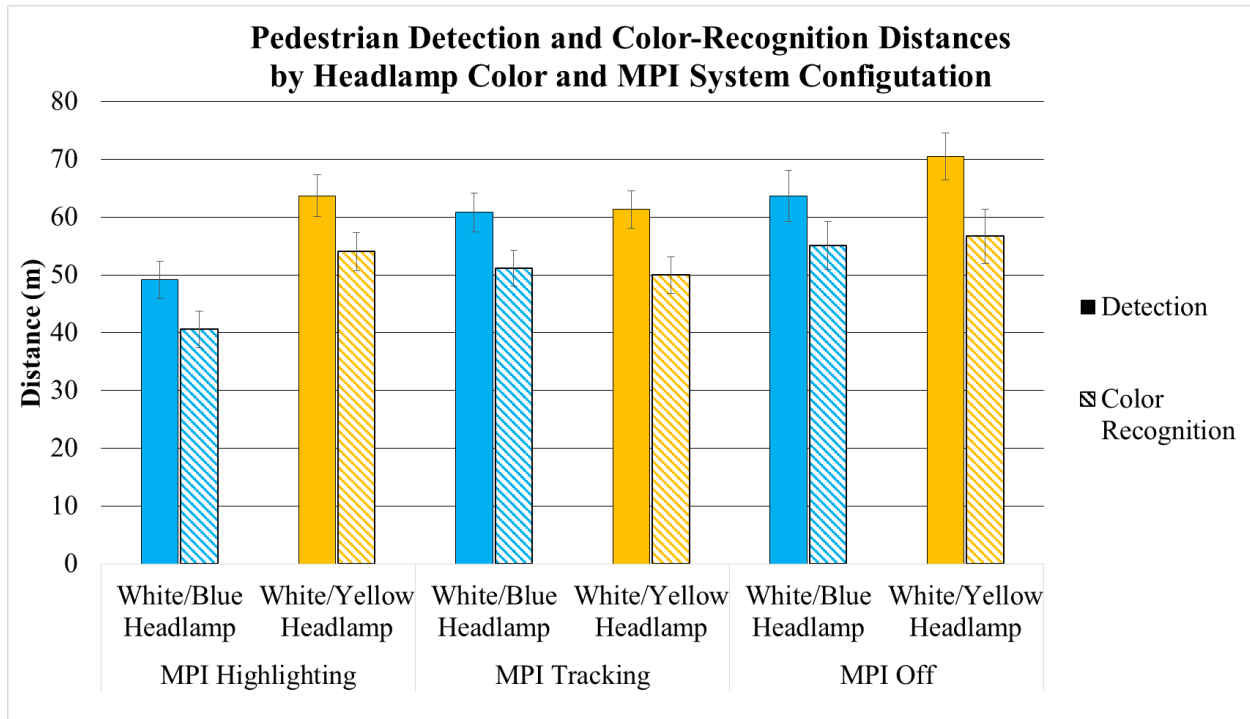


1 m = 3.3 ft

Figure 66. Chart. MPI system performance experiment—pedestrian-detection and color-recognition distances versus MPI system configuration and overhead lighting.

MPI System Configuration and Headlamp Color

There was a statistically significant interaction between the headlamp color and MPI system configuration ($F = 3.90, p < 0.05$). When the MPI system was tracking the pedestrians, headlamp color had almost no effect on detection distance, which was about 61.0 m (200 ft). When the MPI system was off, mean detection distance for the white/yellow headlamps ($M = 70.5$ m (231 ft)) was slightly greater than for the white/blue headlamps ($M = 63.6$ m (209 ft)). The greatest effect was when the MPI system was highlighting the pedestrian. With the white/yellow headlamp, the mean detection distance ($M = 63.7$ m (209 ft)) was significantly greater than with the white/blue headlamp ($M = 49.2$ m (161 ft)). The results are shown in figure 67.



1 m = 3.3 ft

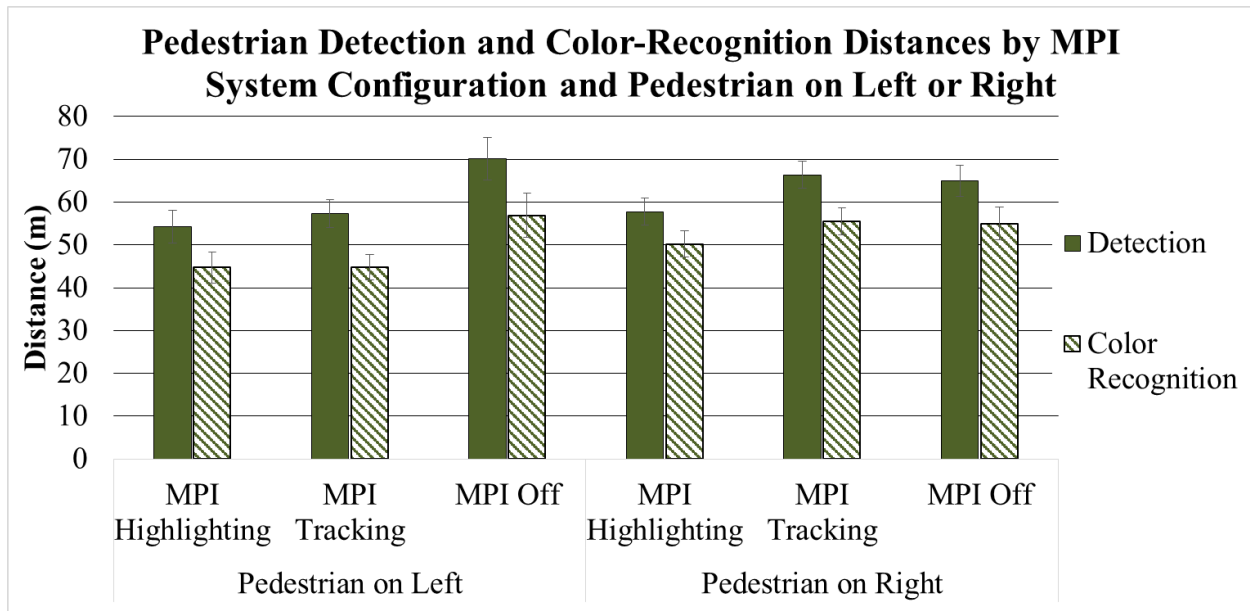
Figure 67. Chart. MPI system performance experiment—pedestrian-detection and color-recognition distances versus MPI system configuration and headlamp color.

MPI System Configuration and Pedestrian on Left or Right

There was no statistically significant effect on detection distance from the interaction between MPI system configuration and pedestrian on the left or right of the road. The shorter detection distances for the highlighting MPI system configuration were apparent whether the pedestrian was on the left or right side of the road.

There was no statistically significant effect on color-recognition distance from the interaction between MPI system configuration and pedestrian on the left or right of the road.

The mean detection and color-recognition distance for pedestrians on the left of the road with the MPI system off was visibly greater than the other means (figure 68). This could possibly be because of a combination of the vehicle's blind spot on the left and the distracting headlamp action. Those two factors could have shortened detection and color-recognition distances when the pedestrian was on the left and the MPI system was on.



1 m = 3.3 ft

Figure 68. Chart. MPI system performance experiment—pedestrian-detection and color-recognition distances versus MPI system configuration and pedestrian on left or right.

Pedestrian Clothing Color

Clothing color significantly affected detection distance. Pedestrians wearing red ($M = 66.2$ m (217 ft)) were detected significantly farther away than pedestrians wearing blue ($M = 55.6$ m (182 ft), $p = 0.0015$), as shown in Figure 69.

Clothing color also significantly affected color-recognition distance. Participants recognized the clothing color of pedestrians wearing red ($M = 57.9$ m (190 ft)) from significantly farther away than pedestrians wearing blue ($M = 43.0$ (141 ft), $p = 0.0002$), also shown in figure 69.

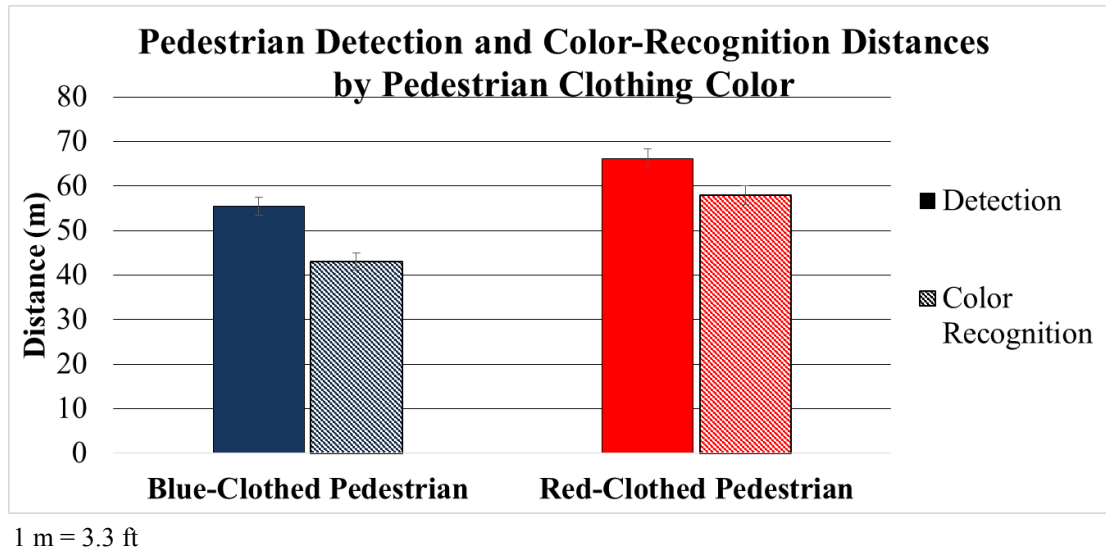
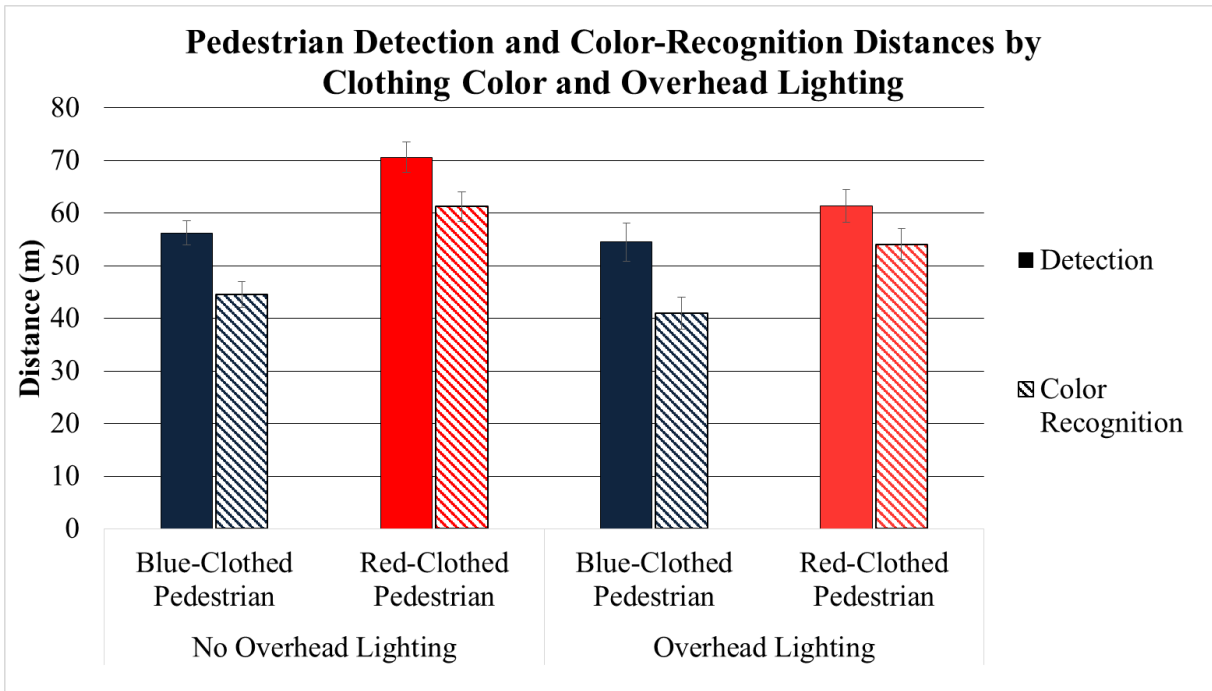


Figure 69. Chart. MPI system performance experiment—pedestrian-detection and color-recognition distances versus pedestrian clothing color.

Pedestrian Clothing Color and Pedestrian in Overhead Lighting

When detection distances were broken down by whether the pedestrian was in an area with overhead lighting, clothing color did not have a significant effect on detection distance for either overhead-lighting condition. With no overhead lighting, red-clothed pedestrians ($M = 70.6$ m (232 ft)) were detected from farther away than blue-clad pedestrians ($M = 56.3$ m (185 ft)). With overhead lighting, red-clothed pedestrians ($M = 61.4$ m (201 ft)) were also detected from farther away than blue-clad pedestrians ($M = 54.5$ m (179 ft)), but this interaction of presence/absence of overhead lighting and pedestrian clothing color was not found to be statistically significant.

The same trend held for color-recognition distances. With no overhead lighting, participants recognized the color of red-clothed pedestrians ($M = 61.3$ m (201 ft)) from farther away than blue-clad pedestrians ($M = 44.6$ m (146 ft)). With overhead lighting, participants recognized the color of red-clothed pedestrians ($M = 54.1$ m (177 ft)) from farther away than blue-clad pedestrians ($M = 41.0$ m (134 ft)), but again, this was not statistically significant. Both detection and color-recognition distance results by pedestrian clothing color and overhead lighting are shown in figure 70.



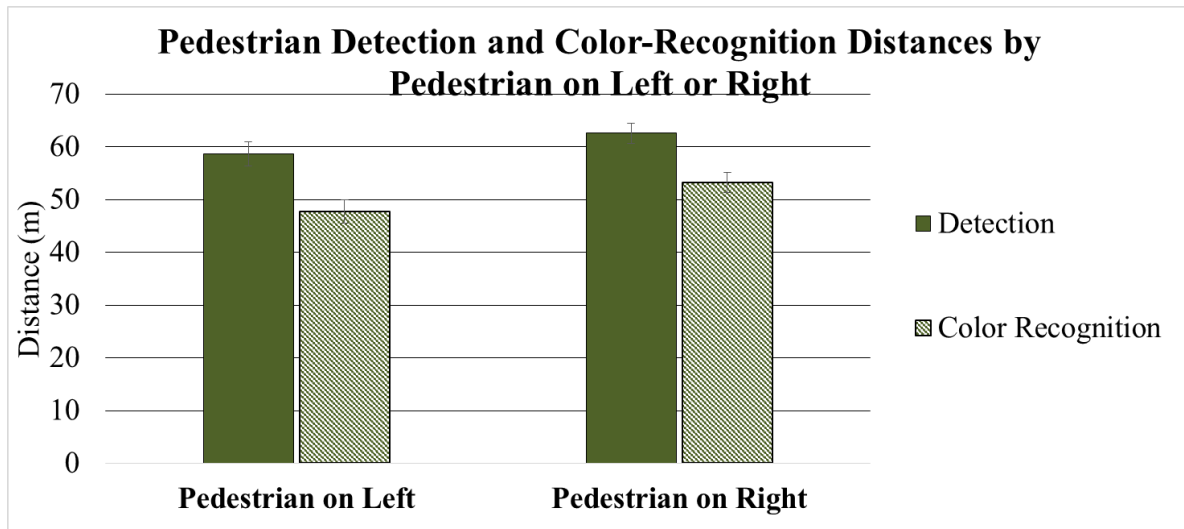
1 m = 3.3 ft

Figure 70. Chart. MPI system performance experiment—pedestrian-detection and color-recognition distances versus pedestrian clothing color and overhead lighting.

Pedestrian on Left or Right

Pedestrians on the right side of the road ($M = 62.6$ m (205 ft)) were detected from farther away than pedestrians on the left side of the road ($M = 58.7$ m (193 ft)) but not to a statistically significant degree.

Participants recognized the clothing color of pedestrians on the right side of the road ($M = 53.2$ m (175 ft)) from farther away than clothing color of pedestrians on the left side or the road ($M = 47.7$ m (157 ft)); this effect was also not statistically significant. Both effects are illustrated in figure 71.



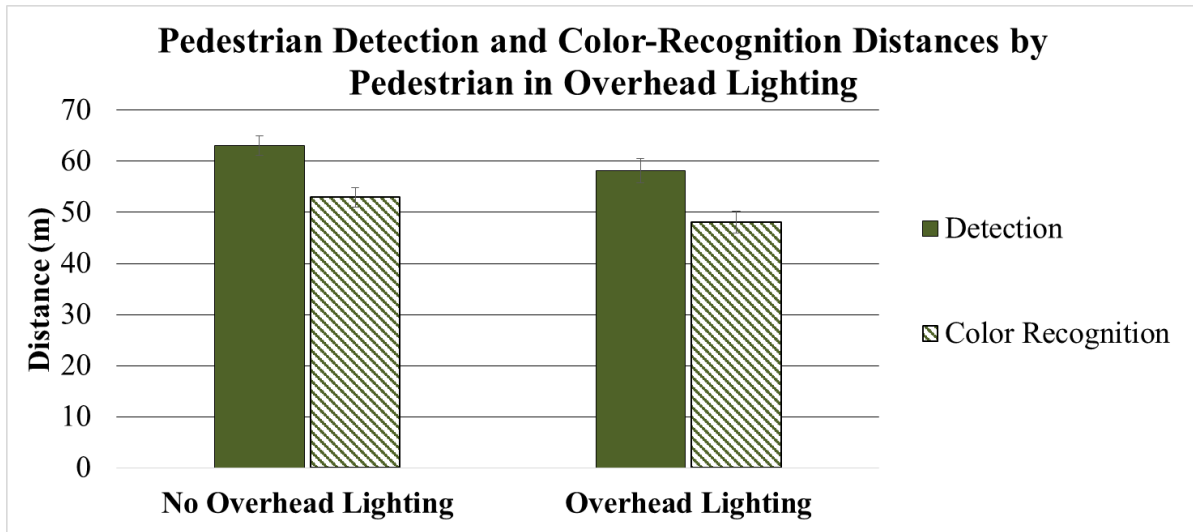
1 m = 3.3 ft

Figure 71. Chart. MPI system performance experiment—pedestrian-detection and color-recognition distances versus pedestrian on left or right.

Pedestrians could be detected and their clothing colors recognized from farther away when they stood on the right-hand side of the road because of the headlamp beam pattern: the headlamp cutoffs that prevent light from creating glare for oncoming vehicles also prevent light from shining on the left-hand shoulder of the road and illuminating pedestrians there.

Pedestrian in Overhead Lighting

The mean detection distance for pedestrians in areas with no overhead lighting ($M = 63.1$ m (207 ft)) was greater than the mean detection distance for pedestrians in areas with overhead lighting ($M = 58.2$ m (191 ft), $p = .2430$). An SNK test indicates that while these results are not statistically significant in terms of an analysis of variance, these mean detection distances were meaningfully different from each other, as shown in figure 72. Results of the mean color-recognition distances were similar in terms of significance for with ($M = 48.1$ m (158 ft)) and without ($M = 53.0$ m (174 ft)) overhead lighting.



1 m = 3.3 ft

Figure 72. Chart. MPI system performance experiment—pedestrian-detection and color-recognition distances versus pedestrian in overhead lighting.

It should be noted that for this comparison and the clothing color and overhead-lighting conditions, Stations with overhead lighting had more visual clutter than the stations without overhead lighting, and that clutter could have masked the pedestrians, as illustrated in figure 73. Therefore, the above results must be interpreted with caution.



Figure 73. Photo. MPI system performance experiment—visual clutter on the Smart Road.

Detection Rate by Pedestrian Illuminated by MPI System

Some trials were performed with a pedestrian on the side of the road opposite the location where the MPI beam tracked to determine whether the MPI system interrupted the participants' normal scanning behavior.

When the MPI system illuminated the pedestrian, participants detected the pedestrian about 70 to 80 percent of the time. When the MPI system illuminated the roadway opposite the pedestrian, participants detected the pedestrian about 50 to 60 percent of the time. The results, illustrated in figure 74, show that participant drivers either trusted the MPI system or expected the experimental configuration to be predictable.

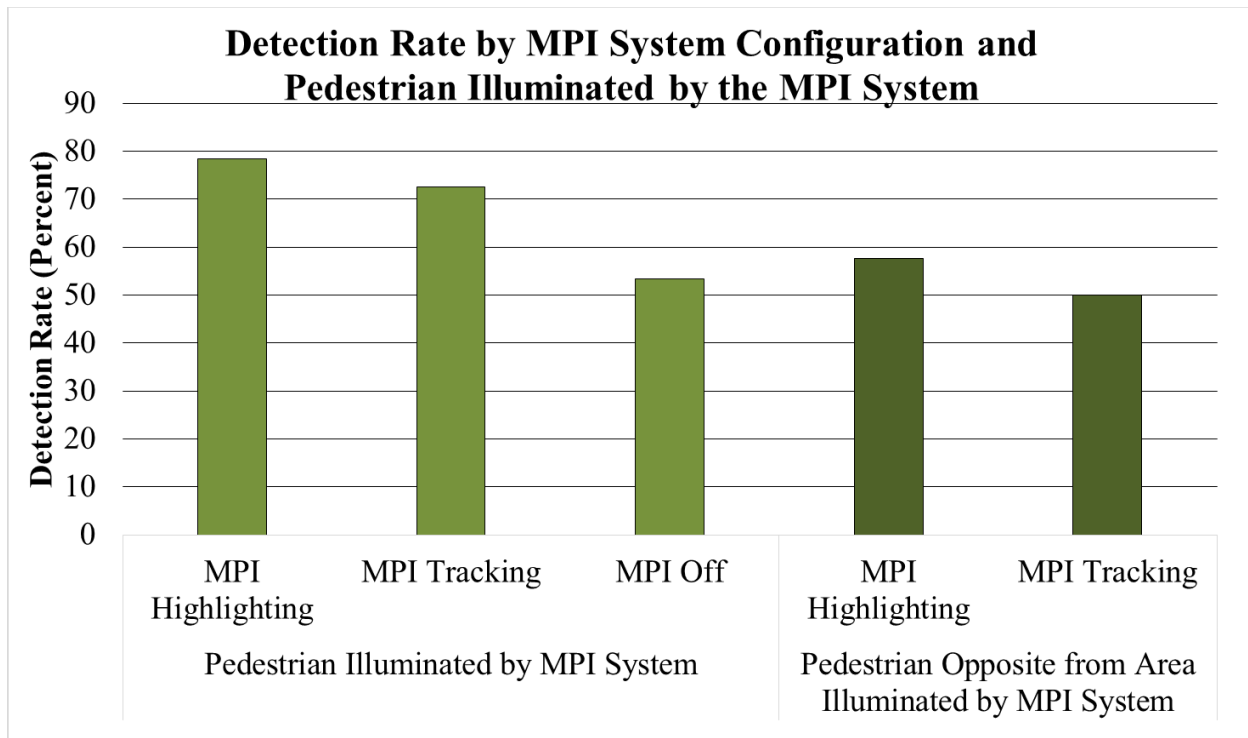


Figure 74. Chart. MPI system performance experiment—percentage of detections of pedestrian versus MPI system configuration and whether the pedestrian was illuminated by the MPI system.

Mean Fixation Duration by MPI System Configuration

When the MPI system was configured to track the pedestrian, it began illuminating the pedestrian when the vehicle was 183 m (600 ft) away and swiveled to keep the pedestrian illuminated as the vehicle approached. When the MPI system was configured to highlight the pedestrian, it shined on the pedestrian when the vehicle was 46.7 m (150 ft) away.

Mean fixation duration per MPI system configuration was calculated, but the fixation duration data was not normally distributed, so comparing means to determine statistical significance was not valid. Therefore, a non-parametric statistical analysis, the Kruskal-Wallis test, was used to compare the groups of fixation durations between MPI system configurations. There was no statistically significant difference in fixation duration between the three MPI system configurations ($p = 0.8040$). The mean fixation durations by MPI system configuration are shown in figure 75.

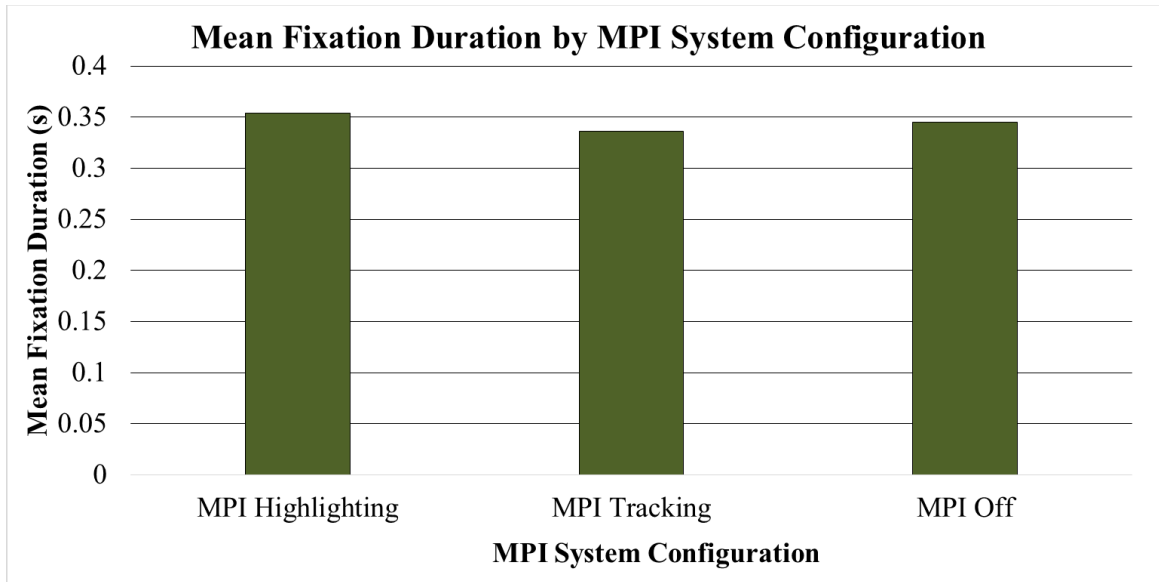


Figure 75. Chart. MPI system performance experiment—mean fixation duration versus MPI system configuration.

DISCUSSION

An objective of this project was to evaluate the effect of a peripheral illumination system on driver visibility. In the absence of overhead lighting, headlamps were the only source of light the driver had available to aid in object detection, and the effects of the MPI system were isolated. Results were mixed, with the MPI system increasing participant detection rates for pedestrians but decreasing detection distances. This result indicates that in a vehicle with an active MPI system, drivers rely on the MPI system to help them detect pedestrians. An MPI system that can detect and highlight pedestrians in the periphery better than human scanning alone would likely increase detection rates for those pedestrians. However, the MPI system may distract the driver's attention from the roadway, because the driver would follow the moving headlamp beam. So while the system may distract in one case, it focuses the driver's attention in another. Refocusing a driver's attention may not always lead to better driving, as seen in the cases where the MPI headlamp beam was directed to a position opposite the pedestrian, reducing detection distances and rates for those pedestrians.

In instances where pedestrians were located on the right side of the vehicle, the MPI highlighting and tracking configurations resulted in detection distances similar to when the MPI system was inactive. However, when pedestrians were located on the left side of the vehicle, the inactive MPI scenarios resulted in the longest detection distances. A possible explanation for this would be the design of the vehicle, where the A pillar may have impeded the driver's view of the left-hand side of the roadway. With a moving headlamp, drivers would have a higher cognitive load trying to search for pedestrians around the A pillar than trying to search for them on the right side of the road with no obstruction,.

A significant interaction took place between headlamp color and the behavior of the MPI system, resulting in findings that are more telling than those found in the scoping experiment, which had too few off-axis detections to draw firm conclusions. The findings from this experiment showed

that the white/yellow headlamps might have allowed drivers to detect peripheral pedestrians from farther away, possibly indicating an effect of the light source's SPD.

CONCLUSIONS

The first objective of this experiment was to evaluate how MPI system configuration affected driver visual performance. Results showed that participants detected pedestrians from the greatest distances when the MPI system was off. That was the case for sections of the road both with and without overhead lighting. This could be because the MPI system's moving beam distracted the participants and prevented them from scanning normally. Additionally, participants seemed to assume the MPI system would accurately illuminate pedestrians; they detected the pedestrian between about 70 to 80 percent of the time with the MPI system illuminating the pedestrian, compared with about 50 to 60 percent of the time with the MPI system illuminating the roadway opposite the pedestrian. This could have serious implications for an MPI system that failed to detect all pedestrians or malfunctioned to illuminate a "false-positive" pedestrian; drivers might assume the system was working and be less vigilant, causing more pedestrian crashes and casualties.

Other research objectives of the experiment was to evaluate how headlamp color of the MPI system affected driver visual performance and how the MPI system and overhead lighting interacted to affect driver visual performance. The white/yellow headlamps had greater detection distances than white/blue headlamps in sections of the road with and without overhead lighting. That could be partially because the white/yellow gels had slightly higher transmittance than the white/blue gels (see table 3). Although mesopic vision is more efficient for blue than for yellow light, drivers were allowed to turn their heads and move their eyes as they scanned the road, and pedestrian detection occurred foveally where mesopic effects are minimal.

An eye tracker was used to determine how the MPI system affected driver eye-glance behavior, the last research objective of the experiment. There were no statistically significant differences among the different MPI system configurations for glance duration.

FUTURE RESEARCH

The experiment described in this chapter was performed with a single overhead-lighting color with pedestrians placed at the same distance from the shoulder for each run. To better characterize mesopic vision and its interaction with an MPI system, future experiments should use other overhead-lighting colors and add off-axis angles for object detection. The final experiment in this project takes these concerns into account.

Drivers typically glance around the roadway as they drive. Future analyses should characterize exactly how an MPI system affects glance behavior.

Participants apparently trusted the MPI system to the extent that they missed important visual information. Therefore, any MPI system would have to be accurate enough that it would seldom, if ever, miss detecting a pedestrian on the side of the road.

CHAPTER 6. OVERHEAD-LIGHTING LEVEL EXPERIMENT

INTRODUCTION

The goal of the overhead-lighting level experiment was to investigate the interaction of overhead-lighting level and vehicle headlamps. The performance of a lighting system is based on the adaptation level of the driver, so it is critical to identify whether the dominant component of a driver's visual field is the vehicle headlamps or the overhead-lighting system. This experiment was designed to investigate the relative dominance of overhead lighting and headlamps with regard to visibility.

Only the 6,000-K LED lighting was used in this experiment because, of the three lighting types used in this project, its spectrum was the most efficient in the mesopic region. Consequently, it provided the best visibility at the lowest illuminance. Eleven lighting levels were tested, ranging from off to the 100 percent.

Pavement type, color, and reflectance all affect object contrast and visibility. Therefore, experiments were performed on two types of pavement: lighter-colored concrete and darker asphalt. The position of the target with respect to the overhead-lighting masts also affects visibility. By combining target placement with respect to the luminaire and pavement type, two worst-case scenarios for target visibility were created to test minimum VLs. In the first case, a target was placed on dark asphalt in a position with low VI. In the second case, a target was placed on light concrete in a position with high VI. Pedestrians were also used to test visibility, representing a real-life dangerous driving scenario.

To get a detailed picture regarding visibility at the various lighting levels, both targets and pedestrians were used to measure detection distance. Only gray clothing and targets were used, because this experiment focused on overhead-lighting level and mesopic vision, not object color. Participants detected the targets and pedestrians. To add a level of detail, participants were also asked to recognize which direction the targets and pedestrians were facing.

Tests were performed with headlamps on to simulate real-life driving scenarios and with headlamps off to examine the effect of overhead lighting alone.

Research Objectives

The research objectives of the overhead-lighting level experiment were to evaluate the following:

- Impact of headlamps driver visual performance.
- Impact of overhead-lighting level on driver visual performance.
- How headlamps and overhead lighting interact to affect driver visual performance.
- Minimum overhead-lighting level where driver visual performance is not compromised.

In addition to the stated research objectives, the results of this experiment informed the remaining experiments regarding adaptation luminance in mesopic conditions. This information was the basis for light levels and object locations used in subsequent experiments in this project.

EXPERIMENTAL DESIGN

An experiment was designed to measure the relationship of overhead-lighting level and headlamps on nighttime driving visual performance in mesopic conditions. Variables used in the experiment are listed in table 20 and table 21.

Table 20. Overhead-lighting level experiment independent variables.

Variable Type	Variable Options
Age	Younger (25–35), Older (65+)
Vehicle Headlamps	On, Off
Overhead-Lighting Level (percent)	Off, 10, 20, 30, 40, 50, 60, 70, 80, 90, 100
Target Type	Target I (low VI), target II (high VI), pedestrians

Table 21. Overhead-lighting level experiment dependent variables.

Dependent Variable	Maximum Times Measured Per Participant
Target I Detection Distance	21
Target II Detection Distance	21
Pedestrian-Detection Distance	21
Target I Orientation-Recognition Distance	21
Target II Orientation-Recognition Distance	21
Pedestrian Orientation-Recognition Distance	21
Object Luminance and Contrast	N/A

N/A = Not applicable.

All variable combinations were tested except for the headlamp-off and the overhead-lighting-off conditions together. In that combination, no lighting would be present, which would present a significant safety hazard.

Independent Variables

Age

Participants were divided into the same age groups as in previous experiments: drivers (25–35 years old) and older drivers (65 years old and older). These ages were selected on the basis of visual ability and driving experience. Younger drivers typically have better vision for driving at night, while the older population has more experience with driving in general.

Vehicle Headlamps

Vehicle headlamps were either turned on or off; when on, they were used with the neutral-density low-intensity filters described in chapter 3.

Overhead-Lighting Level

The overhead roadway lighting used was the 6,000-K LED system. Dim levels varied in 10-percent intervals from 0-percent illuminance to 100-percent illuminance. The horizontal illuminances were measured on the roadway surface at the target II location. (Target positioning will be described in the next section.) The 100-percent level was 10 lx (0.93 fc). The 10-percent level was actually 1.37 lx (0.13 fc) because the control system and luminaire characteristics do not allow for lower dimming levels. The headlamps used were the white/yellow filters with the 30-percent neutral density filters. Vehicle headlamps were either turned on or off.

Target Type

This experiment used gray-clad pedestrians and gray targets. The pedestrians were positioned on the shoulder, 0.03 m (1 ft) away from the road, on the same side of the road as the overhead-lighting system. The targets were placed on the shoulder, also 0.03 m (1 ft) away from the road but on the opposite side of the road from the overhead lighting.

The target placement longitudinally along the roadway was selected to produce worst-case scenarios in terms of target contrast—one with high VI and one with low VI. The pedestrians were located so that the VI at head level matched that of the high VI targets. Target and pedestrian placement is described in detail in the following paragraphs.

Target I Placement:

The placement of target I attempted to create a low VI condition. It was placed on a dark asphalt surface and positioned directly across from a luminaire (figure 76), so very little light from the luminaire shone directly on the face visible to the oncoming vehicle.

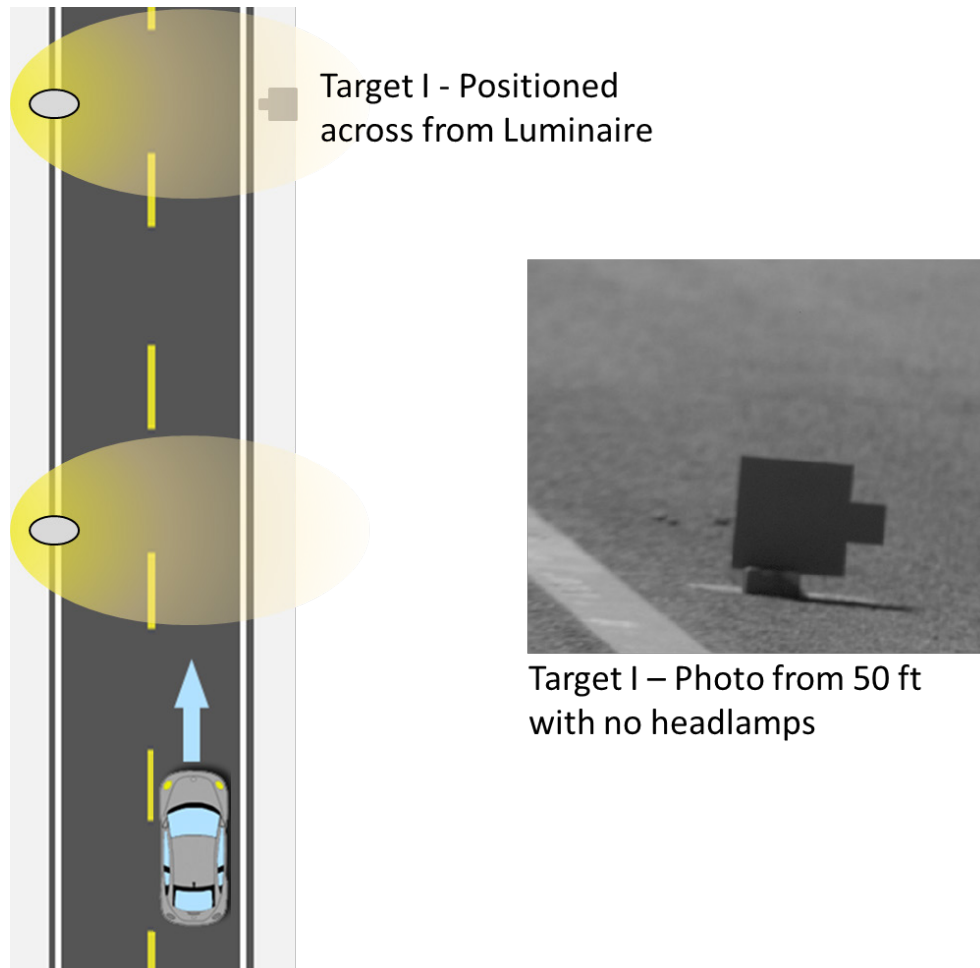


Figure 76. Diagram. Overhead-lighting level experiment—target I (low VI) placement.

Target II Placement:

The placement of target II attempted to create a high VI condition. It was placed on a light asphalt surface halfway between two luminaires (figure 77), the area of maximum VI with respect to the luminaire, and as much light as possible shone on the face visible to the oncoming vehicle.

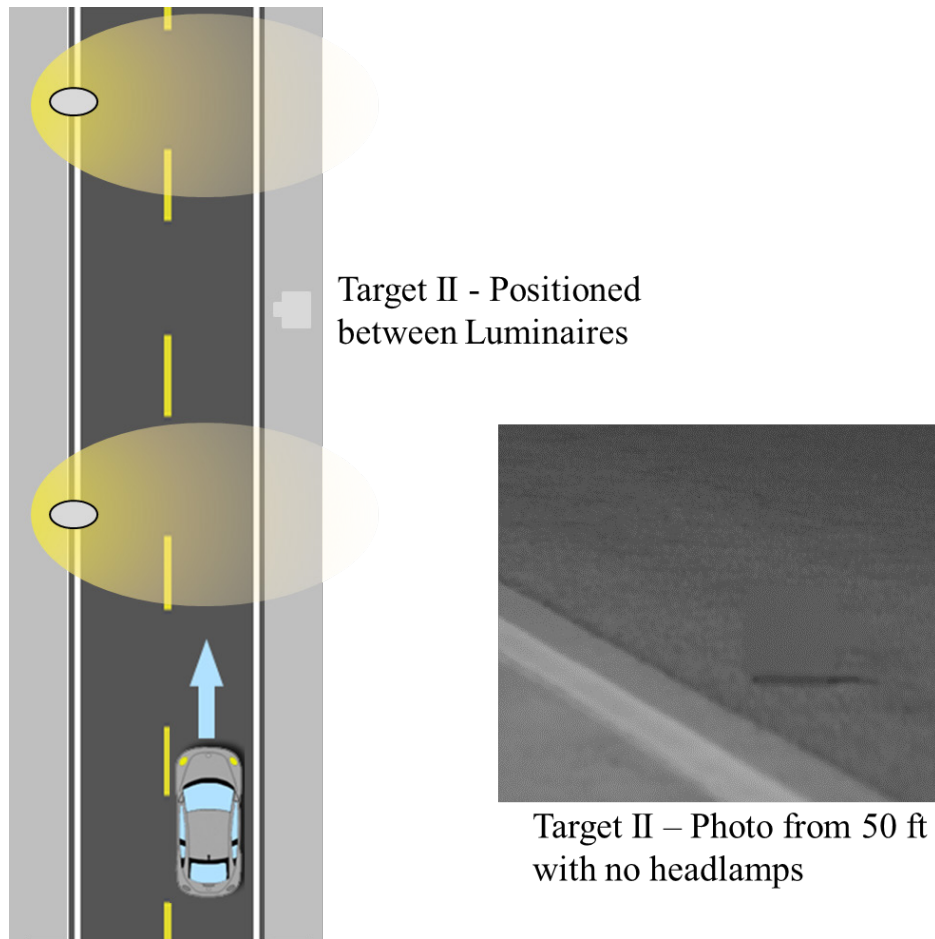


Figure 77. Diagram. Overhead-lighting level experiment—target II (high VI) placement.

Pedestrian Placement:

The placement of the pedestrian with respect to the luminaires was chosen so that the VI at approximately face height, about 1.5 to 1.8 m (5 to 6 ft), matched the VI at target II, the high-VI target.

To do so, first the VIs at target II's position were measured. Measurements were repeated with the overhead lighting varying in 10-percent intervals from 0 to 100 percent. Then, VI measurements were taken at various locations on the same side of the road as the luminaires and at 1.5 to 1.8 m (5 to 6 ft) (head height). The pedestrian was positioned where these VI measurements were approximately equal to those at target II for the same illumination condition. Table 22 lists illuminance measurements at the target I, target II, and the best-match pedestrian position. Figure 78 graphs those illuminances.

Table 22. Overhead-lighting level experiment—VI of targets and pedestrian with luminaires and no headlamps.

Dim Level of Luminaire	Target I VI (lx (fc))	Target II VI (lx (fc))	Pedestrian VI (lx (fc))
100 percent	1.6 (0.15)	5.73 (0.53)	6.75 (0.63)
90 percent	1.5 (0.14)	5.68 (0.53)	5.92 (0.55)
80 percent	1.3 (0.12)	4.79 (0.44)	5.45 (0.51)
70 percent	1.07 (0.099)	4.06 (0.38)	4.53 (0.42)
60 percent	0.98 (0.091)	3.44 (0.32)	3.8 (0.35)
50 percent	0.83 (0.077)	2.85 (0.26)	3.21 (0.30)
40 percent	0.67 (0.062)	2.29 (0.21)	2.59 (0.24)
30 percent	0.5 (0.046)	1.67 (0.16)	1.96 (0.18)
20 percent	0.34 (0.032)	1.11 (0.103)	1.3 (0.12)
10 percent	0.27 (0.025)	0.79 (0.073)	0.88 (0.082)

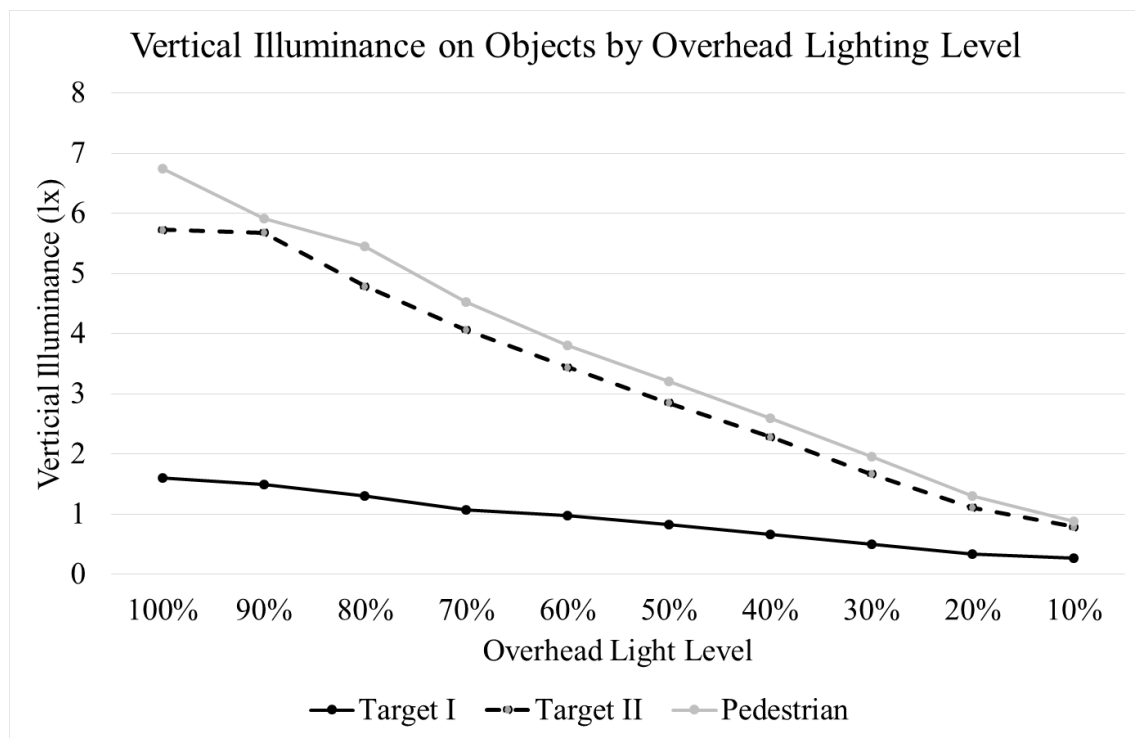


Figure 78. Graph. Overhead-lighting level experiment—VI on objects by overhead-lighting level.

Dependent Variables

Detection and orientation-recognition distances were measured in this experiment. Color-recognition distance was not measured; all objects were gray.

Object Luminance and Contrast

Photometric images of the pedestrians and targets were taken post hoc with a calibrated ProMetric® Radiant Imaging® camera mounted inside the test vehicle. Images were taken with headlamps on and off. For the targets, photometric images were recorded every 15 m (50 ft) out to 122 m (400 ft) from the target. For pedestrians, images were recorded every 30 m (100 ft) out to 244 m (800 ft) from the pedestrian.

The images taken were analyzed using Radiant Imaging® software. A data reductionist traced the contour of the pedestrian or target, and the software calculated the average luminance within that polygon. The luminances of the targets, pedestrians, and their backgrounds were measured to calculate contrast.

METHODS

Participants

Twenty-four participants took part in the study. However, data for two of the participants were unusable because an anomaly during data collection rendered that data unreliable. Of the 22 participants whose data were kept, 12 were in the older group, and 10 were in the younger group. There were 11 males and 11 females. Mean and standard deviation of participant age, visual acuity, mesopic visual acuity, and low contrast visual acuity are listed in table 23.

Table 23. Overhead-lighting level experiment participant characteristics.

Participant Characteristic	Older Drivers Mean	Older Drivers Standard Deviation	Young Drivers Mean	Younger Drivers Standard Deviation
Age	67.4	1.3	25.6	1
Visual Acuity	20/21.2	4.9	20/16.2	5.8
Mesopic Visual Acuity	20/36.3	14.1	20/23.5	6.3
Low Contrast Visual Acuity	20/29.8	7.2	20/21.2	6.8
UFOV	1.4	0.5	1.2	0.4

Procedure

Data Collection

Upon arrival for an experimental session, participants were directed to the test vehicles, familiarized with their operation and the experiment, and then asked to proceed to the Smart Road for the experiment. As in previous experiments, two participants in two vehicles completed the experiment at one time. Participants drove 22 laps on the Smart Road, including one practice lap. One lap was from turn 2 to turn 3, as shown in figure 23. In the remaining 21 laps, the same objects (targets and pedestrians) were in the same location for each lap. Participants were told the objects would be in the same position for each lap and were reminded to say when they could see the objects and object orientations, not when they expected to see the objects. On-road researchers changed the overhead-lighting configuration and object orientations, and in-vehicle

researchers turned the headlamps on and off and recorded detection and orientation-recognition. There were no laps without headlamps and without overhead lighting to avoid creating hazardous test conditions.

Data Analysis

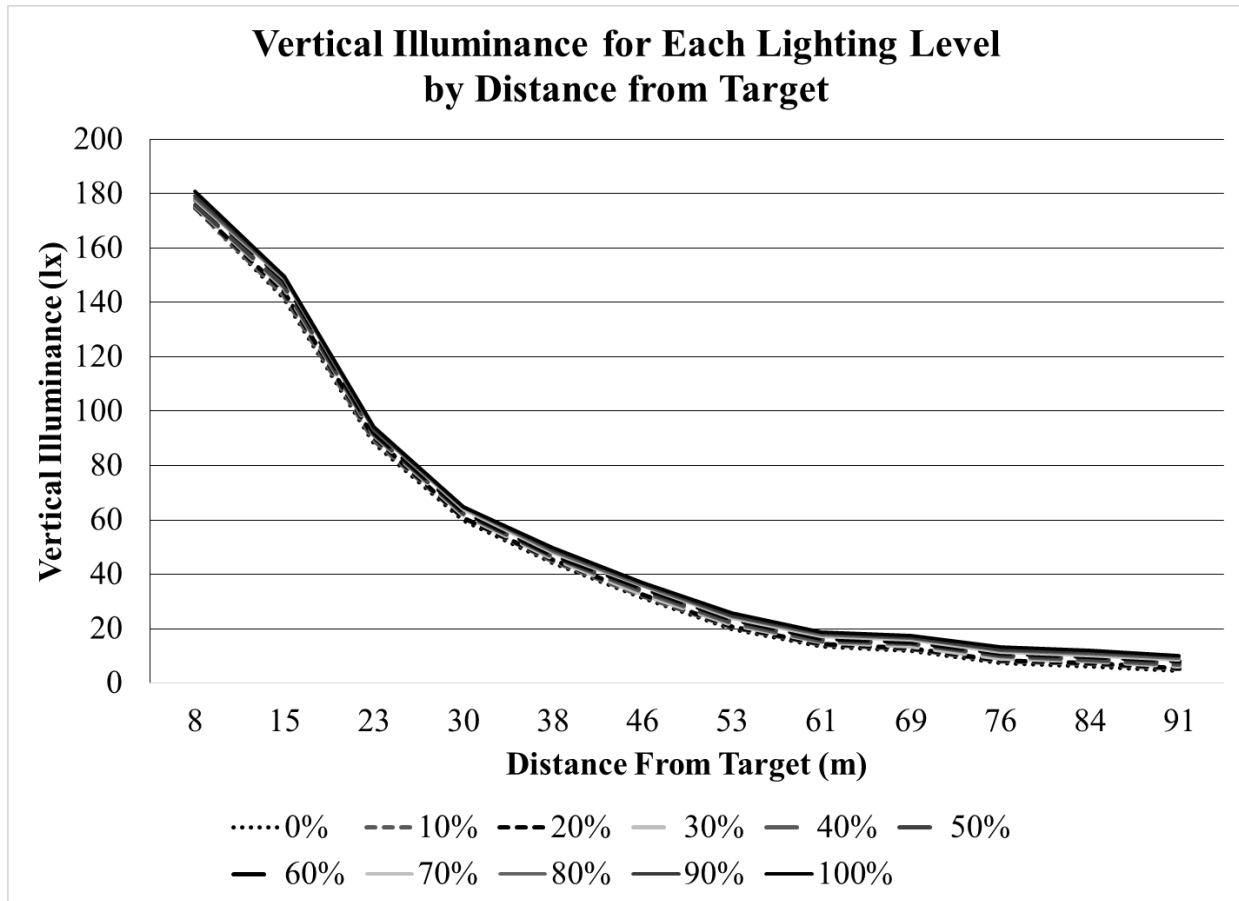
After video reduction of the data, an ANOVA was conducted for analyses related to detection and orientation-recognition distances. An ANCOVA was conducted for analyses related to contrast.

The photometric results were also analyzed in terms of contrast and average detection distance for the objects.

RESULTS

Lighting Characteristics

The distance at which headlamps contribute illuminance to a small target was determined by measuring VI using a light meter placed in front of the target at ground level with the vehicle headlamps on. Luminaire dim levels did not noticeably affect the VI at the target while headlamps were on. When the vehicle was within 91.4 m (300 ft) of the target, there was only about a 10-lx (0.93 fc) difference in VI between no overhead lighting and 100-percent overhead lighting at each distance. VI measurements by distance from target are graphed in figure 79.



1 m = 3.3 ft

Figure 79. Graph. Overhead-lighting level experiment—VI at target, vehicle with headlamps on at between 91 and 8 m (300 and 25 ft) from target, luminaires from 0 to 100 percent.

Detection Distance Versus Lighting Conditions

The data were analyzed using a mixed-models analysis to determine significant effects of headlamp lighting condition and overhead-lighting level on detection and orientation-recognition distances.

Significant Results Summary

Separate analyses were run for the targets and the pedestrian to isolate the effects of lighting. Overhead-lighting level significantly affected pedestrian-detection distances. Overhead-lighting level significantly affected detection distance for both targets, as did headlamp condition, but there was no effect from interaction between the two (table 24).

Table 24. Overhead-lighting level experiment—significant effects on detection distance of targets and pedestrian.

Object	Effect	<i>F</i>-value	Pr > <i>F</i>
Pedestrian	Headlamps on/off	0.39	0.5315
Pedestrian	Overhead-lighting level	18.65	< 0.0001 ^a
Pedestrian	Headlamps by overhead-lighting level	1.34	0.2153
Target I	Headlamps on/off	27.52	< 0.0001 ^a
Target I	Overhead-lighting level	4.41	< 0.0001 ^a
Target I	Headlamps by overhead-lighting level	0.14	0.9985
Target II	Headlamps on/off	13.93	0.0002 ^a
Target II	Overhead-lighting level	3.7	< 0.0001 ^a
Target II	Headlamps by overhead-lighting level	0.34	0.9603

^aSignificant at $p < 0.05$.

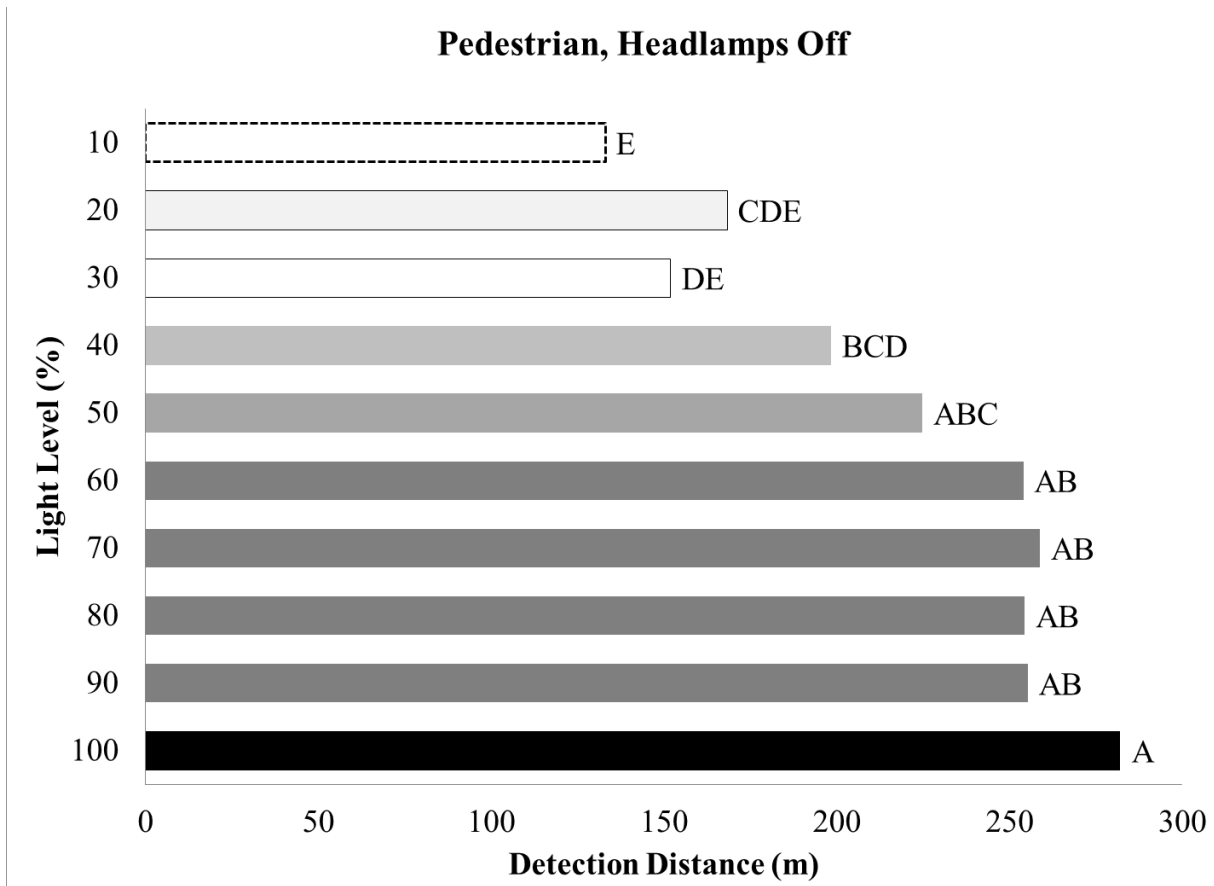
Pr = Probability.

Detection Distance Versus Overhead-Lighting Level

An SNK test was conducted to isolate the extent that overhead-lighting level affected detection distance, with headlamps off and with headlamps on, for the targets and pedestrians. In the figures reporting results of SNK tests, bars sharing a letter do not significantly differ from each other.

Pedestrian, Headlamps Off:

For pedestrian detection with headlamps off, 100-percent overhead-lighting level provided the greatest mean detection distance. However, although lighting levels of 50 through 90 percent were not significantly different from 100 percent, they had mean detection distances significantly greater than for the 10- to 30-percent overhead-lighting levels. The same was true for the dimmest levels; 10 percent had the shortest mean detection distance, but this was not significantly different from 20- and 30-percent overhead lighting. The general trend was for increasingly intense overhead lighting to correspond with greater mean detection distances, except for 30 percent, which had an unexpectedly short mean detection distance given the general trend. Those results are shown in figure 80.

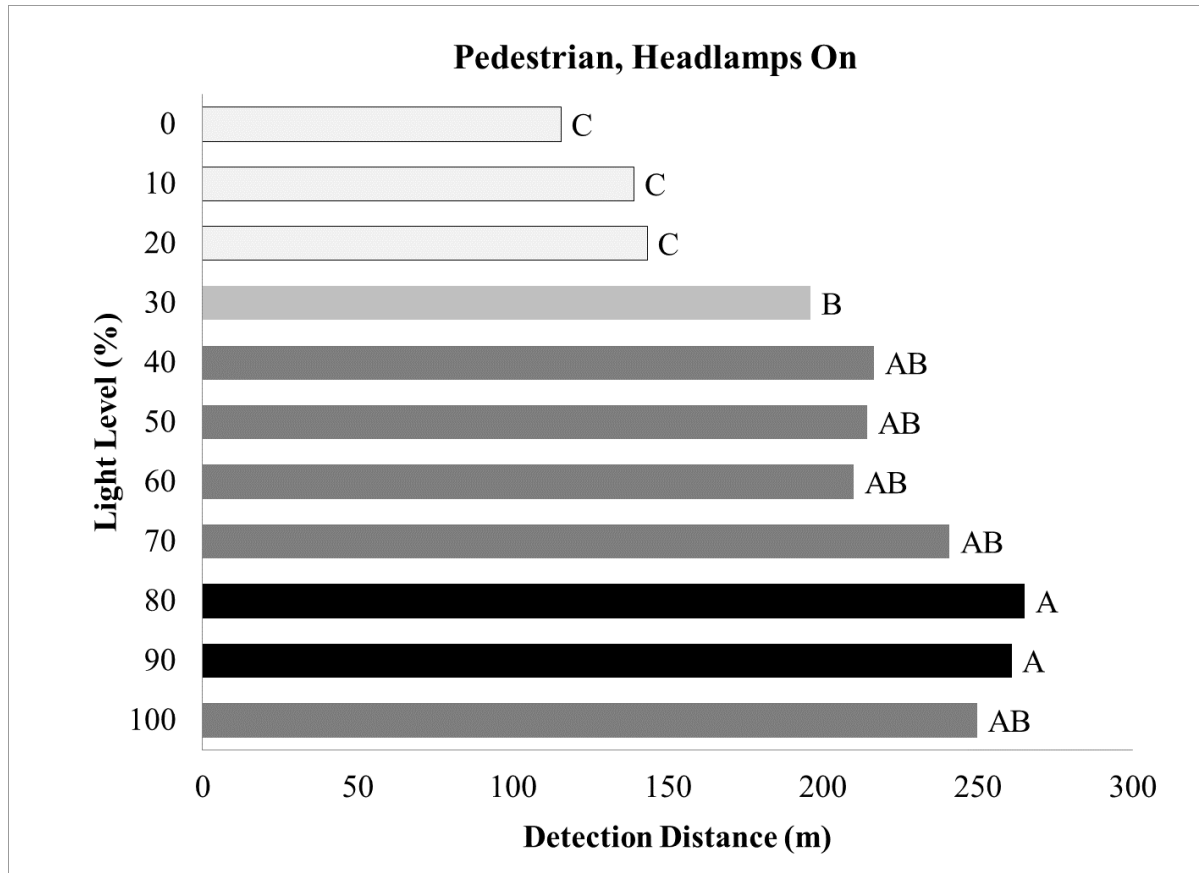


1 m = 3.3 ft

Figure 80. Chart. Overhead-lighting level experiment—SNK groupings for pedestrian-detection distance with headlamps off by overhead-lighting level.

Pedestrian, Headlamps On:

For pedestrian detection with headlamps on, the SNK results show a sharp decrease in mean detection distance when the overhead-lighting level drops from 30 to 20 percent (figure 81).

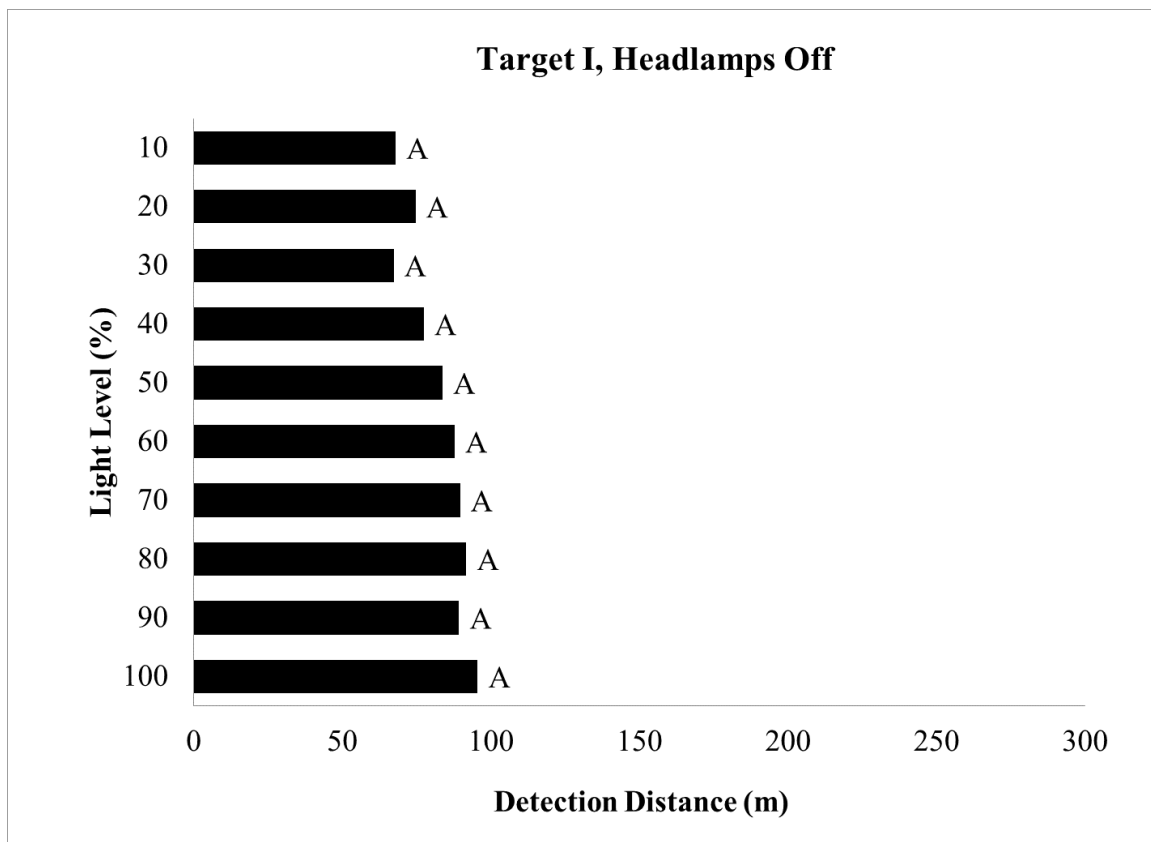


1 m = 3.3 ft

Figure 81. Chart. Overhead-lighting level experiment—SNK groupings for pedestrian-detection distance with headlamps on by overhead-lighting level.

Target I, Low VI, Headlamps Off:

There were no significant differences in target I mean detection distances for the different overhead-lighting levels, but a trend of greater mean detection distances with greater overhead lighting is apparent (figure 82).



1 m = 3.3 ft

Figure 82. Chart. Overhead-lighting level experiment—SNK groupings for target I detection distance with headlamps off by overhead-lighting level.

Target I, Low VI, Headlamps On:

The target I mean detection distances were significantly different for the different overhead-lighting levels when headlamps were on. There was a significant difference in mean detection distances between 100 and 10 percent and between 0 and levels 80 percent and higher, as illustrated in figure 83.

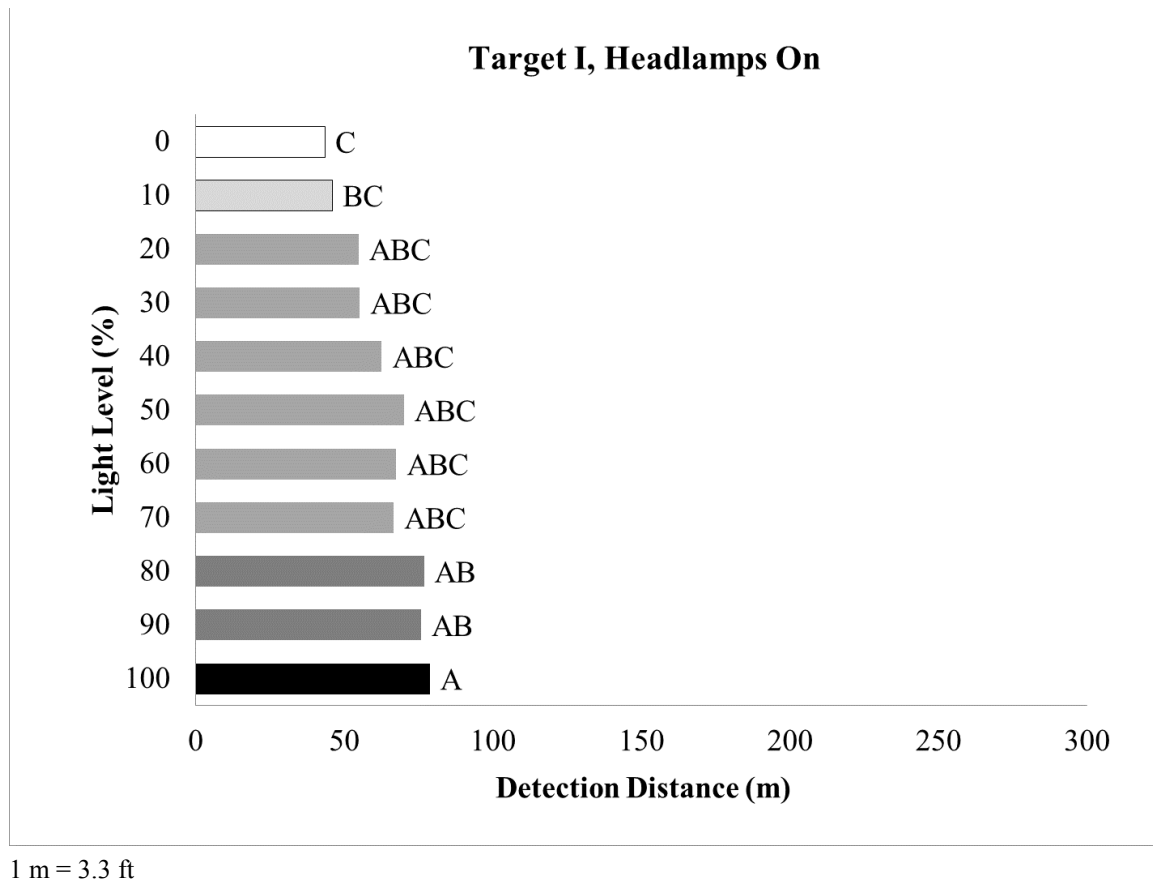


Figure 83. Chart. Overhead-lighting level experiment—SNK groupings for target I detection distance with headlamps on by overhead-lighting level.

Target II, High VI, Headlamps Off:

The mean detection distances for target II with headlamps off did not show a strong trend of greater detection distance with more intense overhead lighting. The 80-percent overhead-lighting level had a significantly greater mean detection distance than the 30-percent level, as shown in figure 84, but neither differed significantly from any of the other lighting levels.

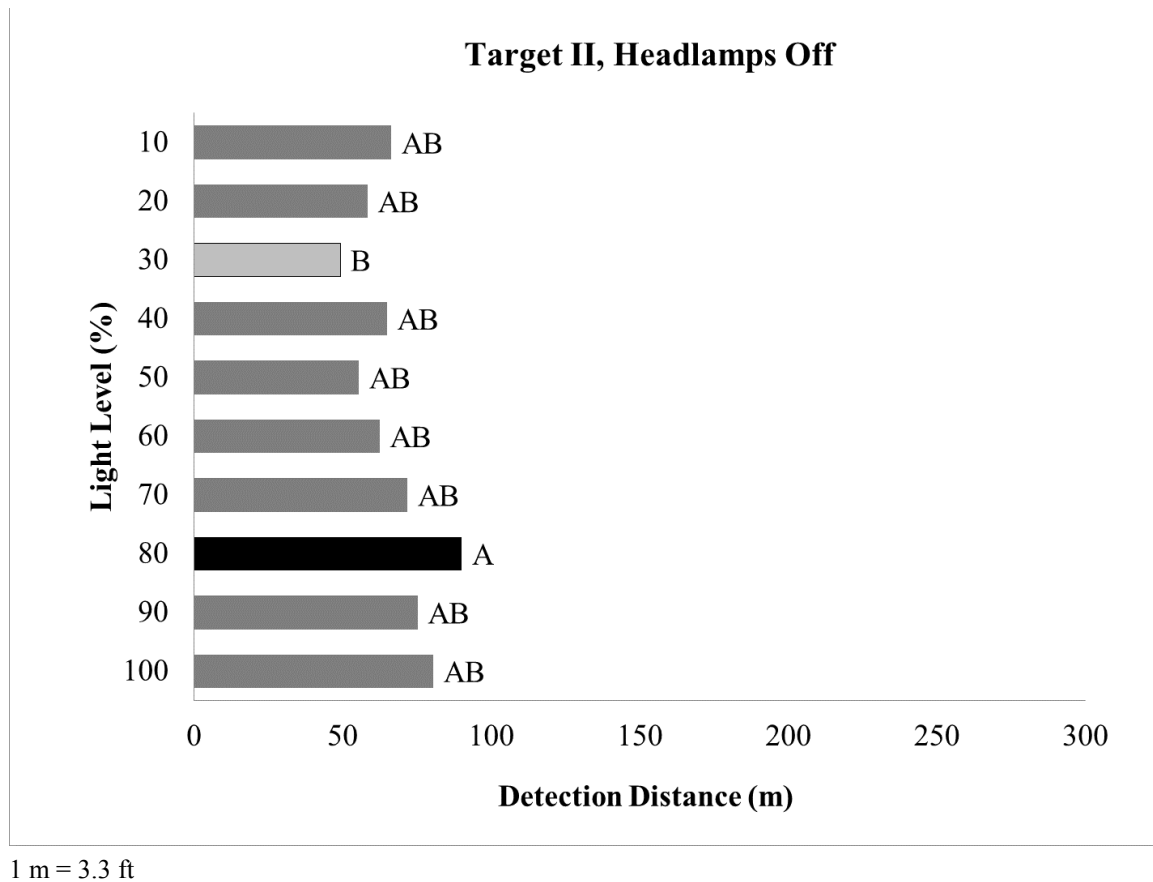


Figure 84. Chart. Overhead-lighting level experiment—SNK groupings for target II detection distance with headlamps off by overhead-lighting level.

Target II, High VI, Headlamps On:

The mean detection distances for target II with no headlamps are similar to those with headlamps; the 80-percent level had a significantly greater mean detection distance than the 30-percent level, but neither differed significantly from any of the other overhead-lighting levels (figure 85).

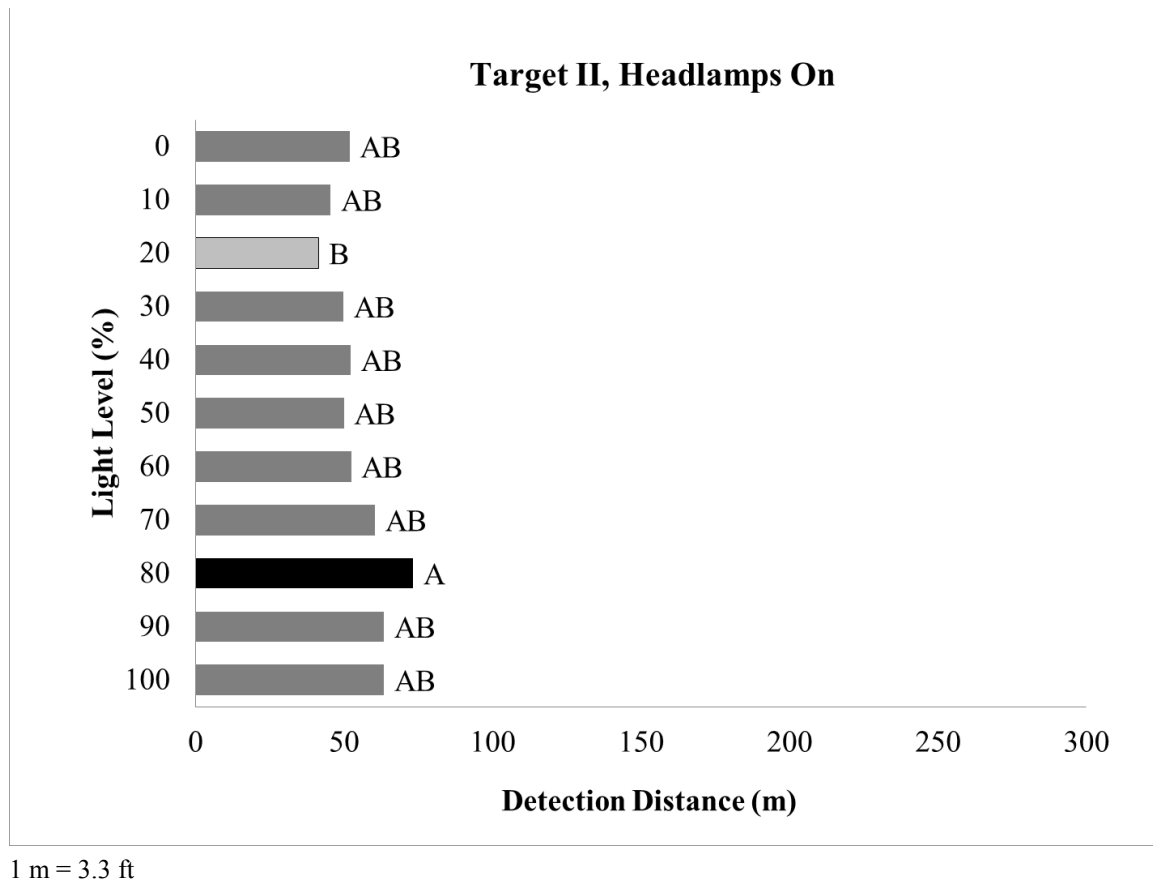


Figure 85. Chart. Overhead-lighting level experiment—SNK groupings for target II detection distance with headlamps on by overhead-lighting level.

Detection Distances Versus Headlamps On or Off

Mean detection distances were greater when the vehicle's headlamps were off for all objects—target I, target II, and the pedestrian—although the difference was not significant for the pedestrian. Those differences are shown in figure 86.

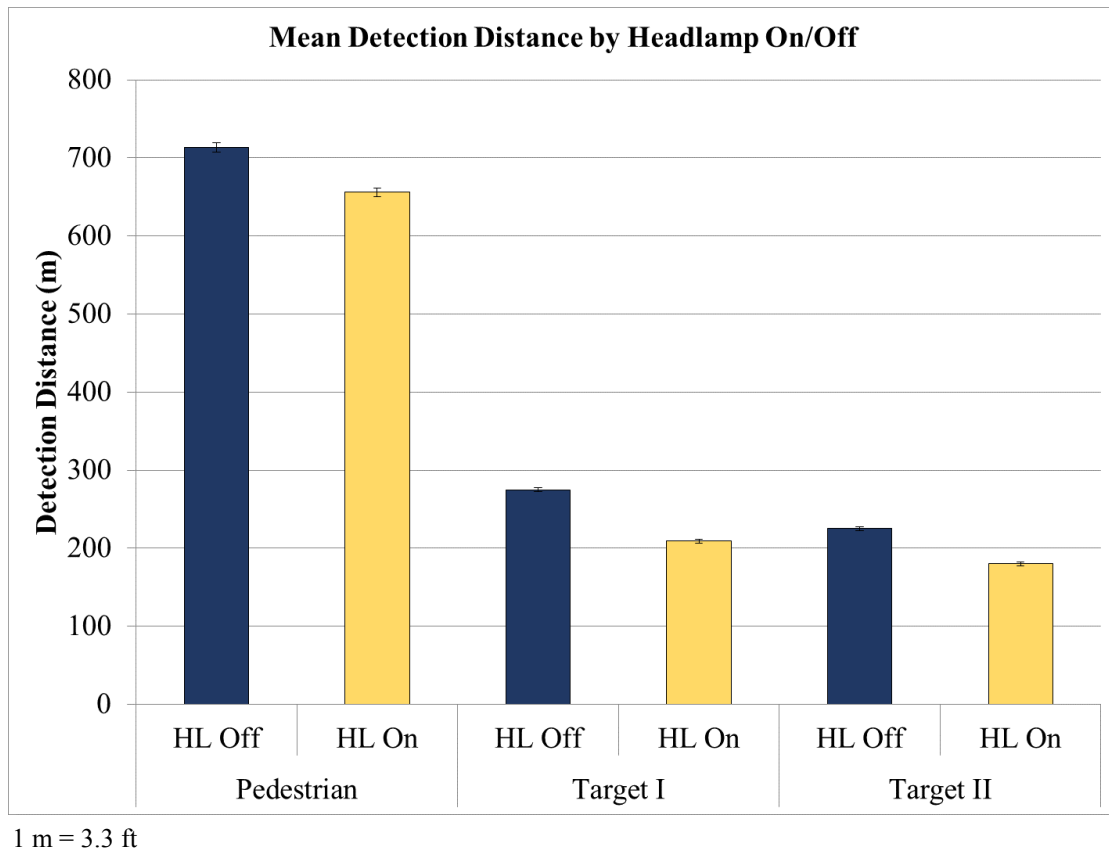


Figure 86. Chart. Overhead-lighting level experiment—mean detection distance for all objects by headlamp on/off.

Detection Distance Versus Participant Age

Young subjects detected the pedestrians and both targets at significantly greater mean distances than older participants, when all overhead-lighting levels and headlamp condition were combined. These results, illustrated in figure 87, do not differentiate between the different lighting levels.

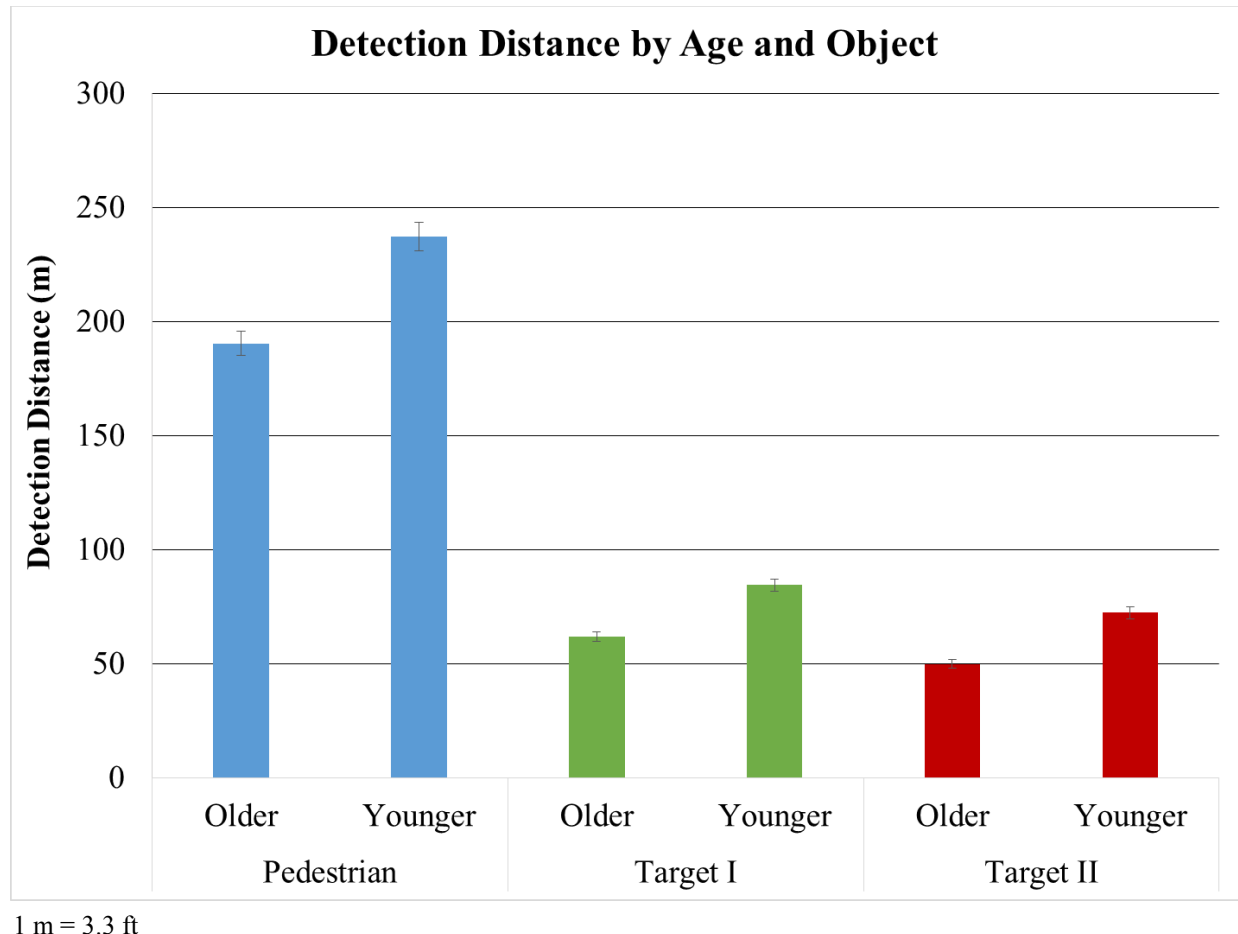
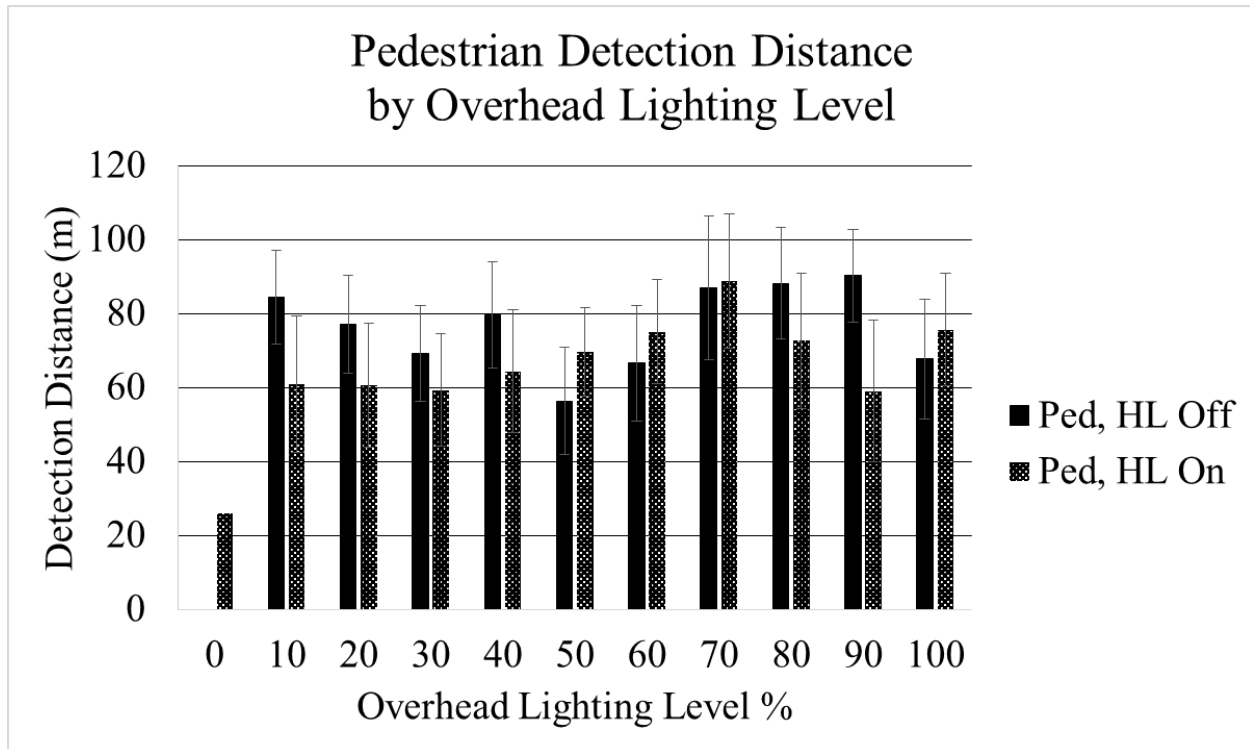


Figure 87. Chart. Overhead-lighting level experiment—mean detection distance for all objects by participant age and lighting conditions combined.

Comparison Among Pedestrian, Target I, and Target II Detection Distances

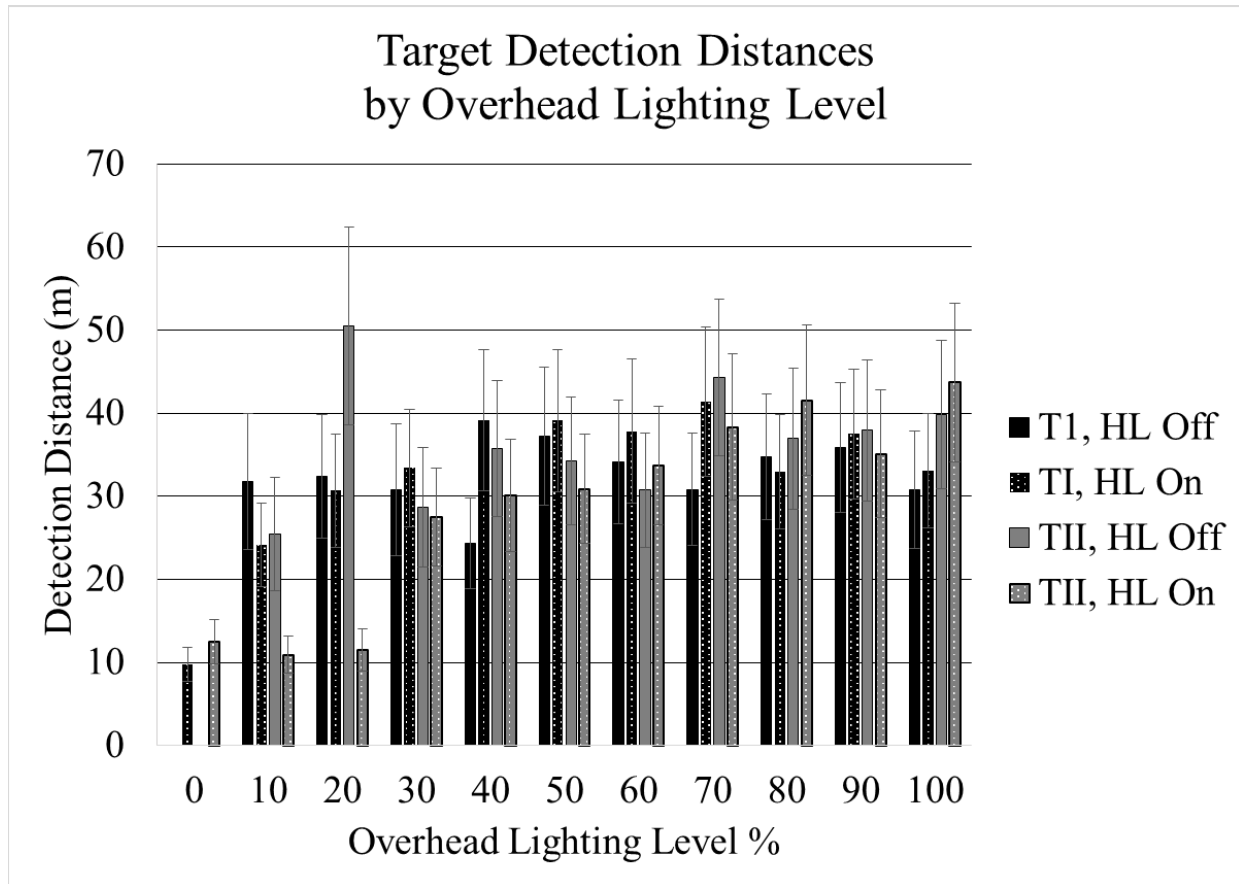
Most pedestrian-detection distances were from more than 122 m (400 ft), but the test vehicle headlamps only contributed to object illumination at between 76.2 and 107 m (250 and 350 ft) away, so overhead lighting, more than headlamps, drove pedestrian visibility. Pedestrian-detection distances were also significantly greater with headlamps off. In addition, detection distances for the pedestrians were not significantly different from each other for overhead-lighting intensities between 60 and 100 percent, as shown in figure 81, figure 82, and figure 88. This shows there might be an opportunity to conserve energy without reducing pedestrian safety.

The target I (low VI) mean detection distances tended to be greater than those for target II (high VI), with headlamps both on and off, because target I had greater contrast with the background than did target II (figure 89). Target detection distances tended to increase with increasing overhead-lighting levels in both headlamp conditions, but the increase was more erratic with target II because of its low contrast and poor general visibility to the participants. Targets were consistently detected from farther away with headlamps off, likely because the headlamps washed out the background behind the target, reducing contrast.



1 m = 3.3 ft

Figure 88. Chart. Overhead-lighting level experiment—mean detection distances for pedestrians by overhead-lighting level.



1 m = 3.3 ft

Figure 89. Chart. Overhead-lighting level experiment—mean detection distances for targets by overhead-lighting level.

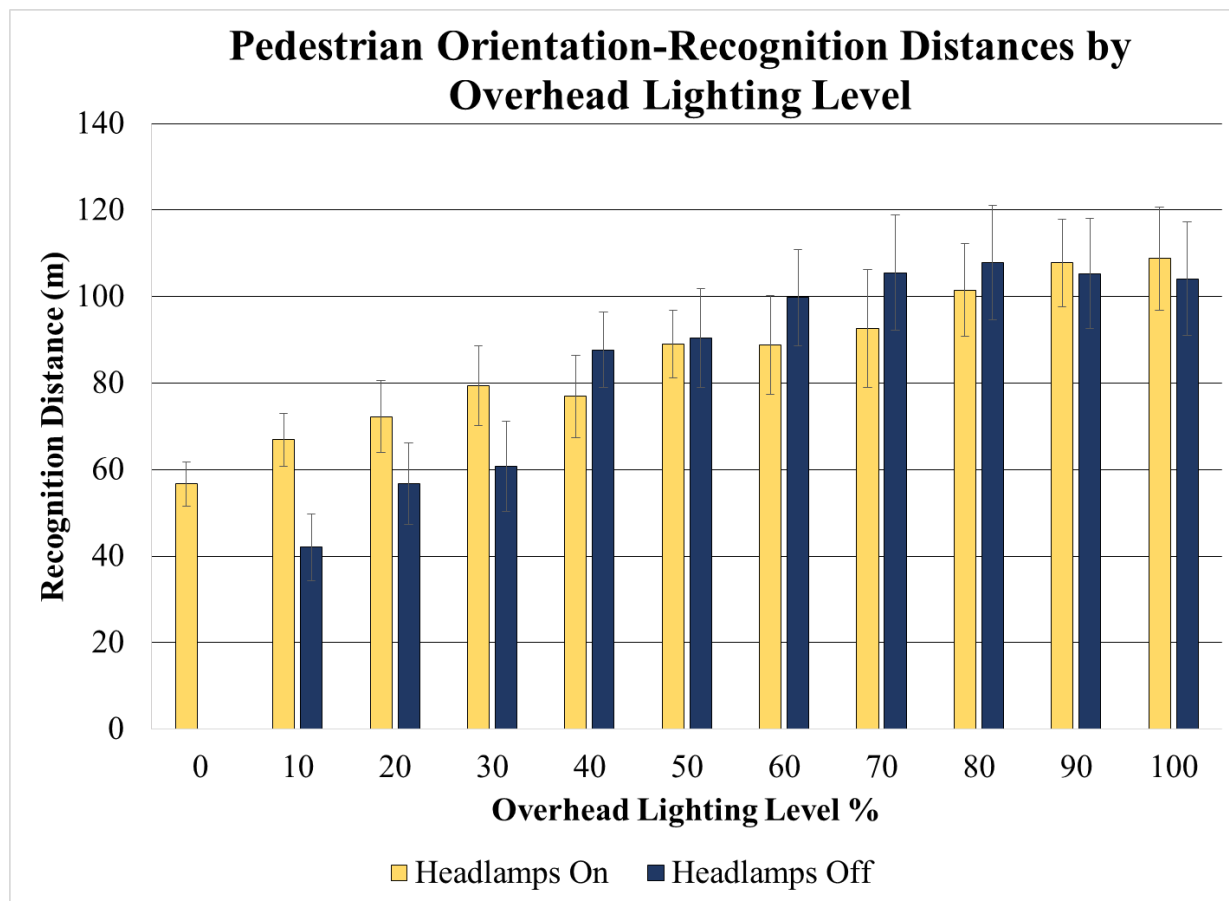
Orientation-Recognition Distance

Object orientation was randomized, unlike detection distance, because the targets were kept at the same place on the roadway. Because it was randomized, orientation-recognition distance is less likely to have participant-created error.

Pedestrian

Orientation-recognition distances varied more widely with overhead-lighting level with headlamps off than with headlamps on, because without headlamps, overhead-lighting level alone drove visibility (figure 90). At overhead-lighting levels between 0 and 30 percent and no headlamps, the pedestrians were less visible, resulting in shorter detection distances. At those same overhead-lighting levels, however, and with headlamps on, pedestrian orientation was recognized from farther away—about 91.4 m (300 ft)—the limit of the headlamp’s range. Therefore, headlamps create a boundary at about 91.4 m (300 ft) where objects will most likely be visible. Adding overhead lighting increased orientation-recognition distances beyond that 300 ft (91.4 m).

Orientation-recognition distances for the pedestrian varied widely, and that variance was even wider at higher overhead-lighting levels, whether or not the headlamps were on.



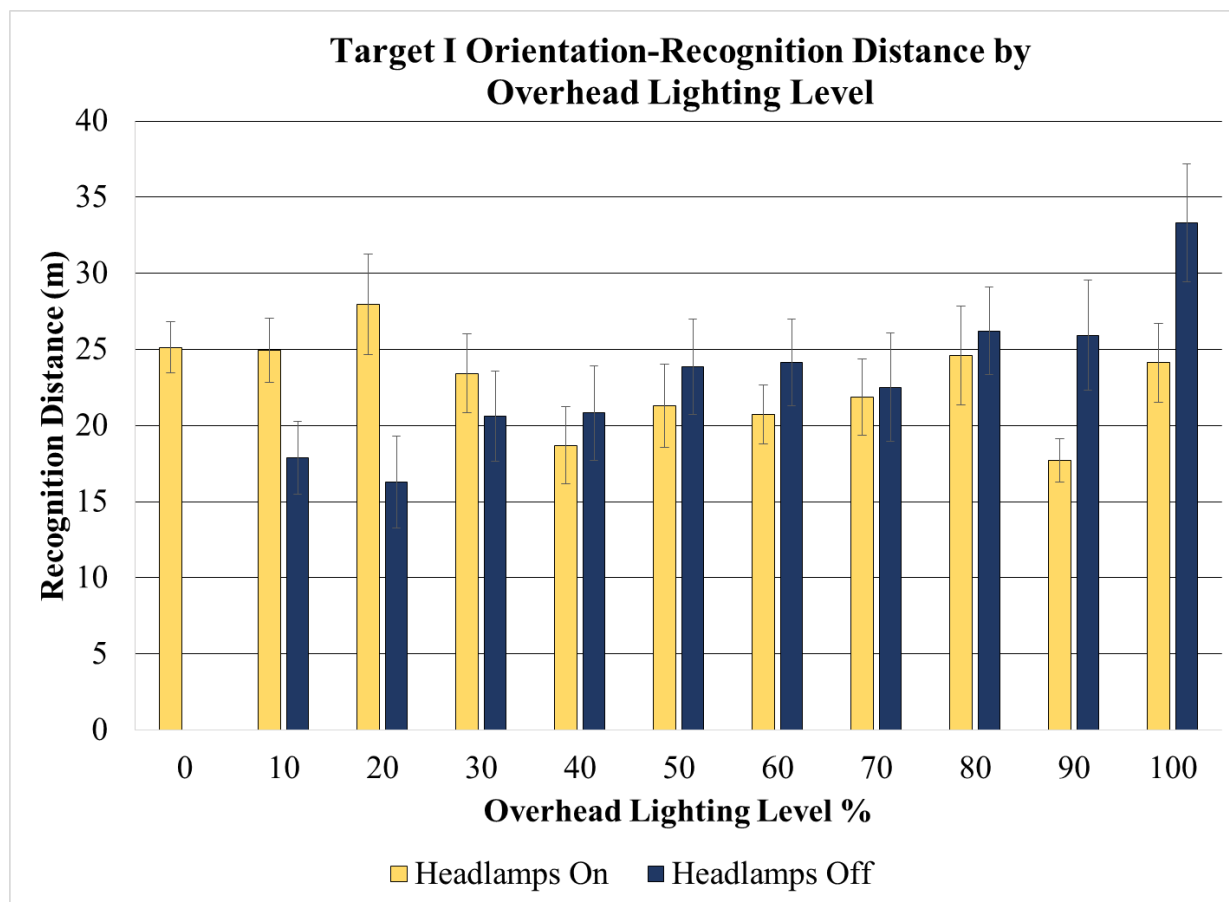
1 m = 3.3 ft

Figure 90. Chart. Overhead-lighting level experiment—mean recognition distance of pedestrian by headlamps on and off and overhead-lighting level.

Target I

Figure 91 shows that for target I, the span of orientation-recognition distances with headlamps off and 10-percent overhead lighting was from 15 to 125 m (50 to 500 ft). With headlamps on, that span was from 24 to 61 m (80 to 200 ft).

With headlamps off and high overhead-lighting levels, participants recognized target orientation from distances beyond where headlamps normally illuminate. With headlamps on and overhead-lighting levels at 30 percent and below, participants recognized targets from farther away. Therefore, headlamps helped drivers see targets at those lower lighting levels.

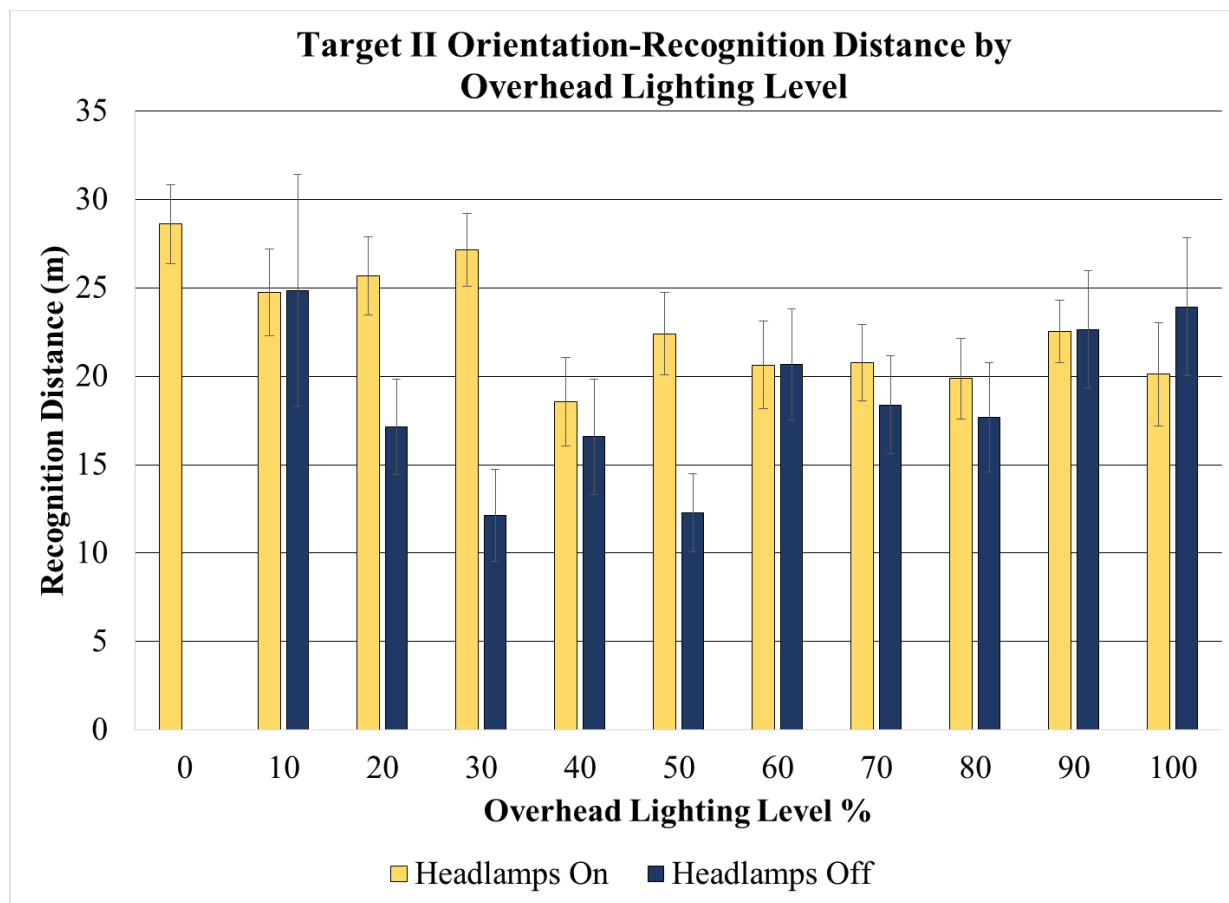


1 m = 3.3 ft

Figure 91. Chart. Overhead-lighting level experiment—mean recognition distance of target I by headlamps on and off and overhead-lighting level.

Target II

The orientation-recognition distances for target II vary widely with headlamps on and off at between 100- and 0-percent overhead lighting (figure 92). One trend is that with headlamps on and with between 20- and 50-percent overhead lighting, participants recognized target II orientation from farther away than with headlamps off.



1 m = 3.3 ft

Figure 92. Chart. Overhead-lighting level experiment—mean recognition distance of target II by headlamps on and off and overhead-lighting level.

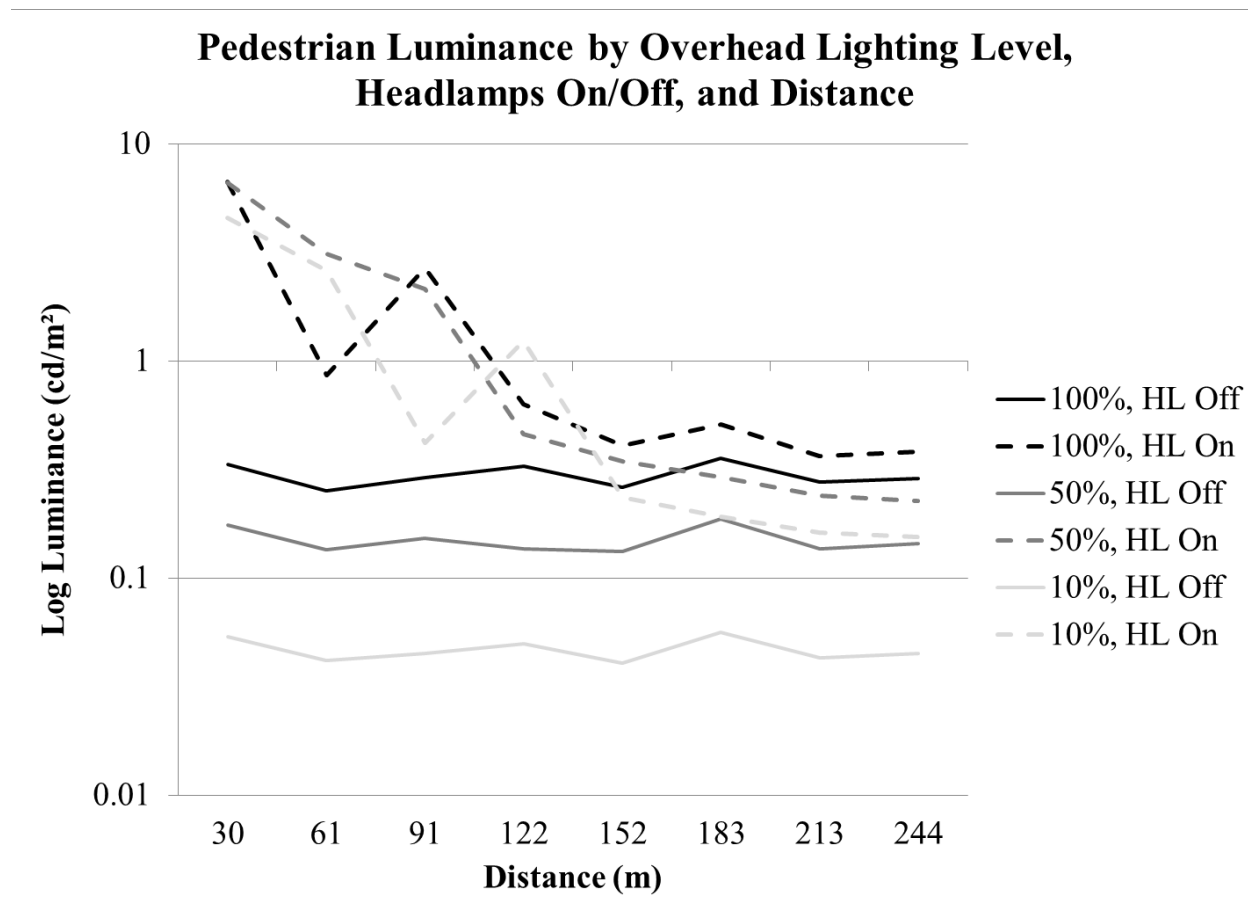
Luminance

The luminance and contrast measures were measured to determine whether detection distance correlated with changes in contrast. If so, photometric measurements could be used to predict driver visual behavior.

Pedestrian

Pedestrian-detection distances differed significantly with the 100-, 50-, and 1- percent overhead-lighting levels, so those lighting levels were chosen for the luminance analysis. Luminance for those overhead-lighting levels was measured from 30.4 to 244 m (100 to 800 ft) in 15.2-m

(100-ft) intervals. Results are shown in figure 93 and described following the figure. Log luminance is used to better show the differences in the conditions without headlamps.



1 cd/m² = 0.3 fL
1 m = 3.3 ft

Figure 93. Graph. Overhead-lighting level experiment—pedestrian log luminance by overhead-lighting level, headlamp condition, and distance.

Overhead Lighting at 100 Percent:

The luminance between 213 and 244 m (700 and 800 ft) was 0.096 cd/m² (0.028 fL) higher with headlamps on, showing some headlamp illumination was reaching the pedestrian even at 244 m (800 ft), probably via reflection off the guard rails and roadway surface. Headlamps illuminated the pedestrian more directly beginning at 122 m (500 ft), and then luminance increased sharply at 91.4 m (300 ft) from the pedestrian, where the headlamps began to directly illuminate them.

Overhead Lighting at 50 Percent:

Dimming the overhead lighting from 100 to 50 percent affected the pedestrian luminance; at 244 m (800 ft) and without headlamps, the pedestrian luminance at 50-percent overhead lighting (0.145 cd/m² (0.042 fL)) was half that at 100-percent overhead lighting (0.288 cd/m² (0.084 fL)). With headlamps, the luminance at 50-percent overhead lighting was 58 percent (0.226 cd/m²

(0.066 fL)) of that at 100-percent overhead lighting (0.384 cd/m^2 (0.112 fL)), showing the percent contribution of headlamp light to luminance was different for the various overhead lighting intensities. This could be because at 100-percent overhead lighting level, the overhead lighting drowned out the headlamps' effect. Also, slightly different vehicle and pedestrian positions between measurements could affect luminance measurements.

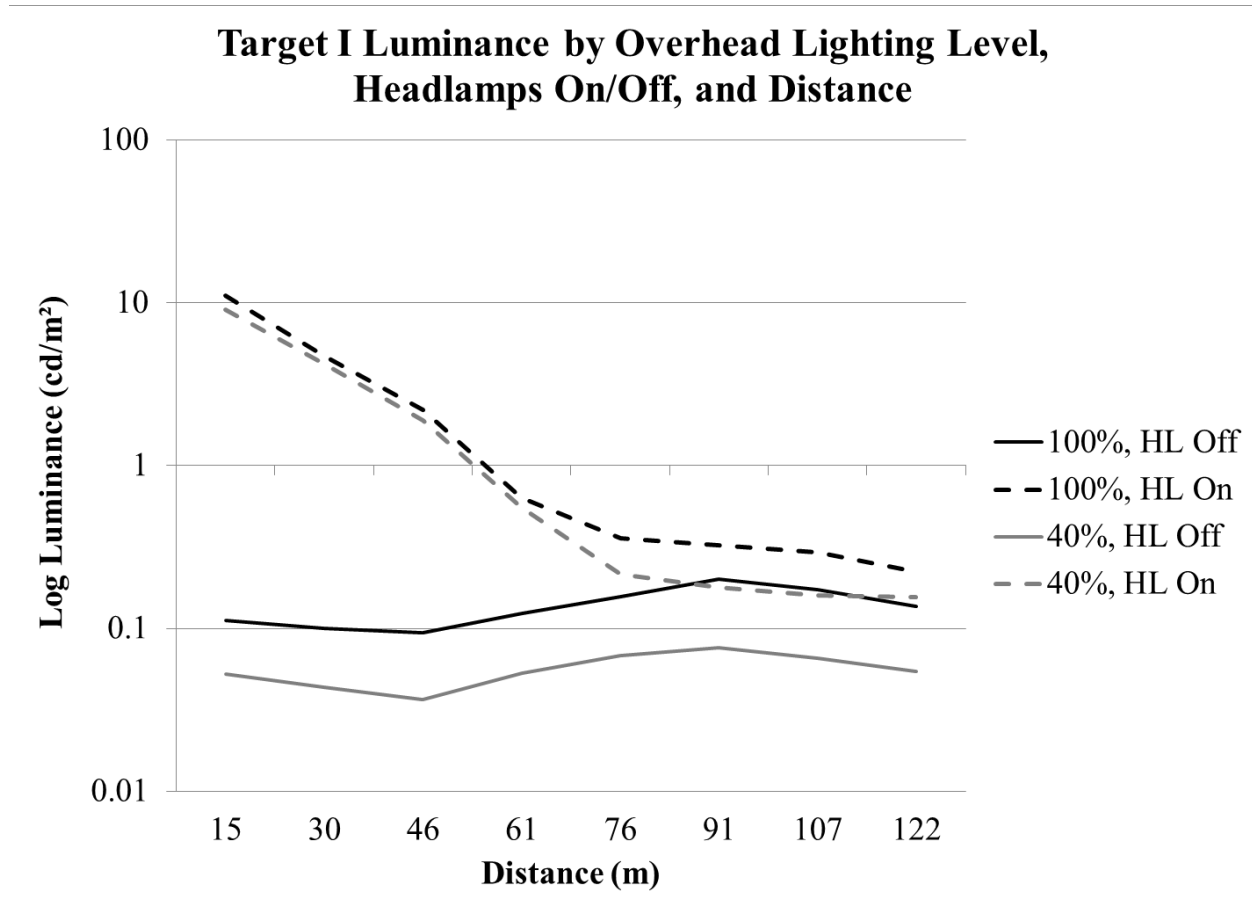
Overhead Lighting at 10 Percent:

Dimming the overhead lighting from 100 to 10 percent affected the pedestrian luminance; at 244 m (800 ft) and without headlamps, the pedestrian luminance at 10-percent overhead lighting (0.045 cd/m^2 (0.013 fL)) was 15 percent of that at 100-percent overhead lighting (0.288 cd/m^2 (0.084 fL)) with the headlamps off. With headlamps, the luminance at 10-percent overhead lighting was 35 percent (0.1375 cd/m^2 (0.040 fL)) of that at 100-percent overhead lighting (0.384 cd/m^2 (0.112 fL)). This shows that headlamp illumination affected pedestrian luminance at that distance.

Another important aspect of this comparison is that the headlamp seemed to dominate the target light level at 152 m (499 ft), where the target luminances from each of the dim levels began to converge.

Target I (Low VI)

The 40-percent overhead-lighting level had considerably shorter detection distances than more intense levels and appears to be the level where overhead lighting and headlamp light contribute similarly to luminance. Therefore, the 100- and 40-percent levels were selected for luminance analyses. Luminance measurements were taken from 15.2 to 122 m (50 to 400 ft) in 15.2-m (50-ft) intervals, and the results are shown in figure 94.



1 cd/m^2 = 0.3 fL
1 m = 3.3 ft

Figure 94. Graph. Overhead-lighting level experiment—target I luminance by overhead-lighting level, headlamp condition, and distance.

Results for 100- and 40-percent overhead lighting were similar, and headlamp condition and vehicle distance to target both affected target I's luminance. For headlamps on and off, the targets had nearly equal luminance between 91.4 and 122 m (300 and 400 ft). At 76.2 m (250 ft) and closer, the luminances diverged, with target I in the headlamp-on condition brighter than in the headlamp-off condition. Luminances were slightly greater with headlamps on at 100-percent overhead lighting than those with headlamps on at 40-percent overhead lighting at distances closer than 60 m (200 ft).

Target II (High VI)

Like target I, the luminance and contrast of target II were analyzed at 100- and 40-percent overhead-lighting levels. Results are illustrated in figure 95.

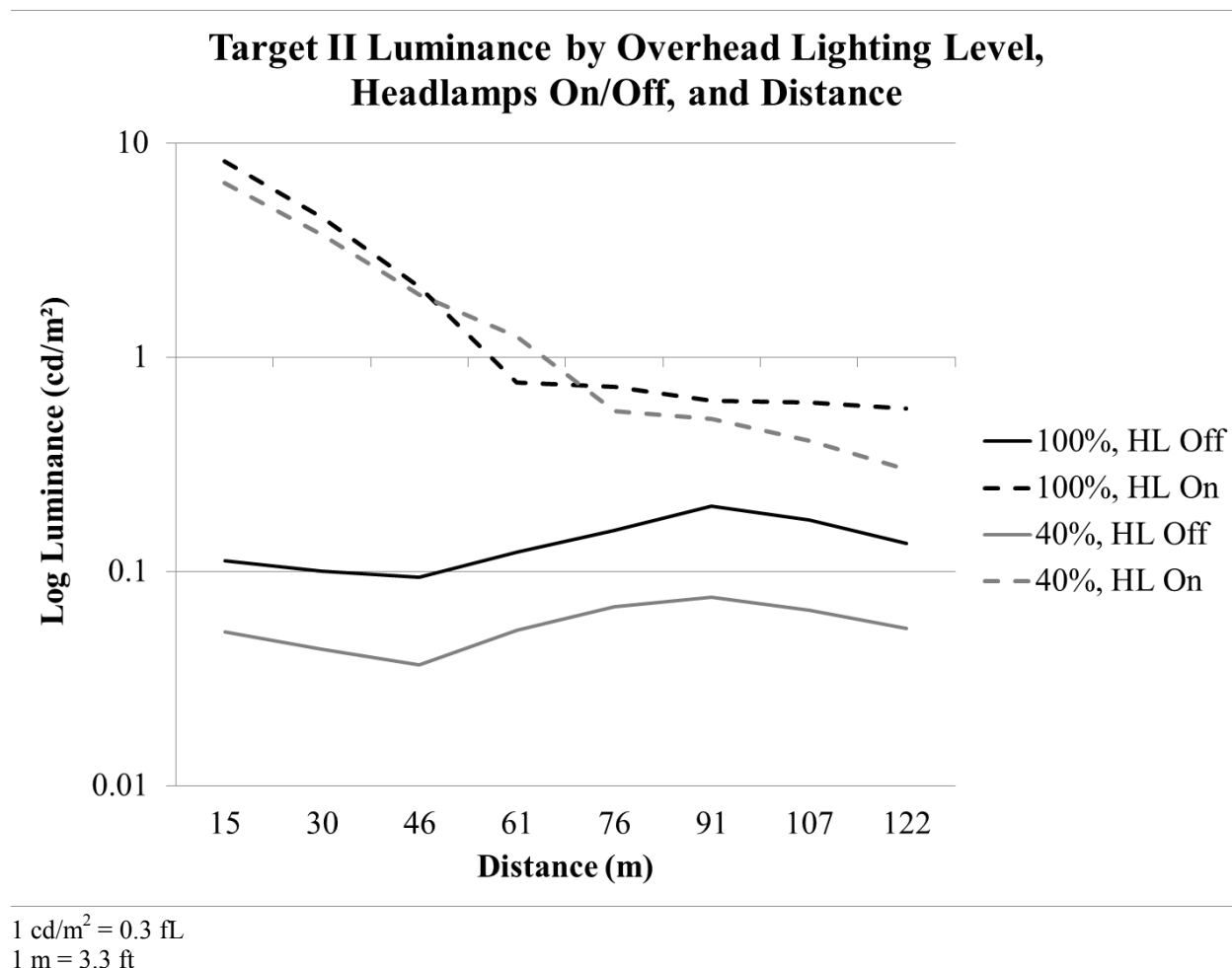


Figure 95. Graph. Overhead-lighting level experiment—target II luminance by overhead-lighting level, headlamp condition, and distance.

Results for 100- and 40-percent overhead lighting were similar, and headlamp condition and vehicle distance to target both affected the target II's luminance. In both overhead-lighting conditions, target luminance with headlamps on was greater than with headlamps off, even at longer distances. Like target I, luminance increased rapidly as measurements were taken from 60 m (200 ft) and closer with the headlamps on because headlamp light contributed to luminance. At greater distances, headlamp contribution to luminance was smaller for target II, but the headlamps-on and headlamps-off curves never converged, showing that even at great distances, headlamps contributed slightly to target luminance.

DISCUSSION

Although this experiment did not specifically evaluate models of mesopic vision—a project objective—its results provide insight on human visual behavior while driving in mesopic conditions as a method to determine the adaptation level of the driver, which is an input to the mesopic model. Pedestrians and small roadside targets were largely visible to participants even in low contrast conditions and without headlamps. Dimming the roadway lighting did not affect luminance ratio and contrast of objects, but object visibility, as measured by detection and object-recognition distances, did change depending on roadway lighting dim level. At 40-percent overhead lighting and below, detection distances were much shorter than at higher lighting levels. At 30-percent overhead lighting and below, orientation-recognition distances were much shorter. The range of orientation-recognition distances narrowed considerably at 30-percent overhead lighting and below. Therefore, participants were able to detect and recognize low-contrast objects, but that ability dropped off at reduced overhead lighting.

Viewing angle affected object visibility, as did the angle of light on the object. Object illuminance combined with contrast affected visibility in terms of quantity, in accordance with Adrian's model.⁽⁵⁴⁾

Contrast polarity also affected object visibility. The negatively contrasting target—target I—had greater detection distances than the positively contrasting target—target II. Adrian's model accounts for the tendency for negatively contrasting objects to have higher visibility.⁽⁵⁴⁾ However, when the vehicle approached the negatively contrasted target, the headlamps illuminated it, increasing its luminance with respect to the background. As the vehicle approached, the target contrast was close to zero for a period of time, rendering it invisible. When the vehicle was close enough, the headlamps illuminated the target enough to produce positive contrast. Thus, negatively contrasted objects are initially more visible than positively contrasted objects, but as a vehicle with headlamps approaches them, there is a span of distance where the object has low contrast and very poor visibility. Positively contrasted objects only increase in contrast as a vehicle approaches.

Zones of Visibility

Headlamps and roadway lighting combine to form three zones of visibility for object detection. These zones, introduced by Boyce, include near, intermediate, and far categories.⁽⁹⁵⁾ The near zone is where visibility is dominated by headlamp light. The intermediate zone is where headlamp and overhead lighting combine to affect visibility. The far zone is where overhead lighting alone contributes to visibility.

The zones of visibility identified in this experiment for pedestrians and targets are listed in table 25. The near zone for target visibility was aligned with previous research that found headlamps were the dominant light source up to approximately 40 m (130 ft).⁽⁹⁵⁾ The differences in visibility zones between the pedestrian and the targets are because they are different sizes and are different distances from the ground. The boundaries for the intermediate zone for pedestrians were not as clear from the data because the pedestrian contrast polarity shift was more gradual than that of the targets.

Table 25. Overhead-lighting level experiment—zones of visibility for pedestrian and targets.

Zone	Pedestrian	Targets
Near Zone	0 to 91.4 m	0 to 30 m
Intermediate Zone	91.4 to 152 m	30 to 76.2 m
Far Zone	152 m and beyond	76.2 m and beyond

1 m = 3.3 ft

Stopping Sight Distance

Lighting design should consider stopping sight distance, because illuminated objects must be visible from far enough away for drivers to stop. The detection distances were assumed to be stopping sight distances, and vehicle speeds corresponding to those distances were calculated using the stopping sight distance formula. The following calculations take into account both headlamp and overhead light, meeting a project objective of evaluating influence of the interaction of vehicle headlamps and overhead lighting on driver visual performance. The results are listed in table 26.

Table 26. Overhead-lighting level experiment—object stopping sight distance and corresponding speed.

Overhead-Lighting Level (percent)	Headlamp Condition	Pedestrian Stopping Sight Distance (m)	Pedestrian Rec. Speed (km/h)	Target I Stopping Sight Distance (m)	Target I Rec. Speed (km/h)	Target II Stopping Sight Distance (m)	Target II Rec. Speed (km/h)
0	ON	76	56	24	24	24	24
10	OFF	24	24	24	24	35	32
10	ON	76	56	24	24	24	24
20	OFF	35	32	24	24	—	< 24
20	ON	76	56	24	24	24	24
30	OFF	—	< 24	—	< 24	—	< 24
30	ON	76	56	—	< 24	—	< 24
40	OFF	61	48	24	24	—	< 24
40	ON	93	64	—	< 24	—	< 24
50	OFF	130	80	—	< 24	—	< 24
50	ON	93	64	—	< 24	—	< 24
60	OFF	130	80	—	< 24	—	< 24
60	ON	130	80	24	24	—	< 24
70	OFF	110	72	24	24	—	< 24
70	ON	76	56	—	< 24	—	< 24
80	OFF	151	88	24	24	24	24
80	ON	151	88	—	< 24	—	< 24
90	OFF	93	64	24	24	—	< 24
90	ON	110	72	24	24	24	24
100	OFF	110	72	35	32	—	< 24
100	ON	110	72	—	< 24	—	< 24

Rec. = Recognition.

— Indicates data were not adequate to provide a meaningful result.

1 km/h = 0.62 mi/h

1 m = 3.3 ft

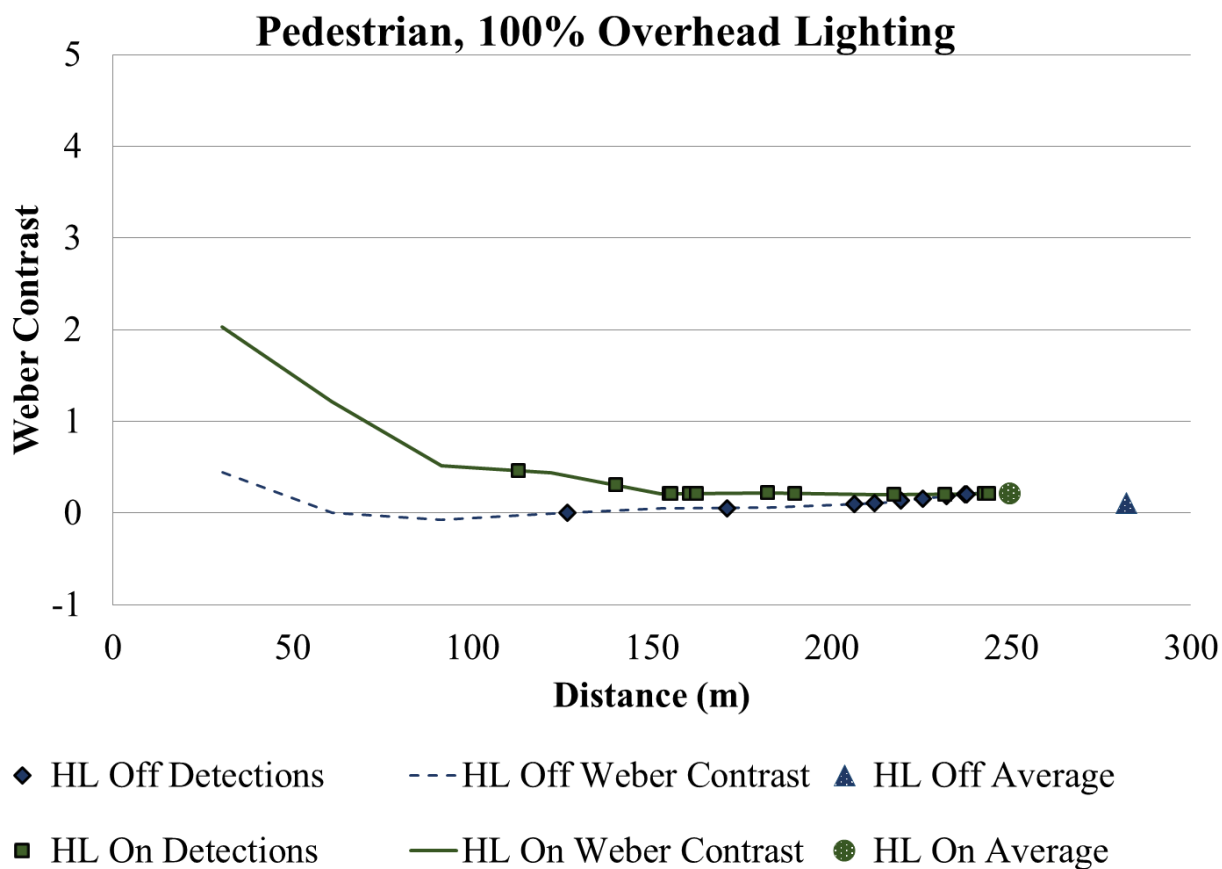
There are many instances in which the minimum detection distance was shorter than suggested by stopping sight distance at a typical speed limit of about 24 km/h (15 mi/h). The implication is that, for those situations, drivers typically cannot see objects in time to stop. That was the case for many conditions using the targets but not so with the pedestrian, where drivers could travel as fast as 88 km/h (55 mi/h) and still see a pedestrian in time to stop. (Most roadways with pedestrians have speed limits of 72 km/h (45 mi/h) or lower.) The results for target detection suggest that headlamp and overhead-lighting design might be inadequate for small-object detection.

Weber Contrast and Detection Distance

Pedestrian

Weber contrasts for the pedestrians and targets were calculated using the same procedure outlined in the scoping experiment. Weber contrast results were related to detection distances and are examined in the discussion.

Overhead Lighting at 100 Percent: The contrasts calculated from the images of the pedestrian are shown in figure 96. Overlaid on the contrast curves are points at which the participant detected the pedestrian. Between 152 and 213 m (500 and 700 ft), the curves slightly diverge, with pedestrians and headlamps on having more contrast. At those greater distances, the headlamps illuminate the roadway in front of the vehicle, causing the eye to adapt to the brighter foreground and causing the background and pedestrian to appear darker.



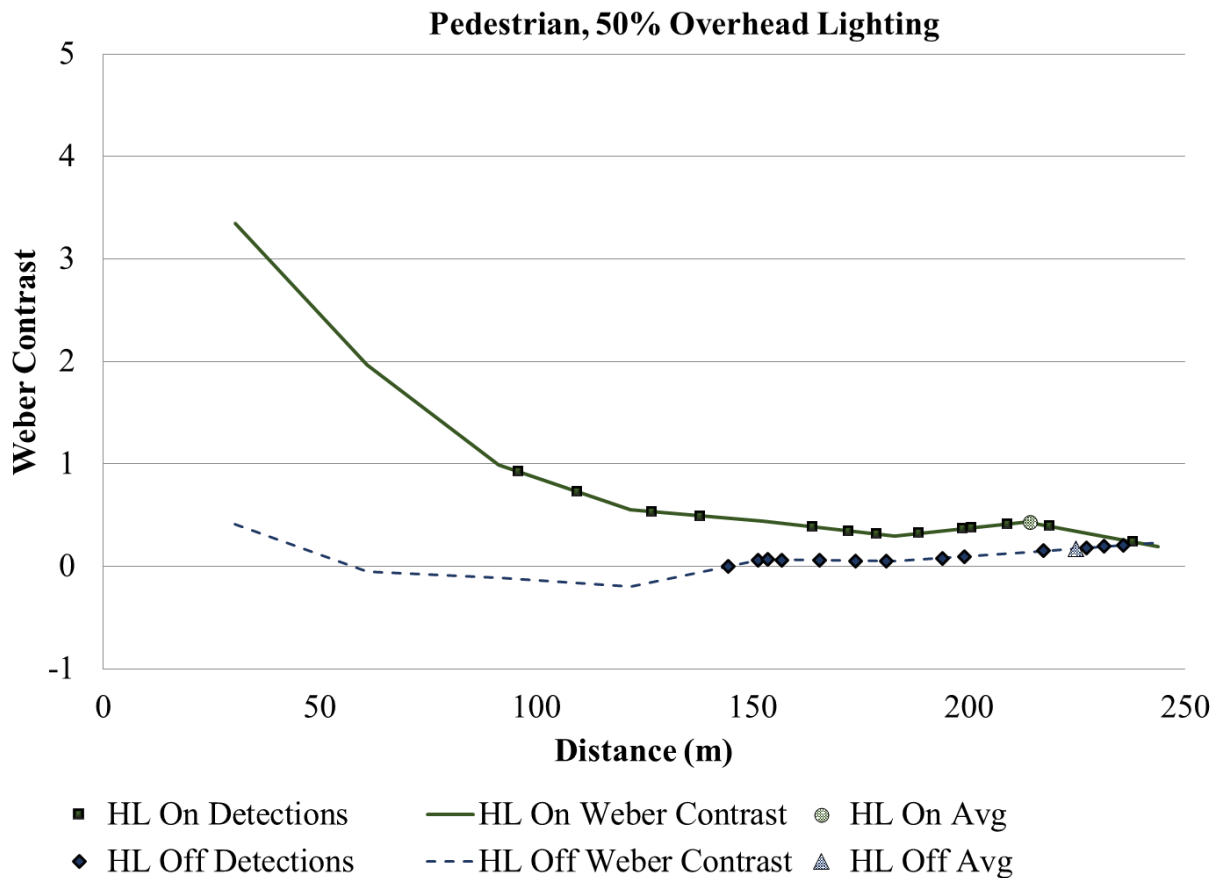
1 m = 3.3 ft

Figure 96. Graph. Overhead-lighting level experiment—pedestrian contrast and detection distance at 100-percent overhead lighting.

The contrast curves diverge more sharply at distances closer than 122 m (500 ft), where the headlamps begin to indirectly illuminate the pedestrian via reflections from the pavement and guardrails, and very sharply at 91.4 m (300 ft) from the pedestrian, where the headlamps begin to directly illuminate the pedestrian.

Changing contrast as the vehicle approaches the pedestrian did not appear to affect detection distance because the average detection distance with headlamps off was 285 m (925 ft) and with headlamps on was 250 m (819 ft), distances with very low measured luminance contrast. This level can be determined to be the threshold contrast for the object. (Note 100-percent detection threshold, not 50-percent detection as typically referenced.) The participants could be detecting pedestrians from farther away without headlamps because headlamps raise the ambient light level, causing the eye to adapt to a higher light level and be less sensitive. It would also be because participants tend to not look beyond the area their headlamps illuminate and do not scan as far ahead with headlamps on. Both detection distances are sufficient for a driver to stop a vehicle traveling at 121 km/h (75 mi/h) before arriving at the pedestrian; however, while it is unlikely a road with that speed limit would have pedestrians, other hazards, such as wildlife, might be present.

Overhead Lighting at 50 Percent: The Weber contrasts of the images were similar to those taken at 100-percent overhead-lighting level, because dimming the overhead lighting dims the entire scene and changes the luminance difference, while the luminance ratio is unchanged. Average detection distances were more than 244 m (800 ft) with 100-percent overhead lighting but are just over 213 m (700 ft) with 50-percent overhead lighting with headlamps on or off. A 50-percent reduction in overhead-lighting output shortened the detection distances by 21 percent without headlamps and 14 percent with headlamps. Results are shown in figure 97.



1 m = 3.3 ft

Figure 97. Graph. Overhead-lighting level experiment—pedestrian contrast and detection distances at 50-percent overhead lighting.

Overhead Lighting at 10 Percent:

The Weber contrast curves for 10-percent overhead lighting are similar to those for the other lighting levels, but the average detection distances are different (figure 98).

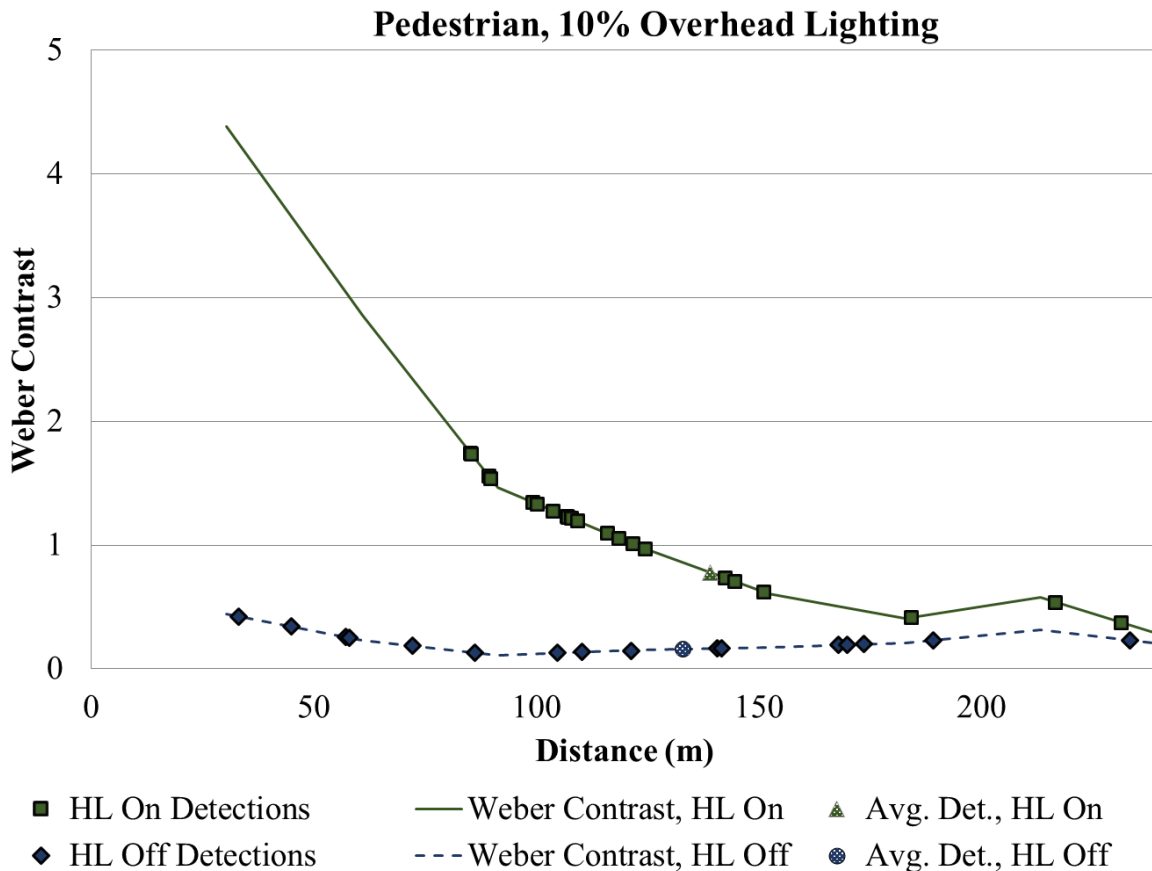


Figure 98. Graph. Overhead-lighting level experiment—pedestrian contrast and detection distances at 10-percent overhead lighting.

Target I (Low VI)

Weber contrast calculations were performed for the targets at 100-percent and 40-percent overhead lighting levels. The 40-percent overhead lighting level had considerably shorter detection distances than more intense levels and appears to be the level at which overhead lighting and headlamp light contribute similarly to luminance. Therefore, those lighting levels were selected for contrast analyses.

Overhead Lighting at 100 Percent:

Images of target I with 100-percent overhead lighting taken from various distances are shown in figure 99 to illustrate that, between 45.7 and 76.2 m (150 and 250 ft), the contrast changes from positive to negative. At 61.0 m (200 ft), the 100-percent overhead lighting creates negative contrast by illuminating the road behind the target, and the headlamps create positive contrast by illuminating the target. The target goes through a stage where it is invisible, and the contrast shifts from negative to positive and crosses the point of zero contrast.




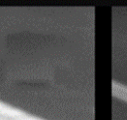
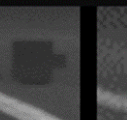
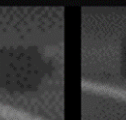
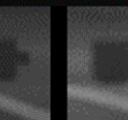

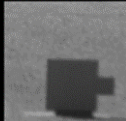
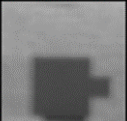
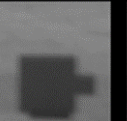
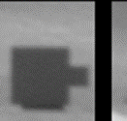

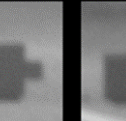
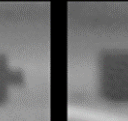
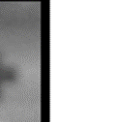
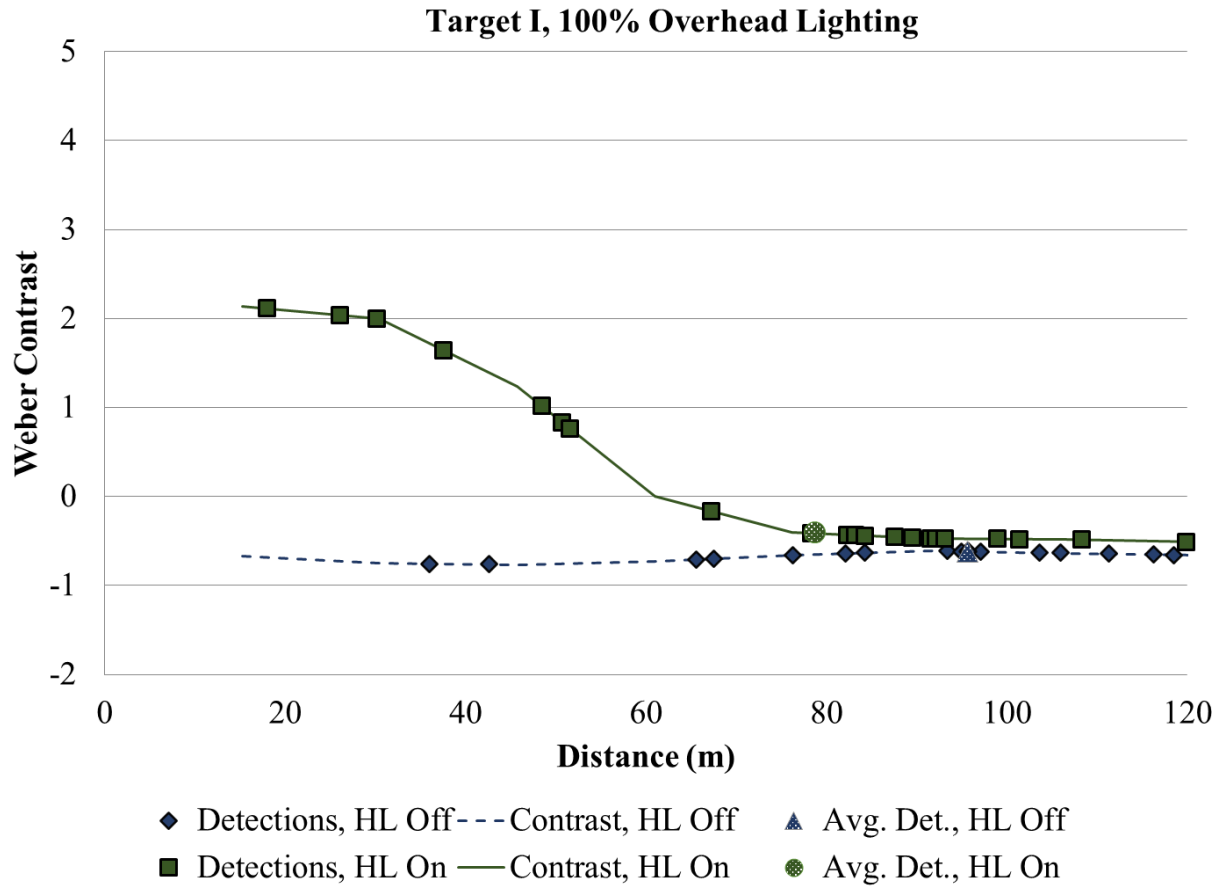
Head-lamps on/off	15.2 m (50 ft)	30.5 m (100 ft)	45.7 m (150 ft)	61.0 m (200 ft)	76.2 (250 ft)	91.4 m (300 ft)	107 m (350 ft)	123 m (400 ft)
On								
Off								

Figure 99. Image Table. Overhead-lighting level experiment—images of target I at 100-percent overhead lighting for from 15.2 to 123 m (50 to 400 ft) to the target.

The Weber contrasts for target I at 100-percent overhead lighting, with and without headlamps, are shown in figure 100. With the headlamps on (solid line), the shift from negative to positive contrast can be seen as the line passes through zero contrast. Detection distances, indicated by squares and diamonds on the two lines, are widely spread. When the vehicle was 76.2 to 122 m (250 to 400 ft) away, the contrasts, for headlamps off and on, like the luminances, were very similar.



1 m = 3.3 ft

Figure 100. Graph. Overhead-lighting level experiment—target I contrast and detection distance at 100-percent overhead lighting.

Overhead Lighting at 40 Percent:

Images of target I at various distances with 40-percent overhead lighting with and without headlamps are shown in figure 101. The ambient luminance is darker than at 100-percent overhead lighting. The same change from positive to negative contrast between 45.7 and 76.2 m (150 and 250 ft) is apparent in these images, as it was in the images with 100-percent overhead lighting.

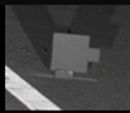
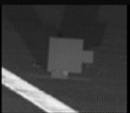
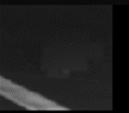
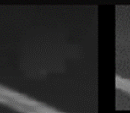
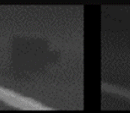
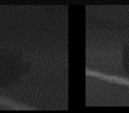
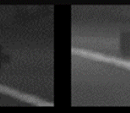
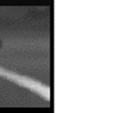
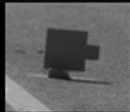
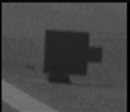
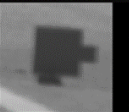
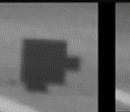
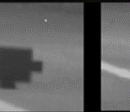
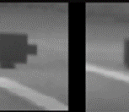
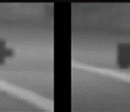
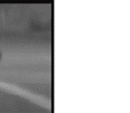
Head-lamps on/off	15.2 m (50 ft)	30.5 m (100 ft)	45.7 m (150 ft)	61.0 m (200 ft)	76.2 (250 ft)	91.4 m (300 ft)	107 m (350 ft)	123 m (400 ft)
On								
Off								

Figure 101. Image Table. Overhead-lighting level experiment—images of target I at 40-percent overhead lighting for from 15.2 to 123 m (50 to 400 ft) to the target.

Weber contrast and detection distances for target I in 40-percent overhead lighting are shown in figure 102. The average detection distance with headlamps on is shorter than with headlamps off, which could be because the headlamps cause the participant's eye to adapt to higher luminance, reducing contrast sensitivity. Also, at 40-percent overhead lighting, because headlamp light dominates the visual environment, participants might be less likely to look beyond the area illuminated by them.

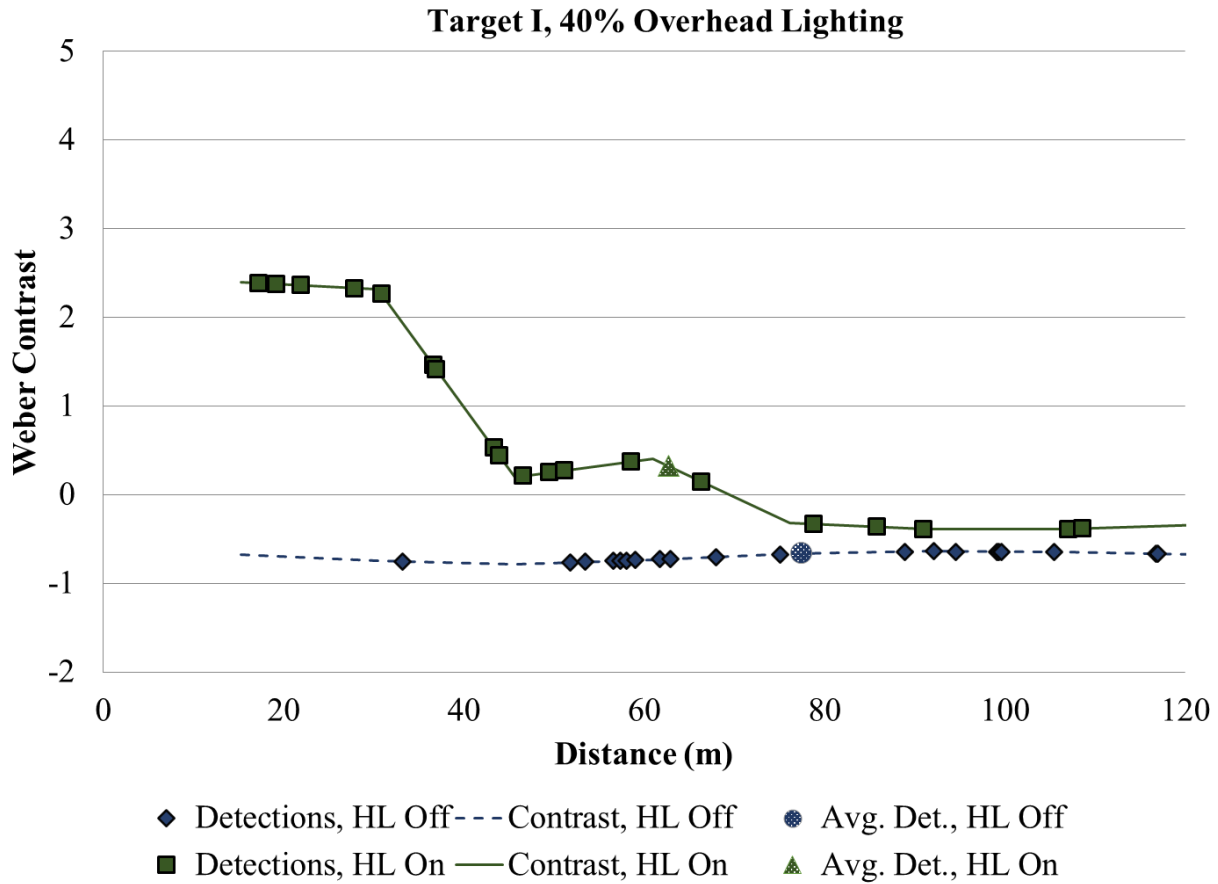


Figure 102. Graph. Overhead-lighting level experiment—target I contrast and detection distances versus distance from target at 40-percent overhead lighting.

Target II (High VI)

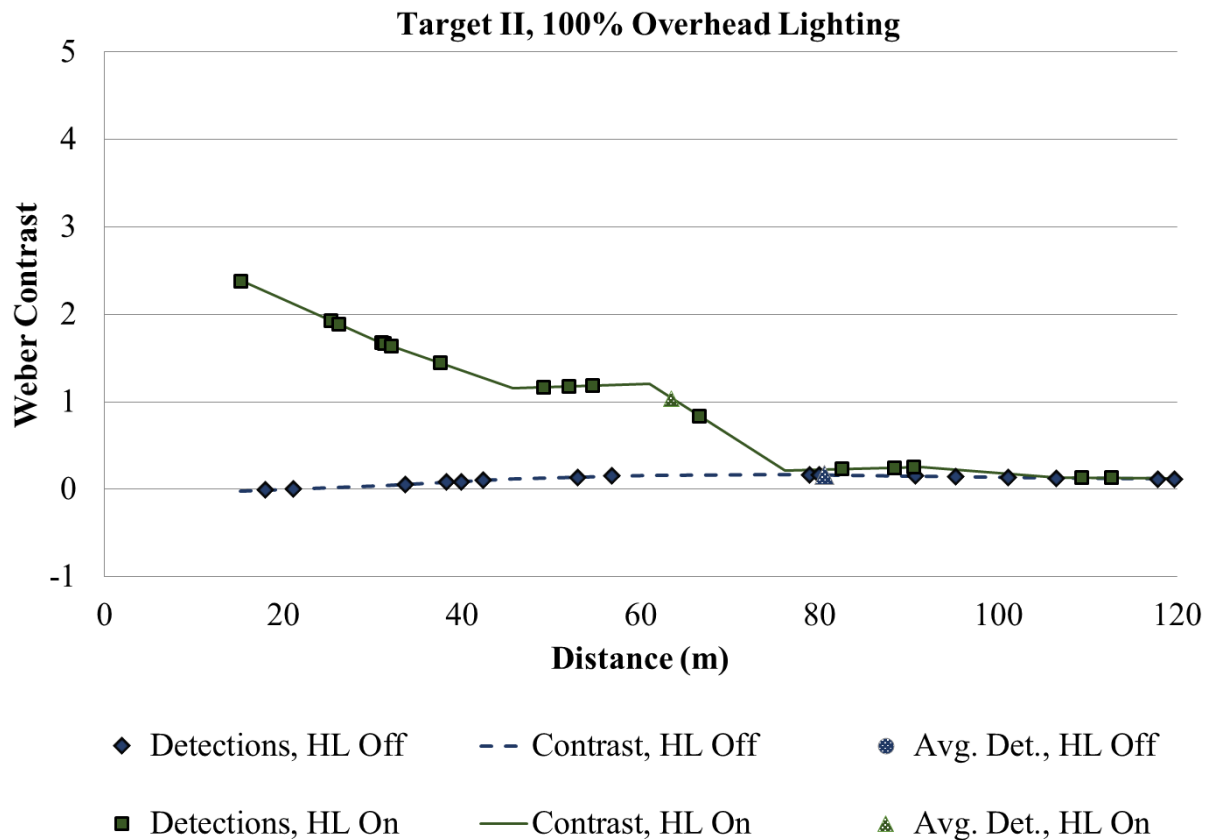
As with target I, the contrast of target II was analyzed at 100-percent and 40-percent overhead-lighting levels.

Overhead Lighting at 100 Percent:

The Weber contrasts for target II are shown in figure 103. With headlamps at distances closer than 76.2 m (250 ft), the headlamps create positive contrast on the target. Beyond that and without headlamps, contrasts are very close to zero but fluctuate owing to differences in the pavement behind the target and the changing visual angle.

Most participants detected the target more than 61.0 m (200 ft) away, showing that luminance contrast was not the only factor driving target visibility. The average detection distance without headlamps decreased by approximately 15 m (50 ft) (19.4 percent) when the lighting level was reduced from 100 percent to 40 percent. With headlamps, the detection distance decreased by approximately 12 m (40 ft), or 17.8 percent. Detection distances are nearly normally distributed

when the headlamps are off. When the headlamps are on, the distribution is skewed toward longer distances.

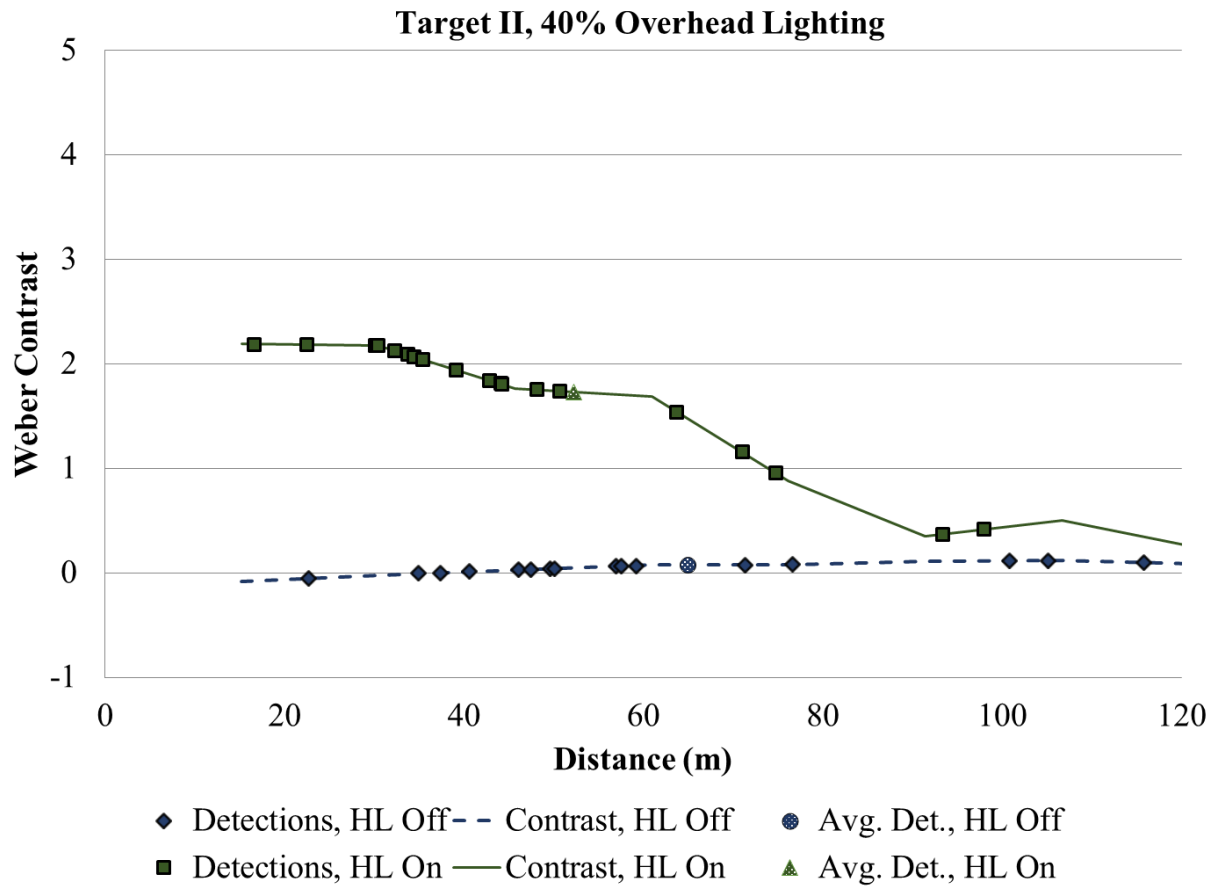


1 m = 3.3 ft

Figure 103. Graph. Overhead-lighting level experiment—target II contrast and detection distances versus distance from target at 100-percent overhead lighting.

Overhead Lighting at 40 Percent:

Weber contrast at 40-percent overhead lighting, shown in figure 104, is similar to that at 100-percent overhead lighting. Without headlamps, the target detection distance is about 15.2 m (50 ft) farther away than with headlamps, even though the contrast with headlamps is higher. Again, this could be because headlamps increase ambient luminance causing the eye to adapt to brighter conditions and become less sensitive to contrast.



1 m = 3.3 ft

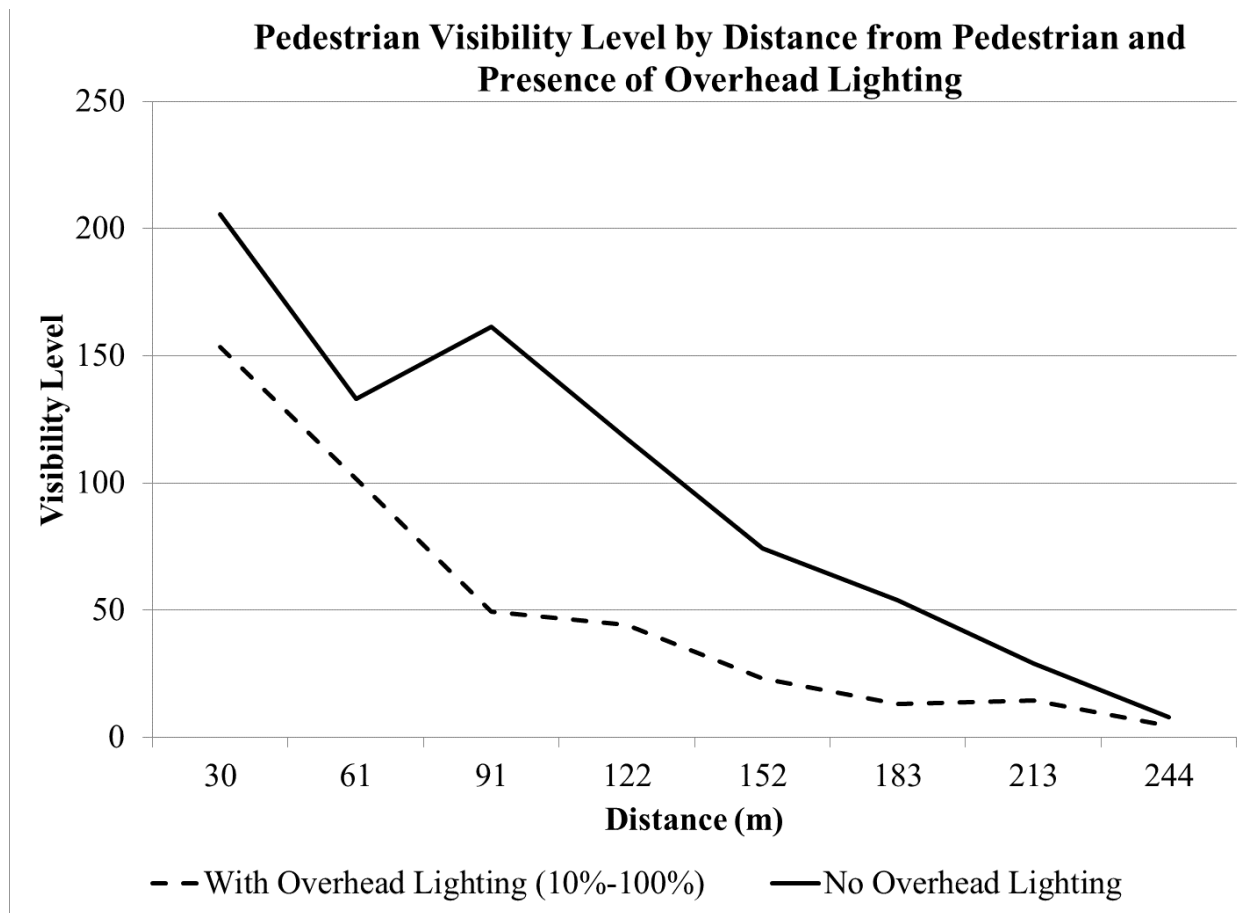
Figure 104. Graph. Overhead-lighting level experiment—target II contrast and detection distances versus distance from target at 40-percent overhead lighting.

Visibility Level

VL is a calculation describing the extent to which a target can be seen. It accounts for the object's size, its contrast, the age of the observer, and the threshold luminance required for an object to be visible to 99 percent of viewers. The higher the VL, the more visible the target should be.⁽⁹⁶⁾

Pedestrian

The VL calculations for the pedestrian with headlamps on are shown in figure 105. Overhead-lighting levels from 10 to 100 percent were averaged (dashed line) because there was very little difference in VL between them. They are compared with VL for no overhead lighting (solid line). The pedestrian VL was higher for no overhead lighting at all distances up to 244 m (800 ft). That roughly corresponds with experimental observations, where pedestrians were visible from slightly greater distances with no overhead lighting.



1 m = 3.3 ft

Figure 105. Graph. Overhead-lighting level experiment—pedestrian VL with headlamps on and with and without overhead lighting.

Target I (Low VI)

Figure 106 shows the VL calculations for target I with headlamps on, grouped by whether or not there was overhead lighting. The VLs are very similar at 30 m (100 ft) from the target and beyond. The VL rapidly increases at closer than 30 m (100 ft). That point is closer than the distance at which headlamp light falls on the target, about 76.2 m (250), showing that the VL calculation does not correspond with experimental observations.

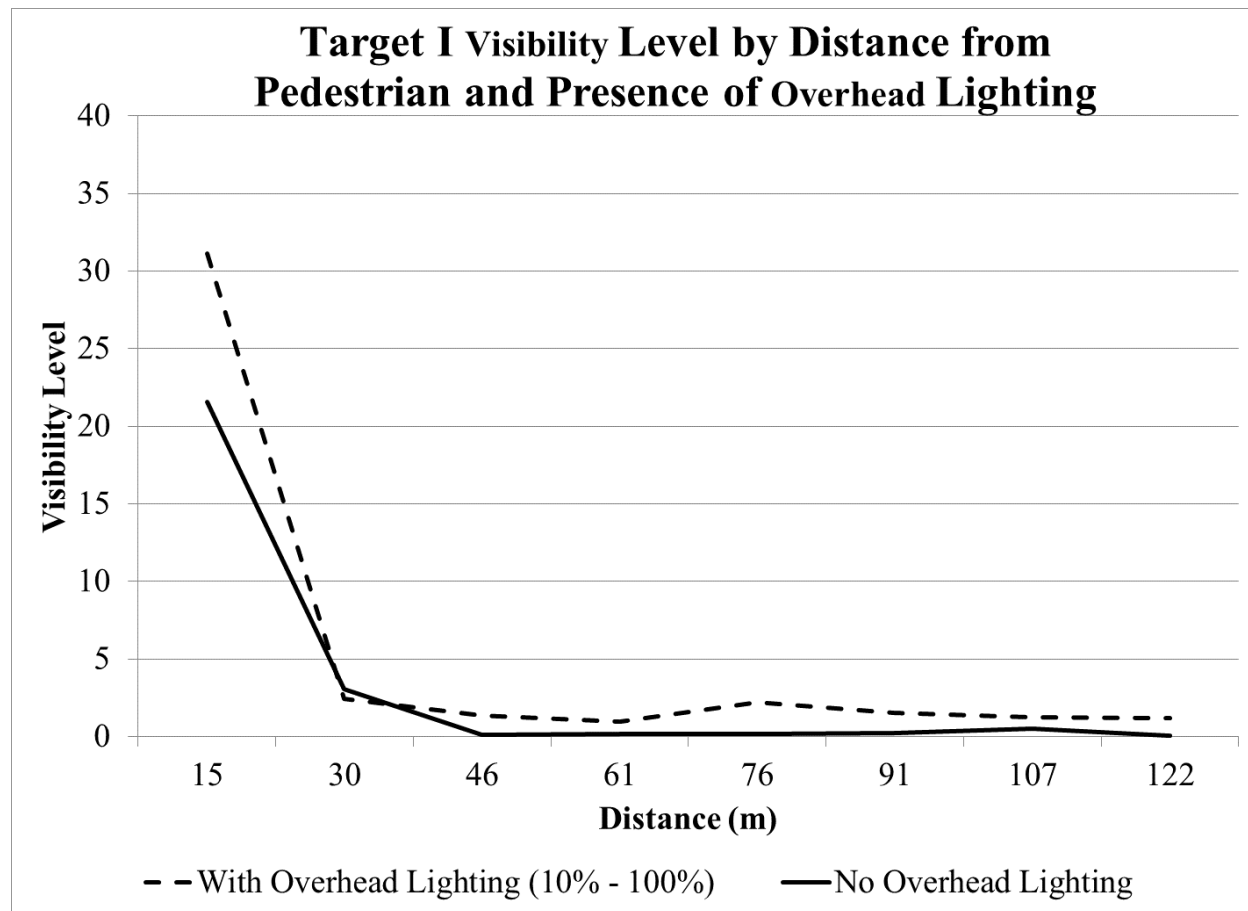
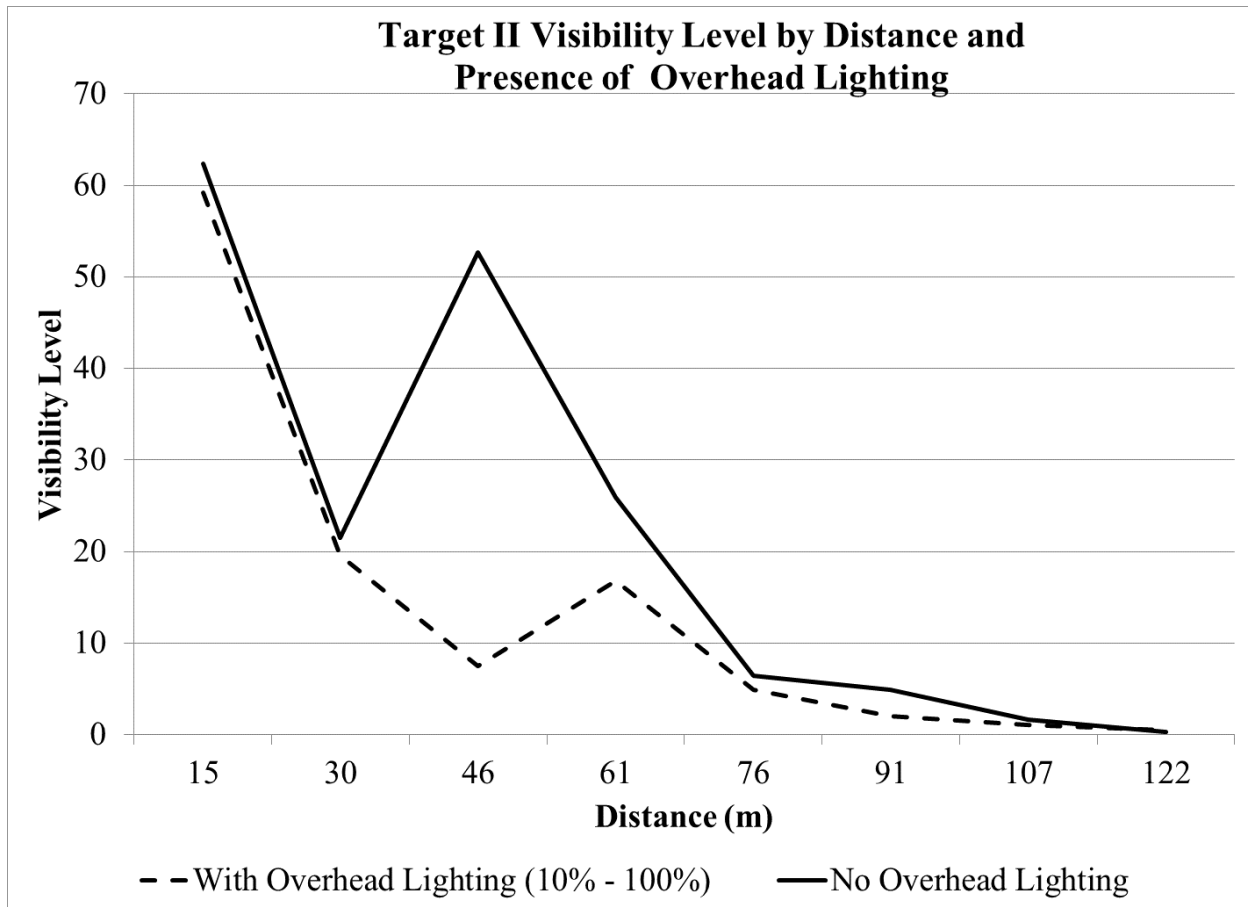


Figure 106. Graph. Overhead-lighting level experiment—target I VL with headlamps on and with and without overhead lighting.

Target II (High VI)

The VL calculations do not align with experimental observations for target II. Target II's contrast transitioned from negative to positive when the vehicle with headlamps on got close to it, but the VL calculations do not show that change (figure 107). At about 46 m (150 ft), the VL calculations also show a spike in visibility for no overhead lighting and a dip in visibility for overhead lighting. Those effects were not supported by the experimental data.



1 m = 3.3 ft

Figure 107. Graph. Overhead-lighting level experiment—target II VL with headlamps on and with and without overhead lighting.

CONCLUSIONS

A research objective for this experiment was to evaluate the impact of headlamps on driver visual performance. Results found that distant objects were more visible without headlamps than with headlamps, likely because the headlamp light caused the eye to adapt to the brighter environment, reducing contrast sensitivity. In addition, headlamps, which produced measurable amounts of VI up to 91.4 m (300 ft) away from a vehicle, affected object visibility at 213 m (700 ft) away, likely owing to light scatter on the roadway and environment. The impact of this indirect light on visibility was negligible.

Evaluating how overhead-lighting level affected driver visual performance was the next research objective. High ambient luminance made a positively contrasting object more difficult to see, and low ambient luminance made a negatively contrasting object easier to see. An object with very low contrast would be difficult to see, regardless of object size and adaptation level; however, that poor visibility can be mitigated by adjusting object size and adaptation luminance. In addition, a target with negative contrast becomes briefly invisible as it is illuminated by headlamps and transitions to positive contrast. The effects of higher adaptation levels to brighter environments are particularly noticeable at night with low-contrast objects.

Other project objectives were to evaluate how headlamps and overhead lighting interacted to affect driver visual performance and to evaluate the minimum overhead-lighting level where target and pedestrian visibility was not compromised. This experiment found that headlamps combined with overhead lighting resulted in better object recognition and detail visibility than with overhead lighting alone, especially when overhead lighting was dim. The combination of headlamps and overhead lighting appears to have its greatest impact when the two sources contribute a nearly equal amount of lighting. This partial contribution can be achieved in two ways and was found primarily with respect to target visibility. The first way was when overhead lighting was dimmed to 30 percent (3 lx (0.28 fc), approximately 0.3 cd/m² (0.09 fL)) or below. Above 30 percent, the overhead lighting was typically the dominating light source, allowing for distant detections, especially for targets. Headlamps competed with overhead lighting when the level was below 30 percent, resulting in effects on the properties of the target—contrast, adaptation luminance, and light angle—that affect visibility. The second way the partial combination was achieved was via proximity, depending on contrast polarity. In the intermediate zone (30.4 to 76.2 m (100 to 250 ft)), a negative contrast target must transition to positive contrast when headlamps become the primary source of lighting, causing it to cross a point of zero contrast. In this same zone, a positive contrast target experiences changes in VL and contrast that can affect visibility. In this situation, whether an object seen in positive contrast remains visible as a vehicle approaches depends on adaptation luminance. The impact of headlamps and overhead lighting was less pronounced in the case of pedestrians, primarily because of their angular size and nonuniform shape.

Additional results found that object size, ambient lighting level, and contrast affected the visibility of gray pedestrians and targets in this experiment. First, the larger an object, the more visible it was, as shown by the VL calculations; pedestrians had higher VLs than targets. Second, the ambient lighting level affected the eye's adaptation, which in turn affected contrast sensitivity. Last, longer pedestrian-detection distances were measured without headlamps (and with overhead lighting), because this condition had a lower adaptation level, making a low-contrast pedestrian discernible beyond 422 m (800 ft). Orientation recognition, however, typically occurred only within 30 m (100 ft) of the object, requiring the driver to drive slower than 24 km/h (15 mi/h) to be able to stop in time to avoid colliding with the object.

CHAPTER 7. MESOPIC MODELING EXPERIMENT

INTRODUCTION

This experiment was designed to investigate the applicability of the CIE Recommended System for Mesopic Photometry, described in chapter 2, to nighttime roadway conditions.⁽¹⁾ It also investigated the relationship between peripheral visual performance and the SPD of overhead-lighting sources in the mesopic range, in both static (parked) and dynamic (driving) conditions. To that end, three types of overhead lighting with different spectral distributions were used: 2,100-K HPS, 3,500-K LED, and 6,000-K LED. The level of the overhead lighting was chosen based on the adaptation luminance at the roadway. All adaptation luminance levels fell in the mesopic range, and all were the same among the different lighting types. The overhead lighting was used in combination with two pavement types—darker asphalt and lighter concrete—so the same level for an overhead-lighting type produced two different adaptation luminance levels, depending on pavement type. The experiment used five adaptation luminances for each lighting type, one of which was the same between asphalt and concrete. Three different off-axis target locations were used because research indicated that overhead-lighting sources whose spectral distributions favored the sensitivity of the rods had better off-axis performance.^(20,21)

This experiment included two portions, one static and one dynamic. The static portion of the experiment was similar to laboratory and simulator studies on mesopic vision but was performed in a stationary vehicle on the roadway. Participants sat behind the steering wheel of the test vehicle and fixated on the center of the roadway while researchers adjusted the contrast of off-axis targets on the shoulder. The dependent variable was the threshold luminance contrast or contrast threshold at which the participant first saw the target. In the dynamic portion of the experiment, participants drove down the road and were instructed to fixate on the roadway and use peripheral vision to detect the targets. Targets at different eccentricities and contrasts were presented, and participant detection distances were measured. The static experiment used a fixed geometry setup, whereas the dynamic experiment used a nonfixed geometry setup.

Target color was not included in this experiment, because the experiment focused on the effects of overhead-lighting configuration, eccentricity, and adaptation luminance rather than effects of object color on mesopic visibility. For the same reason, vehicle headlamps were not used for this experiment, isolating the effects of overhead lighting on mesopic vision.

Research Objectives

The purpose of the mesopic modeling experiment was to evaluate the following:

- Applicability of the CIE Recommended System for Mesopic Photometry in naturalistic nighttime roadway situations.⁽¹⁾
- Effect of the spectrum of an overhead-lighting source on peripheral visual performance of drivers in both static and dynamic conditions.

EXPERIMENTAL DESIGN

For the static portion, a 2 by 3 by 5 by 3 mixed-factors experiment was designed to investigate the effects of age, overhead-lighting type, adaptation luminance, and eccentricity on the threshold contrast where participants first detected a target.

For the dynamic portion, a 2 by 3 by 5 by 3 by 2 mixed-factors experiment was designed to investigate the effects of age, overhead-lighting type, adaptation luminance, eccentricity, target light intensity, and vehicle speed on target detection distance.

Participants of two age groups were exposed to all combinations of factors for the static experiment. The dynamic experiment was a partial factorial experimental design with all second-order interactions and one third-order interaction. Experimental variables are listed in table 27 through table 29.

Table 27. Mesopic modeling experiment—-independent variables and values.

Independent Variable	Used In Static	Used In Dynamic	Values
Age	Yes	Yes	Younger (25–35), Older (65+)
Overhead-Lighting Type	Yes	Yes	6,000-K LED (S/P 1.82), 3,500-K LED (S/P 1.31), 2100-K HPS (S/P 0.64)
Adaptation Luminance	Yes	Yes	0.07 cd/m ² (0.020 fL), 0.1 cd/m ² (0.03 fL), 0.2 cd/m ² (0.06 fL), 0.3 cd/m ² (0.09 fL), 0.5 cd/m ² (0.15 fL)
Eccentricity	Yes	Yes	6 degrees, 10 degrees, and 14 degrees
Speed	No	Yes	56 km/h (35 mi/h), 80 km/h (50 mi/h)

Table 28. Mesopic modeling experiment—covariate and value/measurement method.

Covariate	Used in Static	Used in Dynamic	Value/Measurement Method
Target Contrast	No	Yes	High and Low Contrast (Weber)

Table 29. Mesopic modeling experiment—dependent variables and measurement method.

Dependent Variables	Used in Static	Used in Dynamic	Measurement Method
Threshold Contrast	Yes	No	Weber contrast at which participant can first detect a target
Detection Distance	No	Yes	Distance at which participant can first detect a target

Independent Variables

Age

Participants were divided into the same age groups as previous experiments: younger (25–35 years old) ($M = 28.4$, $SD = 3.2$) and older (65 years old and older) ($M = 67$, $SD = 1.5$).

Overhead-Lighting Type

All three of the overhead-lighting systems were used.

Adaptation Luminance

Adaptation luminance was the photopic luminance viewed from inside the vehicle for a given combination of overhead-lighting level and pavement type. It was controlled for by adjusting the overhead-lighting levels for the three lighting types and two pavement types.

Overhead-Lighting Level:

Each lighting type was used at three intensity levels: low, medium, and high. Those lighting levels were adjusted so that the low, medium, and high intensity levels produced the same adaptation luminance inside the vehicle across the three lighting types, and so they were all in the mesopic range.

Pavement Type:

With the two pavement surfaces on the Smart Road, the pavement color and reflectance differed meaning that the same overhead-lighting level resulted in different adaptation luminances in the two sections. For this experiment, the overhead-lighting levels were adjusted so that the high overhead-lighting level on asphalt produced the same adaptation luminance as the medium overhead-lighting level on concrete. The result was five distinct adaptation luminances, shown in table 30.

Table 30. Mesopic modeling experiment—adaptation luminance by overhead-lighting level and pavement type.

Overhead-Lighting Level	Luminance on Concrete (cd/m² (fL))	Luminance on Asphalt (cd/m² (fL))
Low	0.1113 (0.032)	0.0716 (0.021)
Medium	0.3535 ^a (0.103)	0.1987 (0.056)
High	0.5385 (0.157)	0.3535 ^a (0.103)

^aSame luminance.

Eccentricity

Targets were placed at three angles with respect to the roadway: 6, 10, and 14 degrees, as shown in figure 108. These angles were measured assuming the observer was at a vertical distance of 83 m (272 ft) from the target location.

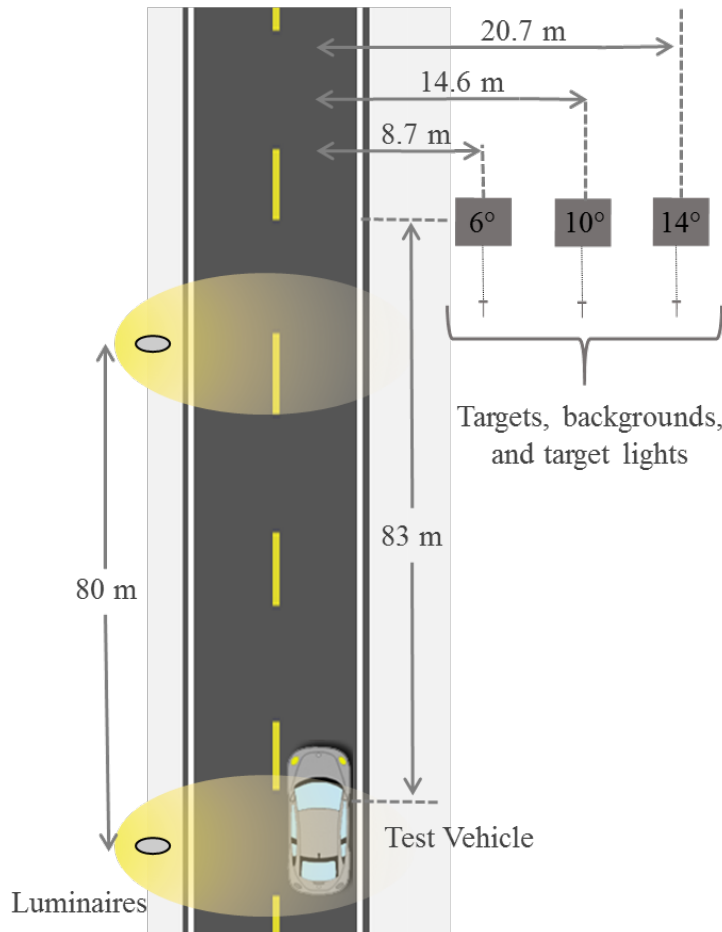


Figure 108. Diagram. Arrangement of target lights for static experiments on the Smart Road.

Speed

For the static portion of the experiment, the vehicle was parked in a specified location with respect to the targets, and speed was not an independent variable.

For the dynamic portion of the experiment, the vehicle traveled at 56 and 80 km/h (35 and 50 mi/h).

Dependent Variables

Threshold Contrast

For the static portion of the experiment, the target's light intensity was increased until the participant could just discern the target. At that point, threshold contrast of the target was calculated by first measuring the luminance of the target and background with a ProMetric® luminance camera inside the test vehicle and then by calculating the target's Weber contrast from those measurements using the formula in figure 8. The threshold-detection measurements in this experiment measured supra-threshold contrast, where the participant definitely detected the

target, whereas threshold contrast typically refers to the contrast at 50-percent detection probability.

Detection Distance

For the dynamic portion of the experiment, the detection distance was the dependent variable.

METHODS

Facilities and Equipment

This experiment was conducted on the Smart Road using the same test vehicles as in previous experiments.

Targets and Backgrounds

The target setup for this experiment was significantly different than those used in the other experiments. While the targets were the same gray targets as used in the previous experiments in this project, they were mounted on vertical posts, and their height was adjustable. Spotlights used to illuminate the targets were mounted on the same apparatus as the targets. The target illuminators were about 2.4 m (8 ft) from the targets and were also adjustable, so the experimenters could ensure the spotlight was centered on the target. The target lights were enclosed in light-tight cases, reducing scatter, so that the only light emitted was directed toward the target. The target stands and target lights were painted in a neutral camouflage pattern so they would not distract the participant drivers. The targets were illuminated using CREE® LED BR30 reflector spotlights rated at 650 lumens. A warm bulb (2,100 K) was used with the 3,500-K LED and 2,100-K HPS lighting, and a cool (5,000 K) bulb was used with the 6,000-K LED lighting.

The backgrounds were 0.91 by 1.2 m (3 by 4 ft) sheets of gray-painted plywood on gray-painted stands. The target-lighting apparatus were placed 4.6 m (15 ft) from the background. A target, a target light, and its background are illustrated in figure 109.

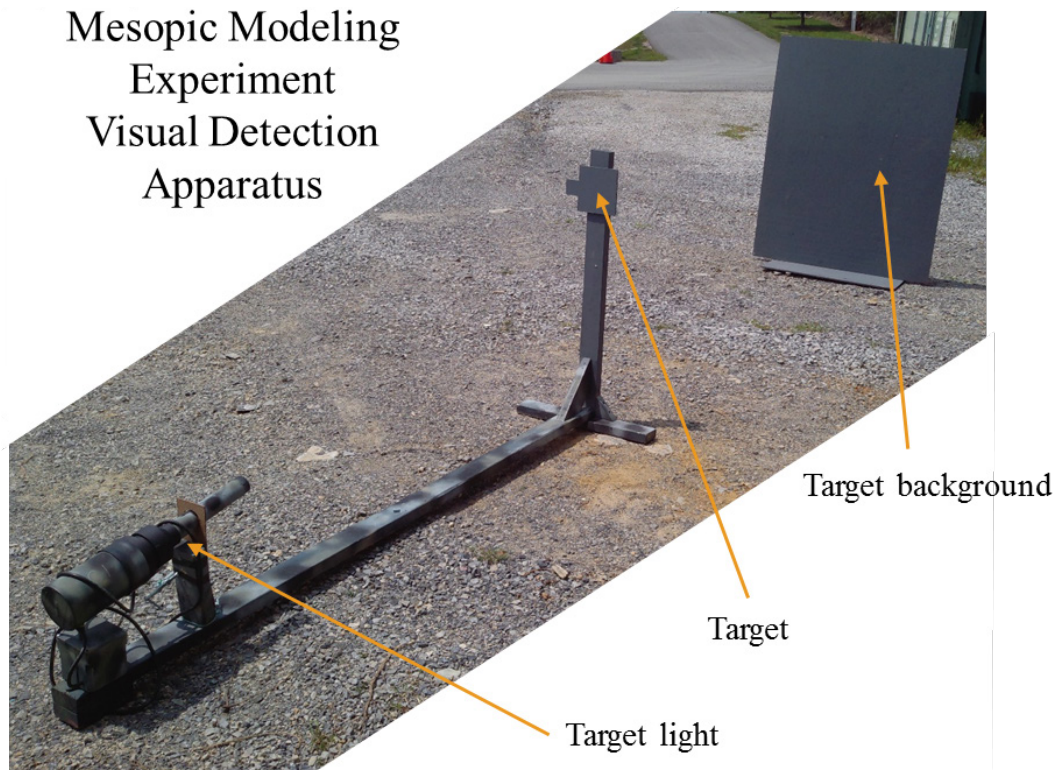


Figure 109. Photo. Mesopic modeling experiment—target, target light, and background.

Four sets of three targets, target lights, and backgrounds were set up alongside the Smart Road to create the three desired viewing angles at those four stations. The two stations in the asphalt section were named A1 and A2, and the two in the concrete section were named C1 and C2. All four stations were used in the dynamic portion of the experiment, but only stations A1 and C2 were used in the static portion of the experiment.

Participants

Participants were recruited and screened as described in chapter 3. A total of 18 participants performed the experiment. Nine were older, and nine were younger. Nine were female, and nine were male. Mean and standard deviation of participant age, visual acuity, mesopic visual acuity, low contrast visual acuity, and UFOV are listed in table 31.

Table 31. Mesopic modeling experiment participant characteristics.

Participant Characteristic	Older Drivers Mean	Older Drivers Standard Deviation	Young Drivers Mean	Younger Drivers Standard Deviation
Age	70.4	6.3	30.5	3.2
Visual Acuity	20/24.2	8.8	20/19.4	8.8
Mesopic Visual Acuity	20/38.8	10.6	20/27.2	13.0
Low Contrast Visual Acuity	20/26.3	10.6	20/18.3	6.4
UFOV	1.55	0.73	1	0

Procedure

Each participant attended three experimental sessions, one for each overhead-lighting type. Each session consisted of a static and dynamic portion, and two participants completed the experiment simultaneously.

Static

One participant was directed to park at the vehicle stopping point for station A1, and the other was directed to park at the vehicle stopping point for station C2. An in-vehicle experimenter asked the participant to focus on a cone placed on the roadway, so that the targets were visible in the participant's peripheral vision. The researcher then slowly increased the intensity of the target light. When the participant was first able to see a target, he or she announced "target" and the researcher recorded the target light intensity. The procedure was repeated for targets at different viewing angles for a total of 24 times. At the end of the static portion of the experiment, the in-vehicle researchers notified other team members that they were finished, and the on-road researchers adjusted the equipment for the dynamic portion of the experiment.

Dynamic

Each participant performed 1 practice run and 12 experimental runs down and up the Smart Road for each overhead-lighting type during an experimental session. For the dynamic portion of the experiment, the on-road experimenters set the target light levels, target positions, and overhead-lighting level for each experimental run. The in-vehicle experimenters directed the participants to focus on the roadway while driving to encourage target detection in peripheral vision, ensured they drove at the correct speed, and recorded detections.

Data Analysis

Static

A mixed-factors ANOVA was performed to determine how the independent variables affected threshold contrast. If results were significant, a Tukey's HSD test was performed to determine which independent variables differed significantly from each other. In the graphs reporting Tukey's HSD results, points sharing a letter are not significantly different from each other.

Dynamic

A partial mixed-factorial ANOVA was performed to determine how the independent variables affected detection distance.

RESULTS

Static

In the static portion of the experiment, researchers varied the contrast of the off-axis targets, and participants told researchers when they could first see them. The threshold contrast, when the participant would first see the target, was the dependent variable.

The effect of the independent variables on threshold contrast is listed in table 32, with results described in detail after the table.

Table 32. Mesopic modeling experiment (static portion)—independent variables and their effect on threshold contrast.

Independent Variable(s)	Degrees of Freedom	<i>F</i>-value	Pr > <i>F</i>
Age	1	3.34	0.0832
Overhead-Lighting Type	2	18.55	< .0001 ^a
Overhead-Lighting Type by Age	2	3.18	0.0549
Adaptation Luminance	4	48.11	< .0001 ^a
Adaptation Luminance by Age	4	1.68	0.1765
Eccentricity	2	32.81	< .0001 ^a
Eccentricity by Age	2	3.04	0.0596
Overhead-Lighting Type by Overhead-Lighting Level	8	6.06	< .0001 ^a
Overhead-Lighting Type by Eccentricity	4	5.77	0.0005 ^a
Adaptation Luminance by Eccentricity	8	14.86	< .0001 ^a
Overhead-Lighting Type by Adaptation Luminance by Eccentricity	16	10.96	< .0001 ^a

^aSignificant at $p < 0.05$.

Pr = Probability

Overhead-Lighting Type

Overhead-lighting type significantly affected threshold contrast, illustrated in figure 110, where points sharing a letter are not significantly different from each other. The 6,000-K LED lighting provided the lowest threshold contrast and the 2,100-K HPS lighting the highest threshold contrast. A Tukey's HSD test found no statistical difference between the two LED lighting types, but HPS light differed significantly from both LED types.

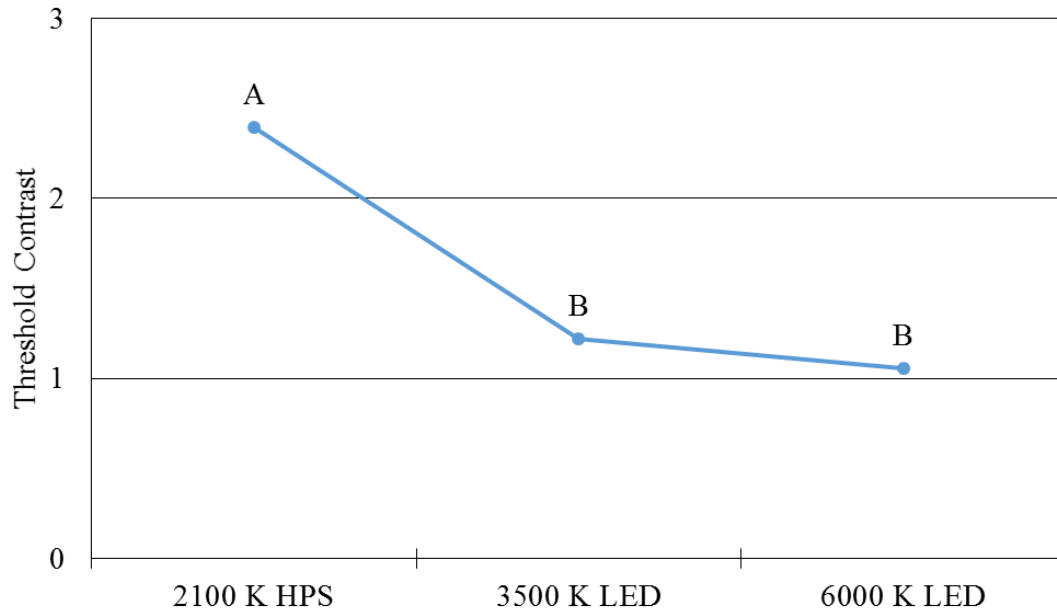
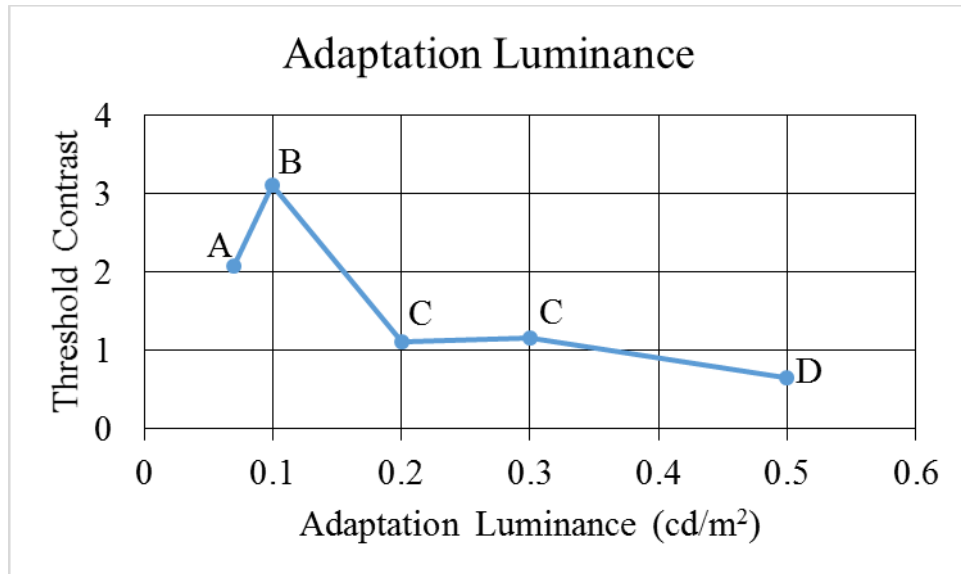


Figure 110. Graph. Mesopic modeling experiment (static portion)—threshold contrast by overhead-lighting type.

Adaptation Luminance

Adaptation luminance significantly affected threshold contrast, with, in general, lower adaptation levels requiring higher contrasts before the target was visible (see figure 111, where points sharing a letter are not significantly different from each other). A Tukey's HSD test found all pairwise comparisons between adaptation luminances were significant, except the comparisons between 0.2 and 0.3 cd/m^2 (0.06 and 0.09 fL) and 0.2 and 0.5 cd/m^2 (0.06 and 0.15 fL). This could be because of a threshold effect where, if the luminance is above a certain level, increasing luminance no longer negatively affects contrast sensitivity. Adaptation luminance was also involved in statistically significant higher order interactions. This main effect could also be significantly influenced by the statistical significance of higher order interactions involving adaptation luminance.



1 cd/m² = 0.3 fL

Figure 111. Graph. Mesopic modeling experiment (static portion)—threshold contrast by adaptation luminance.

Eccentricity

Eccentricity significantly affected threshold contrast, with targets farther off axis requiring greater contrast before they were visible, as shown in figure 112. Pairwise comparisons found that the threshold contrasts at all three eccentricities were significantly different from one another. That increase in threshold contrast cannot be attributed to loss due to probability summation because of the target locations (especially at 10 and 14 degrees) falling in the blind spot of the eyes. Binocular probability summation states that if the probability of detection by each eye is 50 percent (or 0.5), the probability that two eyes detect the signal when the target falls in the blind spot on one eye is now $0.5 + 0.5 - (0.5 \times 0.5) = 0.75$ or 75 percent (a 25-percent decrease compared with when the target is not in the blind spot of one eye). The threshold contrast at 10 degrees was 70-percent greater than that at 6 degrees, and at 14 degrees, it was 140-percent greater than that at 6 degrees. That is greater than the increase in threshold contrast predicted by binocular probability summation alone—25 percent.

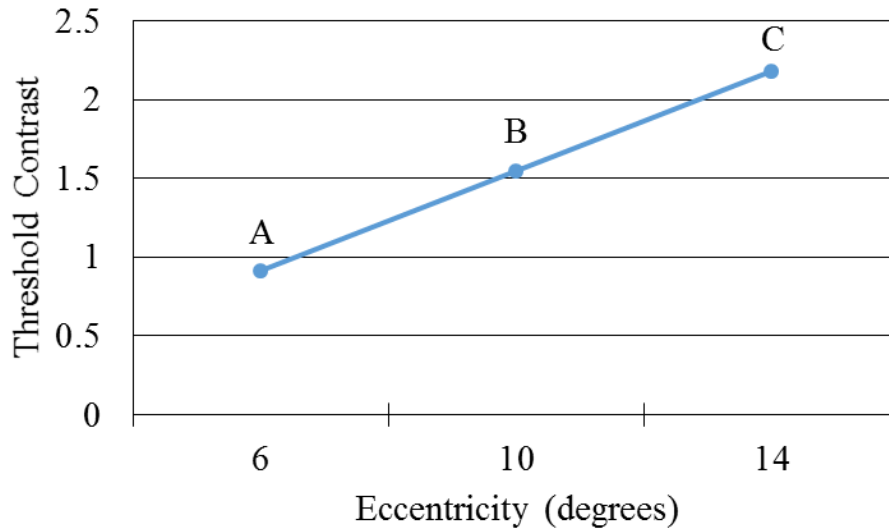


Figure 112. Graph. Mesopic modeling experiment (static portion)—threshold contrast by eccentricity.

Effect of Overhead-Lighting Type, Adaptation Luminance, and Eccentricity on Mesopic and Photopic Threshold Contrast

Luminance, as determined by the luminance meter used in this experiment, assumed measurements were taken in the photopic range. In the mesopic range, luminance calculations are different and account for the eye's different mesopic spectral sensitivity. The above-threshold contrasts were calculated using luminance measurements as determined by the luminance meter, with no mesopic correction.

The mesopic correction factor is calculated by multiplying the photopic luminance by a correction factor based on the S/P ratio of the light source. The S/P ratio is the ratio of the lamp's scotopic output to its photopic output, calculated using $V(\lambda)$ and $V'(\lambda)$ and describes the spectral sensitivity of the eye to the power distribution of a light source in mesopic conditions. The higher a lamp's S/P ratio, the better its light for peripheral detection in the mesopic region.^(28,29) The mesopic output is calculated using the formula in figure 113 and figure 114, taken from the *CIE Recommended System for Mesopic Photometry Based on Visual Performance*.⁽¹⁾

$$L_{Mesopic} = MM \times L_{Photopic}$$

Figure 113. Equation. Formula for calculating mesopic output.

Where:

$L_{mesopic}$ = Mesopic luminance.

MM = Mesopic multiplier from the *CIE Recommended System for Mesopic Photometry Based on Visual Performance*.⁽¹⁾

$L_{Photopic}$ = Photopic luminance.

Mesopic threshold contrasts were calculated by first calculating the mesopic luminance of the target and the mesopic luminance of the target's background using the equation in figure 114:

$$\text{Threshold Contrast}_{\text{Mesopic}} = \frac{L_{\text{Target-Mesopic}} - L_{\text{Background-Mesopic}}}{L_{\text{Background-Mesopic}}}$$

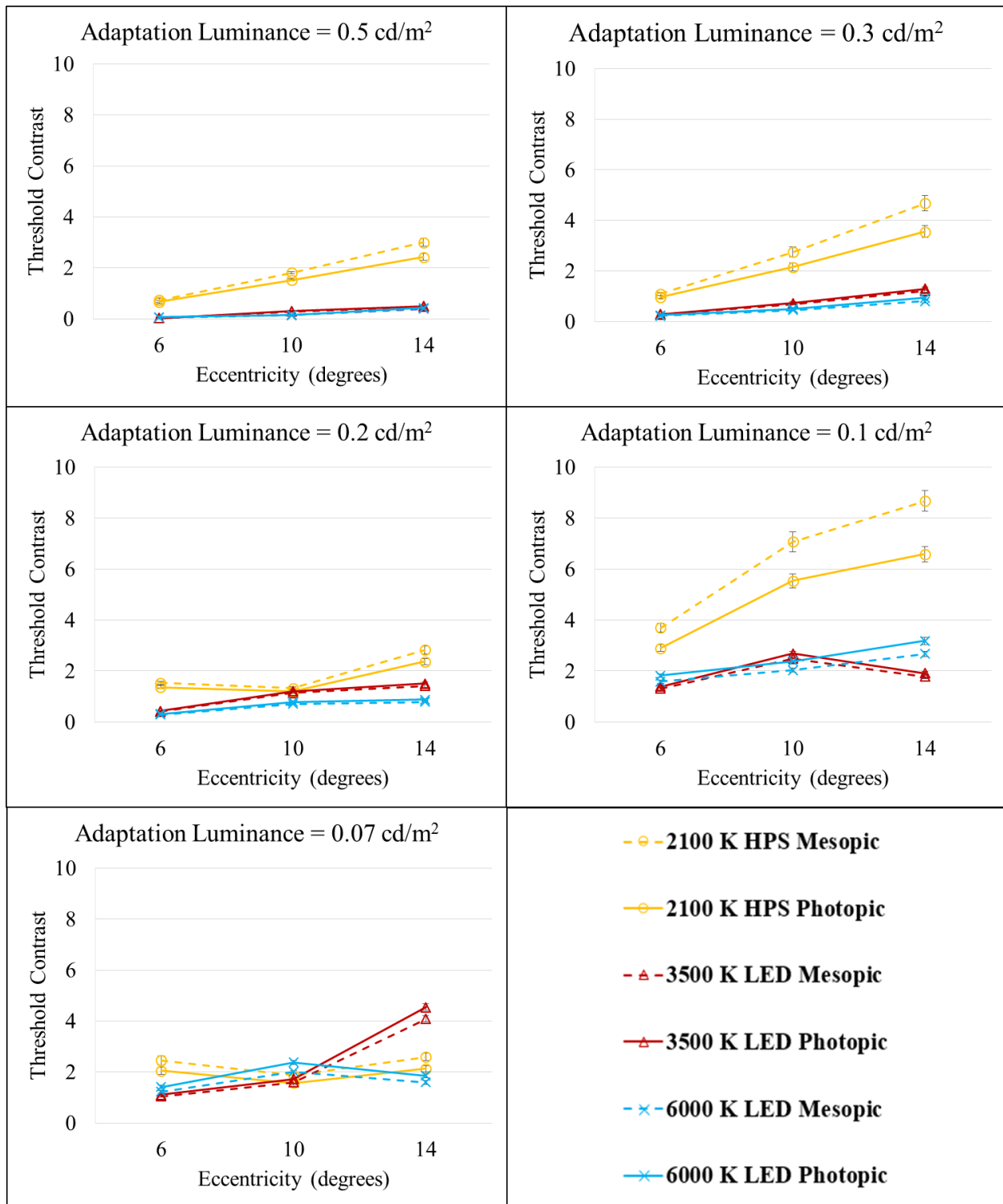
Figure 114. Equation. Formula for calculating mesopic threshold contrast.

Where:

$L_{\text{Target-Mesopic}}$ = Mesopic luminance of the target.

$L_{\text{Background-Mesopic}}$ = Mesopic luminance of the background.

Threshold contrasts using photopic luminance values were compared with those using calculated mesopic luminance values to determine where the results diverge and which luminance calculation best predicts the results. Calculations were repeated for each adaptation luminance and are displayed by lighting type and eccentricity in figure 115.



1 cd/m² = 0.3 fL

Figure 115. Graph. Mesopic modeling experiment (static portion)—threshold contrasts calculated with photopic and mesopic luminances for the three lighting types and three eccentricities.

From figure 115, it is clear that broad spectrum overhead-lighting types with higher S/P ratios (3,500-K LED and 6,000-K LED) had considerably lower off-axis threshold contrast values compared with narrow spectrum 2,100-K HPS lighting. The threshold contrasts were lower for LED lighting at all eccentricities and at four of the five adaptation luminances, showing that greater contrast was needed in HPS than LED lighting to see the same object.

Surprisingly, both threshold contrasts for HPS lighting were highest at 0.1 cd/m^2 (0.03 fL) and not the dimmer 0.07 cd/m^2 (0.020 fL) one would expect.

Photopic threshold contrasts for HPS were lower than the mesopic threshold contrasts. For LED lighting, the opposite was true.

Dynamic

In the dynamic portion of the experiment, participants drove with their eyes focused on the roadway, detecting the off-axis targets in their peripheral vision. Age, overhead-lighting type, adaptation luminance, eccentricity, speed, and target contrast were independent variables. A partial mixed-factors ANOVA was performed to determine how the independent variables affected detection distance.

The effect of the independent variables on detection distance is listed in table 33, with results described in detail after the table.

Table 33. Mesopic modeling experiment (dynamic portion)—independent variables and their effect on threshold contrast.

Factor(s)	Degrees of Freedom	F-value	Pr > F
Age	1	1.2	0.2898
Overhead-Lighting Type	2	0.18	0.8325
Adaptation Luminance	4	2.98	0.0263 ^a
Eccentricity	2	1.69	0.2014
Speed	1	0.23	0.6349
Contrast	1	0.87	0.3654
Overhead-Lighting Type by Adaptation Luminance	8	3.25	0.0027
Overhead-Lighting Type by Eccentricity	4	0.74	0.572
Adaptation Luminance by Eccentricity	8	2.73	0.0091 ^a
Overhead-Lighting Type by Speed	2	0.34	0.7174
Adaptation Luminance by Speed	4	2.29	0.0731 ^a
Eccentricity by Speed	2	3.55	0.0433 ^a
Contrast by Overhead-Lighting Type	2	4.09	0.0303 ^a
Contrast by Adaptation Luminance	4	1.35	0.2636
Contrast by Eccentricity	2	0.98	0.3904
Contrast by Speed	1	0.55	0.4711
Overhead-Lighting Type by Adaptation Luminance by Eccentricity	16	2.08	0.0164 ^a

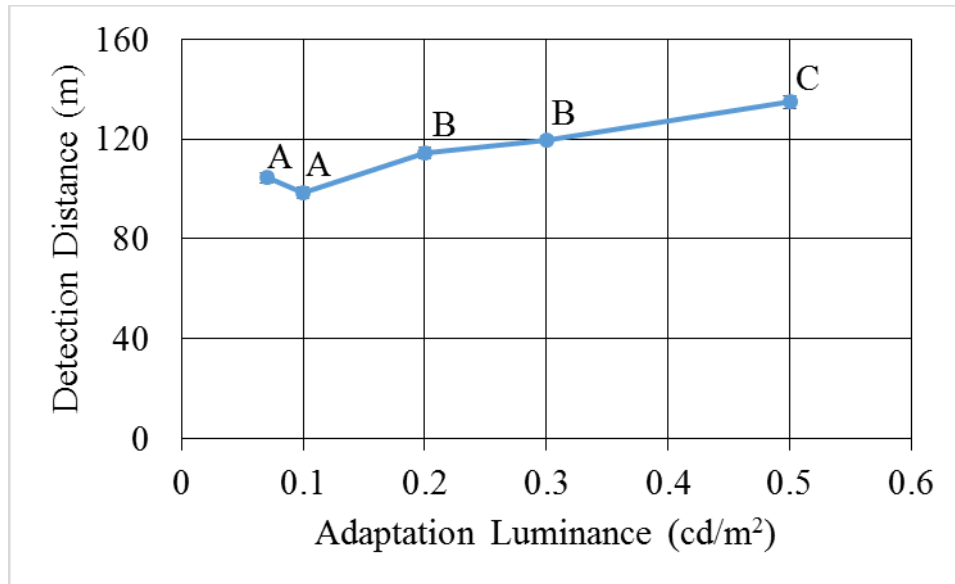
^aSignificant at $p < 0.05$ or marginally significant at $p < 0.1$.

Pr = Probability.

Only the main effect of adaptation luminance was significant. Four two-way interactions and a three-way interaction among overhead-lighting type, adaptation luminance, and eccentricity were also significant.

Adaptation Luminance

The effect of adaptation luminance on detection distance, plotted in figure 116, was significant. Points sharing a letter in the figure do not differ significantly from one another. Targets in the areas with the highest adaptation luminances were detected from farther away than those in areas with the lower adaptation luminances.



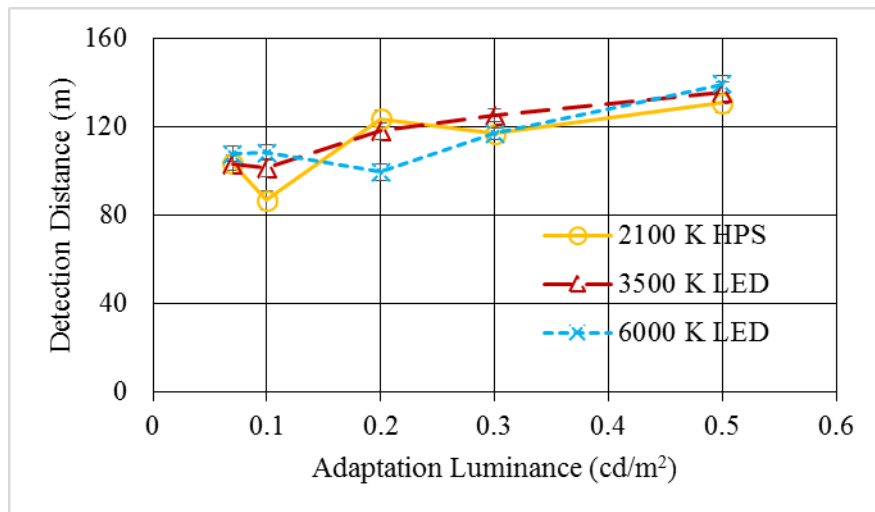
1 cd/m² = 0.3 fL

1 m = 3.3 ft

Figure 116. Graph. Mesopic modeling experiment (dynamic portion)—detection distance by adaptation luminance.

Overhead-Lighting Type and Adaptation Luminance

The effect on detection distance of the interaction between overhead-lighting type and adaptation luminance was significant when all eccentricities were combined. There was no difference in the mean detection distance among the three overhead-lighting types at the highest and lowest adaptation luminance levels (0.5, 0.3, and 0.01 cd/m² (0.15, 0.09, and 0.03 fL)). However, at the intermediate adaptation luminance levels (0.1 and 0.2 cd/m² (0.03 and 0.06 fL)), detection distances were different across the different overhead-light types, as illustrated in figure 117. More information was extracted from these trends by including the eccentricity in these data, as described in the section Overhead Lighting Type, Adaptation Luminance, and Eccentricity.



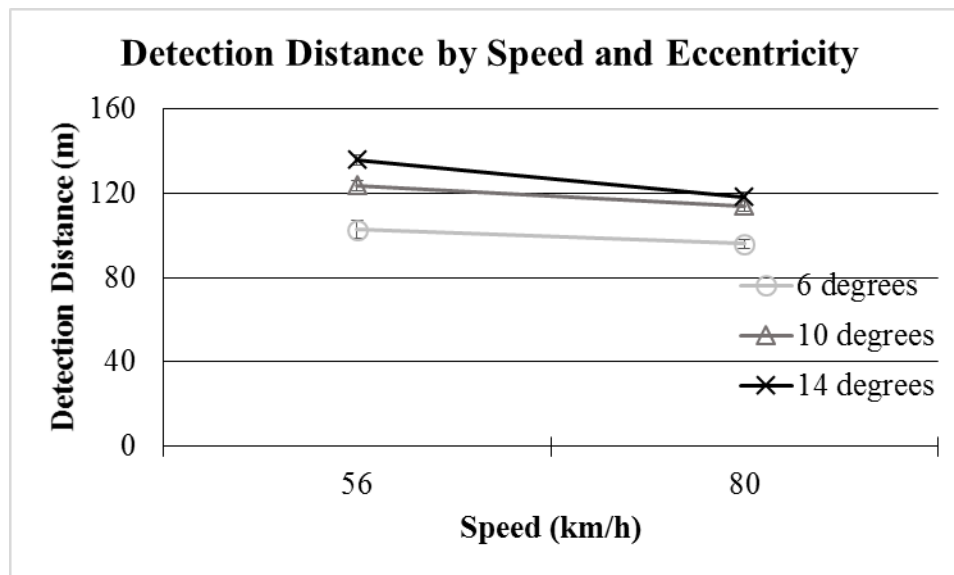
1 cd/m² = 0.3 fL

1 m = 3.3 ft

Figure 117. Graph. Mesopic modeling experiment (dynamic portion)—effect of overhead-lighting type and adaptation luminance on detection distance.

Eccentricity and Speed

The effect on detection distance of the interaction between eccentricity and speed was significant. At both speeds, more eccentric targets were detected from farther away, as illustrated in figure 118. Also, objects were detected from farther away at the lower speed compared with the higher speed.



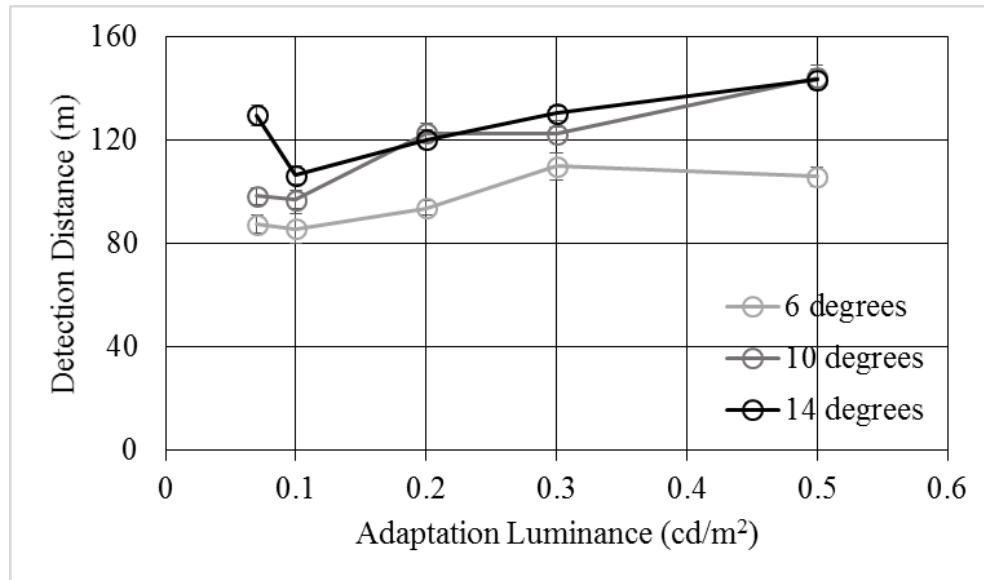
1 m = 3.3 ft

1 km/h = .62 mi/h

Figure 118. Chart. Mesopic modeling experiment (dynamic portion)—effect of eccentricity and speed on detection distance.

Adaptation Luminance and Eccentricity

The interaction between adaptation luminance and eccentricity was also significant. The detection distance was longer for higher adaptation luminances and targets at greater eccentricities. The 6-degree eccentricity target had the lowest mean detection distance across all the adaptation luminances. The 10- and 14-degree targets had higher detection distances at every adaptation luminance. An increase in adaptation luminance was also associated with an increase in the detection distance. The results, illustrated in figure 119, also show that an increase in the adaptation luminance significantly affected the detection distances of objects at higher eccentricities. The 14-degree target at 0.07 cd/m² (0.020 fL) had a higher detection distance than those at the other two angles, 6 and 10 degrees.



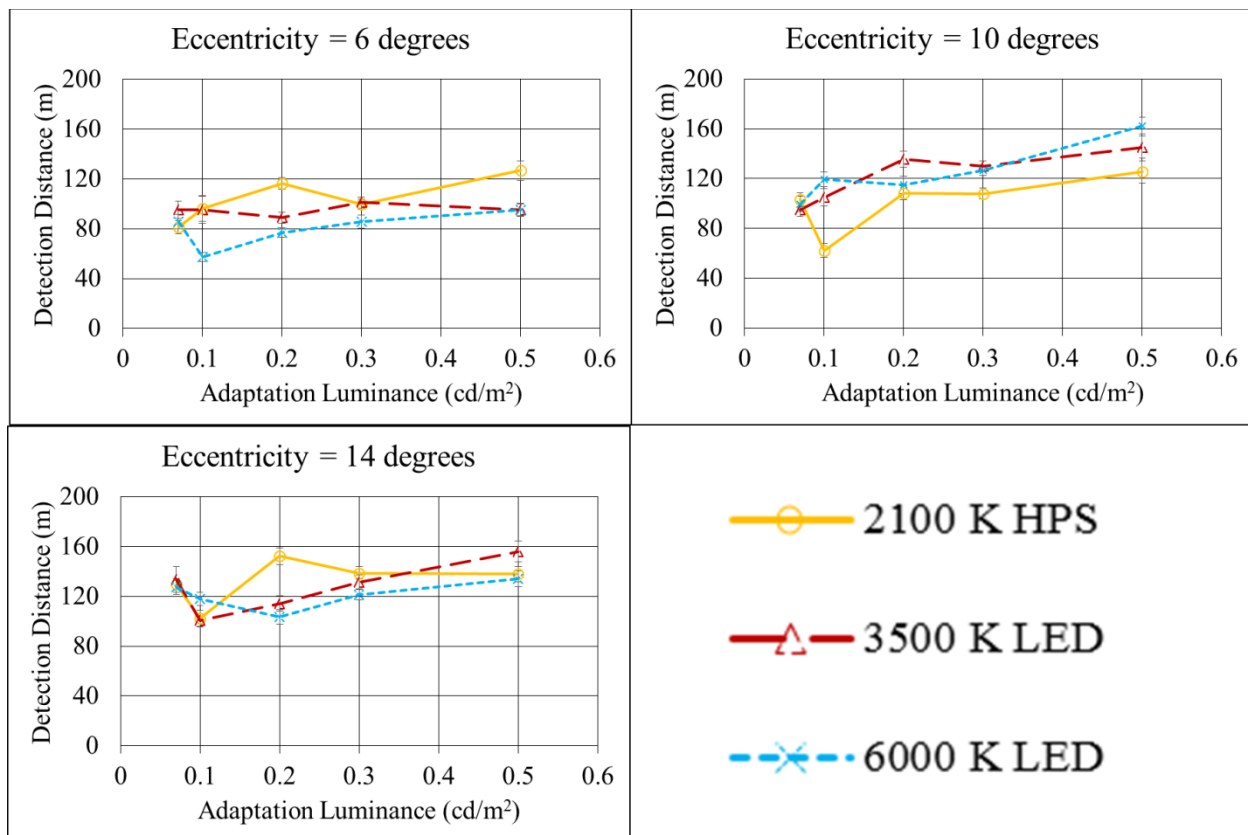
1 cd/m² = 0.3 fL

1 m = 3.3 ft

Figure 119. Graph. Mesopic modeling experiment (dynamic portion)—effect of adaptation luminance and eccentricity on detection distance.

Overhead-Lighting Type, Adaptation Luminance, and Eccentricity

Mean detection distances increased as adaptation luminance increased, and different light sources had longer detection distances at different adaptation luminances, as shown in figure 120. An increase in eccentricity corresponded to both an increase in detection distance and a decrease in the difference between detection distances among the overhead-lighting types. At a 6-degree eccentricity, the 2,100-K HPS lighting resulted in had longer detection distances at adaptation luminances of 0.5 and 0.2 cd/m² (0.15 and 0.06 fL), but the three lighting types had similar detection distances at adaptation luminances of 0.1 and 0.3 cd/m² (0.03 and 0.09 fL). The 6,000-K LED overhead lighting had shorter detection distances than the other lighting types at the 6-degree eccentricity at all adaptation luminance levels. At the 10-degree eccentricity, both of the LED overhead-lighting types had longer detection distances than HPS lighting at every adaptation luminance. However, that trend did not occur at the 14-degree eccentricity, where no lighting type had longer detection distances at all adaptation luminances.



1 cd/m² = 0.3 fL
1 m = 3.3 ft

Figure 120. Graph. Mesopic modeling experiment (dynamic portion)—effect of overhead-lighting type, adaptation luminance, and eccentricity on detection distance.

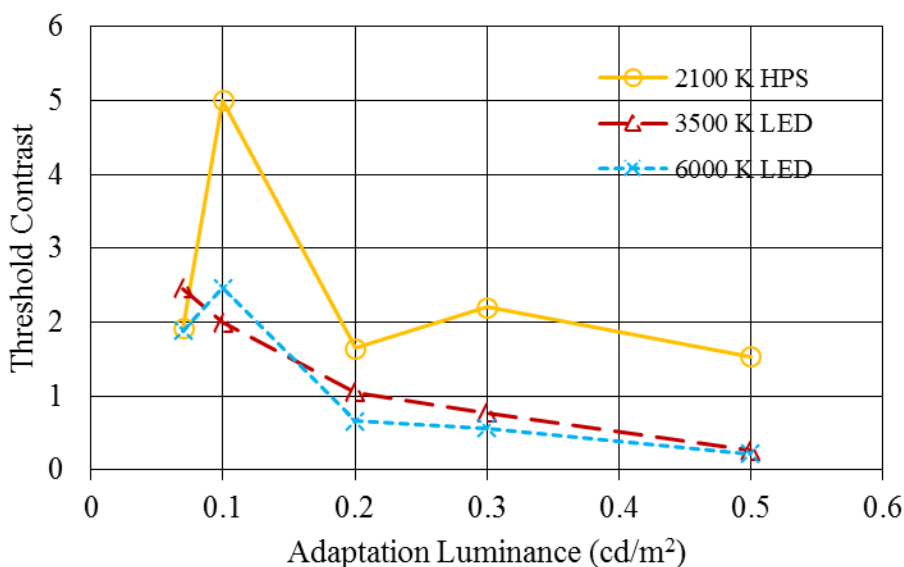
DISCUSSION

This research effort focused on application of the CIE *Recommended System for Mesopic Photometry Based on Visual Performance* to realistic nighttime roadway conditions and directly addressed the project objective to evaluate the effectiveness of mesopic models in a driving environment.⁽¹⁾ A two-pronged approach was used. First, a static experiment was conducted to replicate fixed geometry laboratory tests to understand the effects of overhead-lighting type, adaptation luminance, and eccentricity on peripheral threshold contrasts of participants of different age groups. Second, a dynamic experiment was performed in which the same participants drove at two different speeds to detect targets under the same conditions of overhead lighting, adaptation luminance, and eccentricity. The dynamic experiment helps answer questions regarding how nonfixed geometry affects peripheral visual performance; as in any driving task, the objects on the periphery of the road subtend different angles at different instances. The analysis of the static and dynamic experiments provided insights into not only the applicability of the CIE recommended mesopic system but also how overhead-lighting sources, adaptation luminance, and eccentricities affected peripheral visual performance.

Static Experiment

The results showed that both LED overhead-lighting sources showed significantly lower threshold contrasts compared with the HPS source. Participants found it more difficult to detect the targets in HPS lighting and required higher contrast to do so, likely because HPS spectral distribution does not align with the eye's sensitivity in the mesopic range. A light source with higher S/P ratios, such as the LED light sources tested, produces more light in the wavelengths where the rod photoreceptors are more sensitive and lowers the peripheral contrast threshold of the targets. These results align with previous research, which showed that light sources with higher S/P ratios had better peripheral visual performance. (See references 20, 21, 28, 42, and 44.)

An increase in adaptation luminance is also associated with a decrease in the threshold contrast. These results are in agreement with other studies that indicated that an increase in adaptation luminance reduces threshold contrast.⁽⁴¹⁾ Both the LED light sources required lower contrasts to detect peripheral targets compared with the HPS source, as shown in figure 121. Again, this can be attributed to LED light sources producing light in the wavelengths that make the rods more sensitive. An increase in the eccentricity of the target was associated with an increase in the threshold contrast. These results align with previous research that found visual acuity outside the fovea decreases with eccentricity.⁽⁶⁰⁾



1 cd/m² = 0.3 fL

Figure 121. Graph. Mesopic modeling experiment (static portion)—threshold contrasts of targets under different overhead-lighting sources at different adaptation luminances.

Comparison of Mesopic and Photopic Threshold Contrasts

The mesopic threshold contrasts were calculated from the mesopic luminances of the targets and their backgrounds under different overhead-lighting types and adaptation luminances and at three different eccentricities. These mesopic threshold contrasts were compared with the

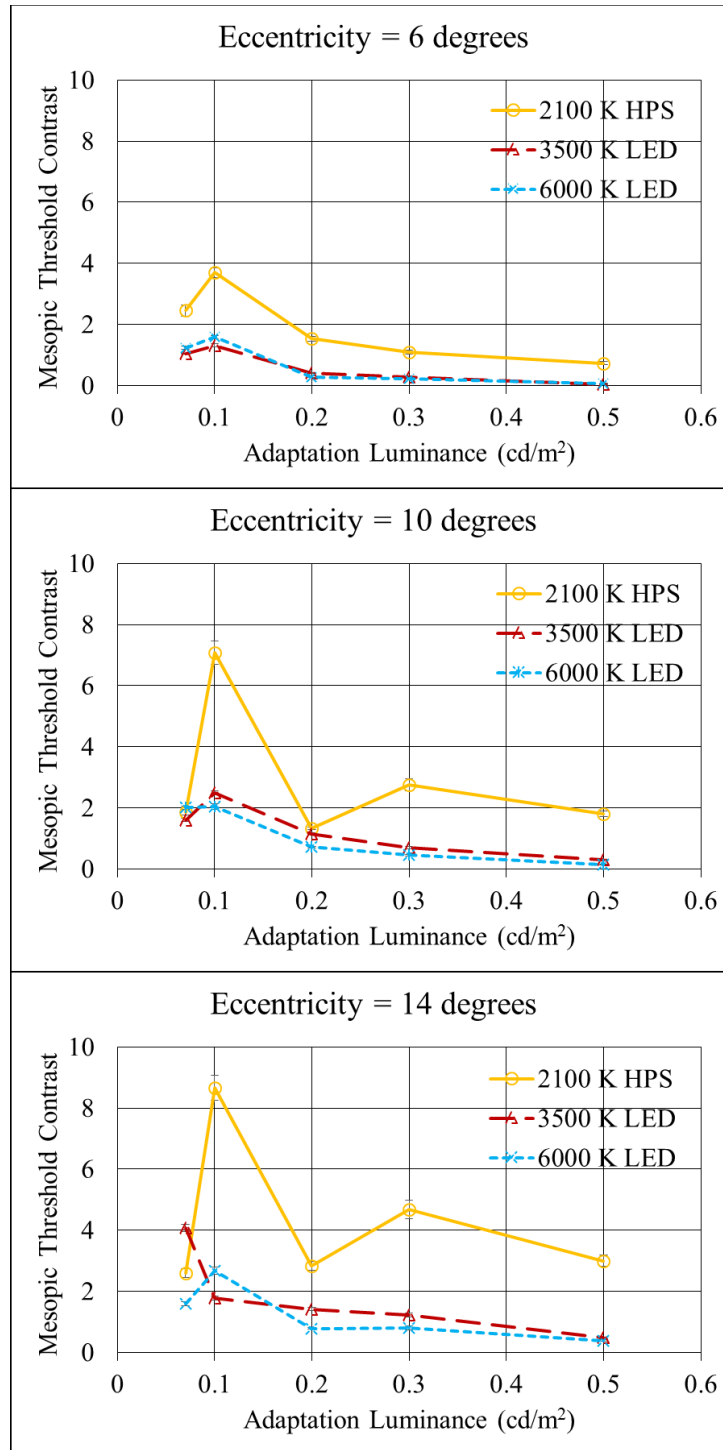
photopic contrasts to see how they varied. The difference between photopic and mesopic threshold contrasts for target detection for the 2,100-K HPS lighting was largest at 0.1 cd/m^2 (0.03 fL) and higher eccentricities. For HPS lighting, the difference in photopic and mesopic threshold contrasts decreased as eccentricity decreased and decreased as adaptation luminance increased. For LED lighting, the differences in photopic and mesopic threshold contrasts were smaller than those for HPS lighting but also became slightly greater for lower luminance levels, mirroring the trend in HPS lighting. This shows that for HPS lighting, photopic luminance measurements may be the least accurate, especially at low light levels. For both lighting types, photopic threshold contrasts were more accurate at higher luminances.

The unexpectedly low threshold contrast at 0.07 cd/m^2 (0.020 fL) could be because at the far periphery, and at the lowest lighting level, the peripheral area of the retina was not adapted to the measured adaptation luminance. The adaptation levels for this study were calculated at the roadway surface, where the drivers were instructed to fixate. At the lowest levels of HPS lighting, the 10- and 14-degree locations were very dark, with a luminance approaching scotopic levels. The difference in adaptation levels between the fovea, where participants were looking at the brighter roadway, and 10 and 14 degrees in the periphery, where they detected the targets, meant the eye's periphery was not adapted to the same level as the fovea. At the periphery, the eye was adapted to darker lighting levels, reducing the threshold contrast for those conditions.

CIE Recommended System for Mesopic Photometry

The CIE model for mesopic spectral sensitivity makes it possible to calculate the mesopic luminance when the photopic luminance and S/P ratio of the light source are known.⁽¹⁾ The outputs of the CIE model for mesopic spectral sensitivity are the mesopic luminance and the weighting factor for calculating the mesopic spectral luminous efficiency function from the photopic spectral luminous efficiency function $V(\lambda)$ and scotopic spectral luminous efficiency function $V'(\lambda)$.

An ideal model for mesopic spectral sensitivity would describe the mesopic luminances of the target and background (and therefore contrast) the same way for the light sources with different spectra; it would be independent of the lighting type's color. The CIE model makes it possible to make the mesopic luminance independent of the spectrum of the light source. However, in figure 122 (which shows the mesopic luminances for the different overhead-lighting types calculated using the CIE model), the mesopic contrast was different for different light sources at the same adaptation luminance. Therefore, for this experiment, the CIE model did not accurately produce mesopic luminance, contrast, and threshold contrast values that were independent from the light-source spectra. The greatest difference was for HPS lighting. The CIE model performed very well for 6- and 10-degree eccentricities for both of the LED lighting types; the mesopic threshold contrast lines are very close to each other for different adaptation luminances, as shown in figure 122. However, at an eccentricity of 14 degrees and adaptation luminance of 0.07 cd/m^2 (0.020 fL), the predicted mesopic contrasts were very different from one another.



1 cd/m² = 0.3 fL

Figure 122. Graph. Mesopic modeling experiment (static portion)—mesopic contrast thresholds as predicted by the CIE Mesopic Spectral Sensitivity Model.

Predicted Versus Actual Difference in Mesopic Luminances

The threshold contrasts in the HPS lighting were significantly different from both LED lighting types. This section compares the actual difference in the mesopic luminance (delta, expressed as a percentage) between the HPS lighting and both LED lighting types to the predicted difference (expressed as a percentage) in mesopic luminance from the *CIE Recommended System for Mesopic Photometry Based on Visual Performance*.⁽¹⁾

For example, the difference between 2,100-K HPS and 6,000-K LED lighting is calculated in the following way (figure 123, from table 11 in *CIE Recommended System for Mesopic Photometry Based on Visual Performance*):

$$\frac{L_{\text{Mesopic-HPS}}}{L_{\text{Photopic-HPS}}} - \frac{L_{\text{Mesopic-LED6K}}}{L_{\text{Photopic-LED6K}}}$$

Figure 123. Equation. Formula for calculating the mesopic luminance difference between 2,100-K HPS and 6,000-K LED lighting.⁽¹⁾

Where:

$L_{\text{mesopic-HPS}}$ = Mesopic target luminance under 2,100-K HPS lighting.

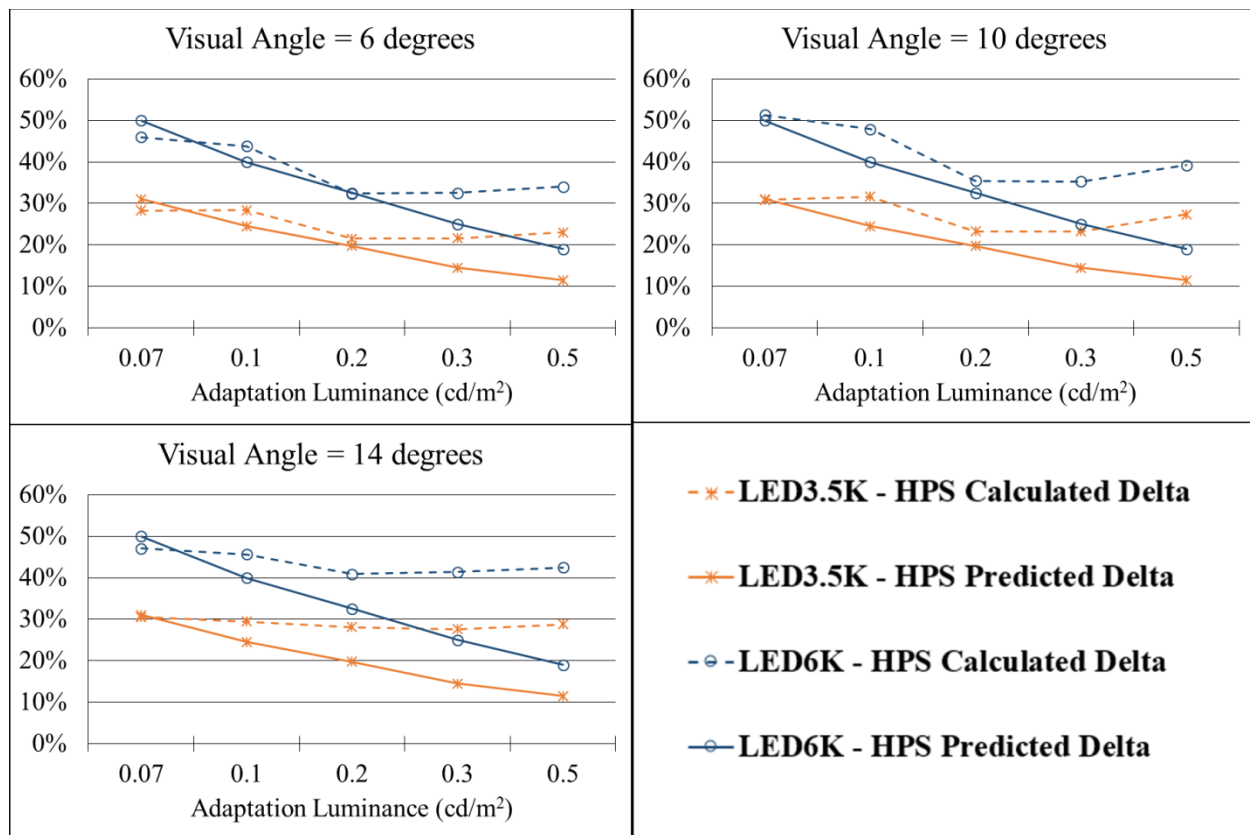
$L_{\text{Photopic-HPS}}$ = Photopic target luminance under 2,100-K HPS lighting.

$L_{\text{Mesopic-LED6K}}$ = Mesopic target luminance under 6,000-K LED lighting.

$L_{\text{Photopic-LED6K}}$ = Photopic target luminance under 6,000-K LED lighting.

For instance, the percentage difference in mesopic and photopic luminance for HPS lighting ($S/P = 0.64$) and LED 6,000-K lighting ($S/P = 1.82$) at 0.1 cd/m^2 (0.03 fL) is -5 and +27 percent, respectively. Therefore, the predicted difference is $(-5 - 27) \text{ percent} = -32 \text{ percent}$.

Figure 124 illustrates the difference in the calculated and predicted delta between the HPS and LED lighting types at each adaptation luminance for each eccentricity. The differences in the calculated and the predicted mesopic luminance between HPS lighting and both the LED lighting types at eccentricities of 6 and 10 degrees show the same trend from the lowest adaptation luminance to 0.2 cd/m^2 (0.06 fL). The calculated difference evened out above this level. For the 14-degree eccentricity, the calculated deltas between the HPS and the LED lighting types were most similar at the lowest adaptation luminances. However, as the adaptation luminance increased, the predicted and calculated deltas diverged, with the greatest difference at 0.5 cd/m^2 (0.15 fL). From this analysis, it is evident that the CIE model accurately predicted the mesopic luminances to about 0.2 cd/m^2 (0.06 fL), up to 10-degree eccentricity off-axis. At higher adaptation luminances and eccentricities, the calculated delta between the HPS and LED lighting types evened out rather than decreased as the model predicted. The differences between calculated and predicted mesopic luminances increase with increasing eccentricity. Because the CIE model does not use eccentricity as an input parameter, the results for this study suggest that a mesopic model with eccentricity as an input parameter might predict the mesopic luminances more accurately.



1 cd/m² = 0.3 fL

Figure 124. Graph. Mesopic modeling experiment (static portion)—calculated versus predicted deltas (difference in mesopic luminance expressed as a percentage) between HPS lighting and each of the LED lighting types.

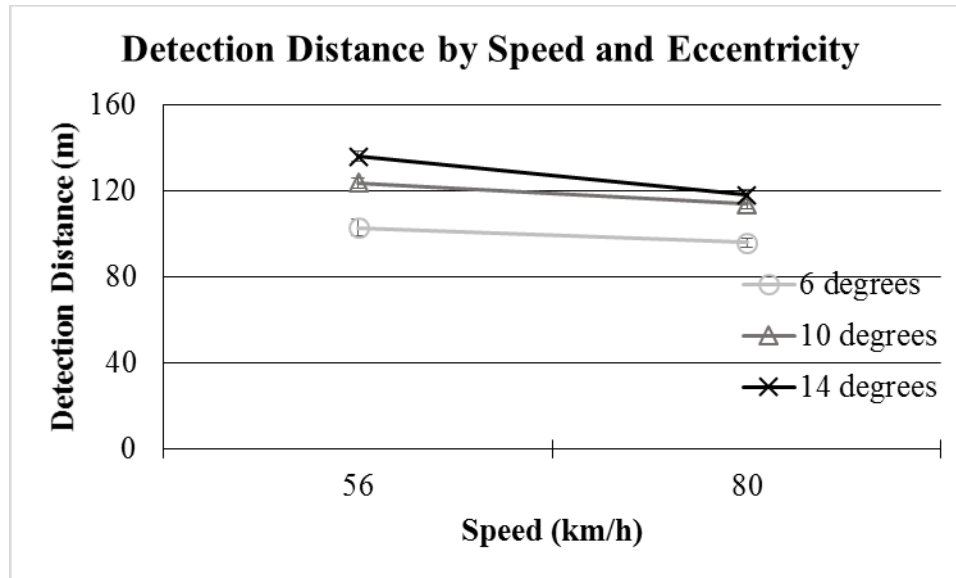
Dynamic Experiment

In the dynamic experiment, adaptation luminance significantly affected the distance at which peripheral targets were detected. An increase in the adaptation luminance resulted in an increase in the detection distance. An increase in the eccentricity was also associated with an increase in the detection distance. Unlike the results of the Akashi and Rea study, where the main effect of overhead-lighting type was significant with the metal halide light (higher S/P ratio) source eliciting shorter response times compared with HPS lighting for targets of eccentricity 15 and 23 degrees, the current study did not show a significant main effect of overhead-lighting type.⁽⁴²⁾ However, there are some significant differences in experimental design between the two studies that could have contributed to the different results. For instance, Akashi and Rea's study did not look at different adaptation luminances. Also, that study used a single vehicle speed, whereas the current study looked at multiple adaptation luminances and two different vehicle speeds. Overhead-lighting type alone did not significantly affect the detection distance of peripheral targets, which is surprising because it was anticipated that light sources with higher S/P ratios would result in significantly better peripheral visual performance. However, overhead-lighting source, along with adaptation luminance, had an effect on visual performance of peripheral targets. Overhead-lighting types with higher S/P ratios (the 3,500-K LED and 6,000-K LED

lighting), had better peripheral visual performance for 10-degree off-axis targets. There were no clear trends regarding overhead-lighting type for the 6- and 14-degree off-axis targets.

For the HPS lighting at larger eccentricities (10 and 14 degrees), the mean detection distances at 0.07 cd/m^2 (0.020 fL) were higher than those at 0.1 cd/m^2 (0.03 fL). This phenomenon could be the result of differential adaptation of the fovea and the periphery of the eye. The adaptation luminances used in the study were measured at the surface of the roadway; the luminance level decreased as distances increased off-axis from the roadway. At a foveal adaptation luminance of 0.07 cd/m^2 (0.020 fL) and an eccentricity of 14 degrees, the adaptation luminance of the periphery of the eye is much lower—possibly close to the lower end of the mesopic range—making the peripheral rod receptors more sensitive and increasing detection distances. That increased sensitivity in the periphery at low adaptation levels could have resulted in better performance at lower lighting levels. HPS was the only overhead-lighting type that displayed differential adaptation at 0.07 cd/m^2 (0.020) at 10 degrees of eccentricity. The low S/P ratio of the HPS lighting could have contributed to the longer detection distances at 0.1 cd/m^2 (0.03 fL). Both LED lighting types have a higher S/P ratios (1.31 and 1.82), which could have made them perform better at this eccentricity for the same adaptation luminance.

The main effect of speed was not significant. However, the interaction between speed and eccentricity was significant. Figure 118 is repeated below as figure 125 for reference. Targets at higher eccentricities were detected at a greater distance at lower speeds than those at lower eccentricities and higher speeds. The target with 14-degree eccentricity at the 56 km/h (35 mi/h) had the highest mean detection distance ($M = 139 \text{ m}$ (456 ft)) and the target with 6-degree eccentricity at (80.47 km/h (50 mi/h) had the lowest mean detection distance ($M = 95.9 \text{ m}$ (315 ft)). These results indicate that at higher speeds, drivers' visual fields narrow, negatively affecting their ability to detect objects in their peripheral vision. These results align with existing research done using driving simulators where peripheral visual performance was poorer at higher speeds.⁽⁹⁷⁾ Because the higher order interactions of eccentricity and speed with either overhead-lighting type or adaptation luminance were not significant, neither overhead-lighting type nor adaptation luminance influenced the change in the size of the visual field caused by driving speed.



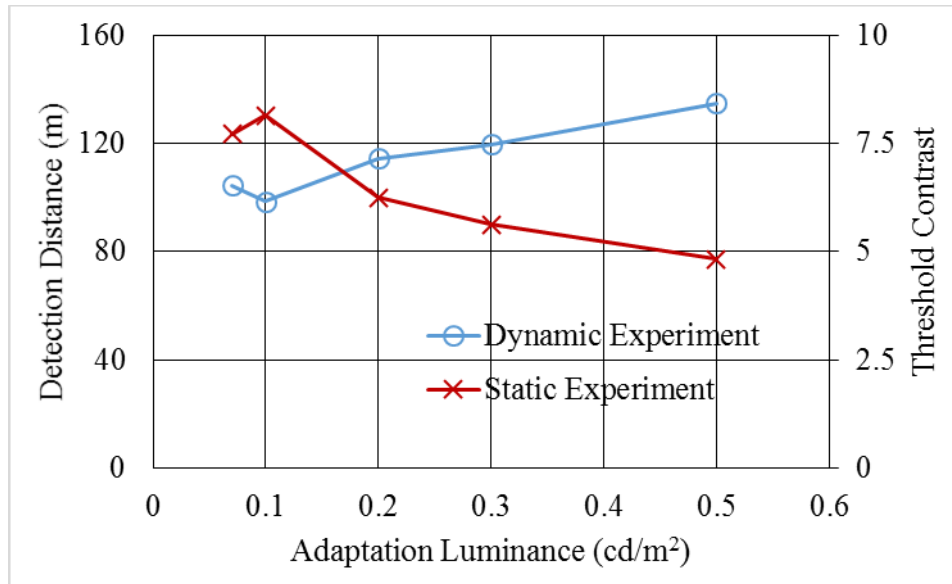
1 m = 3.3 ft
1 km/h = 0.62 mi/h

Figure 125. Graph. Mesopic modeling experiment (dynamic portion)—effect of eccentricity and speed on detection distance.

Transition From Static to Dynamic

Even though in the static (fixed geometry) experiments overhead-lighting type, adaptation luminance, eccentricity, and their interactions were all significant in the dynamic experiment (nonfixed geometry), only the main effect of adaptation luminance and the three-way interaction among overhead-lighting type, adaptation luminance, and eccentricity were significant. This shows that in dynamic conditions, unlike static conditions, overhead lighting alone does not contribute significantly to peripheral visual performance. In dynamic conditions, peripheral visual performance very much depends on factors such as adaptation luminance, eccentricity, and speed. Even though for 10-degree targets, the LED light sources had marginally better performance, this result could not be replicated at either 6- or 14-degree eccentricities. Overall, there were no clear trends in the dynamic experiment that indicate which overhead lighting source resulted in better peripheral visual performance. The only trend clearly evident from the dynamic experiment is the role of adaptation luminance in peripheral visual performance. The results indicate that increased adaptation luminance results in target detection from longer distances, thereby resulting in increased peripheral visual performance. The same result was also observed in the static experiment, where threshold contrasts were lower at higher adaptation luminances. These trends are clearly illustrated in figure 126.

In the static phase of the experiment, the threshold contrasts for the HPS overhead-lighting sources were significantly higher compared with the LED sources. Taking this information into consideration, it was expected that the HPS lighting would perform poorly in the dynamic experiment. From the previous discussion, it is clear the all three overhead-lighting sources had similar performance, with only marginal differences. These differences in peripheral visual performance are illustrated in figure 127.



1 cd/m² = 0.3 fL

1 m = 3.3 ft

Figure 126. Graph. Mesopic modeling experiment—peripheral visual performance in both static and dynamic experiments at different adaptation luminances.

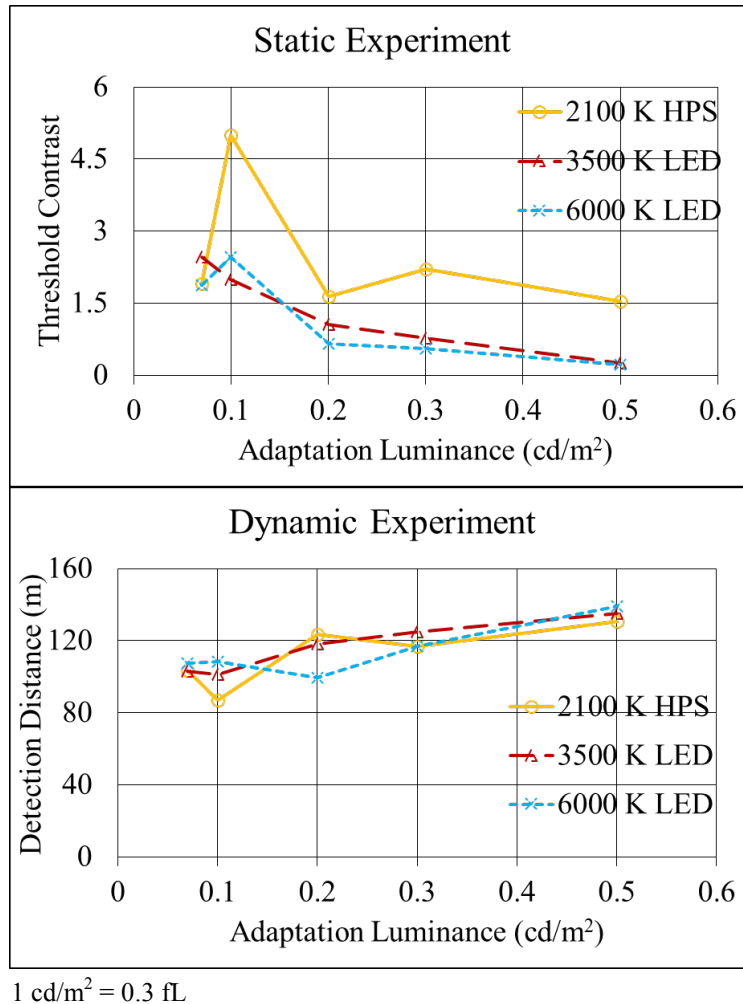


Figure 127. Graph. Mesopic modeling experiment—peripheral visual performance of overhead lighting types at different adaptation luminances.

Age

The effect of age was not statistically significant either in the static experiment or in the dynamic experiment. This was interesting result, because it was expected that age would be a significant factor in peripheral visual performance. Because the average age of the older participants is 67 years, it is also possible that the selected sample of older drivers was not old enough to see statistically significant changes, especially in peripheral contrast sensitivity. There were, however, differences in the threshold contrasts and detection distances of targets in both static and dynamic experiments; younger participants detected targets at lower threshold contrasts ($M_{Young} = 1.27$ m (4.17 ft) versus $M_{Old} = 1.81$ m (5.94 ft)) and longer detection distances ($M_{Young} = 122.58$ m (402.17 ft) versus $M_{Old} = 109.91$ m (360.60 ft)) compared with older participants. These differences were also not statistically significant.

CONCLUSIONS

The primary goal of this mesopic modeling experiment was to verify the applicability of the CIE Recommended System for Mesopic Photometry in naturalistic nighttime roadway situations, addressing the project objective of evaluating mesopic models in a driving environment.⁽¹⁾ The CIE Recommended System for Mesopic Photometry accurately predicted the mesopic luminances and contrasts for both the LED light sources at smaller eccentricities but not for the HPS light source. Differences between the mesopic and the photopic luminances of HPS lighting and both the LED overhead-lighting sources indicated that the calculated differences closely followed the predicted differences from 0.07 to 0.2 cd/m² (0.020 to 0.06 fL). Beyond this range, the calculated differences leveled off, whereas the predicted values continued to decrease. The results show that the existing system does not take eccentricity into account, and the results show that the mesopic luminances calculated at greater eccentricities were less accurate. An ideal mesopic model should also use eccentricity as an input to accurately calculate mesopic luminances.

The secondary goal of the study was to assess the effect of an overhead lighting source's spectrum on drivers' peripheral visual performance in both static and dynamic conditions, addressing the project objective of evaluating the impact of spectra of overhead-lighting systems. In the static experiment, overhead-lighting type, adaptation luminance, and eccentricity significantly affected the threshold contrast at which participants were able to detect a target. Light sources with higher S/P ratios (3,500-K and 6,000-K LEDs) had lower threshold contrasts at detection in the periphery, compared with light sources with lower S/P ratios (2,100-K HPS), as suggested by existing research. An increase in eccentricity resulted in an increase in the threshold contrast. An increase in the adaptation luminance resulted in a decrease in the threshold contrast. In the dynamic experiment, peripheral visual performance was mainly affected by adaptation luminance. Increases in the adaptation luminance resulted in detection of objects from longer distances. Surprisingly, overhead-lighting type did not influence peripheral visual performance in the dynamic experiment. Targets with larger eccentricities and lower speeds were detected from longer distances, indicating that drivers' visual fields narrow at higher speeds, which negatively affects peripheral visual performance.

Other results included an interesting observation in the static experiment: threshold contrast at the lowest adaptation luminance (0.07 cd/m² (0.020 fL)) was lower than at higher adaptation luminances for all overhead lighting types and at all eccentricities. In the dynamic experiment at 0.07 cd/m² (0.020 fL), the detection distance for all overhead-lighting types was also longer than that at 0.1 cd/m² (0.03 fL), especially for 10- and 14-degree eccentricities. These findings could be attributed to the differential adaptation of the fovea compared with that at the periphery of the driver's eye at the lowest adaptation luminance. However, more research is required to confirm these findings. Lastly, age was not a significant factor in either the static or dynamic portions of this experiment.

CHAPTER 8. FINAL PERFORMANCE EXPERIMENT

INTRODUCTION

The purpose of the final experiment for this project was to further investigate variables of interest identified in the previous spectral effects experiments. This experiment melded many factors used in the previous experiments so the combination of their effects could be explored. The configuration of the MPI system performance experiment described in chapter 5 was incorporated to determine the impact on pedestrian visibility at various off-axis positions. The overhead lighting levels incorporated into this study were also used in the mesopic modeling experiment as described in chapter 7. These levels were first researched in the overhead-lighting level experiment described in chapter 6. The impact these factors had in previous experiments were more closely examined in this final performance experiment.

There were no significant main effects for the MPI system configuration on pedestrian-detection distances found in the MPI system performance experiment, but there were significant two-way interactions involving the MPI system. To gather more data on MPI system performance, it was included in this final experiment, but only two configurations were used to reduce the number of variables and test the most likely MPI system configurations: the MPI system off and the MPI system tracking a roadside pedestrian.

The mesopic modeling experiment found mixed results for overhead lighting type. Overhead-lighting type significantly affected threshold contrast in the static portion of the experiment, but as a main effect, it did not significantly affect detection distance. Thus, this final experiment collected more data using the three overhead-lighting types used in previous experiments.

Although reducing the level of overhead lighting results in energy savings, this goal is not acceptable if it compromises visibility. A combination of overhead-lighting level and pavement type affects adaptation luminance, which in turn affects the eye's behavior in the mesopic range. In this experiment, as in the mesopic modeling experiment, the experiment was conducted with five distinct adaptation luminances to determine the points at which visibility might be compromised.

Driver behavior differs at varying driving speeds, possibly resulting in different levels of visual performance. Thus, this experiment included two different speeds common to roadways, 56 km/h and 80 km/h (35 and 50 mi/h).

Pedestrians were employed as the detection targets for this experiment because the current state of machine-vision technology limits an MPI system's ability to detect and highlight small targets. The pedestrians were placed at various distances from the roadway. They wore different colors and appeared on both the left and right sides of the road. These conditions were selected to mimic naturalistic conditions, to reduce the chance that a participant might predict pedestrian position, and to introduce the possibility of detection at multiple eccentricities because eccentricity affects mesopic visual performance. Eccentricity was not controlled in this experiment, however, because participants were not instructed to keep their eyes focused on the roadway. To create the possibility for peripheral detection, pedestrians were placed at various

offsets with respect to the driving lane. Participants could scan for pedestrians, and detection could take place either in the fovea or in the periphery.

Research Objectives

The research objectives of the final performance experiment were the same as those of the overall project. They included evaluating the following:

- Impact of the spectra of overhead-lighting systems on driver visual performance.
- Interaction of vehicle headlamps and overhead lighting in terms of object visibility.
- Applicability of mesopic models and scaling factors in a roadway lighting design.
- Impact of a peripheral illumination system on driver visual performance.

EXPERIMENTAL DESIGN

A 2 by 3 by 5 by 2 by 2 by 4 by 2 by 3 mixed-factors experiment was designed to measure the effect of age, overhead lighting type, adaptation luminance, MPI system configuration, vehicle speed, visual angle, pedestrian position, and pedestrian clothing color on pedestrian-detection and color-recognition distances. The variables used in the experiment are listed in table 34, through table 36.

Table 34. Final experiment—-independent variables and values.

Independent Variable	Levels
Age	Younger (25–35), Older (65+)
Overhead-Lighting Type	2,100-K HPS, 3,500-K LED, 6,000-K LED
Adaptation Luminance	0.07, 0.1, 0.2, 0.3, 0.5 cd/m ² (0.020, 0.03, 0.06, 0.09, 0.15 fL)
MPI System Configuration	Off, Tracking
Speed	56 km/h (35 mi/h), 80 km/h (50 mi/h)
Offset	3.0, 7.7, 8.9, 21.0 m (9.8, 25, 29, 69 ft)
Pedestrian on Left or Right	Left, Right
Pedestrian Clothing Color	Gray, Red, Blue

Table 35. Final experiment—covariate and measurement method.

Dependent Variables	Measurement Method
Contrast	Weber contrast, measured with ProMetric® system

Table 36. Final experiment—dependent variables and measurement method.

Dependent Variables	Measurement Method
Pedestrian-Detection Distance	Participant first sees pedestrian
Pedestrian Color-Recognition Distance	Participant first correctly identifies pedestrian clothing color

Independent Variables

Age

Participants were divided into the same age groups as previous experiments: drivers (25–35 years old) and older drivers (65 years old and older).

Overhead Lighting Type

All three overhead-lighting systems were used.

Adaptation Luminance

Adaptation luminance was the luminance, viewed from inside the test vehicle, for a given combination of overhead-lighting level and pavement type. The same design was used here as in the mesopic modeling experiment, and adaptation luminances are reported in table 37.

Table 37. Final performance experiment—adaptation luminance per overhead lighting level and pavement type.

Overhead-Lighting Level	Luminance on Concrete (cd/m ² (fL))	Luminance on Asphalt (cd/m ² (fL))
Low	0.1113 (0.032)	0.0716 (0.021)
Medium	0.3535 ^a (0.103)	0.1987 (0.056)
High	0.5385 (0.157)	0.3535 ^a (0.103)

^aSame luminance.

MPI System Configuration

The mockup MPI system was configured to behave in two ways: off, with headlamps aimed ahead, like in a normal vehicle; and tracking, with headlamps illuminating a pedestrian from about 183 m (600 ft) away, and then swiveling the headlamp to keep the pedestrian in the beam as the vehicle approached. The configurations are illustrated in figure 59.

Speed

The participant drove the vehicle at 56 and 80 km/h (35 and 50 mi/h).

Pedestrian Offset

The eccentricity at which participants detect pedestrians for dynamic experiments cannot be fixed, because as the driver approaches the pedestrian, the eccentricity is constantly changing. Also, for this experiment, participants were not instructed to focus along the roadway. To create the possibility for peripheral detection, pedestrians were placed at four offsets with respect to the travel lane. To determine the pedestrian positions, a theoretical detection distance was fixed at 83 m (277 ft), because based on a 1-degree downward viewing angle with a vehicle height of 1.45 m (4.76 ft), this is the resulting distance.⁽⁵⁾ Four offsets were calculated based on detection from that distance—3.0, 7.7, 8.9, and 21.0 m (9.8, 25, 29, and 69 ft)—and are described in figure 128.

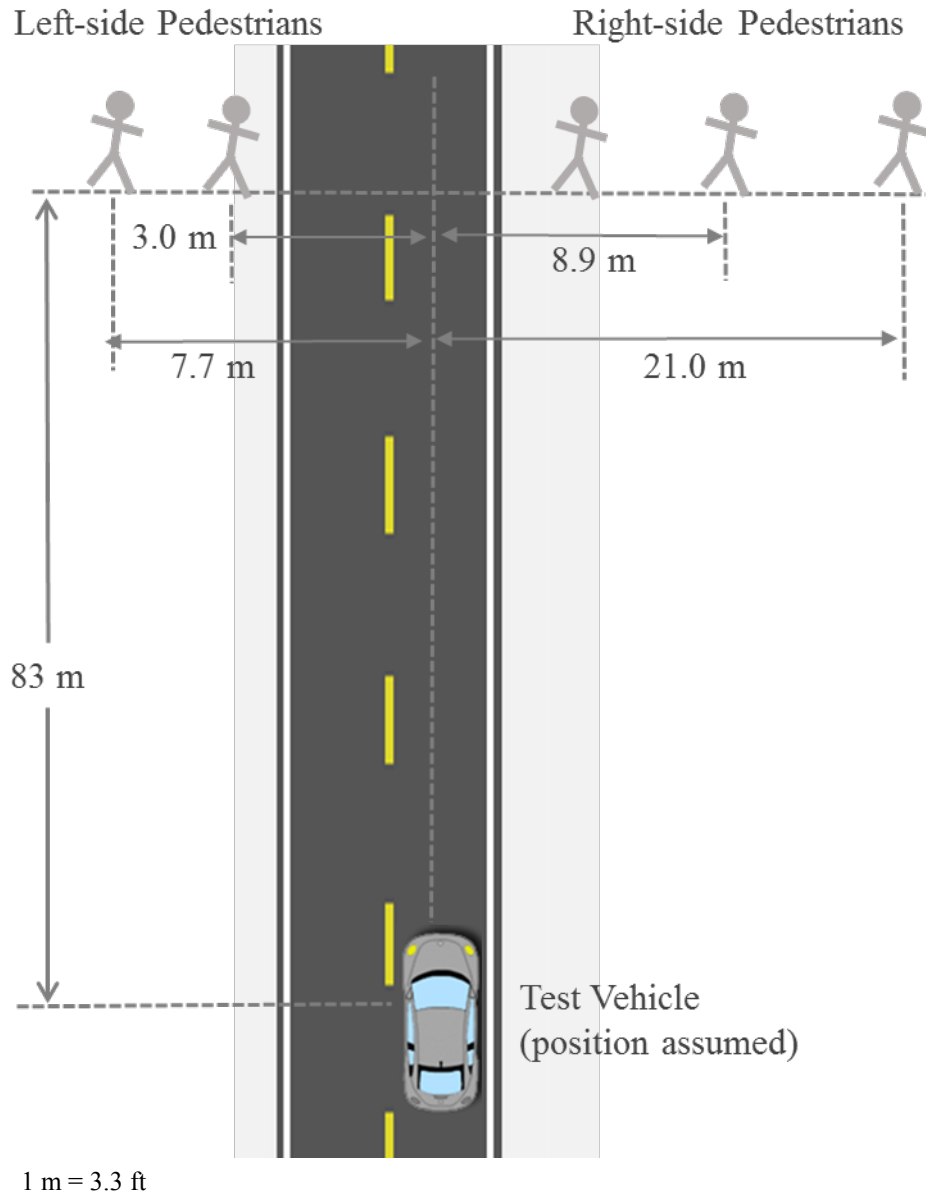


Figure 128. Diagram. Final performance experiment—pedestrian positions and offsets from the roadway.

All pedestrian positions were in the lighted section of the Smart Road, and all pedestrian positions had VI on the pedestrian's face as similar as possible to each other within a specified lighting condition. VI levels are listed in table 38.

Table 38. Final performance experiment—VI for all pedestrian positions, overhead lighting levels, and visual angles.

Offset (m)	Light Level	Average VI (lx (fc))	Standard Deviation (lx (fc))
3.0	Low	0.35 (0.03)	0.027 (0.0025)
3.0	Medium	1.05 (0.1)	0.307 (0.0285)
3.0	High	1.6 (0.15)	0.316 (0.0294)
7.7	Low	0.27 (0.025)	0.027 (0.0025)
7.7	Medium	0.88 (0.082)	0.267 (0.0248)
7.7	High	1.25 (0.116)	0.261 (0.0242)
8.9	Low	0.27 (0.025)	0.023 (0.0021)
8.9	Medium	0.88 (0.082)	0.342 (0.0318)
8.9	High	1.3 (0.121)	0.343 (0.0319)
21.0	Low	0.1 (0.009)	0.047 (0.0044)
21.0	Medium	0.36 (0.033)	0.287 (0.0267)
21.0	High	0.47 (0.044)	0.298 (0.0277)

1 m = 3.3 ft

Pedestrian on Left or Right

The pedestrian stood on the left or right of the road with respect to the participant vehicle. Pedestrians at 3.0 m (9.8 ft) offset were located on both sides of the road. Pedestrians at 7.7 m (25 ft) offset were located only on the left side of the road, and pedestrians at 8.9 and 21.0 m (29 and 69 ft) offset were located only on the right side of the road, as shown in figure 128.

Pedestrian Clothing Color

Pedestrians wore clothing in three colors: gray, red, and blue, as described in chapter 3.

Covariate

Contrast

The luminance of the pedestrians and the background behind them was measured using the ProMetric® luminance system from 83 m (277 ft) up the road from the pedestrian, the same distance at which RP-8 advises roadway lighting designers to measure roadway luminance from a luminaire.⁽⁵⁾ The Weber contrast was calculated from that measurement.

Dependent Variables

Detection and color-recognition distances were the dependent variables. Orientation-recognition distance was not measured, and pedestrians all faced toward the roadway.

METHODS

Facilities and Equipment

This experiment was conducted on the Virginia Smart Road using the same test vehicles as in previous experiments. The headlamps were the HID headlamps installed on the test vehicles for the previous experiments in this project but with low-intensity neutral-density filter with a CCT of 3,530 K and transmittance of .3413.

Participants

Participants were recruited and screened as described in Chapter 3; however, for this experiment, they were not tested for UFOV.

A total of 36 participants performed the experiment, 18 older and 18 younger. Within each age group, participants were divided equally by gender. Mean and standard deviation of participant age, visual acuity, mesopic visual acuity, and low contrast visual acuity are listed in table 39.

Table 39. Final performance experiment participant characteristics.

Participant Characteristic	Older Drivers Mean	Older Drivers Standard Deviation	Young Drivers Mean	Younger Drivers Standard Deviation
Age	70.4	6.3	30.5	3.2
Visual Acuity	20/21.6	5.25	20/17.3	3.53
Mesopic Visual Acuity	20/38.1	13.5	20/25.8	6.4
Low Contrast Visual Acuity	20/27.8	7.3	20/20.9	5.3

Procedure

Participants were recruited, screened, and directed to the Smart Road as described in chapter 3. Each participant attended three experimental sessions, one for each overhead-lighting type. Each session consisted of 1 practice run and 12 experimental runs up and down the Smart Road, for a total of 24 trials for each lighting type. Lighting level was changed twice during each session, so all three intensities were tested. Two participants in two vehicles typically completed the experiment at one time.

During the experiment, on-road experimenters adjusted the overhead lighting level and pedestrian positions for the each experimental run. In-vehicle experimenters directed participants to drive at the speed called for by the protocol and recorded detection distances.

Data Analysis

Detection and Color Recognition Distances

After video data reduction, an ANOVA was used to determine whether the independent variables significantly affected pedestrian-detection and color-recognition distances. When results were

significant, Tukey HSD tests were performed to determine which factors differed from each other. When Tukey HSD tests are reported on charts, data points sharing a letter do not significantly differ from each other.

For missed detections, Fisher's Exact Test was conducted to determine the degree of difference between two binomial variables. The results of the test are reported as the probability that one variable occurs over another variable.

This experiment focused mainly on gray-target detection; colored targets were not distributed evenly among the visual angles. Therefore, although data analysis was performed on all target colors, it was repeated only for the gray targets.

Contrast

Weber contrast was calculated for the pedestrians the same way it was calculated for the other experiments in this project. An ANCOVA using contrast as a covariate was performed to determine the relationship between contrast and detection distance. Contrast was not analyzed with respect to color-recognition distance. Detection is more crucial for driving safety than color recognition. Only luminance contrast, not color contrast, was measured.

Contrast and detection-distance data were analyzed separately for when the MPI system was off and when it was on, but results indicated the MPI system introduced a great deal of variation in the data—system-on data and system-off data were not necessarily comparable. In addition, it was not possible to calculate the contrast for the instant a participant detected a pedestrian, because it was calculated from luminance measurements taken 83 m (277 ft) along the road from the pedestrian. Actual detection occurred at between 124 and 97.4 m (407 and 320 ft), introducing error in the contrast measurement.

RESULTS

Main Effects

Main effects on detection distance and color-recognition distance occurred for many of the same independent variables. Significant main effects are listed in table 40 with results explained in detail following the table.

Table 40. Final performance experiment results.

Factor(s)	Detection Distance <i>F</i>	Detection Distance <i>p</i>	Color- Recognition Distance <i>F</i>	Color- Recognition Distance <i>p</i>
Adaptation Luminance	5.24	0.0006 ^a	2.75	0.0313 ^a
Age	2.9	0.0987	2.3	0.1401
Color	20.69	< 0.0001 ^a	2.46	0.0947
Offset	3.28	0.0253 ^a	3.1	0.0316 ^a
Overhead-Lighting Type	0.14	0.8718	0.04	0.9622

Factor(s)	Detection Distance <i>F</i>	Detection Distance <i>p</i>	Color-Recognition Distance <i>F</i>	Color-Recognition Distance <i>p</i>
MPI Configuration	0.5	0.4865	1.68	0.205
Speed	1.43	0.2414	0.13	0.7218
Age by Color	1.38	0.2589	0.57	0.5706
Age by MPI Configuration	0.35	0.5605	1.12	0.2989
Age by Speed	0.02	0.8791	0.68	0.4164
Color by MPI Configuration	2.62	0.0816	0.36	0.7008
Color by Speed	0.25	0.7782	0.35	0.7097
Offset by Adaptation Luminance	6.52	< .0001 ^a	1.72	0.0777
Offset by Age	0.03	0.9919	0.41	0.7481
Offset by Color	2.9	0.0649	0.95	0.3967
Offset by Overhead-Lighting Type	1.97	0.0799	1.3	0.2666
Offset by MPI Configuration	0.45	0.6422	0.27	0.7672
Offset by Speed	3.55	0.0184 ^a	2.01	0.1201
Overhead-Lighting Type by Adaptation Luminance	2.78	0.0071 ^a	0.77	0.6298
Overhead-Lighting Type by Age	0.04	0.9561	0.1	0.9089
Overhead-Lighting Type by Age by Color	0.69	0.6027	1.03	0.402
Overhead-Lighting Type by Color	0.81	0.5236	1.38	0.2523
Overhead-Lighting Type by MPI Configuration	1.35	0.2734	0.29	0.7535
Overhead Lighting Type by Speed	0.56	0.5784	0.46	0.6331
MPI Configuration by Speed	0.26	0.6137	0	0.9567
Adaptation Luminance by Speed	2.31	0.0619	2.23	0.0697
Age by Adaptation Luminance	1.34	0.2605	0.38	0.8241
Age by Adaptation Luminance by Speed	1.07	0.3727	1.14	0.3387
Age by Color by Adaptation Luminance	1.08	0.3768	0.6	0.7327
Age by Color by MPI Configuration	2.98	0.0588	1.27	0.29
Age by Color by Speed	0.24	0.7892	0.06	0.9394
Age by MPI by Adaptation Luminance	0.25	0.9066	1.79	0.1356
Age by MPI by Speed	0.56	0.4593	0.15	0.7002
Color by Adaptation Luminance	1.16	0.3296	1.17	0.3247
Color by MPI Configuration By Adaptation Luminance	1.08	0.3759	2.23	0.0435 ^a
Color by MPI Configuration by Speed	0.08	0.9245	0.56	0.5725
Offset by Adaptation Luminance by Speed	1.92	0.0432 ^a	1.53	0.1291

Factor(s)	Detection Distance <i>F</i>	Detection Distance <i>p</i>	Color-Recognition Distance <i>F</i>	Color-Recognition Distance <i>p</i>
Offset by Age by Adaptation Luminance	1.9	0.0462 ^a	1.24	0.2652
Offset by Age by Color	2.55	0.0889	2.88	0.0676
Offset by Age by MPI Configuration	0.54	0.5828	2.06	0.1343
Offset by Age by Speed	1.28	0.287	3.51	0.0194 ^a
Offset by Color by Adaptation Luminance	0.24	0.7887	0.49	0.6187
Offset by Color by MPI Configuration	0.61	0.548	0.26	0.7736
Offset by Overhead-Lighting Type by Adaptation Luminance	1.27	0.1971	0.97	0.5041
Offset by Overhead-Lighting Type by Age	0.47	0.8298	0.44	0.851
Offset by Overhead-Lighting Type by Color	6.72	0.0004 ^a	2.71	0.0503 ^a
Offset by Overhead-Lighting Type by MPI Configuration	0.4	0.806	1.7	0.1578
Eccentricity by Overhead-Lighting Type by Speed	2.12	0.0583	0.99	0.4386
Offset by MPI Configuration by Adaptation Luminance	0.46	0.8352	0.97	0.445
Offset By MPI Configuration by Speed	0.81	0.447	2.98	0.0568
Overhead-Lighting Type by Age by Adaptation Luminance	1.37	0.2168	0.35	0.9457
Overhead-Lighting Type by Age by MPI Configuration	1.25	0.2998	0.01	0.9879
Overhead-Lighting Type by Age by Speed	0.32	0.7286	0.14	0.8671
Overhead-Lighting Type by Color by Adaptation Luminance	2.03	0.0254 ^a	0.94	0.5134
Overhead-Lighting Type by Color by MPI Configuration	1.1	0.364	4.01	0.0065 ^a
Overhead-Lighting Type by Color by Speed	0.91	0.4639	0.8	0.5343
Overhead-Lighting Type by MPI Configuration by Adaptation Luminance	1	0.4395	2.07	0.043 ^a
Overhead-Lighting Type by MPI Configuration By Speed	0.26	0.7696	0.56	0.5771
MPI Configuration by Adaptation Luminance	0.57	0.6855	1.4	0.2387

^aSignificant at $p < 0.05$.

Table 41. Final performance experiment significant main effects, gray only.

Independent Variable	Detection Distance <i>F</i>	Detection Distance <i>p</i>
Adaptation Luminance	8.26	< 0.0001 ^a
Age	7.16	0.0119 ^a
Offset	1.75	0.163
Overhead-Lighting Type	1.71	0.1966
MPI Configuration	0.05	0.8272
Speed	0.62	0.4379
Adaptation Luminance by Speed	2.35	0.0579
Age by Adaptation Luminance	0.64	0.6327
Age by MPI Configuration	1.66	0.2079
Age by Speed	0.1	0.7484
Offset by Adaptation Luminance	7.69	<0.0001 ^a
Offset by Age	0.41	0.7498
Offset by Overhead-Lighting Type	1.46	0.2017
Offset by MPI Configuration	1.44	0.2437
Offset by Speed	3.96	0.0114 ^a
Overhead-Lighting Type by Adaptation Luminance	0.43	0.9033
Overhead-Lighting Type by Age	0.41	0.6693
Overhead-Lighting Type by MPI Configuration	0.41	0.6701
Overhead-Lighting Type by Speed	0.6	0.5543
MPI Configuration by Adaptation Luminance	0.28	0.8935
MPI Configuration by Speed	0.25	0.6219
Age by Adaptation Luminance by Speed	1.04	0.3909
Age by MPI Configuration by Adaptation Luminance	0.91	0.46
Age by MPI Configuration by Speed	0.12	0.7306
Offset by Adaptation Luminance by Speed	2.33	0.0123 ^a
Offset by Age by Adaptation Luminance	2.23	0.0172 ^a
Offset by Age by MPI Configuration	1	0.3713
Offset by Age by Speed	1.24	0.3001
Offset by Overhead Lighting Type by Adaptation Luminance	1.21	0.2467
Offset by Overhead Lighting Type by Age	0.21	0.974
Offset by Overhead Lighting Type by MPI Configuration	0.74	0.5706
Offset by Overhead Lighting Type by Speed	2.2	0.0505
Offset by MPI Configuration x Adaptation Luminance	0.86	0.5222
Offset by MPI Configuration x Speed	0.83	0.4384
Overhead Lighting Type by Age by Adaptation Luminance	1.31	0.2437
Overhead Lighting Type by Age by MPI Configuration	3.37	0.0464 ^a
Overhead Lighting Type by Age by Speed	3.68	0.0356 ^a

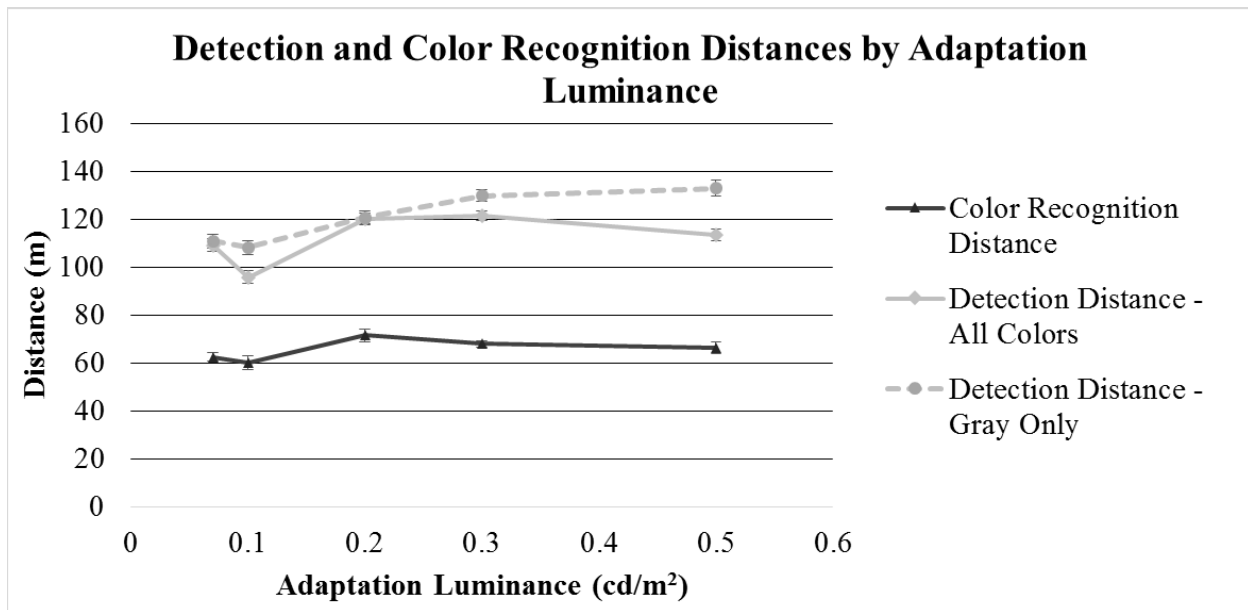
Independent Variable	Detection Distance <i>F</i>	Detection Distance <i>p</i>
Overhead-Lighting Type by MPI Configuration by Adaptation Luminance	0.91	0.5072
Overhead-Lighting Type by MPI Configuration by Speed	1.78	0.1841

^aSignificant at $p < 0.05$.

Adaptation Luminance

The results for adaptation luminance's effect on detection and color-recognition distances are shown in figure 129. When all pedestrian clothing colors were analyzed, it was found adaptation luminance significantly affected detection distance, with mean detection distance at 0.1 cd/m^2 (0.03 fL) shorter ($M = 95.7 \text{ m}$ (314 ft)) than at the other adaptation luminances (all more than 109 m (358 ft)). The same effect was seen in the previous experiment. Adaptation luminance also significantly affected color-recognition distance, following the same trend as described for detection distance but to a lesser extent. This could be because of poor target contrast at that luminance, a condition described in more detail in the contrast section of the results.

When only gray-clothed pedestrians were analyzed, it was found that adaptation luminance also significantly affected detection distance, with a general trend of higher adaptation luminances having longer detection distances.



1 $\text{cd/m}^2 = 0.3 \text{ fL}$

1 m = 3.3 ft

Figure 129. Graph. Final performance experiment—detection distance and color-recognition distance by adaptation luminance.

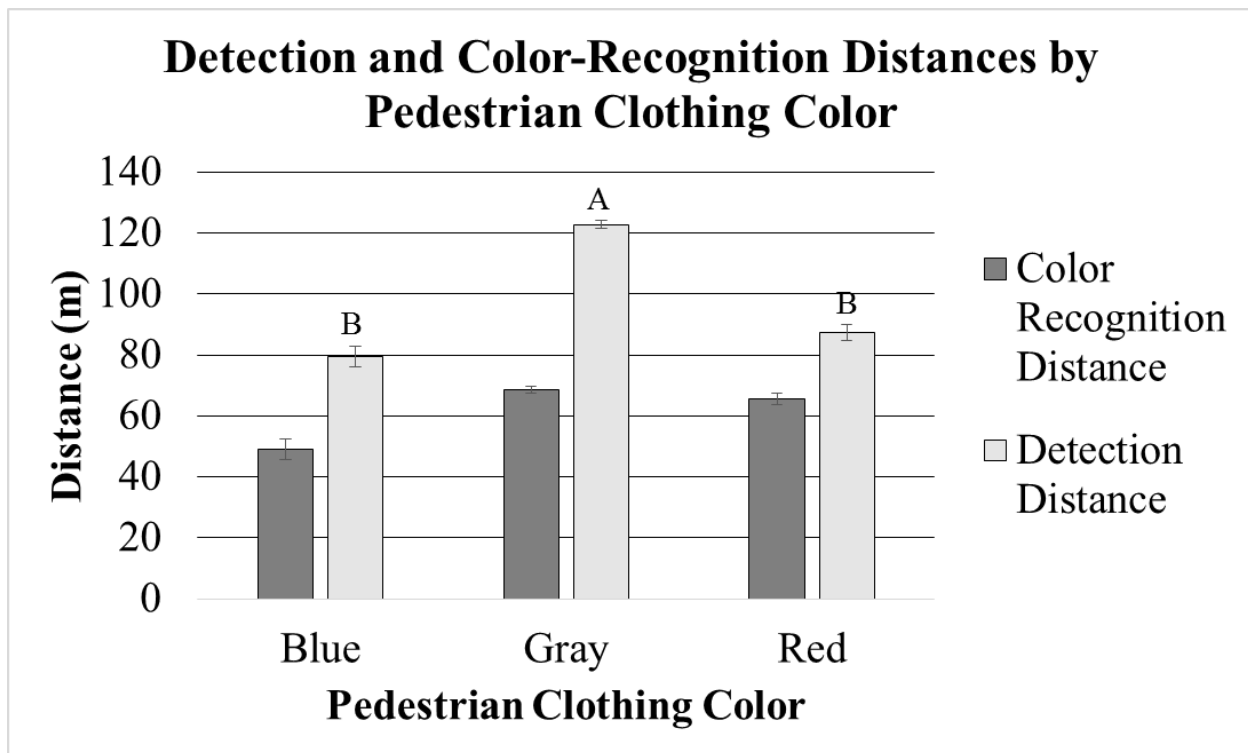
Age

Age significantly affected pedestrian-detection distance when data for only gray-clothed pedestrians were analyzed. The mean detection distance for older participants ($M = 107$ m (351 ft)) was significantly shorter than that for younger participants ($M = 135$ m (440 ft)).

The Snellen visual acuity test performed during participant screenings found that older participants had poorer visual acuity than younger participants. While normal vision is 20/20, younger participants had average visual acuity of 20/17.2, while older participants had an average visual acuity of 20/21.6. Older participants also had poorer contrast sensitivity than younger participants. When the contrast sensitivity exam was administered with lighter-colored gray letters on the Snellen eye chart, younger participants had an average acuity of 20/20.8, while the older participants had an average of 20/27.8. These two exams were performed in photopic conditions. A third Snellen acuity test was performed in mesopic conditions; for that exam, younger participants had an average visual acuity of 20/25.7, while older participants had an average visual acuity of 20/38.1. As the difficulty of the Snellen eye exams increased, from normal-to-low contrast to mesopic conditions, older participants' visual acuity decreased when compared with the younger participants. That difference in visual acuity was reflected in the gray-only target detection distances because the colored targets were distributed unevenly among the visual angles, introducing variations in the detection distances not caused by color alone.

Pedestrian Clothing Color

Mean detection distances were significantly different among the three pedestrian clothing colors, with gray ($M = 123$ m (404 ft)) seen from farther away than red ($M = 87.3$ m (286 ft)) and blue ($M = 79.4$ m (260 ft)). Mean color-recognition distances did not differ significantly by pedestrian clothing color. Pedestrian clothing color results are shown in figure 130.



1 m = 3.3 ft

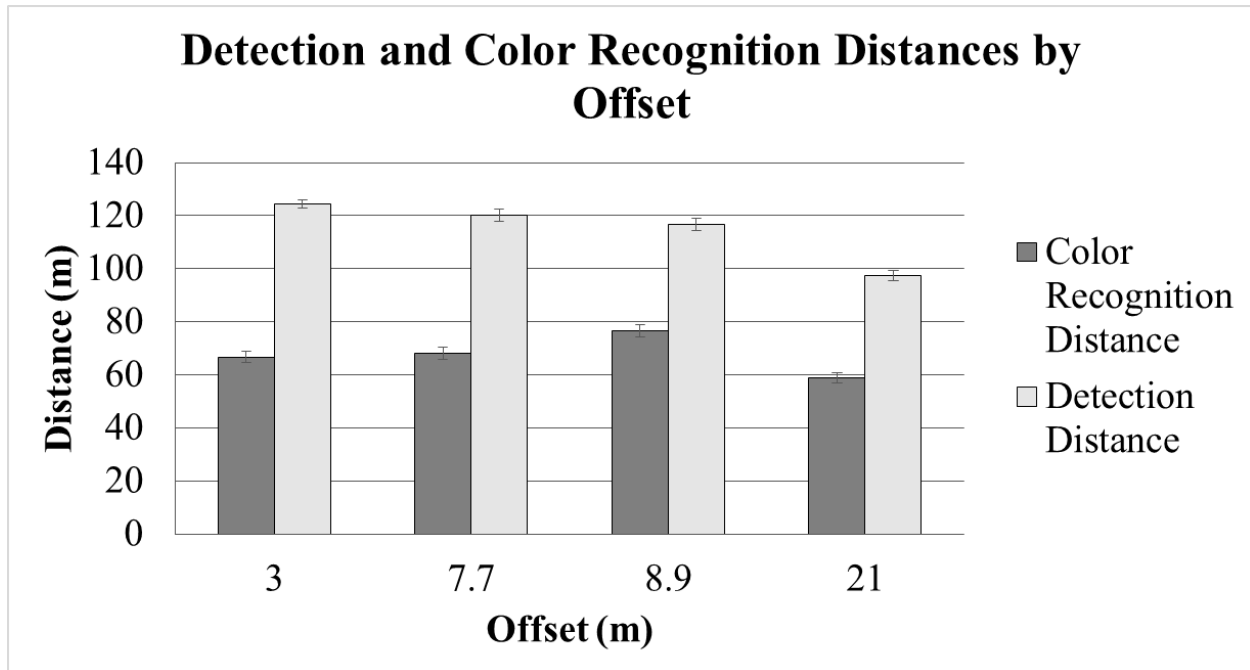
Figure 130. Chart. Final performance experiment—detection and color-recognition distances by pedestrian clothing color.

The experiment was designed so that pedestrians wearing gray were seen 10 times more frequently than those wearing red or blue, and the visual angle was not divided evenly among the colors. Therefore, definitive results regarding pedestrian clothing color cannot be obtained.

Offset

For all pedestrian clothing colors, detection distance differed significantly with offset. As offset increased, detection distance decreased. A Tukey HSD test found that the only detection distances that differed significantly from each other were those at 3.0 m (9.8 ft) offset ($M = 124$ m (407 ft)) and 21.0 m (69 ft) offset ($M = 97.4$ m (320 ft)). This result was expected, because visual acuity decreases as offset increases and objects are viewed more in the eye's periphery. Figure 131 illustrates the results.

Color-recognition distance differed significantly with offset but followed a different trend (figure 131). Color-recognition distance was shortest at 21.0 m (69 ft) offset ($M = 58.8$ m (193 ft)) and longest at 8.9 m (29 ft) offset ($M = 76.6$ m (251 ft)), but the standard deviation of the color-recognition data, between 47.5 and 68.9 m (156 and 225 ft) depending on offset, warrants caution when attempting to draw meaning from the results.



1 m = 3.3 ft

Figure 131. Chart. Final performance experiment—detection distance and color-recognition distance versus offset for all pedestrian clothing colors.

MPI System Configuration

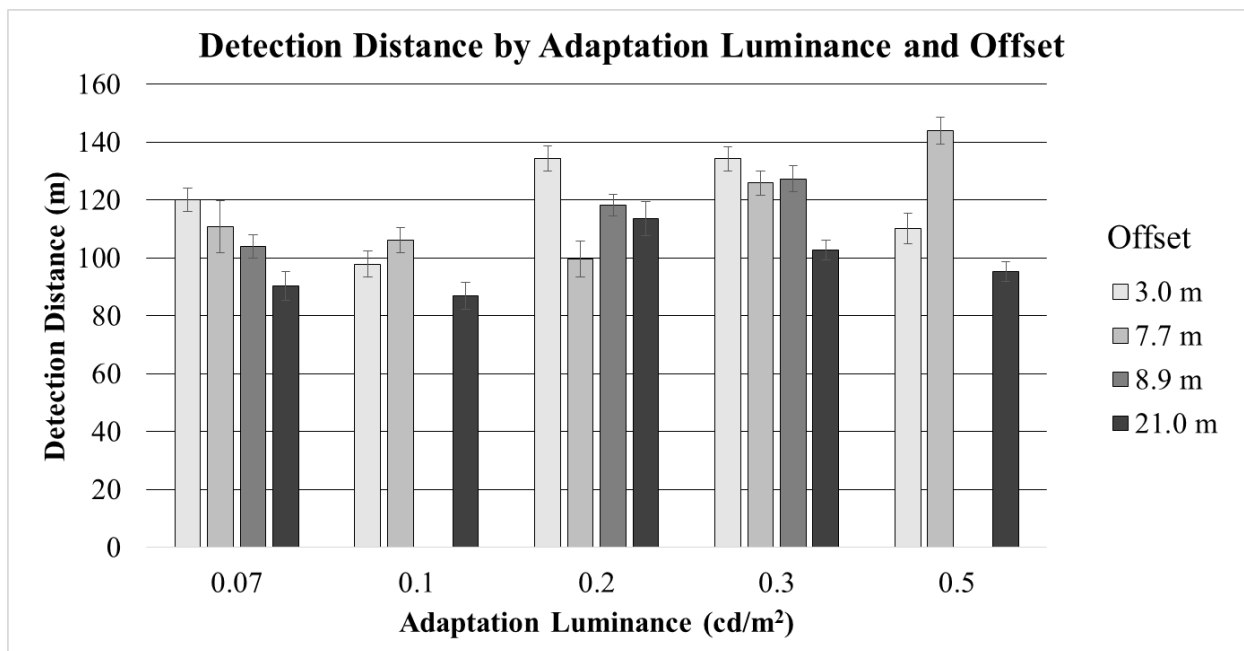
The MPI system configuration did not significantly affect detection distance but did significantly affect the percent of detections, as tested with a Fisher’s Exact Test. The probability that MPI-off resulted in significantly more misses than MPI-on was significant. With the MPI system on, drivers either missed or did not detect 24 percent of the pedestrians. With the MPI system off, drivers missed 38 percent of pedestrians.

Two-Way Interactions

There were a number of significant and marginally significant two-way effects on detection distance and percent of missed detections.

Offset and Adaptation Luminance

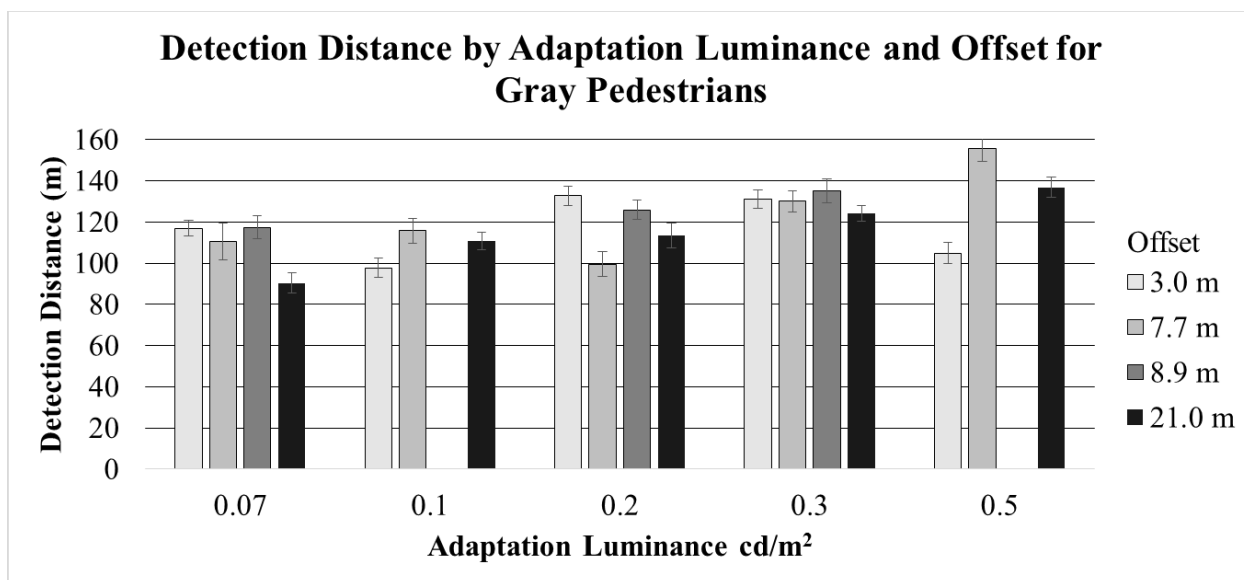
For all pedestrian clothing colors, the combination of adaptation luminance and offset affected detection distance (figure 132). At an adaptation luminance of 0.07 cd/m² (0.020 fL), detection distances decreased with increasing offset. This is expected, given that visual acuity decreases as eccentricity increases, and if drivers’ eyes were focused on the roadway, higher offset would correspond to higher eccentricity. At higher adaptation luminance levels, however, the relationship between offset and detection distance changed; detection distance decreased with increasing offset, but the trend was less clear and more general. A similar trend was seen for only gray-clothed pedestrians, as shown in figure 133.



1 cd/m² = 0.3 fL

1 m = 3.3 ft

Figure 132. Chart. Final performance experiment—detection distance by adaptation luminance and offset for all clothing colors.



1 cd/m² = 0.3 fL

1 m = 3.3 ft

Figure 133. Chart. Final performance experiment—detection distance by adaptation luminance and offset for gray-clothed pedestrians only.

Offset and Age

The number of missed detections at each location indicated that there was a much greater probability for missed detections at 21 m (69 ft) offset than at the other offset distances (figure 134). The effect was greater for older participants, who missed 61 percent of pedestrians at 21.0 m (69 ft) offset, than it was for younger participants, who missed 29 percent of pedestrians at 21.0 m (69 ft) offset (Fisher's Exact Test, $p \leq 0.0001$).

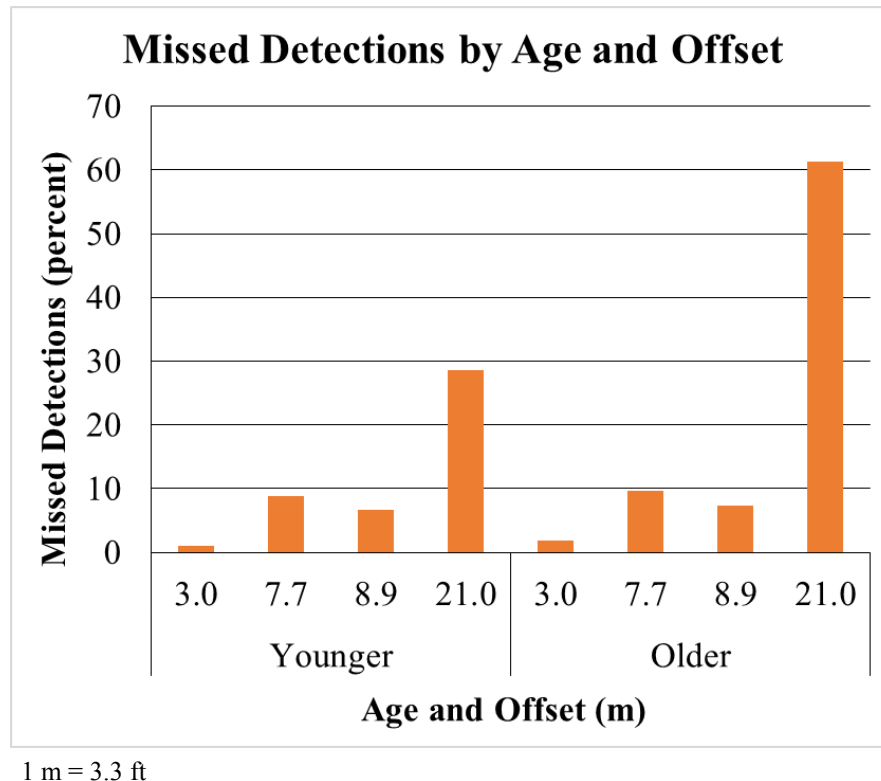
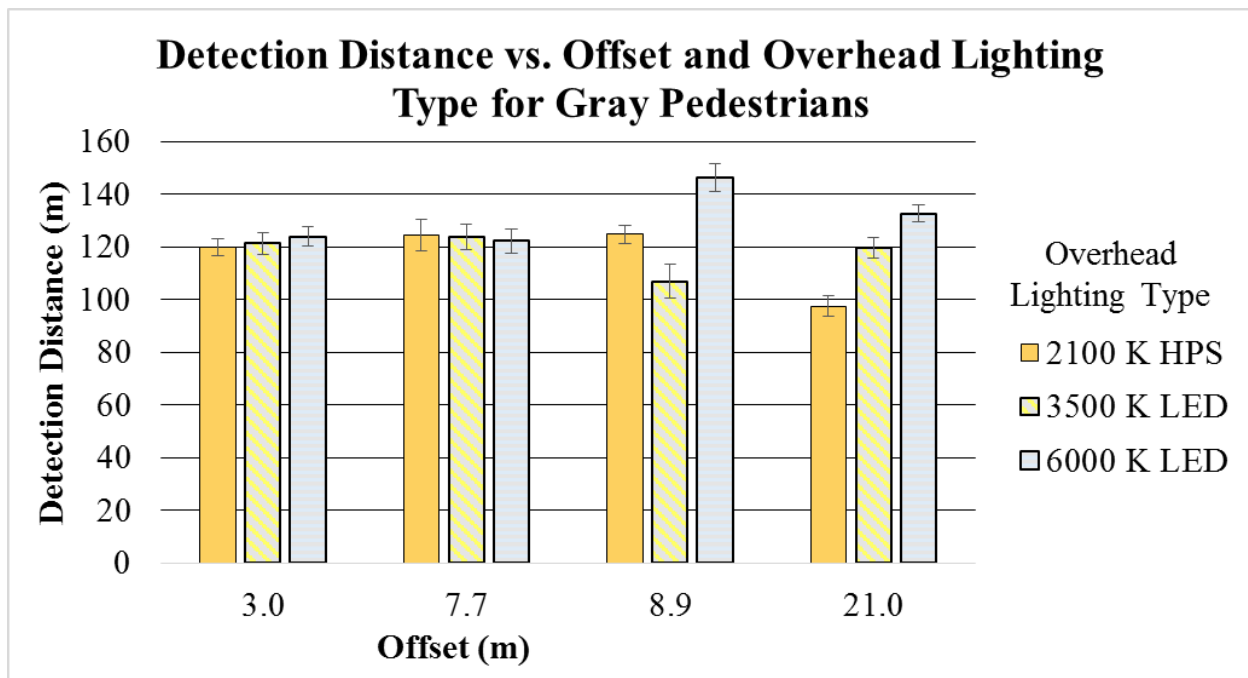


Figure 134. Chart. Final performance experiment—missed detections by age and offset.

Offset and Overhead Lighting Type

For gray-clothed pedestrians, the interaction effect between offset and overhead-lighting type was not significant; however, there were differences in detection distances among the overhead-lighting types that depended on offset. At 3.0 and 7.7 m (9.8 and 25 ft) offset, the overhead-lighting types had similar detection distances. At 8.9 and 21.0 m (29 and 69 ft) offset, the 6,000-K LED lighting had greater detection distances, possibly because the 6,000-K LED lighting's spectral distribution is more efficient in the mesopic range, and mesopic effects are only seen in the periphery. At 21.0 m (69 ft) offset, the lighting types' detection distances increased with increasing color temperature. The results are illustrated in figure 135.



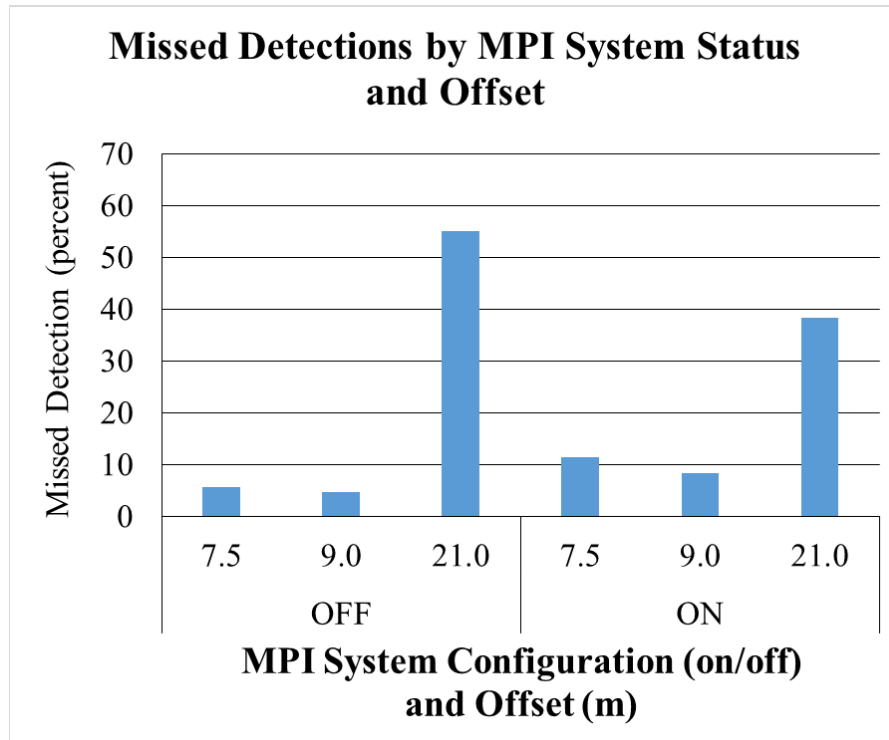
1 m = 3.3 ft

Figure 135. Chart. Final performance experiment—detection distance by offset and overhead-lighting type for gray-clothed pedestrians.

Offset and MPI System Configuration

Offset and MPI system did not have an interaction effect on detection distance but did have an interaction effect on missed detections. The MPI system was not used for pedestrians at the 3.0 m (9.8 ft) offset. When detection rates were analyzed without the 3.0 m (9.8 ft) offset data, it was found that when the MPI system was on, participants missed the pedestrians at 7.7 and 8.9 m (25 and 29 ft) offsets more than when it was off (figure 136). Conversely, for the pedestrians at 21.0 m (69 ft) offset, participants missed more pedestrians with the MPI system off than with it on (Fisher’s Exact Test, $p \leq 0.0001$).

Similarly to its main effect, the MPI system’s on or off status did not affect detection distance but did affect detection rate; however, it did so differently for different offsets. It was most beneficial in increasing detection rates for the pedestrian at 21.0 m (69 ft) offset. It could have had a slight negative effect on detection rates for the pedestrians at 7.7 and 8.8 m (25 and 29 ft) offsets because the MPI system swiveling beam could have caused an extreme change in contrast. At the 7.7 m (25 ft) offset, missed detections were significantly greater with the MPI system on than off (Fisher’s Exact Test, $p = 0.0226$). At the 8.9 m (29 ft) offset, the difference was not significant.

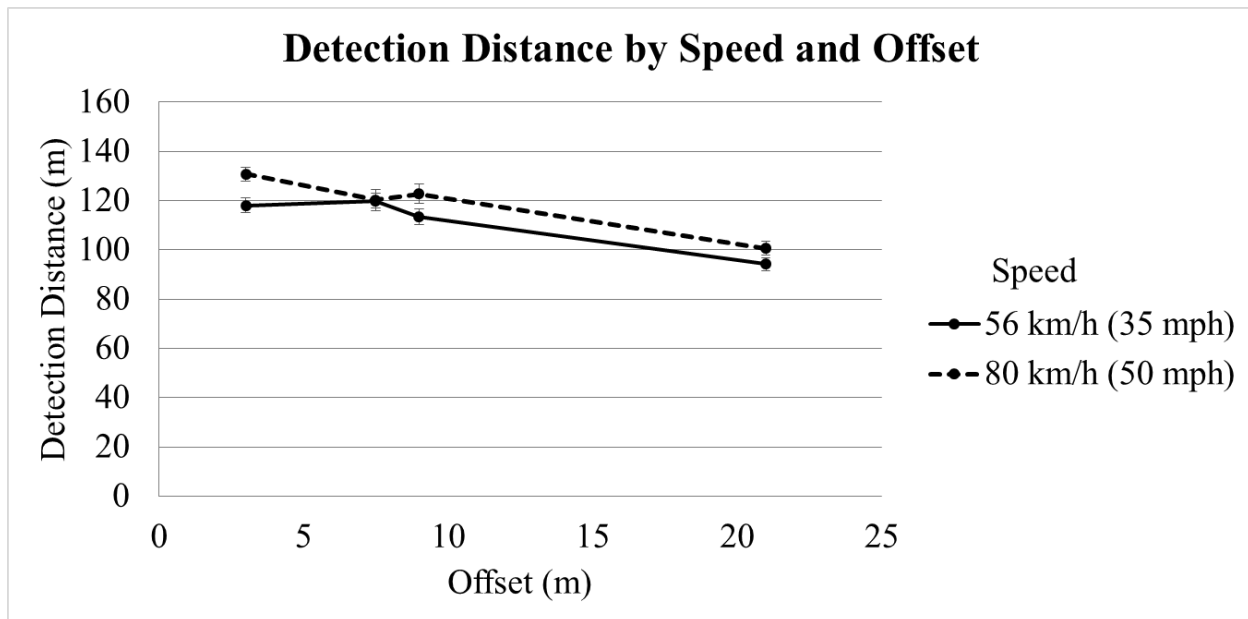


1 m = 3.3 ft

Figure 136. Chart. Final performance experiment—missed detections by MPI system configuration and offset.

Offset and Speed

For all clothing colors, participants driving 80 km/h (50 mi/h) detected the pedestrians from slightly farther away ($M = 111$ m (364 ft)) than those driving 56 km/h (35 mi/h) ($M = 119$ m (390 ft)), but the main effect was not significant. However, a two-way interaction between speed and offset found that detection distances were longer for higher speeds at 3.0, 8.9, and 21.0 m (9.8, 29, and 69 ft) offsets but not at the 7.7 m (25 ft) offset (figure 137).

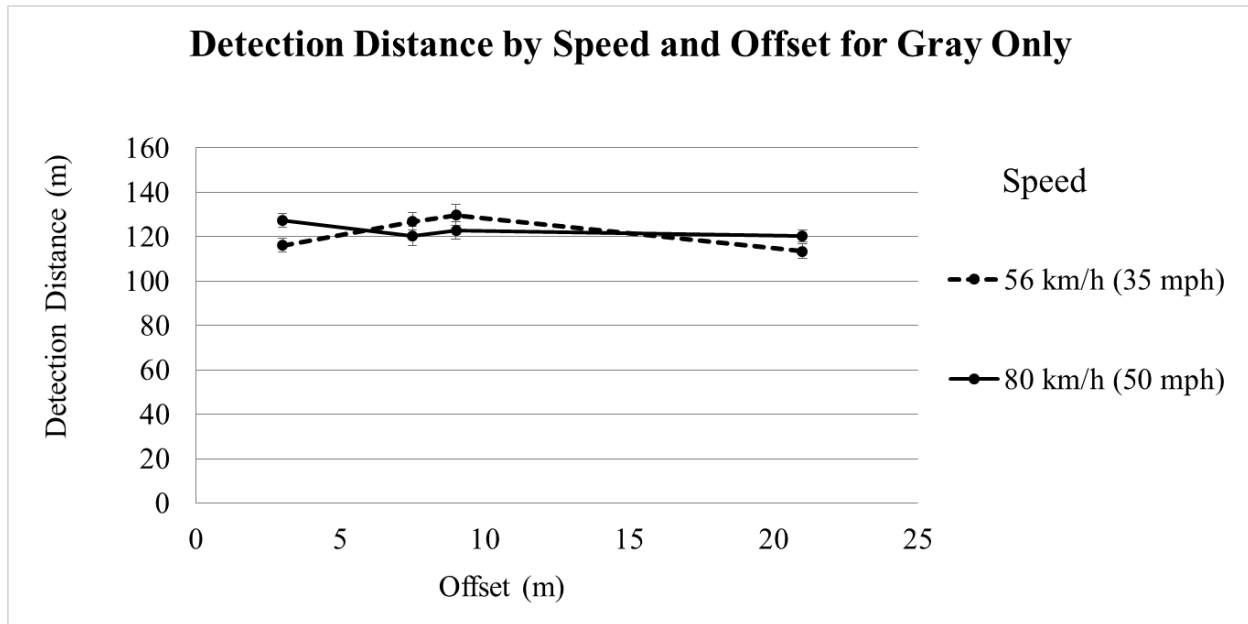


1 m = 3.3 ft
1 km/h = 0.62 mi/h

Figure 137. Graph. Final performance experiment—detection distance by speed and offset for all clothing colors.

Some explanations for these results could stem from roadway design, driving speed, and scanning behavior. At faster speeds, drivers are likely more vigilant and might have different scanning behavior. Drivers at higher speeds might be more vigilant, scanning might be restricted to within a few degrees of the roadway on the left but cover a broader angle on the right, or rely more on periphery. Therefore, at higher speeds, more-vigilant drivers would detect pedestrians from farther away within their scanning region. The pedestrians at 7.7 m (25 ft) offset, corresponding to 5 degrees, were only on the left side of the road, and the location of the vehicle A pillar might have hindered scanning patterns and limited detection distances at that visual angle for both speeds.

A similar effect was seen when only data for gray-clad pedestrians were analyzed. Detection distances were longer for higher speeds at 3.0 and 21.0 m (9.8 and 69 ft) offsets (2 and 14 degrees at 83 m (277 ft)), but detection distances were shorter for higher speeds at 7.7 and 8.9 m (25 and 29 ft) offsets (5 and 6 degrees at 83 m (277 ft)) (figure 138).

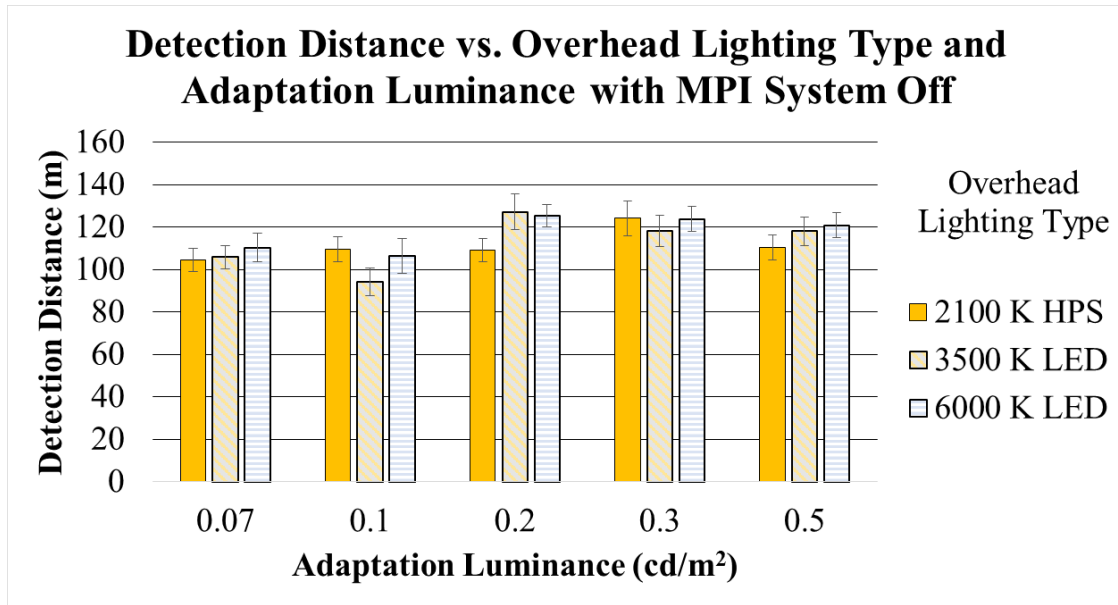


1 m = 3.3 ft
1 km/h = 0.62 mi/h

Figure 138. Graph. Final performance experiment—detection distance by speed and offset for gray only.

Overhead Lighting Type and Adaptation Luminance

To isolate the effects of overhead lighting and adaptation luminance, figure 139 shows their combined effect on detection distance in cases when the MPI system was off. Figure 135 shows that overhead lighting with a higher CCT and with an SPD more efficient in the mesopic range had longer detection distances but only for larger eccentricities, where mesopic effects are expected. One would also expect higher adaptation luminances to correlate with longer detection distances for large-object detection because the general environment is brighter. However, that effect was only seen for the LED lighting; at adaptation luminances of 0.07 and 0.1 cd/m^2 (0.020 and 0.03 fL), detection distances for the LED lighting types were shorter than for adaption luminances of 0.2 cd/m^2 (0.06 fL) and higher. There may exist a threshold adaptation luminance, above which brighter lighting does not significantly increase the visibility of large objects such as pedestrians, thus creating a limited return to additional lighting. The interaction of adaptation luminance and color might also explain the difference because overhead-lighting type and adaptation luminance did not significantly affect detection distances for gray-clothed pedestrians.



1 cd/m² = 0.3 fL
 1 m = 3.3 ft

Figure 139. Chart. Final performance experiment—detection distance by adaptation luminance and overhead-lighting type with the MPI system off.

Contrast and Detection Distance

Weber contrast was calculated from luminance measurements taken 83 m (277 ft) along the road from the pedestrian positions. An ANCOVA was performed using contrast as a covariate. Contrast and detection-distance data were only analyzed for gray pedestrians because only luminance contrast, not color contrast, was measured. The ANCOVA was only performed for detection distance. The results are listed in table 42.

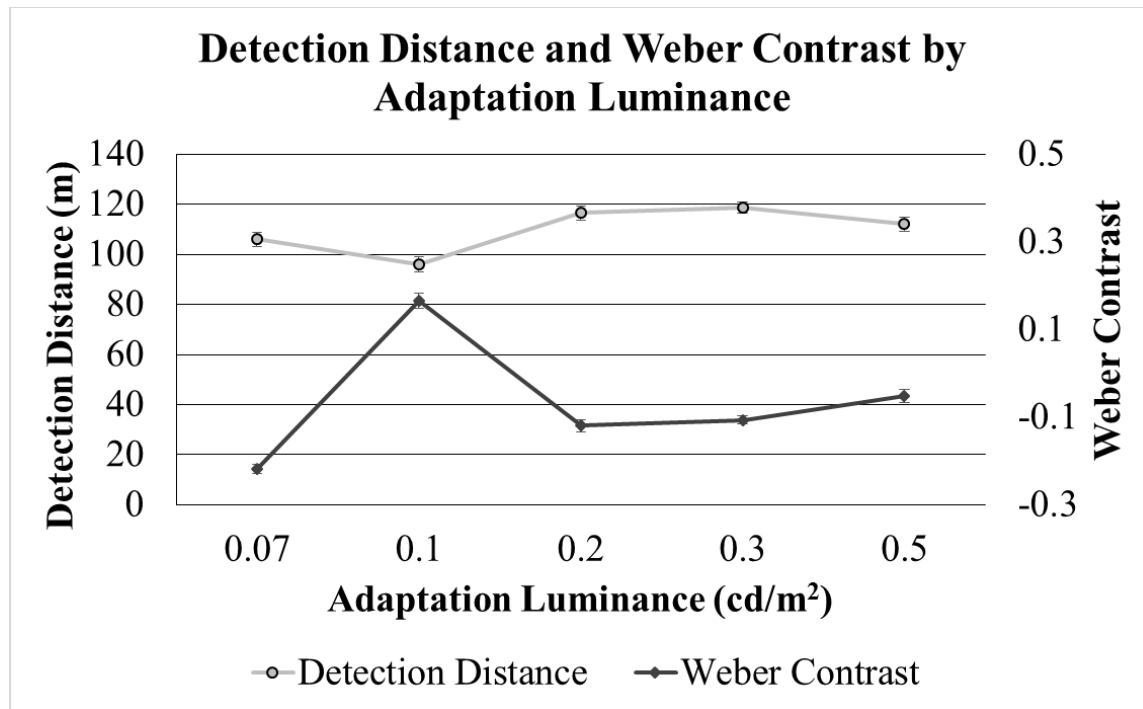
Table 42. Final performance experiment results for Weber contrast and detection distance for gray pedestrians only.

Factor(s)	Detection Distance <i>F</i>	Detection Distance <i>p</i>
Adaptation Luminance	8.46	< 0.0001 ^a
Offset	1.88	0.1393
Overhead-Lighting Type	1.61	0.2142
MPI System Configuration	0.04	0.8386
Speed	0.69	0.4136
Offset by Adaptation Luminance	6.57	< 0.0001 ^a
Offset by Overhead-Lighting Type	1.49	0.1909
Offset by MPI System Configuration	1.45	0.2413
Overhead-Lighting Type by Adaptation Luminance	0.39	0.9256
Overhead-Lighting Type by MPI System Configuration	0.43	0.655
MPI System Configuration by Adaptation Luminance	0.28	0.8897
Age by MPI System Configuration by Adaptation Luminance	0.92	0.4546
Offset by Overhead-Lighting Type by Adaptation Luminance	1.23	0.2313
Offset by Overhead-Lighting Type by MPI System Configuration	0.74	0.5677
Offset by MPI System Configuration by Adaptation Luminance	0.97	0.4463
Overhead-Lighting Type by MPI System Configuration by Adaptation Luminance	0.98	0.4582

^aSignificant at $p < 0.05$.

Adaptation Luminance

The detection distance at 0.1 cd/m² (0.03 fL) was lower than at the other adaptation luminance levels, and the Weber contrast results could explain why. At 0.1 cd/m² (0.03 fL), the pedestrian was seen in positive contrast, but at all the other adaptation luminance levels, the contrast was negative, as illustrated in figure 140. At some point, when the vehicle approached the pedestrian, the pedestrian contrast passed from negative to positive. Detection is much more difficult as contrast passes through zero, causing longer detection distances.

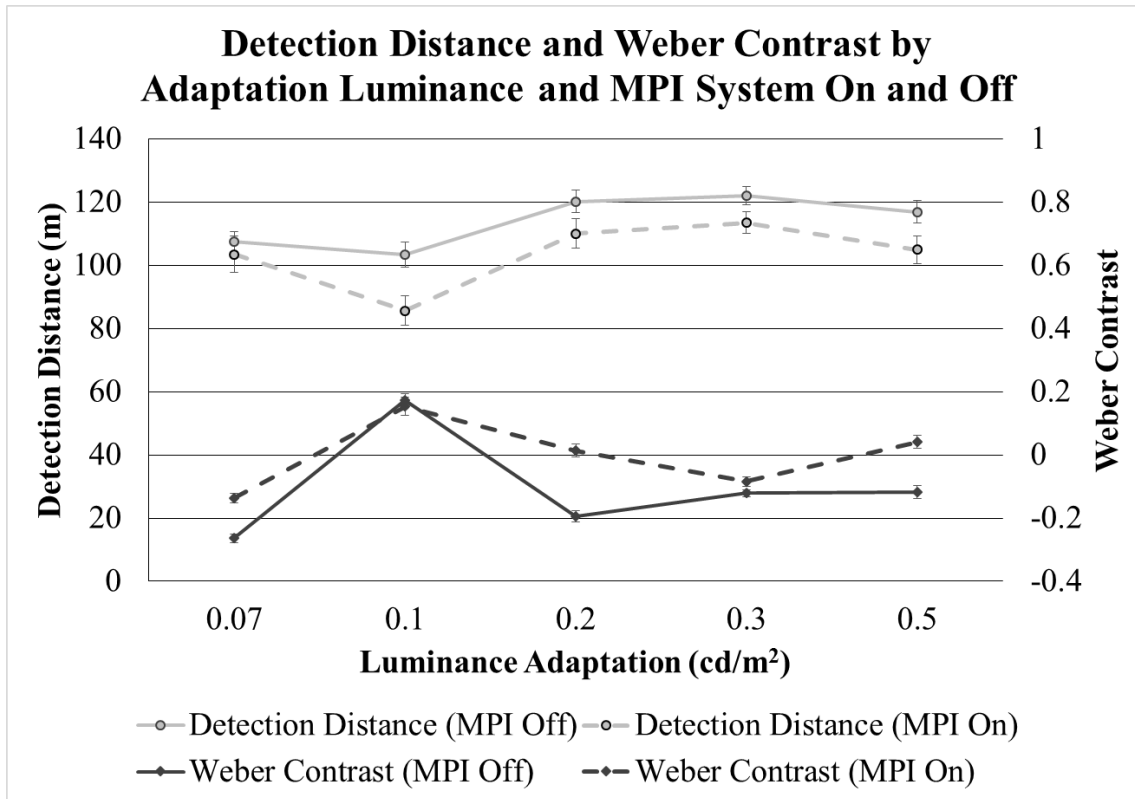


1 cd/m² = 0.3 fL
 1 m = 3.3 ft

Figure 140. Graph. Final performance experiment—detection distance and Weber contrast by adaptation luminance.

MPI and Adaptation Luminance

When the MPI system was on, detection distances were shorter, albeit not statistically significantly. That effect was greatest at 0.1 cd/m² (0.03 fL). At most adaptation luminance levels, the MPI-on condition caused the Weber contrast to be closer to zero because the headlamps illuminated the pedestrian, bringing him or her closer to positive contrast, as shown in figure 141. Thus, while the MPI system illuminated the pedestrian, it also decreased contrast, making detection more difficult. The MPI system could have also distracted the participant, negatively affecting detection distances.



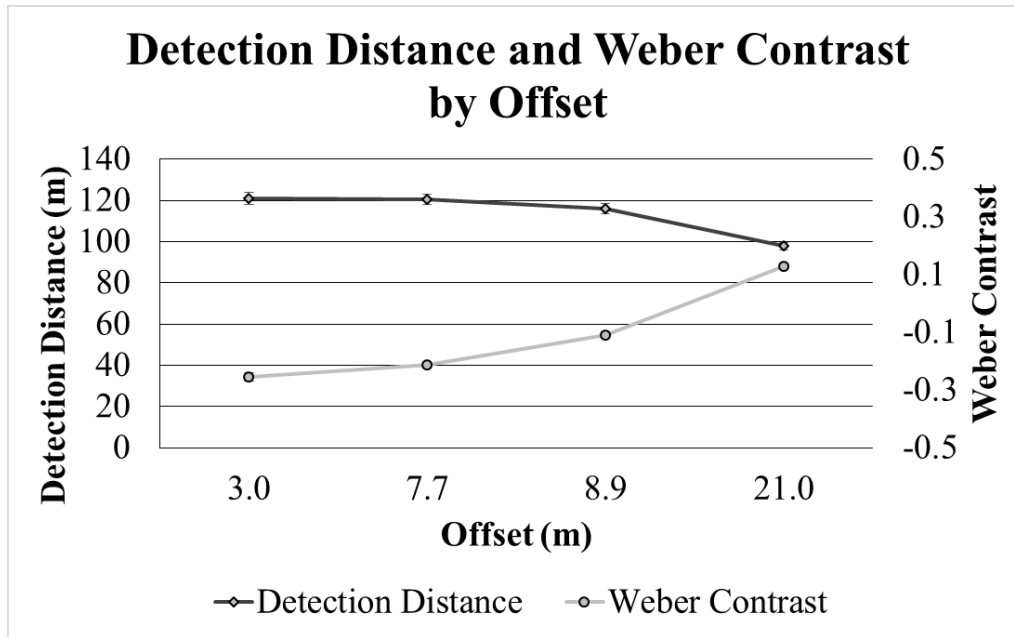
1 cd/m² = 0.3 fL
1 m = 3.3 ft

Figure 141. Graph. Detection distance and Weber contrast by adaptation luminance for MPI system on and off.

Offset

As offset increased, contrast approached zero and detection distance decreased (figure 142). There was a sharp increase in contrast, and contrast passed through 0, 8.9, and 21.0 m (29 and 69 ft) offsets. There was also a sharp decrease in detection distance between 8.9 and 21.0 (29 and 69 ft) offsets. Contrast polarity factor (C_{FP}), described by Adrian, states that objects in negative contrast are easier to detect than those in positive contrast.⁽⁵⁴⁾ In this experiment, the contrast at the 21.0 m (69 ft) offset was positive, but at the other offsets, the contrast was negative. That could help explain why detection distances were so much shorter at the 21.0 m (69 ft) offset than at the other offsets, even though the contrast at 21.0 m (69 ft) offset was close to 0.1.

Probability summation, or the probability of detecting an object with both eyes, cannot be factored into the visibility of the targets at the various offsets because of this study's lack of control over the participants' eye gaze behavior, and offsets did not necessarily correspond to eccentricity.



1 m = 3.3 ft

Figure 142. Graph. Final performance experiment—detection distance and Weber contrast by offset.

DISCUSSION

The main purpose of this experiment was to further evaluate the variables of interest identified in previous experiments in this project.

One of the outcomes of the scoping experiment was that more information was needed on the effect of overhead-lighting type and level on peripheral visibility, and a project objective was to address the effect of the SPD of overhead lighting on driver visual performance. The mesopic modeling experiment found that the spectral distribution of overhead lighting affected detection distances but only at higher eccentricities. This experiment attempted to extend the investigation to determine the effects of overhead lighting's SPD on visibility while driving.

The final performance experiment found no significant differences in detection and color-recognition distances between overhead-lighting types at any offset, although results showed a trend toward longer detection distances with 6,000-K LED lighting at greater offsets. The results do not strongly support a spectral effect of overhead lighting on mesopic visibility in the periphery. That result, different from the one in the mesopic modeling experiment where eccentricity was fixed, means that drivers depended on glance patterns to scan their driving environment and detect peripheral objects. Therefore, they likely detected objects in the fovea, where mesopic effects do not occur.

MPI

Evaluating the performance of drivers when using a peripheral illumination system was a project objective. This experiment found that the MPI system configuration did not significantly affect

detection distance. This is consistent with findings from the spectral interaction experiment, where the headlamp's effect on visibility was much less than that of the overhead-lighting level. In the final performance experiment, most detection occurred at distances greater than the 75 to 90 m (246 to 295 ft) window where the headlamps first illuminated the pedestrian. Therefore, in most cases, the MPI system highlighted the off-axis pedestrians after participants had detected them.

The MPI system configuration did significantly affect the probability that a pedestrian was detected, but the results varied among offsets. For the pedestrian at 21.0 m (69 ft) offset, the MPI system significantly increased detection rates. For the pedestrians at 7.7 and 8.9 m (25 and 29 ft) offsets, the MPI system slightly decreased detection rates. Congruent with the results of the spectral interaction experiment, at the 21.0 m (25 ft) offset location, luminance from overhead lighting was low, and headlamps were the primary light sources driving detection. At the 7.7 and 8.9 m (25 and 29 ft) offset locations, the pedestrians were largely illuminated by overhead lighting and were in negative contrast. When the headlamp light struck them, it reduced their contrast until they shifted into positive contrast. Near-zero contrast conditions reduced visibility and detection distances.

Because the MPI system only increased the detection rate for pedestrians farthest from the roadway, it is important to consider how far an object is from the roadway to evaluate its potential as a hazard. The pedestrian at the highest offset was 21.0 m (69 ft) to the right of the test vehicle (figure 128). If the pedestrian is traveling directly toward the road, and the vehicle is traveling at 80.4 km/h (50 mi/h) and 83 m (272 ft) from the point where the pedestrian would intersect the road, the pedestrian would have to be moving 20.3 km/h (12.6 mi/h) for it to intersect the vehicle and cause a collision. Large animals native to North America, such as deer and black bear, can easily achieve that speed, as can some runners and cyclists.^(98,99)

The MPI system might be distracting to drivers. Results of the MPI system performance experiment indicated the MPI system illuminating an area of road with no pedestrian interfered with drivers detecting pedestrians on the opposite side of the road. This research has shown that when overhead lighting is in place, the MPI system does not significantly alter detection distances, but it did increase the probability of detection, especially at high eccentricity angles. Further research should explore these limits. In addition, driver behavior associated with false positives and other potential errors the system should be further investigated.

Age

Age did not significantly affect detection or color-recognition distances for this group of participants, who were all experienced drivers and comfortable with nighttime driving. The difference in detection distances between the younger and older groups, however, was effectively different at 22 m (72 ft), the difference in safe stopping distances for vehicles traveling 50 and 60 km/h (31 and 37 mi/h). Other studies reported in chapter 2 found diminishing visual acuity with age, but peripheral contrast sensitivity diminishes with age more slowly than foveal contrast sensitivity.⁽⁹⁵⁾ If participants initially detected the pedestrians using peripheral vision, that could explain the lack of age effects, similar to the lack of age effects in the mesopic modeling experiment, which ensured peripheral detection.

Color

Gray-clad pedestrians were often detected from farther away than red- or blue-clad pedestrians. Color-recognition distances for the red- and gray-clad pedestrians were longer than for the blue-clad pedestrians. The experimental design, and the fact that color contrast was not measured, meant that it was difficult to determine why those results occurred.

Adaptation Luminance

Although this experiment did not specifically evaluate mesopic models in a driving environment—a project objective—it did address visual performance in the mesopic range. The detection differences among the adaptation luminance levels were in line with Adrian's model.⁽⁵⁴⁾ As adaptation luminance changed, so did contrast threshold. Comparing VL to Weber contrast (figure 143) showed that as adaptation luminance increased, contrast decreased and VL increased. This is because higher adaptation luminances require higher threshold contrasts for object detection.

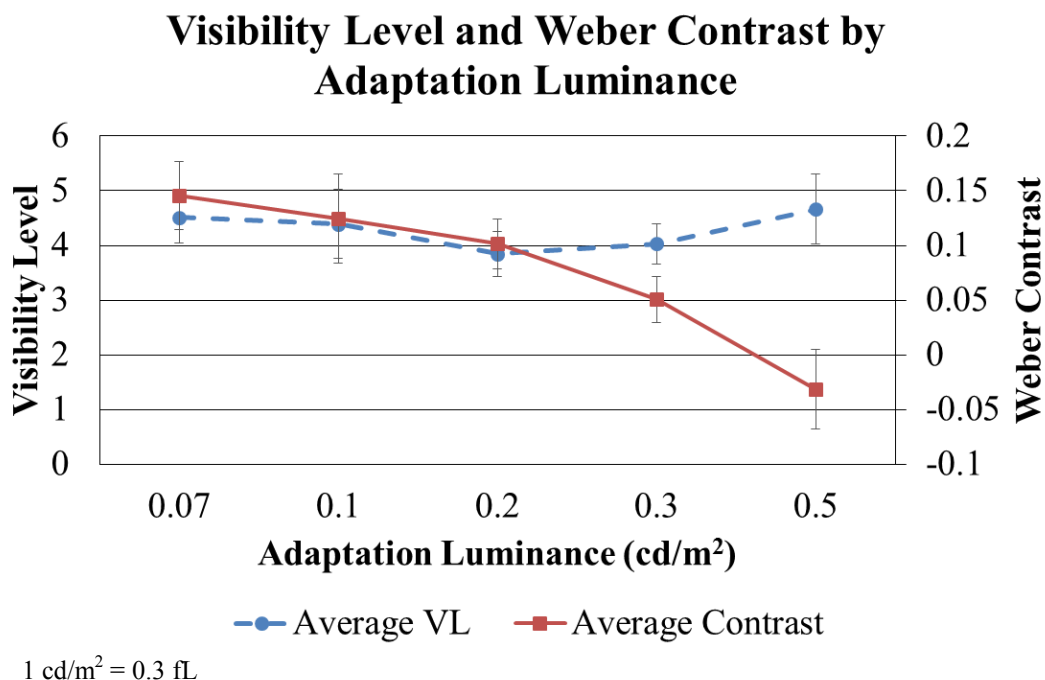


Figure 143. Graph. Final performance experiment—VL and Weber contrast by adaptation luminance.

At the lowest adaptation luminance level, 0.07 cd/m^2 (0.020 fL) and at 14 degrees (corresponding to a 21.0 m (69 ft) offset at 83 m (277 ft) distant), light levels approached the lower end of mesopic vision. The eye is more adapted to darkness and more contrast-sensitive in those conditions, possibly causing the longer detection distances than those at 0.1 cd/m^2 (0.03 fL), where vision is more mesopic.

In general, visual performance depended more on adaptation luminance than on overhead-lighting type. At higher adaptation luminances and closer to the photopic region, overhead-

lighting type had even less effect on visual performance. At the lowest adaptation luminance, detection was only about 10 m (30.5 ft) shorter than at higher adaptation levels, likely because a dark-adapted eye is more contrast sensitive. The fact that detection distances were longer at the larger visual angles, where both pedestrians and background were darker, supports that conclusion. The 0.1 cd/m² (0.03 fL) adaptation luminance showed the shortest detection distances and was the only adaptation luminance level where the target had positive contrast. The contrast of that adaptation level probably passed through zero as the vehicle approached the pedestrian, reducing the pedestrian's visibility.

Offset

There was no difference in detection or color-recognition distances among the different lighting types for the pedestrians stationed closest to the roadway. For pedestrians at 21.0 m (69 ft) offset, the two LED lighting types had longer detection distances than HPS lighting, because the LED lighting had a greater S/P ratio and better SPD in the mesopic range. That result might have occurred only at 21.0 m (69 ft) offset (corresponding to 14-degree eccentricity at 83 m (277 ft) away) because the maximum rod density is at 15 degrees and is where a mesopic effect would most likely occur.⁽¹⁰⁰⁾ However, without restricting the participants' eye-glance behavior, it is difficult to determine whether detection occurred in the fovea or periphery.

Speed

Speed interacted with visual angle to significantly affect detection distance, with detections longer for 3.0, 8.9, and 21.0 m (9.8, 29, and 69 ft) offsets but not the 7.7 m (25 ft) offset, when the participant was driving faster. This could be because driver scanning behavior is broader when driving slower and more vigilantly and narrower when focused down the road and driving faster. At faster speeds, drivers might also focus more on the roadway and rely more on peripheral cues for object detection on the shoulder.

CONCLUSIONS

The four objectives of this project—and of the final performance experiment—were to evaluate the following: (1) impact of the spectra of overhead lighting systems on driver visual performance; (2) interaction of vehicle headlamps and overhead lighting in terms of object visibility; (3) applicability of mesopic models and scaling factors in a roadway lighting design; and (4) impact of a peripheral illumination system on driver visual performance.

First, the impact of spectra of overhead-lighting systems on off-axis visibility was minimal because changes in lighting type did not affect visibility or color recognition significantly. The results of the mesopic modeling experiment indicated significant differences in the overhead-lighting systems were found in the static but not in the dynamic portions of the experiment. The results of this experiment indicate the same is true for pedestrian visibility as it was for targets.

Second, peripheral models were found to be not effective in predicting visual behavior in a driving environment. The inability to control where drivers are looking and what they are attending to at any given moment during a driving task, makes predicting visibility of any roadway object difficult, especially those in low contrast.

Third, this experiment found that the MPI system provides a benefit for off-axis visibility in terms of whether pedestrians are detected or not detected, but the system does not provide a clear benefit of detection distance and may be considered a distraction from the forward roadway.

Other findings were that object size, ambient lighting level, and contrast affected the visibility of gray-clad pedestrians and gray targets in this experiment. The larger an object, the more visible it is, as shown by the VL calculations; pedestrians had higher VLs than targets. Also, the ambient lighting level affects the eye's adaptation, which in turn affects contrast sensitivity. Findings related to contrast polarity and ambient luminance were that high ambient luminance can make a positively contrasting object difficult to see, and low ambient luminance can make a negatively contrasting object difficult to see. An object with very low contrast will be difficult to see regardless of object size and adaptation level; however, that poor visibility can be mitigated by adjusting object size and adaptation luminance. In addition, a target in negative contrast becomes briefly invisible as it transitions to positive contrast when it starts to be illuminated by headlamps. The effects of higher adaptation levels to brighter environments are particularly noticeable at night with low-contrast objects. Findings related to detail recognition were that orientation recognition typically occurred only within 30 m (100 ft) of the object, requiring the driver to drive slower than 24 km/h (15 mi/h) to be able to stop in time to avoid colliding with the object. Distant objects were more visible without headlamps than with headlamps, likely because the headlamp light caused the eye to adapt to the brighter environment.

CHAPTER 9. SUMMARY

This project is a comprehensive review of the applicability of mesopic functions to roadway applications. While the model to determine the impact of mesopic adaptation to visual performance has been well-established and verified, both in the laboratory and in some very carefully prescribed experiments, the real-world applicability of the model has remained in question. Determining the impact of mesopic lighting on high-speed roadways was the focus of this effort. In addition, an MPI system for highlighting pedestrians was developed and tested. The MPI system's effect on visibility may have also been affected by the overhead-lighting source's SPD and level; pedestrians on the roadside might be detected in the periphery, where mesopic effects occur.

This project was developed as a stepwise approach to these problems. The first two steps were to develop a scoping experiment that defined the nature of the effect of the spectral distribution of overhead lighting on visibility and to provide guidance for the development of the subsequent experiments. The primary outcomes from this scoping experiment were that both the type and level of overhead lighting significantly affected the detection and recognition of objects on the roadway. This was also evident for objects that were off of the roadway. One of the primary determinants for detection was the color of pedestrian clothing and targets in the roadway, thus indicating that color contrast is a significant component of object detection. The results also indicated that roadway lighting uniformity has an important role in object detection. The final aspect was that of headlamp color and intensity. In scenarios when overhead lighting was used, headlamp configuration did not affect visibility.

These results drove the direction of the next two experiments. The first was an investigation of conditions when headlamps have an impact on object detection and when they do not have an impact. The second was an investigation of the applicability of the mesopic model to roadway lighting.

Before these experiments were performed, however, an investigation of the applicability of an MPI system was conducted. Although the scoping experiment showed a minimal spectral effect of the headlamp color on detection distance, two headlamp colors were used to further explore this relationship. A mock-up MPI system was created with servo-activated headlamps that either tracked the pedestrians as the vehicle approached or highlighted them for a short time as the vehicle approached. The results of this experiment were that use of the MPI system resulted in both shorter detection distances and an increase in detection rate. Headlamp color did not seem to have a significant impact on detection. When the MPI system highlighted an area across from a pedestrian, participants' detection rates and distances for that pedestrian were lower. This highlights the importance of careful design in a full-featured MPI system; participants' behavior indicated that they expected it to work properly, so it must not produce false positives, which could distract drivers from actual roadside hazards.

The next experiment was an investigation of the interaction of vehicle headlamps and overhead lighting on roadway-object detection. Small targets and a pedestrian were located in specific locations along the roadway that created high- and low-visibility conditions. The overhead lighting was then dimmed and headlamps turned off and on while participant drivers tried to detect the objects. Results indicated that the impact of the headlamps varied by object size. For

most lighting levels, the overhead lighting was the dominant force driving object detection, but that was not the case when the overhead lighting was at the lowest levels. The results of the experiment show that when a vehicle approaches a negatively contrasted target and the vehicle's headlamps begin to illuminate that target, the target contrast passes from negative to positive contrast and, importantly, through a point of invisibility—zero contrast—during that transition. Therefore, it is desirable for roadside objects to be positively contrasted at all times. The results also show that headlamps affect pedestrian luminance up to 91.4 m (300 ft) away. Headlamps were the driving factor for orientation-recognition distances, the direction the object was facing. The applicability of these results are critical for roadway lighting design. Headlamps dominate object recognition and also drive adaptation luminance. Therefore, the effect of the SPD of the roadway lighting may be overridden by the headlamps' effect on adaptation level and the contribution of headlamp illumination to object luminance.

The other experiment resulting from the scoping experiment considered the mesopic model. Here both static and dynamic target detection experiments allowed the research team to evaluate the mesopic model in the field. The static portion of the experiment was performed by determining the threshold contrast for small targets, and the dynamic portion examined target detection from a moving vehicle. In both cases the drivers were instructed to fix their gaze on the roadway, with the targets located at a number of peripheral angles. Gray targets were used to minimize the contribution of color contrast on object detection. The results indicate that overhead-lighting level significantly affected object detection; higher adaptation levels resulted in a lower threshold contrast. The results also showed that in the dynamic experiment, higher speeds typically resulted in longer detection distances. In terms of the mesopic model, for white overhead-lighting sources, the experimental results corresponded well to the model; however, for HPS lighting, they did not. An issue with the mesopic model could be that it does not include a term for eccentricity that accounts for different retinal sensitivities at different angles. The main conclusion was that although the mesopic model predicted some of the results at lower lighting levels, it also has limitations.

The final experiment performed did not attempt to limit driver eye glances or fix eccentricities at detection. This experiment included an MPI system, overhead lighting, two speeds, and pedestrian detection at different offsets from the roadway. The results indicate that for pedestrians close to the roadway, there was no impact of overhead lighting's spectral distribution on detection distance. For those pedestrians, adaptation luminance was the most influential factor on visibility. For pedestrians farther from the roadway, spectral effects were more significant, but those results might not be applicable to roadway lighting design, because objects that far away would have to be moving fairly quickly and on a collision path with the vehicle to become a hazard. The MPI performance results were similar to those of the initial MPI experiment. The MPI reduced detection distances and increased detection rates for objects in the periphery. The results of this experiment show that in a natural driving environment at the speeds tested, there is limited applicability of the mesopic model to lighting design. It is likely that drivers scan the roadway and detect objects in the fovea, where mesopic effects are not seen. Headlamps might also cause a high adaptation luminance, further limiting the applicability of the mesopic model to lighting design for nighttime driving.

CHAPTER 10. CONCLUSIONS AND FUTURE CONSIDERATIONS

CONCLUSIONS

Effect of Overhead-Lighting SPD on Driver Visual Performance

The primary result of this project shows that the SPD of overhead lighting affects object visibility but only in selected conditions. Adaptation luminance affected detection distance more so than light source type and correlated color temperature. Eccentricity affected the extent to which overhead-lighting spectrum affected detection distance; objects closer to the line of sight of the driver were less affected by source spectrum than objects farther from the line of sight. This may be a result of driver scanning behavior. For off-axis pedestrians, broad-spectrum overhead lighting had greater, albeit not statistically significant, color-recognition distances than HPS lighting. It is noteworthy that this result is related to the light sources used for the experiment, and this result may vary based on a different light source.

The contrast of the overhead lighting system appeared to affect pedestrian visibility. At the time of detection, pedestrians contrasted more against the background under HPS lighting than they did under the other light sources, likely because HPS lighting is less uniform and created bright lines across the roadway. This result may be related to the light source intensity distribution and the inefficiencies in lighting design with the HPS light source. Future experiments should investigate the effect of overhead lighting uniformity on object detection.

Combined Effect of Overhead Lighting and Headlamps on Driver Visual Performance

When only overhead lighting was used and headlamps were off, objects could be detected from farther away than with overhead lighting and headlamps on because adding vehicle headlamps increased the ambient luminance of the forward roadway, increasing adaptation luminance and decreasing contrast sensitivity. The result was that with headlamps, distant objects were more difficult to detect under the same overhead lighting levels. When only headlamps were used and overhead lighting was off, visibility was confined to the limits of the vehicle headlamps. Adding overhead lighting increased the probability of detecting objects off-axis or from distances beyond the reach of the vehicle's headlamps.

The combination of headlamps and overhead lighting appears to have its greatest impact when the two sources contribute nearly equal amounts of lighting. This requires the object to be within the area illuminated by the vehicle's headlamps, approximately 91 m (300 ft) for the vehicles used in this study. When headlamps and overhead lighting were combined, detail recognition increased because multiple sources of light illuminated the object from different angles.

The effects of visibility caused by the combination of headlamps and overhead lighting depend on ambient luminance and contrast. High ambient luminance causes objects in positive contrast to be more difficult to detect, and low ambient luminance causes negatively contrasted objects to be more difficult to detect. Also, the extent of ambient luminance's impact on visibility depends on the amount of luminance contrast between object and background; for example, concrete surfaces reflect more light than asphalt and result in a higher ambient luminance. These results highlighted the complex relationship between ambient luminance, contrast, and visibility. Future research should consider additional factors, such as the impact of headlamps and overhead

lighting on object visibility from different vehicle types, with and without oncoming vehicles, in different road profiles, and in twilight conditions.

Applicability of Mesopic Models to the Driving Environment

The CIE Recommended System for Mesopic Photometry accurately predicted the mesopic luminances and contrasts for both the LED light sources but not for HPS lighting. The change in the calculated difference to the predicted difference between the mesopic and the photopic luminances of HPS lighting and both LED overhead-lighting sources indicated that the calculated differences closely followed the predicted differences from 0.07 to 0.2 cd/m^2 (0.020 to 0.06 fL). Above that luminance value, the calculated differences leveled off while the predicted values continued to decrease. An ideal mesopic model should also have the eccentricity as an input to accurately calculate mesopic luminances.

Impact of MPI System on Driver Visual Performance

The MPI system did not improve the detection distance of off-axis pedestrians but did improve the rate at which they were detected. Also, participants detected pedestrians from the greatest distances when the MPI system was off. This was the case for sections of the road with and without overhead lighting. This could be because the MPI system's moving beam distracted the participants and prevented them from scanning normally. Lastly, participants seemed to assume the MPI system would accurately illuminate pedestrians. They detected the pedestrian about 70 to 80 percent of the time with the MPI system illuminating the pedestrian, compared with about 50 to 60 percent of the time with the MPI system illuminating the roadway opposite the pedestrian position rather than illuminating the pedestrian.

Additional Findings

Pedestrian clothing color and target color both significantly affected detection and color-recognition distances, whether or not overhead lighting was used.

Object size, ambient lighting level, and contrast affected the visibility of pedestrians and targets in this experiment. The larger an object, the more visible it was, as shown by the VL calculations; pedestrians had higher VLs than targets.

Speed appeared to affect driver attention and gaze patterns, and detection distances increased with speed. When the vehicle was traveling faster, it appeared that the driver focused more on the roadway ahead and glanced less to the side of the roadway.

Distant objects were more visible without headlamps than with headlamps, likely because the headlamp light caused the eye to adapt to the brighter environment. The pool of light in front of the driver made by the headlamps has an impact on the adaptation luminance of the driver. The other results of the experiment show that a higher adaptation luminance required a higher threshold contrast. Distant objects that typically have low contrast would be harder to detect with higher adaptation luminance from the headlamps.

CONSIDERATIONS

With overhead lighting systems and standard headlamps, the design of higher speed roads need not consider spectral effects because the gaze behavior of a driver cannot be controlled in a real-world driving situation.

Mesopic factors should be applied for low-speed roadways where lighting is designed to provide more benefit to pedestrians than drivers.

Significant effort in the detection and warning methods for the MPI system require significant effort and regulation. While the system shows promise, care must be taken to ensure that negative outcomes are not encountered.

FUTURE RESEARCH

The results of this project are limited by the conditions tested. These tests were for drivers in vehicles only. Additional testing to study the application of mesopic factors should be investigated for pedestrians and slower-moving roadway users.

The other aspect noted in these results is the applicability of the mesopic model in a variety of conditions with objects at various eccentricities to the roadway. The relationship of these results to the mesopic model shows that an eccentricity factor may apply to the model and should be investigated further.

CHAPTER 11. APPLICATION TO PRACTICE

The interpretation of these results is an important aspect of this project. As mentioned, the results of the experiments show that the impact of overhead lighting spectrum on driver visual performance is limited to specific situations. It is important to note that, in many situations, the broad-spectrum light source did not improve driver visual performance over the narrow-spectrum light source, but neither did it worsen driver visual performance. Other studies have shown benefits of the use of broad-spectrum light sources beyond providing better visual performance. In user preference studies, broad-spectrum light sources were preferred for their user comfort and acceptance.^(23,101) Other research has shown that broad-spectrum sources provide for better object contrast, thus increasing the detection of objects along the roadside. These results indicate that broad-spectrum lighting is a valid choice in general and likely a desirable choice for roadway lighting.

LED lighting is the optimal broad-spectrum source for roadway lighting. The benefits of LED lighting, in addition to those of other broad-spectrum sources, are significant. Typically LED installations use half the energy of that used by traditional HPS roadway lighting. Similarly, LED lighting can be controlled and dimmed in adaptive-lighting designs that actively correlate lighting levels to environmental demands, saving even more energy. These are compelling reasons to use LED lighting, which does not reduce driver visual performance. Other factors such as circadian impacts, sky glow, and glare should be considered but were outside of the scope of this project.

The final aspect to consider regarding broad-spectrum lighting is the application of mesopic scaling factors. A significant finding of this research is the non-applicability of these scaling factors, based on the spectral component of the light source, to roadway lighting design criteria. It is important, however, to highlight that the results of this project are consistent with the Illuminating Engineering Society (IES) RP-8-14 Recommended Practice.⁽⁵⁾ The IES position is that lighting levels can be scaled based on the light source spectrum if the lighting design is for a roadway with a posted speed limit of less than 40 km/h (25 mi/h). Scaling can be performed on roads in this category because the lighting system is primarily for the benefit of pedestrians, and vehicle headlamps provide adequate lighting for drivers. This project shows that there are no spectral effects of roadway lighting on driver visual performance. However, a pedestrian has a wider field of view, and there may be spectral effects of lighting on pedestrian visual performance.

REFERENCES

1. CIE. *Recommended System for Mesopic Photometry Based on Visual Performance*. 2010, CIE: Vienna, Austria.
2. Florida Atlantic University Astronomical Observatory. *Total Electricity Cost of Wasted Outdoor Lighting, United States—2012*. [cited 2015 7/23/2015]; available from http://physics.fau.edu/observatory/lightpol-econ.html#Total_US_Wasted_Lighting).
3. Society of Automotive Engineers. *SAE J1383-2010: Performance Requirements for Motor Vehicle Headlamps*. 2010, Washington, DC.
4. National Highway Traffic Safety Administration (NHTSA). *Federal Motor Vehicle Safety Standards and Regulations, Standard No. 108: Lamps, Reflective Devices, and Associated Equipment*. 1969, Washington, DC.
5. Illuminating Engineering Society of North America (IESNA). “RP-8-14,” *American National Standard Practice for Roadway Lighting*. American National Standards Institute (ANSI)/IESNA. 2014, New York, NY.
6. American Association of State Highway and Transportation Officials (AASHTO). *AASHTO Roadway Lighting Design Guide*, A.A.o.S.H.a.T. Officials, editors. 2005, Washington, DC.
7. Griffith, M.S. “Comparison of the Safety of Lighting Options on Urban Freeways,” *Public Roads*, 1994. 58(2): p. 8–15.
8. Janoff, M.S., Staplin, L.K., and Arens, J.B. “The Potential for Reduced Lighting on Roadways,” *Public Roads*, 1986. 50(2): p. 33–42.
9. ANSI/IESNA. “RP-8-00,” *American National Standard Practice for Roadway Lighting*. 2000, reaffirmed 2005, Washington, DC.
10. Box, P.C. “Major Road Accident Reduction by Illumination,” *Transportation Research Record 1247*. Transportation Research Board, National Research Council. 1989, Washington DC.
11. Ketron, Inc., and FHWA. *Reduced Lighting on Freeways During Periods of Low Traffic Density*. FHWA/RD-86/018 9308 8508. FHWA. 1985, Washington DC.
12. Green, E.R., Agent, K.R., Barrett, M.L., and Pigman, J.G. *Roadway Lighting and Driver Safety*. University of Kentucky. 2003, Lexington, KY.
13. Oya, H., Ando, K., and Kanoshima, H. “Research on the Interrelation Between Illuminance at Intersections and the Reduction in Traffic Accidents,” *The Lighting Journal*, 2003. 68(11): p. 14–15.

14. Box, P.C. "Relationship Between Illumination and Freeway Accidents, IERI Project 85-67," *Illuminating Engineering*, 1971. 66(5): p. 365–393.
15. Bruneau, J.-F., Morin, D., and Pouliot, M. "Safety of Motorway Lighting," *Transportation Research Record: Journal of the Transportation Research Board*, 2001. 1758: p. 1–5.
16. Gibbons, R.B., Guo, F., Medina, A., Terry, T., Du, J., Lutkevich, P., Corkum, D., and Vetere, P. *Guidelines for the Implementation of Reduced Lighting on Roadways*. FHWA-HRT-14-050. FHWA. 2014, Washington, DC.
17. Gibbons, R.B., Guo, F., Medina, A., Terry, T., Du, J., Lutkevich, P., and Li, Q. *Design Criteria for Adaptive Roadway Lighting*. FHWA-HRT-14-051. FHWA. 2014, Washington DC.
18. Green, M. *Seeing Pedestrians at Night*. 2008 [cited 2011 10/28/2011]; available from <http://www.visualexpert.com/Resources/pedestrian.html>.
19. Fotios, S.A. and Cheal, C. "Lighting for Subsidiary Streets: Investigation of Lamps of Different SPD. Part 1—Visual Performance," *Lighting Research & Technology*, 2007. 39(3): p. 215–232.
20. He, Y., Rea, M., Bierman, A., and Bullough, J. "Evaluating Light Source Efficacy Under Mesopic Conditions Using Reaction Times," *Journal of the Illuminating Engineering Society*, 1997. 26(1): p. 125–138.
21. Lewis, A.L. "Visual Performance as a Function of Spectral Power Distribution of Light Sources at Luminances Used for General Outdoor Lighting," *Journal of the Illuminating Engineering Society*, 1999. 28(1): p. 37–42.
22. Mutmanský, M., Gilver, T., Clanton, N., Gibbons, R.B., and Edwards, C. *Street Lighting Survey for Commercial Areas in the Municipality of Anchorage*. Clanton and Associates & Associates at the Virginia Tech Transportation Institute. 2009, City of Anchorage, AK.
23. Mutmanský, M., Gilver, T., Garcia, J., Clanton, N., Gibbons, R.B., and Edwards, C. *Advanced Street Lighting Technologies Assessment Project—City of San Jose*. Clanton and Associates & Associates at the Virginia Tech Transportation Institute. 2010, City of San Jose, CA.
24. Shaflik, C. *Information Sheet 125: Environmental Effects of Roadway Lighting*. International Dark-Sky Association, 1997, Tucson, AZ.
25. Terry, T. and Gibbons, R.B. *Assessment of the Impact of Color Contrast in the Detection and Recognition of Objects in a Road Environment*. Virginia Tech Transportation Institute. 2011, Blacksburg, VA.
26. ANSI/IESNA. "TM-12," *Spectral Effects of Lighting on Visual Performance at Mesopic Light Levels*. IESNA. 2014, New York, NY

27. He, Y., Bierman, A., and Rea, M. "A System of Mesopic Photometry," *Lighting Research and Technology*, 1998. 30(4): p. 175–181.
28. Bullough, J.D. and Rea, M. "Visual Performance Under Mesopic Conditions—Consequences for Roadway Lighting," *Traffic Control Devices, Visibility, and Rail-Highway Grade Crossings 2004*, 2004(1862): p. 89–94.
29. Berman, S.M. "Energy Efficiency Consequences of Scotopic Sensitivity," *Journal of the Illuminating Engineering Society*, 1992. 21(1): p. 3–14.
30. Sagawa, K. and Takeichi, K. "Mesopic Spectral Luminous Efficiency Functions: Final Experimental Report," *Journal of Light & Visual Environment*, 1987. 11(1): p. 22–29.
31. Ikeda, M. and Shimozono, H. "Mesopic Luminous-Efficiency Functions," *Journal of the Optical Society of America*, 1981. 71(3): p. 280–284.
32. Yaguchi, H. and Ikeda, M. Mesopic Luminous-Efficiency Functions for Various Adapting Levels. *Journal of the Optical Society of America A-Optics Image Science and Vision*, 1984. 1(1): p. 120–123.
33. Sagawa, K. "Toward a CIE Supplementary System of Photometry: Brightness at Any Level Including Mesopic Vision," *Ophthalmic and Physiological Optics*, 2006. 26(3): p. 240–245.
34. Sagawa, K. and Takeichi, K. "Spectral Luminous Efficiency Functions in the Mesopic Range," *Journal of the Optical Society of America a-Optics Image Science and Vision*, 1986. 3(1): p. 71–75.
35. Eloholma, M., Viikari, M., Halonen, L., Walkey, H., Goodman, T., Alderdinck, J., Freiding, A., Bodrogi, P., and Varady, G. "Mesopic Models—From Brightness Matching to Visual Performance in Night-Time Driving: A Review," *Lighting Research and Technology*, 2005. 37(2): p. 155–175.
36. Rea, M., Bullough, J.D., Freyssinier-Nova, J.P., and Bierman, A. "A Proposed Unified System of Photometry," *Lighting Research and Technology*, 2004. 36(2): p. 81–111.
37. Helsinki University of Technology Lighting Laboratory. *MOVE Mesopic Optimisation of Visual Efficiency: Performance Based Model for Mesopic Photometry*. M. Eloholma and L. Halonen, eds. 2005, Wspoo, Finland.
38. Eloholma, M. and Halonen, L. "New Model for Mesopic Photometry and Its Application to Road Lighting," *Leukos*, 2006. 2(4): p. 263–293.
39. Viikari, M., Ekrias, A., Eloholma, M., and Halonen, L. "Modeling Spectral Sensitivity at Low Light Levels Based on Mesopic Visual Performance," *Clinical Ophthalmology*, 2008. 2(1): p. 173–185.

40. Gibbons, R.B., Edwards, C., Williams, B., and Andersen, C. *Information Report on Lighting Design for Midblock Crosswalks*. FHWA-HRT-08-052. FHWA. 2008, Washington, DC.
41. Raphael, S. and Leibenfer, M. "Models of Mesopic Photometry Applied to the Contrast Threshold of Peripheral and Foveal Objects," *26th Session of the CIE*. CIE. 2007, Beijing, China.
42. Akashi, Y. and Rea, M. "Peripheral Detection While Driving Under a Mesopic Light Level," *Journal of the Illuminating Engineering Society*, 2002. 31(1): p. 85–94.
43. Rea, M.S., Bierman, T., McGowan, F., Dickey, F., and Javard, J. "A Field Test Comparing the Effectiveness of Metal Halide and High Pressure Sodium Illuminants Under Mesopic Conditions," *CIE Symposium on Visual Scales*. 1997, Teddington, UK.
44. Bullough, J.D. and Rea, M.S. "Simulated Performance and Peripheral Detection at Mesopic and Low Photopic Light Levels," *Lighting Research and Technology*, 2000. 32(4): p. 194–198.
45. Lingard, R. and Rea, M. "Off-Axis Detection at Mesopic Light Levels in a Driving Context," *Journal of the Illuminating Engineering Society*, 2002. 31(1): p. 33–39.
46. Kostic, M. and Djokic, L. "Recommendations for Energy Efficient and Visually Acceptable Street Lighting," *Energy*, 2009. 34(10): p. 1,565–1,572.
47. Kostic, M., Djokic, L., Pojatar, D., and Strbac-Hadzibegovic, N. "Technical and Economic Analysis of Road Lighting Solutions Based on Mesopic Vision," *Building and Environment*, 2009. 44(1): p. 66–75.
48. Bierne, R.O., L. McIlreavy, L., and Zlatkova, M.B. "The Effect of Age-Related Lens Yellowing on Farnsworth-Munsell 100 Hue Error Score," *Ophthalmic & Physiological Optics*, 2008. 28(5): p. 448–456.
49. Horswill, M.S., Marrington, S.A., McCullough, C.M., Wood, J., Pachana, N.A., and McWilliam, J. "The Hazard Perception Ability of Older Drivers," *The Journals of Gerontology Series B: Psychological and Social Sciences*, 2008. 63: p. 212–219.
50. Owens, D.A., Wood, J.M., and Owens, J.M. "Effects of Age and Illumination on Night Driving: A Road Test," *Human Factors: The Journal of the Human Factors and Ergonomics Society*, 2007. 49(6): p. 17.
51. Wood, J.M., Tyrrell, R.A., and Carberry, T.P. "Limitations in Drivers' Ability to Recognize Pedestrians at Night," *Human Factors: The Journal of the Human Factors and Ergonomics Society*, 2005. 47(3): p. 10.
52. Owens, D.A. and Tyrrell, R.A. "Effects of Luminance, Blur, and Age on Nighttime Visual Guidance: A Test of the Selective Degradation Hypothesis," *Journal of Experimental Psychology*, 1999. 5(2): p. 14.

53. NHTSA. *Fatality Reporting System*. 2014 [cited 2014, 4/22/2014]; available from <http://www.nhtsa.gov/FARS>.
54. Adrian, I.W. "Visibility of Targets: Model for Calculation," *Lighting Research & Technology*, 1988. 21(4): p. 181–188.
55. Blackwell, O.M. and Blackwell, R.H. "Individual Responses to Lighting Parameters for a Population of 235 Observers of Varying Ages," *Journal of the Illuminating Engineering Society*, 1980. 9(4): p. 205–232.
56. Stiles, W.S. and Burch, J.M. "NPL Colour-Matching, Investigation: Final Report (1958)," *Optica Acta: International Journal of Optics*, 1959. 6(1): p. 1–26.
57. Coren, S. and Girgus, J.S. "Density of Human Lens Pigmentation: In Vivo Measures Over an Extended Age Range [Letter]," *Vision Research*, 1972. 12(2): p. 343–346.
58. Moreland, J.D. "The Effect of Inert Ocular Pigments on Anomaloscope Matches and Its Reduction," *Modern Problems in Ophthalmology*, 1972. 11: p. 12–18.
59. Rinalduci, E.J. and Beare, A.N. "Losses in Nighttime Visibility Caused by Transient Adaptation," *Journal of the Illuminating Engineering Society*, 1974. 3(4): p. 336–345.
60. Gibbons, R.B. *Fields of Visibility for the Nighttime Driver*. University of Waterloo. 1993, Waterloo, ON, Canada.
61. NHTSA. *Traffic Safety Facts 2009*. U.S. Department of Transportation. 2010, Washington, DC.
62. Pöppel, E. and Harvey, L.O. "Light-Difference Threshold and Subjective Brightness in the Periphery of the Visual Field," *Psychological Research*, 1973. 36(2): p. 145–161.
63. Gibbons, R.L. "Fields of Visibility for the Nighttime Driver," *Systems Design Engineering*. University of Waterloo. 1993, Waterloo, ON. p. 122.
64. Van Derlofske, J.F., Bullough, J.D., and Watkinson, J. *Spectral Effects of LED Forward Lighting*. Lighting Research Center, Rensselaer Polytechnic Institute. 2005, Troy, NY.
65. Bullough, J.D. "Modeling Peripheral Visibility Under Headlamp Illumination," *Transportation Research Board 16th Biennial Symposium on Visibility and Simulation*, Iowa City, IA, June 2–4, 2002.
66. Van Derlofske, J.F., Bullough, J.D., and Hunter, C.M. "Evaluation of High-Intensity Discharge Automotive Forward Lighting," *SAE 2001 World Congress*. SAE International. 2001, Detroit, MI.
67. O'Malley, R., Glavin, M., and Jones, E. "A Review of Automotive Infrared Pedestrian Detection Techniques," *IET Irish Signals and Systems Conference, 2008. (ISSC 2008)*.

68. Zhenjiang, L., Kunfeng, W., Li, L., and Fei-Yue, W. "A Review on Vision-Based Pedestrian Detection for Intelligent Vehicles," *IEEE International Conference on Vehicular Electronics and Safety*, 2006. 2006, Shanghai, China. p. 57–62.
69. Gavrilu, D.M. "Sensor-Based Pedestrian Protection," *IEEE Intelligent Systems*, 2001. 16(6): p. 77–81.
70. Abramson, Y. and Steux, B. "Hardware-Friendly Pedestrian Detection and Impact Prediction," *IEEE Intelligent Vehicles Symposium*, 2004. 2004, Parma Italy.
71. Hashiyama, T., Mochizuki, D., Yano, Y., and Okuma, S. "Active Frame Subtraction for Pedestrian Detection From Images of Moving Camera," *IEEE International Conference on Systems, Man and Cybernetics*, 2003. 2003, Washington, DC.
72. Shashua, A., Gdalyahu, Y., and Hayun, G. "Pedestrian Detection for Driving Assistance Systems: Single-Frame Classification and System Level Performance," *IEEE Intelligent Vehicles Symposium*, 2004. 2004, Parma, Italy.
73. Viola, P., Jones, M.J., and Snow, D. "Detecting Pedestrians Using Patterns of Motion and Appearance," *International Journal of Computer Vision*, 2005. 63(2): p. 153–161.
74. Havasi, L., Szlavik, Z., and Sziranyi, T. "Pedestrian Detection Using Derived Third-Order Symmetry of Legs," *Proceedings of the International Conference on Computer Vision and Graphics*, 2004, Warsaw, Poland.
75. Gandhi, T. and Trivedi, M.M. "Vehicle Mounted Wide FOV Stereo for Traffic and Pedestrian Detection," *IEEE International Conference on Image Processing*, 2005. 2005, Genova, Italy.
76. Papageorgiou, C. and Poggio, T. "Trainable Pedestrian Detection," *Proceedings of the 1999 International Conference on Image Processing*, 1999, Kobe, Japan.
77. Fengliang, X., Xia, L., and Fujimura, K. "Pedestrian Detection and Tracking With Night Vision," *IEEE Transactions on Intelligent Transportation Systems*, 2005. 6(1): p. 63–71.
78. Xia, L. and Fujimura K. "Pedestrian Detection Using Stereo Night Vision," *IEEE Transactions on Vehicular Technology*, 2004. 53(6): p. 1,657–1,665.
79. Broggi, A., Fascioli, A., Carletti, M., Graf, T., and Meinecke, M. "A Multi-Resolution Approach for Infrared Vision-Based Pedestrian Detection," *IEEE Intelligent Vehicles Symposium*, 2004. 2004, Parma, Italy.
80. Yajun, F., Yamada, K., Ninomiya, Y., Horn, B.K.P., and Masaki, I. "A Shape-Independent Method for Pedestrian Detection With Far-Infrared Images," *IEEE Transactions on Vehicular Technology*, 2004. 53(6): p. 1,679–1,697.
81. Saito, H., Hagihara, T., Hatanka, K., and Sawai, T. "Development of Pedestrian Detection System Using Far-Infrared Ray Camera," *SEI Technical Review*, 2008. 66: p. 112–117.

82. Tsuji, T., Hattori, H., Watanabe, M., and Nagaoka, N. "Development of Night-Vision System, *IEEE Transactions on Intelligent Transportation Systems*, 2002. 3(3): p. 203–209.
83. Milch, S. and Behrens, M. *Pedestrian Detection with Radar and Computer Vision*. Pennsylvania State University. 2001, State College, PA.
84. Scheunert, U., Cramer, H., Fardi, B., and Wanielik, G. "Multi Sensor Based Tracking of Pedestrians: A Survey of Suitable Movement Models," *IEEE Intelligent Vehicles Symposium, 2004*. 2004, Parma, Italy.
85. Gavrila, D.M., Giebel, J., and Munder, S. "Vision-Based Pedestrian Detection: The PROTECTOR System," *IEEE Intelligent Vehicles Symposium, 2004*. 2004, Parma, Italy.
86. Volvo Cars of North America. *Volvo Unveils Innovative Safety Technology—Pedestrian Detection With Full Auto Brake Debuts on the All-New Volvo S60*. 2011 [cited 2011 4/12/2011]; available from <https://www.media.volvocars.com/us/enhanced/en-us/Media/Preview.aspx?mediaid=31773>.
87. Mobileye. *MOBILEYE Advance Warning System*. 2008, Jerusalem, Israel.
88. Van Derlofske, J.F., Bullough, J.D., and Gribbin, C. "Comfort and Visibility Characteristics of Spectrally-Tuned High Intensity Discharge Forward Lighting Systems," *European Journal of Scientific Research*, 2007. 17(1): p. 73–84.
89. Van Derlofske, J.F. and McColgan, M.W. *White LED Sources for Vehicle Forward Lighting*. SPIE. 2002, Seattle, WA.
90. Chen, W., Lin, Y., Kojima, S., and Chen, D. "A Study on Peripheral Visibility Under Different Headlamp Low-Beam Pattern," *Journal of Light & Visual Environment*, 2008. 32(4): p. 358–365.
91. Harley, M. *Audi R8 Gets First Full LED Headlamps*. 2008 [cited 2011, 7/23/2015]; available from: <http://www.autoblog.com/2008/05/30/audi-r8-gets-first-full-led-headlamps/>.
92. Meyer, J.E., Gibbons, R.B., and Edwards, C. *Development and Validation of a Luminance Camera*. Virginia Tech Transportation Institute. 2009, Blacksburg, VA.
93. Meyer, J.E. and Gibbons, R.B. *Luminance Metrics for Roadway Lighting*. The National Surface Transportation Safety Center for Excellence. 2011, Blacksburg, VA.
94. Burton, K.B., Owsley, C., and Sloane, M.E. "Aging and Neural Spatial Contrast Sensitivity—Photopic Vision," *Vision Research*, 1993. 33(7): p. 939–946.
95. Boyce, P.R. *Light for Driving: Roads, Vehicles, Signs, and Signals*. CRC Press. 2009, Boca Raton, FL.

96. Adrian, I.W. "Visibility of Targets: Model for Calculation," *Lighting Research & Technology*, 1988. 21(4): p. 8.
97. Alferdinck, J.W.A.M. "Target Detection and Driving Behaviour Measurements in a Driving Simulator at Mesopic Light Levels," *Ophthalmic and Physiological Optics*, 2006. 26(3): p. 264–280.
98. Saunders, D.A. *Adirondack Mammals*. State University of New York, College of Environmental Science and Forestry. 1988, Syracuse, NY. p. 216.
99. Brown, G. *The Great Bear Almanac*. Lyons & Burfurd, 1996, New York, NY.
100. DiLaura, D., Houser, K., Mistrick, R., and Steffy, G., eds. *Lighting Handbook, 10th Edition*. Illuminating Engineering Society of North America. 2010, New York, NY. p. 1,328.
101. Clanton & Associates Inc. *Seattle LED Adaptive Lighting Study*. 2014, Boulder, CO.

